Structural geology of South Hadhramaut area Yemen Republic

Ahmed Mohammed Abdullah Al-Kotbah

B.Sc. (Al-Azhar, Egypt), M.Sc. (Sana'a, Yemen)

Volume I

Thesis submitted for the degree of Doctor of Philosophy in the Faculty of Science, Department of Geology and Applied Geology, University of Glasgow.

September 1996

Declaration

The material presented in this thesis summaries the results of three years of research carried out at Glasgow University under the supervision of Dr. Iain Allison.

This study is based on my own independent research and any previously published or unpublished results of other authors used in this thesis have been given full acknowledgement in the text.

A. M. Al-Kotbah

Abstract

The northern margin of the Gulf of Aden has a long history of extension from the Cambrian to the present. The dominant structures are related to Oligo-Miocene rifting in the early stages of development of the Gulf of Aden and they overprint Palaeozoic and Mesozoic structures. An area of 170 km by 50 km was mapped at scale of 1:50,000.

Landsat images of the whole area, at 1:50,000 and 1:100,000 and air photographs of part of the area were used as base maps. The resulting maps are the first detailed geological maps to be made for this area and are a major outcome of this research. Precambrian basement which was affected by the oldest stage of extension is overlain by a sedimentary cover sequence from upper Cretaceous through the Tertiary in age. The lower part of this sequence represents the Mesozoic post-rift succession deposited after the second period of extension recorded in this margin. Oligo-Miocene extension has resulted in a highly dissected rift shoulder in which the horizontal cover sequence at an elevation of 1500m to 2500m on the plateau is brought down in a series of tilted fault blocks to sea level at the Gulf coast. The massive, nodular Palaeocene limestone of the Umm er Radhuma Formation forms steep inaccessible fault scarps throughout the area. The faults vary in size from major ones which have strike lengths in excess of 50 km and throws over 1000 m to those that are too small to be recorded on the maps.

By measuring the geometry of bedding in the rollover anticlines in the hanging walls of selected faults, the trajectories of the faults at depth were computed. These show that the major faults extend steeply down into metamorphic basement. Balanced cross sections constructed along the main north-south valleys allow values of extension in the range 5-12% to be calculated. These low values on a rift margin which has oceanic crust along the Sheba ridge in the central Gulf of Aden imply that major faults with kilometric throws must lie off-shore or, less likely, are buried beneath the syn- and post-rift sediments of the coastal plain. The extension varies along the area and four zones of even lower extension are recognised. These are transfer zones on a regional scale and are parallel to the trend of the off-shore fracture zones extending NNE from the Sheba ridge. Horizontal movements which are recorded in slickensides from various places throughout the area are reported for the first time. They affect the Palaeocene limestone and are overprinted by steeply pitching slickensides related to the Oligo-Miocene rifting and are probably Eocene in age. The extensional faults could be classified into three groups according to their size and dimensions,

the first group are the major faults which control the shape and morphology of the southern part of the south Hadhramaut area. The second group, which includes most of the faults, are those of medium size with average displacements between 40m and 400m. This group has also contributed to the present shape and morphology of the area and shows the characteristic style of structures in the area which are half grabens with, less commonly, full grabens. The third group are the smallest faults which are mappable at a scale of 1:50,000 and have displacements of between 10m and 40m. The faults display a swing in strike from ESE-WNW in the eastern part through east-west in the middle to ENE-WSW in the west.

The extension direction in the southern part of Hadhramaut area is N-S. The fractures belong to two main trends, namely ESE-WNW and NE-SW, and indicate that there are two subsidary extension directions in the area. Regional implications show that the both north and south margins of the Gulf of Aden could be matched to their initial position before rifting.

A cknowledgements

This research was carried out in the Department of Geology & Applied Geology, University of Glasgow under the supervision of Dr. Iain Allison. This project was funded by Canadian Occidental International Petroleum Co. Ltd., contract no. 9685L010, which also provided logistical and scientific support. Gord Graham is thanked for initiating this project and for his continuing interest and support. Jerry Sykora, Eric Bolton, Kate Glazebrook and Ed Bell are thanked for their assistance.

I would like to thank my supervisor Dr. Iain Allison who was behind this project and selected me to do this research. Also I would like to thank him for his considerable help in guidance, unlimited support, discussion, comments, criticisms and in correcting the drafts of this thesis. His friendliness and hospitality at all times encouraged me to work hard. This project would have never completed on time without his help.

I am grateful to my father and my brothers Saleh and Abdullah for their support financially and encouragement during my study in Britain and to my wife and children for their patience and help during the preparation of this research.

I would like to thank all staff in the Department of Geology and Applied Geology, University of Glasgow. My thanks goes to Dr. Brian Bell, Gary Couples and Colin Braithwaite for their help in discussions and comments during the analysis of field data and preparation of maps. Especial thank goes to Dr. Yhya Alqzaz who provided me the stereoplot programme which is used partially in this thesis.

I send thanks to my colleagues in the Department of Geology in University of Sana'a, in particularly Dr. Abdel Karim Al-Subbary who provided me with many references and continuous encouragement and Dr. Khalid Al-Thour for his support and discussion and Dr. Mohammed Al-Kadsi who guided me to related references on the study area and provided some references and Dr. Mohammed Hazam Alawah for his support. Also especial thanks are due to Gamal Baharmuz who provided me with valuable references.

I would like to thank all staff in the University of Sana'a, in particularly the Faculty of Science and the Department of Higher Studies Affairs for their efforts and help.

My appreciation goes to the technical staff in the Department of Geology & Applied Geology, University of Glasgow in particularly Mrs. Sheila Hall who drew the draft maps and cross sections and for her help at all times. The

photographer, Mr. Douglas Maclean is thanked very much for printing photographs and making slides for talks in conferences and his help at all times. Roddy Morrison is also thanked very much for his help at all times and for copying the maps. A warm greeting goes to Mr. Jim Kavanagh who was helpful with computer software.

My thanks are due to my postgraduate student colleagues, in particular Dr. Abderhammane Abumazber, Amar Gammudi, Abdullah Ghouth, Abu-Al-Kassim Esaiti, Chris McKeown and Simon Peers for their friendlliness and kind help.

List of contents

Abstract ---------- I

Acknowledgements ---------- III

List of contents ---------- VI

List of figures ---------- XI

List of table ---------- XX

Chapter 1 Introduction

1.1. Aim of project ---------- 1

1.2. Location of the study area ---------- 5

1.3. Accessibility and topographic features ---------- 5

1.4. Drainage systems ---------- 6

1.5 Climate and vegetation ---------- 8

1.6. Previous work ---------- 10

1.7. Methods employed ---------- 12

1.7.1. Landsat images ---------- 13

1.7.2. Air photographs ---------- 13

1.7.3 Field work ---------- 14

1.7.4. Laboratory ---------- 14

1.8. Format of the thesis ---------- 15

Chapter 2 Stratigraphic setting

2.1. Introduction ---------- 16

2.2. The basement rocks ---------- 20

2.3. Jurassic ---------- 22

2.3.1. Kholan Formation (Middle to ? Lower Jurassic) ---------- 22

2.3.2 Amran Group (Upper Jurassic) ---------- 23

2.4. Qishn Formation (Barremian-Aptian) ---------- 23

2.5. The Harshiyat Formation (Albian-Cenomanian) ---------- 25

2.6. Fartaq Formation (Albian-Turonian) ---------- 31

2.7. The Mukalla Formation (Senomian)---------- 32

2.8. The Umm er Radhuma Formation (Palaeocene) ---------- 35

2.9. The Jeza Formation (Lower Eocene)---------- 36

2.10. The Rus Formation (Middle Eocene) ---------- 36

2.11. The Habshiya Formation (Middle Eocene)---------- 42

2.12. The Shihr Group (Oligo-Miocene)---------- 42

2.13. Pliocene sediments. ---------- 43

2.14/. River deposits---------- 43

2.15. Alluvium deposits---------- 46

2.16. Aeolian deposits ---------- 46

2.17. Younger lavas ---------- 46

Chapter 3 Review of the extensional faulting

3.1. Introduction ---------- 48

3.2. Geometry and classification of extensional faults---------- 50

3.3. Accommodation structures in extension region---------- 54

3.4. Evolution of transfer zones ---------- 55

3.5. Models of rifting---------- 61

3.6. Discussion of rifts ---------- 65

3.7. Summary ---------- 67

Chapter 4 The geometries of fault surfaces

4.1. Introduction ---------- 69

4.2. Models of the geometry of faults---------- 70

4.3. Methodology ---------- 72

4.4. Location of traverses ---------- 74

4.5. The Switchbacks area ---------- 75

4.7. Gayl Bawazir area---------- 77

4.8. Addition traverses through the whole area ---------- 79

4.9. Conclusion ---------- 81

Chapter 5 Estimation of strain

5.1 Balanced cross sections ---- 84

5.1.1. Introduction ---- 84

5.1.2. Difficulties of balancing cross sections ---- 88

5.1.3. The study area ---- 89

5.1.4. Wadi Hawayrah cross section ---- 89

5.1.5. Restoration of wadi Hawayrah section ---- 91

5.1.6. Switchbacks cross section ---- 92

5.1.7. Restoration of the Switchbacks cross section ---- 93

5.1.8. Wadi Araf cross section ---- 94

5.1.9. Restoration of wadi Araf cross section ---- 95

5.1.10 Wadi Kharid cross section ---- 99

5.1.11. Restoration of wadi Kharid cross section ---- 101

5.1.12. Wadi Assad cross section ---- 101

5.1.13. Restoration of wadi Assad cross section ---- 104

5.1.14. Wadi Bidish cross section ---- 104

5.1.15. Restoration of wadi Bidish cross section ---- 107

5.1.16. Discussion and conclusion ---- 107

5.2. Estimates of strain by brittle faulting ---- 109

5.2.1. Fault displacement populations ---- 113

Chapter 6 Analysis of faults and fractures

6.1. Introduction ---- 116

6.2. Major structures in the northern margin of the Gulf of Aden ---- 119

6.2.1. Major faults ---- 119

6.2.2. Strike slip faults ---- 121

6.2.3. Folds ---- 122

6.3. Structural patterns ---- 122

6.3.2. Transfer zones ---- 125

6.3.3. Accommodation structures ---- 139

6.4. Geometrical analysis of faults and fractures ---- 140

6.4.1. Fault and fractures in basement rock ---- 147

6.4.2. Slip movement in basement rocks ---- 149

6.4.3. Faults and fractures in Ydmah-Hawayrah area ---- 149

6.4.4. Slip movement in Ydmah-Hawayrah area ---- 151

6.4.5. Slip movement in the Switchbacks area ---- 151

6.4.6. Faults and fractures in wadi Araf-wadi Tamah area ---- 151

6.4.7. Slip movement in wadi Araf-wadi Tamah area ---- 152

6.4.8. Faults and fractures in wadi Kharid ---- 152

6.4.9. Slip movement in wadi Kharid ---- 153

6.4.10. Faults and fractures in wadi Assad ---- 158

6.4.11. Slip movement in wadi Assad ---- 158

6.4.12. Faults and fractures in wadi Bidish ---- 158

6.4.13. Slip movement in wadi Bidish ---- 159

6.4.14. Faults and fractures in wadi Shakhawi ---- 159

6.4.15. Slip movement in wadi Shakhawi ---- 160

6.4.16. Shihr Group ---- 160

6.5. Bedding analysis ---- 160

6.6. Conclusion ---- 161

Chapter 7 Geological evolution

7.1. Introduction ---- 167

7.2. Basement structures ---- 173

7.3. Jurassic structures ---- 182

7.4. Cretaceous structures ---- 183

7.5. Palaeocene-Eocene structures ---- 186

7.6. Oligo-Miocene structures ---- 188

7.7. Pliocene-Recent structures ---- 189

Chapter 8. Regional implications

8.1. Introduction ---------- 194

8.2 Precambrian ---------- 195

8.3 Jurassic ---------- 197

8.4 Cretaceous ---------- 198

8.5 Palaeocene-Eocene ---------- 200

8.6 Oligo-Miocene ---------- 201

8.7 Pliocene-Recent ---------- 203

Chapter 9 Conclusion

9.1. Summary of results ---------- 204

9.2. Conclusions ---------- 210

9.3. Recommendation for further work ---------- 211

References ---------- 212

Appendices ---------- 231

List of figures

Chapter 1

Fig. 1.1. Location of the Arabian plate---------- 2

Fig .1.2. Regional tectonic map of Arabian plate---------- 3

Fig. 1.3. Tectonic elements in the northern margin of the Gulf of Aden -------- 4

Fig. 1.4. Location map of the study area ---------- 8

Fig. 1.5. Map of south Hadhramaut area showing the main wadis ---------- 9

Chapter 2

Fig .2.1. Structural geological map of wadi Shakhawi---------- 18

Fig. 2.2. Stratigraphic column of Hadhramaut area---------- 22

Fig. 2.3. High intensity of fractures with different trend in Ydmah area ------- 26

Fig. 2.4. The unconformity between the sedimentary sequence and the basement rocks---------- 27

Fig. 2.5. The Qishn Formation is completely recrystallised to dolomite in the Ydmah area---------- 27

Fig. 2.6. The conglomerate is highly fossiliferous in the lower Qishn ---------- 28

Fig. 2.7. The Qishn Formation is exposed in a horst at 200m above sea level -- 28

Fig. 2.8. The Qishn Formation became shaly and marly with alternating thin layers of limestone in wadi Shakhawi---------- 29

Fig. 2.9. The Harshiyat Formation contains silicified wood---------- 29

Fig. 2.10. Photograph shows the complete Harshiyat Formation with its two limestone members (Rays and Sufla) ---------- 30

Fig. 2.11. The Sufla member contains mainly fossil Rudists ---------- 33

Fig. 2.12. The Fartaq Formation is completely exposed in the footwall of wadi Al-Rakdoon fault in wadi Assad---------- 34

Fig. 2.13. The Dhasohis member recrystallised to dolomite---------- 37

Fig. 2.14. The Umm er Radhuma Formation becomes thin ---------- 37

Fig. 2.15. Characteristic cliffs of the Umm er Radhuma Formation ---------- 38

Fig. 2.16. The Umm er Radhuma Formation forms very steep scarp ---------- 38

Fig. 2.17. The marker unit in the Umm er Radhuma Formation which is used as reference to calculate the vertical displacement ---------- 39

Fig. 2.18. The Umm er Radhuma Formation is highly eroded along the main wadis and sometimes forms screes in many places ---------- 39

Fig. 2.19. The Jeza Formation conformably overlies the Umm er Radhuma Formation. ---------- 40

Fig. 2.20. The Jeza Formation is highly eroded away and sometimes stands as isolated exposures in the flat area ---------- 40

Fig. 2.21. The Jeza Formation sometimes consists of alternating layers of limestones and gypsum ---------- 41

Fig. 2.22. The Rus Formation is rarely found in the southern part of the area - 41

Fig. 2.23. The characteristic feature of the Rus Formation is the irregular shape of its outcrop ---------- 44

Fig. 2.24. This photograph shows the Habshiya Formation brought down against the Rus Formation by a north dipping fault ---------- 44

Fig. 2.25. The Shihr Group shows high deformation and slumping ---------- 45

Fig. 2.26. The Shihr Group is in general of gentle dip, but sometimes has very steep dip ---------- 45

Fig. 2.27. The relationship between the Shihr Group and the Pliocene deposits is an unconformity ---------- 47

Fig. 2.28. Volcanic flows occur on the flat area along the coast plain ---------- 47

Chapter 3

Fig. 3.1. Lithospheric stretching model ---------- 51

Fig. 3.2. Heterogeneous lithospheric stretching ---------- 51

Fig. 3.3. Ramp/flat listric extensional fault model ---------- 53

Fig. 3.4. Classification of transfer zones ---------- 56

Fig. 3.5. Block diagram of a displacement-normal offset (A) and a displacement parallel offsets (B) ---- 58

Fig. 3.6. Schematic diagram of three possible structures underlying a segmented fault zone as seen in map view (a-b) ---- 58

Fig. 3.7. Development of a detached hanging wall relay system ---- 59

Fig. 3.8. Classification of half graben linkage ---- 59

Fig. 3.9. Simple classification of relay zones ---- 61

Fig. 3.10. Model for the rift episode in the development of the Red Sea and Gulf of Aden ---- 64

Fig. 3.11. Proposition that the Gulf of Aden propogated along old lineaments. ---- 66

Chapter 4

Fig. 4.1. Summary of different methods used to calculate the geometry of faults with depth ---- 73

Fig. 4.2. 0.40m aluminium disk attached to a Clar compass ---- 74

Fig. 4.3. Location of the traverses throughout the area ---- 78

Fig. 4.4. The calculation of fault geometry with depth in the Switchbacks area (a-i) and north Gayl Bawazir area (j) ---- 82

Fig. 4.5. The calculation of faults with depth in north Gayl Bawazir area (a-d), - south wadi Hawayrah (e), southeast wadi Araf (f), wadi Assad (g) and wadi Bidish (h-j) ---- 83

Chapter 5

Fig. 5.1. Map showing the major faults in the study area and the locations of cross sections ---- 87

Fig. 5.3. Structural cross section along the Switchbacks area ---- 96

Fig. 5.4. The typical half grabens in the Switchbacks area ---- 97

Fig. 5.5. Block diagram showing the geometry of faults with depth ---- 98

Fig. 5.6. Switchbacks fault brings the Jeza Formation into contact with the Mukalla formation, looking ENE ---- 99

Fig. 5.10. The bedding of the Mukalla Formation are rotated to more than 40° ---------- 106

Fig. 5.12. Displacement-trace length data---------- 112

Fig. 5.13. Fault displacement population curve from seismic reflection data and field data---------- 115

Chapter 6

Fig. 6.1. Horizontal slickensides on a steep fault surface ---------- 127

Fig. 6.2. Slickensides in both horizontal and vertical directions on a fault surface ---------- 128

Fig. 6.3. Clastic sedimentary rocks and dolomite of the Mukalla Formation - overlies the Jeza Formation ---------- 129

Fig. 6.4. Low angle fault and thrust fault in wadi Al-Masila ---------- 130

Fig. 6.5. Map showing the sites of measurements ---------- 131

Fig. 6.6. Landsat image and map showing the Hasis graben ---------- 132

Fig. 6.7. Oblique air photograph and map the Switchbacks ---------- 133

Fig. 6.8. Graben formed by asymmetrical conjugate faults in the Switchback area, ---------- 134

Fig. 6.9. Landsat image and map of the Al-Madi graben ---------- 135

Fig. 6.10. Landsat image showing the linear faults---------- 136

Fig. 6.11. The dominant structures are mainly half-grabens ---------- 136

Fig. 6.12. Development of a detached hanging wall relay system ---------- 137

Fig. 6.13. Small faults formed parallel to the relay ramps ---------- 137

Fig. 6.14. Contour map of vertical displacement of faults ---------- 141

Fig. 6.15. Monocline in Mukalla Formation ---------- 142

Fig. 6.16. Monocline formed at the tip of south dipping fault ---------- 142

Fig. 6.17. Rollover anticline showing the rotation of the hanging wall-------- 143

Fig. 6.18. Rollover anticline showing the rotation of the Jeza bedding-------- 143

Fig. 6.19. Folds in Jeza Formation formed above a reverse fault---------- 144

Fig. 6.20. Deformation of the Harshiyat Formation ---------- 144

Fig. 6.21. Photograph showing small reverse fault---------- 145

Fig. 6.22. The Umm er Radhuma Formation has been rotated to dip at 40° -- 145

Fig. 6.23. Two trends of slickenside lineations in basement rocks---------- 146

Fig. 6.24. Various sets of fractures with dips from steep to low angle in basement rocks ---------- 146

Fig. 6.25. High intensity of fracturing in basement rocks in the lower part --- 147

Fig. 6.26. Lower-hemisphere equal area projection of faults and fractures in basement rocks, (a-b) poles of faults in basement (c) slip sense of faults, and star indicates the oblique slip, (d-e) contour and scatter of fractures in basement rocks. Contours are in points per 1% area and have been generated using a computer programme---------- 154

Fig. 6.27. (a-b) Contour and scatter plots of fractures in Ydmah area (c-d) contour and scatter plots of faults in wadi Hawayrah area, (e) slip motion of faults in wadi Hawayrah, the star indicates oblique to horizontal slip (g-h) - contours and scatter plot of poles of fractures in Lusp-Hawayrah areas ---------- 155

Fig. 6.28. (a-b) Contoured and scatter plots of faults in the Switchbacks area, (c) slickenside lineations on faults in the Switchbacks area, the star indicates horizontal slip, (d-e) contoured and scatter plot of fractures,(f-g) contoured and scatter plot of fractures which have been measured at the tip of a fault in the Switchbacks area---------- 156

Fig. 6.29. Contoured and scatter plot of faults in wadi Araf-wadi Tamah area, (c) slip direction of faults (d-e) contoured and scatter of fractures in Araf-Tamah area---------- 157

Fig. 6.30. Plot of faults and fractures in wadi Kharid areas (a-b) contour and scatter plots of faults in wadi Kharid area (c) slip motion of faults in wadi Kharid, (d-e) contour and scatter of fractures in wadi Kharid and (f-g) fractures measured at the tip of a fault in south wadi Kharid ---------- 162

Fig. 6.31. (a-b) Contour and scatter plot of faults in wadi Assad, (c) slip of motion of faults, (d-e) contour and scatter of fractures in wadi Assad- ---------- 163

Fig. 6.32. (a-b) Contour and scatter plot of faults and fractures in wadi Bidish (c) slip motion of faults, (d-e) contour and scatter plot of fractures in wadi Bidish ---------- 164

Fig. 6.33. (a-b) Contour and scatter plot of faults in wadi Shakhawi and (c) slip of motion of faults, (d-e) contours and scatter plots of fractures in wadi - Shakhawi, (f-g) contoured and scatter plots of fractures measured in the Shihr Group ---------- 165

Fig. 6.34. (a-b) Bedding planes in Hawayrah area, (c-d) bedding planes in Araf-Kharid area, (e-f) bedding planes in wadi Assad and (g-h) bedding planes in wadi Bidish-Shakhawi area. A c e and g are equal area orientation diagrams of poles to bedding; b d f and h are rose diagrams of dip direction ---------- 166

Chapter 7

Fig. 7.1. Main basins of the northern margin of the Gulf of Aden ---------- 171

Fig. 7.2. Dyke in basement intruded along north-south fracture ---------- 175

Fig. 7.3. Thick sequence of Cretaceous rocks of the Mukalla and Harshiyat ------ Formations, wadi Hawayrah. Prominent layer in middle of sequence is the Sufla member ---------- 175

Fig. 7.4. Cretaceous extensional fault cutting the Fartaq and Mukalla Formations ---------- 176

Fig. 7.5. Stratigraphy and Lithotypes of the Tawilah Group, Hadhramaut -- 177

Fig. 7.6. Older horizontal and younger vertical slickensides on a fault surface ---------- 178

Fig. 7.7. Satellite image showing the southern part of the Hadhramaut area which is highly dissected by the Oligo-Miocene extensional faults --------- 178

Fig. 7.8. Fault with oblique slickensides cutting the syn-rift Shihr Group rock ---------- 179

Fig. 7.9. The Shihr Group is subjected to two stage of fractures, Ad-Deis area ---------- 179

Fig. 7.10. Fractures within basement showing variations in dip ---------- 180

Fig. 7.11. Unconformity between the basement rocks and the Cretaceous Qishn Formation ---------- 180

Fig. 7.12. Unconformity showing a high intensity of fractures in the basement

rocks in the lower part and fewer fractures in the sedimentary cover in the upper part---------- 181

Fig. 7.13. Contact between the basement rocks and the Qishn Formation. Steep younger faults affect both rocks ---------- 181

Fig. 7.14. Oblique slickenside lineations in basement rocks---------- 182

Fig. 7.15. Angular unconformity between the Shihr Group and the Pliocene 190

Fig. 7.16. Pliocene conglomerates affected by extensional fractures ---------- 191

Fig. 7.17. Pliocene deposits dipping to the north due to the rotation towards a fault plane---------- 192

Fig. 7.18. Lava spreads in south wadi Assad overlying the Shihr Group and Pliocene deposits ---------- 193

Fig. 7.19. Coast plain about 100m above the sea level ---------- 193

Chapter 8

Fig. 8.1 Generalised structural features of the Gulf of Aden continental margins restored to preseparation position ---------- 202

List of tables

Chapter 2.1 Table 1 the stratigraphic sequence of the study area ----------20

Chapter 7.1 Table 1 the summary of tectonic movements ---------- 172

content of volume II

Structural geological map of wadi Hawayrah area (sheet I).

Structural geological map of Gayl Bawazir-Al-Madi area (sheet II).

Structural geological map of wadi Araf-Tamah area (sheet III).

Structural geological map of wadi Kharid (sheet IV).

Structural geological map of wadi Assad and wadi Bidish (sheet V).

Fig. 5.2. Sructural cross section of wadi Hawayrah

CHAPTER I

INTRODUCTION

1.1 Aim of project

The northern margin of the Gulf of Aden forms an arcuate mountain chain from Bab-Almandab in the west to the straits of Hormuz in the central part of Oman in the east (Fig. 1.1 and Fig. 1.2). This area includes the southern flank of the south Hadhramaut arch that extends from the eastern border of the Hajar trough to the west of Mukalla to Ras Sharwayn in the east (see chapter 6, Fig. 1.3). The study area, which includes part of the southern part of south Hadhramaut arch, represents part of the concession block of the Canadian Occidental International Petroleum Company (Canadian Oxy). The study area is more than 170km long and its width ranges between 30 and 50km. The elevation difference between the coast plain and plateau is greater than 2,000m. The surface structures of the northern margin of the Gulf of Aden have never been mapped in detail. The stratigraphy has been briefly studied by Beydoun (1964), Greenwood and Bleackley (1967) and Beydoun and Greenwood (1968). Only the major faults had previously been mapped, mainly from remote sensing data.

Fig. 1.1. Location of the Arabian plate showing the curved shape of the northern margin of the Gulf of Aden.

Following the discovery of an economic quantity of oil by Canadian Occidental International Petroleum Company there has been extensive exploration throughout the area. This area has thick sequences of Jurassic-Cretaceous sedimentary rocks containing organic rich potential source rocks as well as suitable reservoir and sealing units and has therefore attracted considerable interest from numerous oil companies.

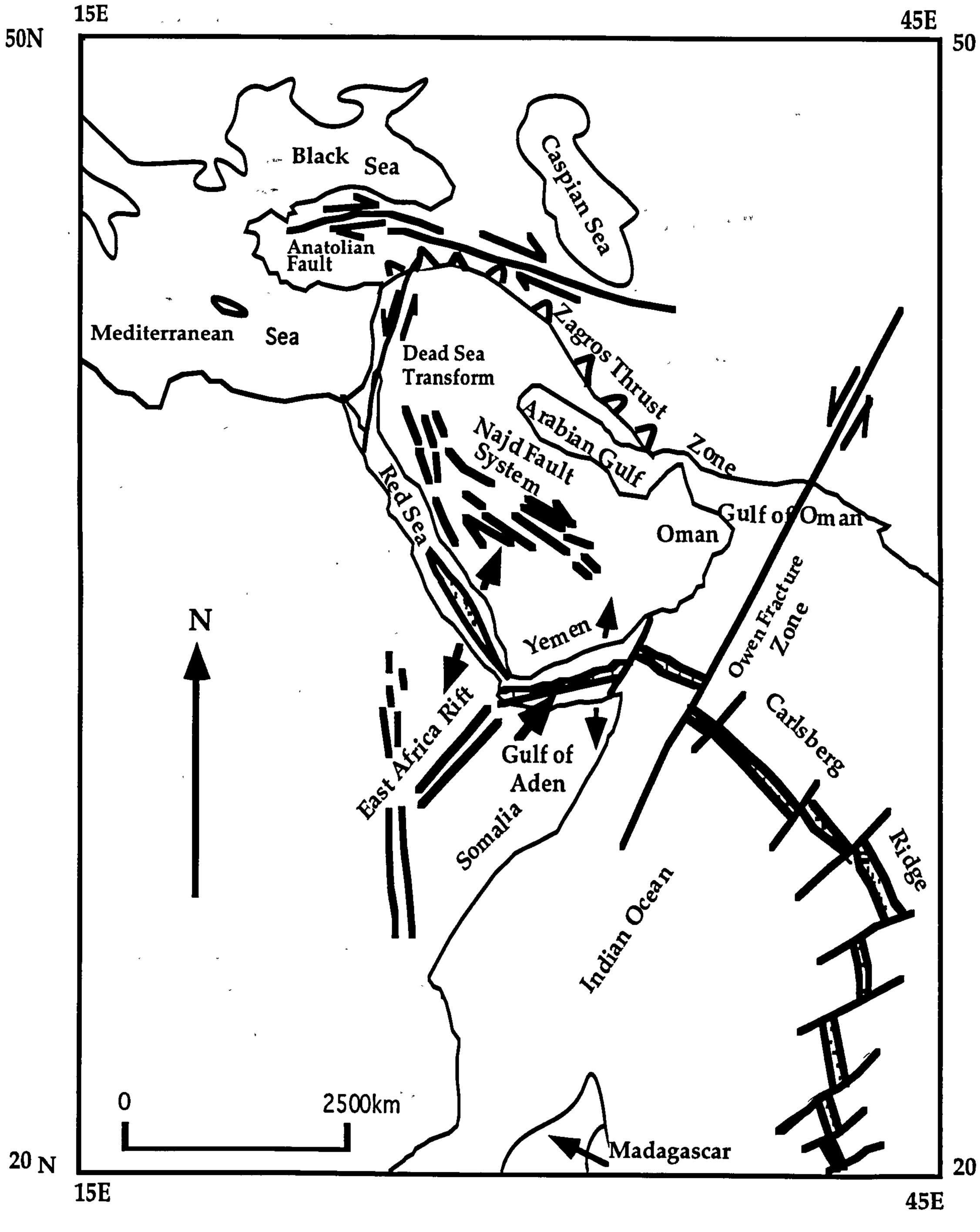

Fig. 1.2. Regional tectonic map of the Arabian plate

Fig. 1.3. Tectonic elements of the northern margin of the Gulf of Aden and the offshore fractures (after Jungwirth and As-Saruri 1990).

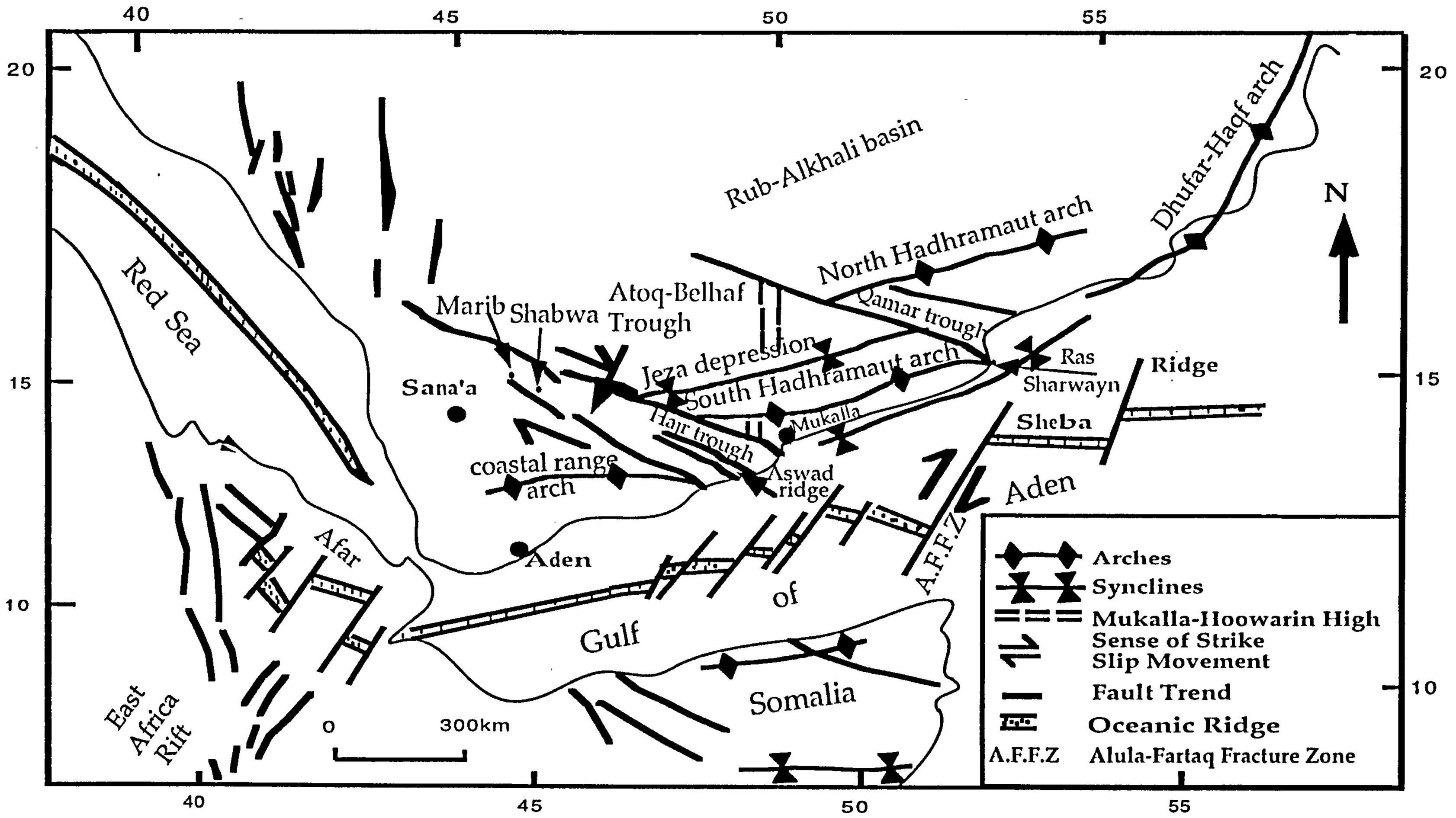

The main objective of this study is to map the southern part of the south Hadhramaut arch within part of Canadian Oxy's concession area and to determine the structural evolution of the south Hadhramaut arch and its relationship to the rifting of the Gulf of Aden. The geometries of faults and estimation of the strain will be done by using published models to show the style and the extent of deformation in the area and the faults and fractures will be analysed to provide a structural evolution of the area.

1.2 Location of the study area

The area is located in the northern margin of the Gulf of Aden, bounded by latitudes 14° N and 15°N and longitudes 48°E and 50°E (Fig. 1.4). It is bounded to the south by the narrow coastal plain consisting mainly of Oligo-Miocene, Pliocene, and younger terrace deposits and to the north by the southern part of the plateau which consists of Umm er Radhuma and Jeza Formations of Palaeocene to Middle Eocene age.

1.3 Accessibility and topographic features

The Hadhramaut as a whole is only accessible by normal vehicles along the two main asphaltic roads; the first links Mukalla city with the interior main cities in the north of plateau, and the second extends along the coastal plain. In addition there are motor tracks which link the main wadis with cities along the coast. These motor tracks are constructed in the main wadis where the nomadic herdsmen live and where water is available and are often less than 15km long. The south Hadhramaut area can be subdivided physically into three parts:

(1) **The plateau area** in the north between 1000m and 2000m elevation which is fluvially dissected.

(2) **The mountainous area** to the north is located between plateau and the

coastal plain and includes the main region of rugged relief. This part can be further divided into two divisions according to the intensity of deformation by extension faults.

(3) The coastal plain is variable in width from 10km in the western part to 3km in the eastern part of the study area and is largely composed of gravel flats and alluvium at various height. Cliffs of older sedimentary Formations such as the Jeza and Umm er Radhuma occur in this coastal plain as well as tracts of Recent volcanic flows, for example, in the Qusayar-Shakhawi area.

In the Mukalla-Al-Raidah section, the Oligo-Miocene sedimentary rocks have been planed down and are overlain by Pliocene-Recent terraces and raised beaches. These flat-lying younger deposits make most of the coast plain area very accessible.

The study area is generally of moderately rough relief. The highest elevation is in the upper part of wadi Tamah at 2200m above sea level. In wadi Hawayarah in the western part of the study area the maximum elevation reaches 1500m and in wadi Shakhawi in the east it is 1400m. Access to the high areas is very difficult due to the very steep cliffs formed by the Umm er Radhuma Formation (see sheet I, II and III, volume II).

1.4 Drainage systems

The drainage system of the area consists of dry-water courses or wadis, which flow as flash floods only in times of heavy rain. Some wadis are deeply cut, while others are wider and with less steep sides and others are broad and flat. Most wadis have a generally north-south trend and are essentially perpendicular to the trough of the Gulf of Aden and open into the sea. The wadi courses are covered by alluvial sand and river terraces.

The drainage systems of the Hadhramaut can be divided into two types: (1) coastal wadis in the south (2) the Hadhramaut-Masila and wadi Jeza systems

in the plateau in the north (Beydoun 1964). The catchment area of the coastal wadis is represented by the southern flank of the south Hadhramaut arch. The drainage is of a parallel pattern, with a general flow from north to south in the middle and east of the area and NW to SE in the west of the area. Wadi Hadhramaut-Masila and wadi Jeza which are to the north and northeast of the study area are of dendritic pattern and their catchment areas are the northern flank of the south arch and south flank of the north Hadhramaut arch as observed from the satellite images.

The main wadis in the southern part of the south Hadhramaut arch can be classified genetically into two types. The wadis in the eastern part of the study area probably formed by erosion along fractures of approximately north-south trend while the wadis in the western part are controlled by faults of NW-SE trend passing through these wadis, for example, wadi Hawayrah and wadi Al-Madi to the north of Gayl-Bawazir town (Fig. 1.5 and sheet II).

At a more detailed scale there are some subsidiary wadis throughout the whole area controlled by faults with an east-west to ESE-WNW trend parallel to the dominant extension faults, for example, wadi Al-Rakdoon (which branches westward of wadi Assad), south wadi Bidish and the upper parts of wadi Shakhawi (Fig. 1.5).

There are many small natural hot springs in the south Hadhramaut area; for example, one north east of Mukalla and close to the city and another located north of Ash-Shihr city at Tabalah village which has temperatures in excess of 50°C and where travertine is still being precipitated. This hot spring is very famous among the local people who use it for treatment. A third one in the south of wadi Bidish flows up a normal fault. These hot springs may be related to the recent volcanic activity which is associated with rifting in the latest stage of opening of the Gulf of Aden.

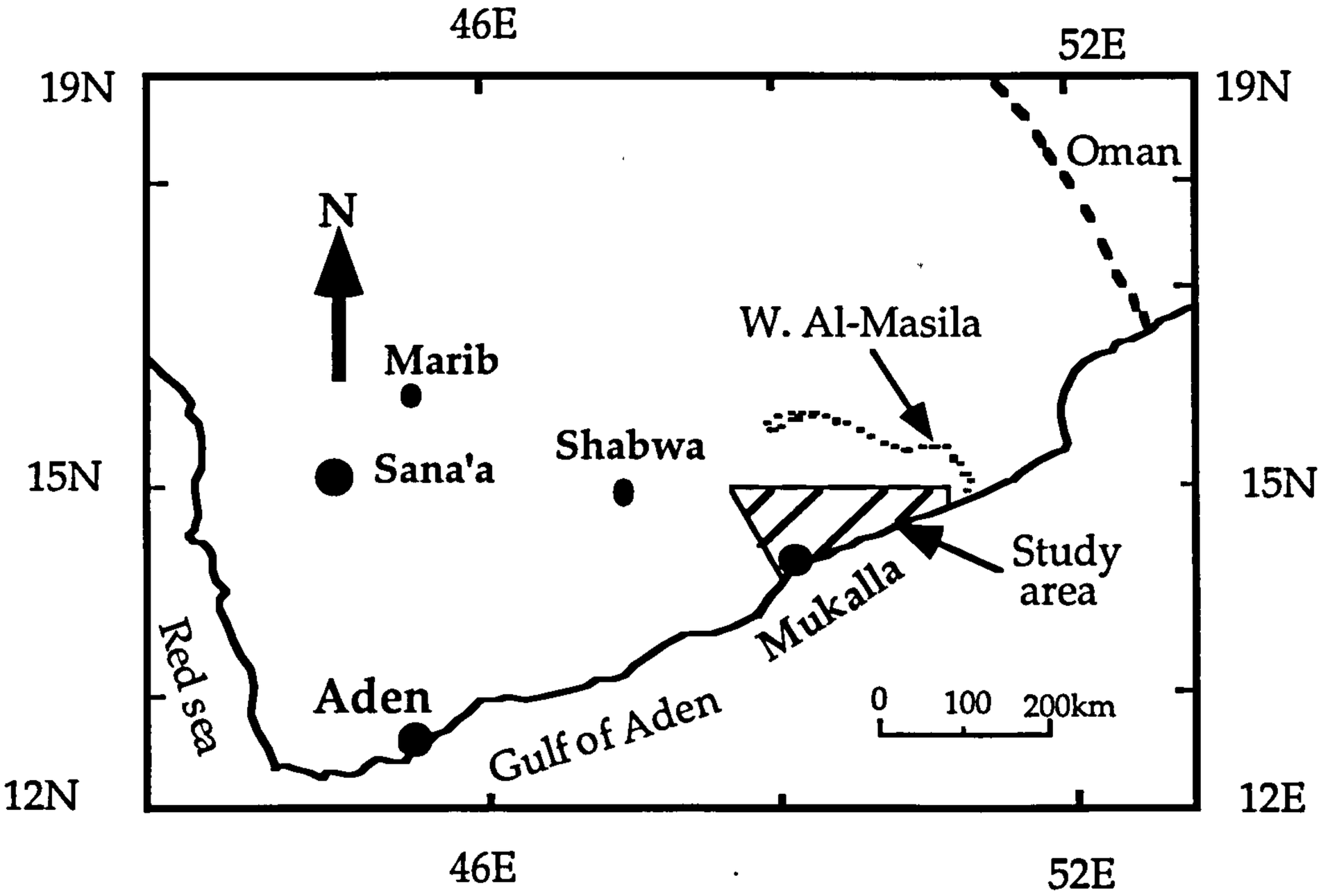

Fig. 1.4 Location map of the study area.

1.5 Climate and vegetation

The climate is affected by the winds coming from the Indian ocean region but these, because of regional physical considerations, do not bring regular rainfall to the Hadhramaut area. Clouds are frequent, but rain is sporadic and often occurs only as localised showers although, at the end of winter, the monsoon may sometimes bring heavy rain over a great part of the area. In summer again only sporadic rain falls. The maximum temperature in summer is more than 35°C and in winter about 28°C.

The vegetation is on the whole sparse, the plateau being mainly barren except in wadi beds where bunch grass, camel thorn, and acacia grow. In the main wadis and parts of the flat-lying coast plain where the water is present either from rain or by pumping, date palms, millet, coconut, corn, vegetables, and tobacco are grown.

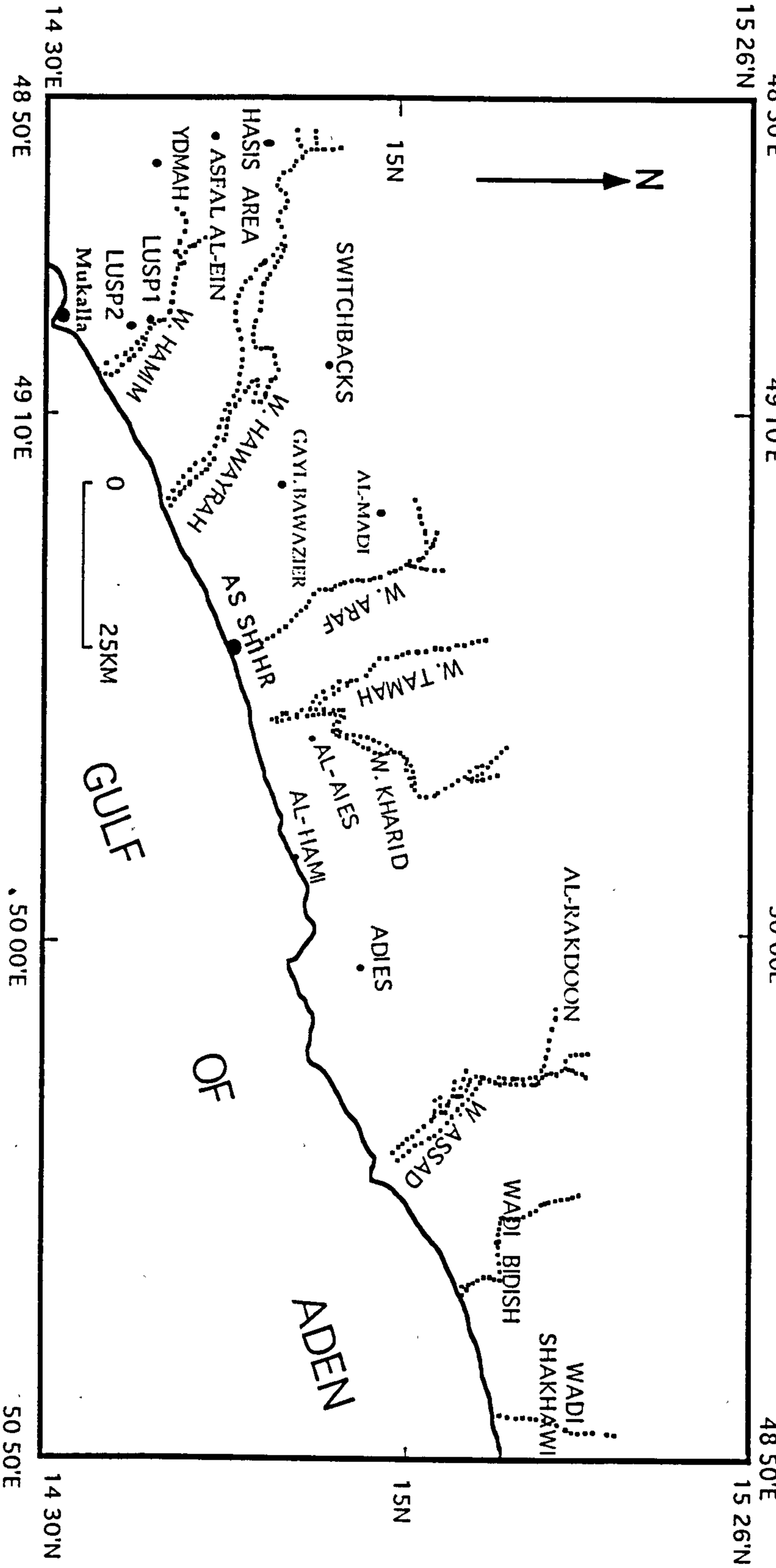

Fig. 1.5. The main wadis in South Hadhramaut area.

1.6 Previous work

Many workers have studied the northern margin of the Gulf of Aden from the early 1950's. However, the area has attracted greater attention since 1985 when the Canadian Occidental International Petroleum Company announced that there was a commercial quantity of oil in the Hadhramaut area.

For example, the Aramco company in 1952 drilled three boreholes along the axis of the north Hadhramaut arch (cited in Beydoun 1969), and these drilled through Tertiary and Cretaceous sedimentary rocks to reach depths of more than 3500m (cited in Beydoun 1969). Beydoun (1964) mapped the northern margin of the Gulf of Aden at a scale of 1:1,000,000 and during his study he classified the stratigraphic sequence into Formations. This study mainly highlighted the stratigraphic and biostratigraphic characters, and he did not study in detail the structures except giving some remarks on the major structures in the margin. He is regarded as the first worker to record the two Hadhramaut arches. Most workers concentrated on the off-shore oceanic ridge using geophysical data such as magnetic anomalies to study the opening of the Gulf of Aden and interpret the evolution of the margins of this rift.

The central portion of the Gulf of Aden east of 45° E is dominated by a NNE-SSW trend which Laughton (1966a) interprets as fracture zones. He was able to trace the oceanic ridge east to the Alula Fartaq fracture zone near 52° E. Laughton *et al.* (1970) suggest that the initial separation of Arabia and Africa occurred about 20 Ma, on the basis of early Miocene block faulting in Somalia and Arabia and that an initial period of movement was followed by a hiatus that allowed thick sediments to accumulate in the basins flanking the Sheba Ridge prior to the beginning of the present spreading episode at about 10 Ma.

Matthews *et al.* (1967) confirmed the existence of a mid ocean ridge structure in the Gulf of Aden west of the Owen Fracture Zone and gave it the

name "Sheba Ridge" and proved that it existed along the Gulf of Aden and played the main role in the separation of the Arabian plate from the African plate. Girdler and Styles (1978) interpret magnetic data obtained on closely spaced tracks in the western Gulf of Aden as indicating a much more complicated history. They suggest that the Gulf of Aden downwarp began to form about 40 Ma, and that seafloor spreading occurred in two distinct phases. The first phase lasted from 30 Ma to 15 Ma, and was followed by a 10 m.y. hiatus. The second stage of spreading began about 5 Ma, and has continued to the present.

Cochran (1981) describes the structure and history of the Gulf of Aden using marine geophysical data such as magnetic anomalies to identify the oceanic ridges along the axial trough and delineate the continental margins within the gulf. He used the offset on the Dead Sea rift to estimate that from 80 to 160 km of opening, amounting to an extension of between 65% and 200% of the initial rift valley, occurred in the Gulf of Aden and Red Sea prior to the establishment of a mid-ocean ridge. It is suggested that the development of a new ocean basin occurs in two stages. The first involves diffuse extension over an area perhaps 100 km wide in a rift valley environment without an organised spreading centre. This is followed by concentration of the extension at a single axis and the beginning of true seafloor spreading.

Isaev *et al.* (1984) have recorded the longitudinal and transverse structures dividing the marginal swell (Von Wissman 1932, 1942), into several depressions with high-grounds in between from the interpretation of air photographs of the northern margin of the Gulf of Aden. Jungwirth and As-Saruri (1990) note that the transverse faults are considered to be inherited from older fracture systems distinguished by the NW-SE trending major faults running parallel to the ancient Najd fault system, for example, Brown and Jackson (1960) in Saudia Arabia, Al-Kotbah (1992) in the Al-Bayda district,

Yemen, and they attribute the north-south striking structures such as the Mukalla-Hoowarin high to the principal old tectonic trend (Hijaz tectonic cycle) (Brown and Coleman 1972).

Haitham and Nani (1990) interpret the general major tectonic movements affecting the northern margin from their study of eight offshore exploration wells (see sheet V). Their study focused on stratigraphic characteristics and the availability of a potential source rocks in the area and they interpret the evolution of the margin in the light of formation thickness changes in these offshore wells. Paul (1990) recognises six basinal areas which are prospective for oil and all these basins show great thickness of Jurassic and Cretaceous Formations. Five of these basins are onshore along the margin from the Aden-Abyan basin in the west to the Hadhramaut-Jeza basin in the east, while the sixth basin is the off-shore Socotra basin. Redfern and Jones (1995) evaluate the stratigraphy and basin structure of the interior rift basins of the northern margin of the Gulf of Aden. They conclude that there are two main rift basins reflecting an inheritance from deep-seated Precambrian (Najd) structural lineaments, although the rifting occurred in the Jurassic and Cretaceous, as part of the Mesozoic break-up of Gondwanaland.

Recently, Ellis *et al.* (1996) describe the northern margin as having been subjected to two phases of rifting during the Jurassic and another rift phase during the Cretaceous. This conclusion is based on seismic lines and well data from the Marib, Shabwa and Hadhramaut areas.

1.7 Methods employed

During the present study air photographs, Landsat images and field work were integrated together to map the south Hadhramaut area. The use of remotely sensed images alone cannot provide the accurate maps without work on the ground. The resulting geological map comprises five sheets at a scale of

1: 50,000. These sheets cover the whole area from the west of Mukalla to wadi Kobbeer east of wadi Bidish, with the exception of wadi Shakhawi at the eastern edge of the area which was mapped at a scale 1:100,000.

1.7.1 Landsat images

The most important advance in remote sensing during the last few decades has been the development of continuously orbiting satellites with various remote-sensing systems. Despite the non-geological aspirations of their sponsors, these satellites have produced an almost complete coverage of the continental surface, and have accelerated the prospect of beginning to match the greatest challenge facing Earth Science, that of completing the geological map of the world. Despite 150 years of conventional effort by a growing community of geologists, only about 25 percent of the Earth's land surface is covered by geological maps at a scale that is useful for resource exploration. However, the new ideas about geological evolution means that many geological maps will need to be reassessed in the light of satellite images.

These satellite images have reduced the need to use air photographs. Landsat images at scales of 1:100,000 and 1:50,000 were used as base maps during this study and detailed maps were produced from the Landsat images of scale 1:50,000 for which contoured topographic maps are available as overlays.

1.7.2 Air photographs

Air photographs were used for some areas to supplement the detail available on the satellite images especially for areas which are cloud covered and also when a stereo view is necessary to show throw on faults.

1.7.3 Field work

More than eight months were spent in the field mapping the area and collecting stratigraphic and structural data. On one occasion a helicopter was used to complete the maps. The geometry of curved bedding surfaces in the hanging wall of faults was measured in detail to allow the shape of the fault at depth to be computed. Traverses perpendicular to strike were taken and the attitude of bedding was measured using a 0.4 m disk attached to a Clar compass. Reading were taken every 20 m and altimeter readings were taken at the beginning and end of traverses to control better the geometry of the bedding surface.

1.7.4 Laboratory

In the laboratory the geological maps of the whole area were completed and more detailed maps were prepared of some localities of especial interest which show the different structure styles in the area.

Six cross sections were drawn parallel to the main wadis. The structural detail was taken from the field surveys and the stratigraphic thickness of Formations was taken mainly from published reports and with extra detail from this study. The laboratory work concentrated on analysing the geometry of faulting for comparison with the models proposed for the geometry of faults with depth. A map at a small scale was produced to show the structure style of the faults and their relationships throughout the whole area. The vertical displacement of mappable faults and their lengths were calculated using these maps together with the topographic maps and plotted on the growth fault model to show the relationship between the vertical displacement and the length of faults. The analysis of orientation data was aided by computer programmes FABRIC (Starkey 1977) and STEREONET (Allmendinger 1993).

1.8 Format of the thesis

The thesis consists of two volumes; the first volume comprises the text subdivided into nine chapters, the second volume comprises five maps and five cross sections. Chapter 1 provides an overview of the nature of the area, previous work, the aim of the research and the methods employed in this work. Chapter 2 is concerned with the field description of the stratigraphic Formations and their relationships with the structures controlling their thickness. Chapter 3 reviews the literature of extension faults, the terminology and models for extensional regimes. Chapter 4 deals with the geometry of faults with depth by applying the data to the previously models. Chapter 5 contains the interpretation of the six balanced cross-sections. Chapter 6 describes the major and minor faults and fractures together with the analysis of the field data collected from the area. Discussion of the present results from chapter 2 to chapter 6 with regard to similar studies in different areas and also with previous study in the surrounding area is presented in chapter 7. Chapter 8 includes regional implications of the northern margin of the Gulf of Aden in the light of the final results of the present research and the surrounding areas and the final chapter, chapter 9, summarises all the results obtained and presents the conclusions of this research.

CHAPTER 2

STRATIGRAPHIC SETTING

2.1 Introduction

The south Hadhramaut area is the southern part of the northern margin of the Gulf of Aden. The most characteristic feature of the south Hadhramaut area is the pattern of arcuate faults striking WSW-ENE more or less parallel to the axis of the Gulf of Aden. The structural and stratigraphic character of the south Hadhramaut arch is highly variable, indicating contrasting basin forming mechanisms and subsequent subsidence histories during the evolution of this northern margin. The southern part of this margin is the southern flank of the south Hadhramaut arch and it may be divided topographically into three parts, namely, the plateau, the faulted rift shoulder and the coastal plain. The plateau ranges in elevation from 1000m up to 2,000m above sea level and is dissected by extension faults. The dip of bedding is very gentle on the top of the plateau and increases southward to become more steep in the faulted rift shoulder towards the coast. This highly faulted rift shoulder exhibits steep scarps of different heights depending on the amount of fault displacement. The majority of these scarps are formed of the Umm er Radhuma Formation. The plateau and the

faulted rift shoulder consist mainly of Cretaceous and Tertiary sedimentary rocks older than the rift while the coastal plain consists mainly of Oligo-Miocene syn-rift rocks of the Shihr Group and later Pliocene sedimentary rocks. Throughout the coastal plain inliers of the older Umm er Radhuma and Jeza Formations occur as hills, for example, at Jabal Dabdab, north of Ad-Deis town (see sheet V and VI, volume II).

Within the study area the rocks range in age from Precambrian to Recent although there is a major gap in the Phanerozoic stratigraphy where the whole middle Cambrian to Jurassic section is missing in the western part of the area (see sheet I). The study area is completely covered by satellite images and partially covered by air photos which were used as base maps in the field mapping programme. The area was mapped at a scale of 1:50,000 with certain areas covered at 1:100,000 scale. The eight months field work resulted in five map sheets covering the whole area from west of Mukalla city to wadi Khobeer in the east (see sheets, I, II, III, VI, V, volume II) at a scale of 1:50,000. Wadi Shakhawi was mapped separately at a scale of 1:100,000 because this eastern area was not included in the 1:50,000 scale satellite images (Fig. 2.1). In addition, many detailed maps were produced to show the relationships of different structure styles. For example, the Switchbacks area was mapped at a scale of 1:23,000 because it best represents the typical structures in the area (see sheet I).

The metamorphic and igneous basement rocks which are predominantly Proterozoic but may range up to Early Cambrian are overlain by a sedimentary cover sequence ranging in age from Cretaceous to Recent which contains five major unconformities. The major unconformity occurs between the basement rocks and the Cretaceous Qishn Formation in the Harshiyat-Ydmah area. In this locality a later unconformity is recorded by the absence of the upper part of the Harshiyat Formation (Sufla member) and the Mukalla Formation where the Umm er Radhuma Formation rests directly on the upper clastic Harshiyat.

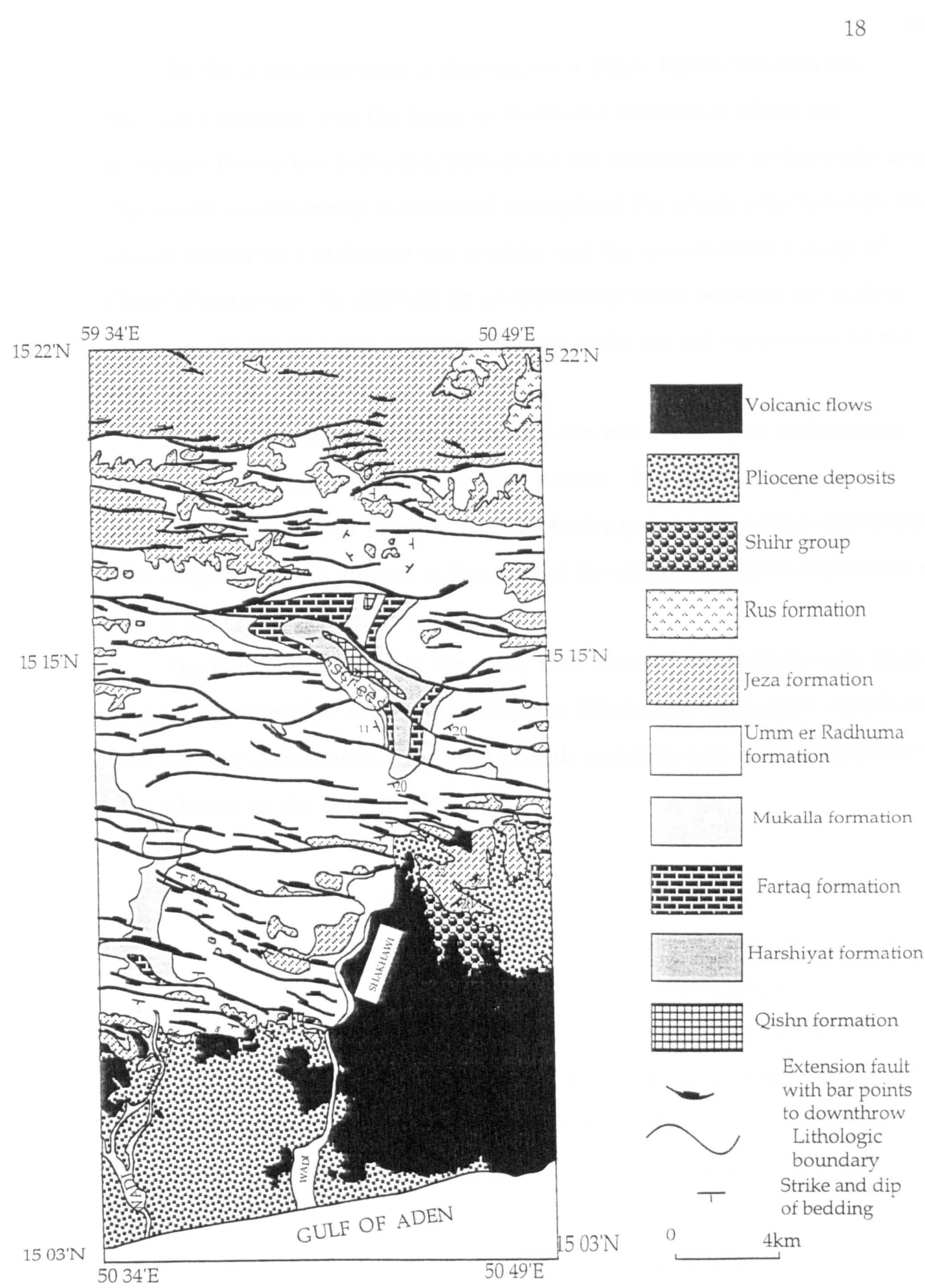

Fig. 2.1. Structural geological map of wadi Shakhawi.

The third unconformity is observed as a minor hiatus between the Mukalla Formation and the Umm er Radhuma Formation where the Sharwayn Formation is missing throughout the western part of the study area. The fourth unconformity is observed throughout the whole area between the pre-rift Formations of Eocene age or older and the syn-rift Shihr Group of Oligo-Miocene age. In addition an unconformity exists between the middle Miocene and the Pliocene as upper Miocene rocks are not represented in the area (Agip 1981, Haitham and Nani 1990).

The northern margin of the Gulf of Aden has a variety of sedimentary strata overlying a peneplaned basement surface. The sedimentary cover of south Hadhramaut area as recorded from both exposures and from subsurface data ranges from the Jurassic to Recent, but the oldest Formation exposed in the area is the Qishn Formation (see table 2.1).

The field observations in the study area revealed the characteristic features and the relationships between the different lithological units, their distribution and the later deformation. The stratigraphic sequence now will be described in detail based on the field observations.

Table 2. 1. Stratigraphic framework of the Hadhramaut area.

Quaternary	Recent	Alluvium and wadi deposits
	Pliocene or younger	Volcanic lava
	Pliocene	Pliocene deposits
Tertiary	Oligo-Miocene	Shihr Group
	Middle Eocene	Habshiya Formation
	Middle Eocene	Rus Formation
	Lower Eocene	Jeza Formation
	Palaeocene	Umm er Radhuma Formation
Cretaceous	Maastrichtian	Sharwayn Formation
	Senonian	Mukalla Formation
	Albian-Turonian	Fartaq Formation
	Albian-Cenomanian	Harshiyat Formation
	Barremian-Aptian	Qishn Formation
Jurassic	Upper Jurassic	Amran Group
	Lower-Middle Jurassic	Kohlan Formation
Precambrian	Proterozioc-Early Cambrian	Basement

2.2 The basement blocks

The basement rocks of Precambrian age are exposed in the western part of the study area in the footwall of a large arcuate north-dipping fault which has brought the whole sedimentary sequence down against the basement blocks (see sheet I). The basement rocks between Jabal Ydmah and wadi Hamim represent part of the Mukalla high. They are of metadolerite to metagranodiorite in composition and are dissected by several trends of younger Precambrian dykes, mainly basaltic in composition.

The basement rocks types are not of great value to this study but their relationship to the sedimentary cover and, in particular, structures which may

have been inherited from the basement rocks are of value since they may have controlled the formation of the younger structures. These basement rocks are not well foliated, but are highly fractured with a number of different trends (Fig. 2.3).

The resistant nature of these basement rocks means that they tend to form hilly areas. The Mukalla-Hoowarin and Fartaq highs may be related to the oldest Hijaz tectonic movement of north-south trend (Beydoun *et al.* 1993). The late Proterozoic to Cambrian Najd fault systems of NW-SE trend, for example, in the Al-Bayda district (Al Kotbah 1992), played a very important part in the formation of the large basins in the Hadhramaut and areas to the west and east of the study area, such as the Jeza basin, Shabwa-Belhaf basin and Al- Juf-Marib basin (Fig. 7.1).

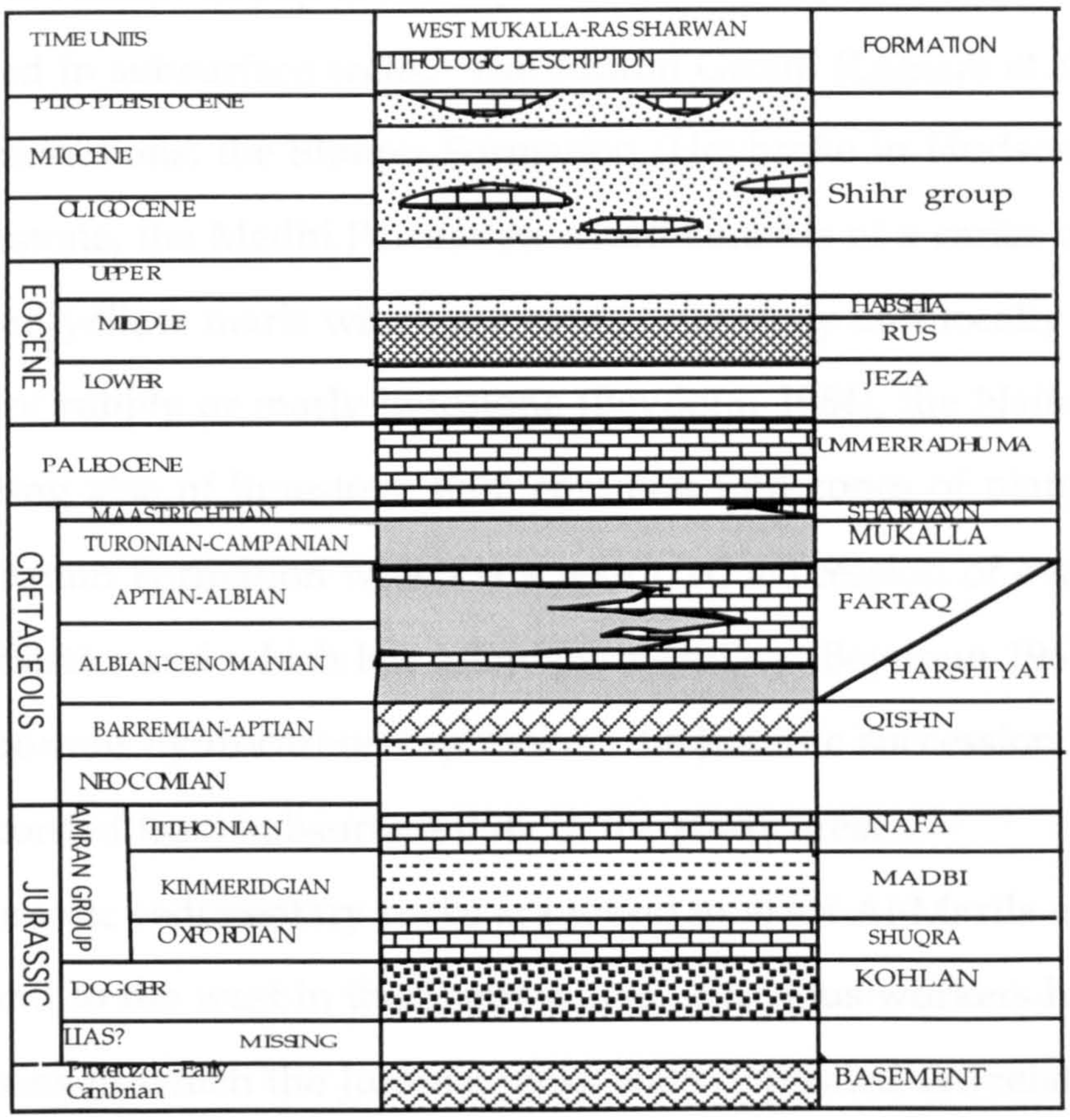

Fig. 2.2. Stratigraphic column of the Hadhramaut area from subsurface wells (after Agip 1981 and Haitham and Nani 1990).

2.3 Jurassic

2.3.1 Kohlan Formation: (Lower to middle ? Jurassic)

The Kohlan Formation constitutes the basal unit of the Jurassic succession in Yemen. The name Kohlan was first used by Lamare (1930) for the succession exposed in the Kohlan area northwest of Sana'a. It consist of marls with sandstone and conglomerate layers containing basement fragments followed by sandstone and interbedded sandstones and sandy marls with plant impressions (Lamare 1930, Beydoun 1964). In the study area the Kohlan Formation is not exposed but it is recognised in the subsurface off-shore wells (see sheet V).

2.3.2 Amran Group (Upper Jurassic)

The Amran Group is not exposed at the surface in the study area, but is recorded in subsurface wells. The Amran Group (Lamare *et al.* 1930) consists of four Formations; the Shuqra Formation (Heybroke in Hudson 1954) consisting of limestone, the Madbi Formation which consists of a series of grey to dark grey and yellow marls which are commonly shaly and locally gypsiferous with layers of rubbly or marly limestone (Beydoun 1964), the Naifa Formation, consisting also of limestone with common thin zones of platy dolomite, and the Sabatain Formation which is a restricted succession of evaporites with some clastics and which has a low permeability (Beydoun 1964) and represents an important hydrocarbon cap rock in the Jurassic succession in Marib area but not recorded from subsurface data in the study area.

Jurassic sedimentary rocks are found in wadi Al-Masila east of the study area, and to the west in the Shabwa area. Previous workers have suggested that the basins in which the Jurassic rocks were deposited are related to the rejuvenation of the Najd fault system and represent rifts throughout Yemen (Beydoun 1964, Isaevs *et al.* 1984, Jungwirth and As-Saruri 1990, Diggens *et al.* 1988, Al-Thour 1992, Redfern and Jones 1995, Ellis *et al.* 1996). Within the Jurassic sedimentary rocks are the main source and reservoir rocks of the oil which is produced from the Marib and Shabwa areas whereas in Canadian Oxy's Al-Masila block (Canadian Occidental Company) the reservoir is the Qishn Formation (see below).

2.4 Qishn Formation (Barremian-Aptian)

The type section of the Qishn Formation is at Ras Sharwayn but it is also well exposed in wadi Al-Masila, with a maximum thickness of 411m (Beydoun 1964, Beydoun *et al.* 1993). The Qishn Formation has been recognised in the study area at three separate localities (see sheets I and V). In the western part of the

area, the Qishn Formation, representing the Barremian transgression, overlies unconformably a peneplaned basement surface (Fig. 2.4), and comprises clastic sedimentary rocks of conglomerate at the base which gradually change upwards into sandstones and finally to dolomite and highly fossiliferous limestone which is sometimes recrystallized to dolomite such as in the Ydmah area (Fig. 2.5). The base of the Qishn Formation consists of an 8m to 10m thickness of conglomerate containing clasts of basement rocks and many fossils (Fig. 2.6), especially in the Ydmah area (see sheet I). Here the Qishn Formation does not exceed 40m in thickness. To the east it is not observed for 170km until it is exposed again in the eastern part of the study area in wadi Bidish, and in a horst block in wadi Al-Andeep to the east of wadi Bidish (Fig. 2.7). Here the thickness is 70m (Smewing 1993 personal communication), and it consists of grey, highly fossiliferous limestone with bivalves and gastropods and some nodular chert. The third locality at which the Qishn Formation is exposed is in wadi Shakhawi in the easternmost part of the area where it consists of limestone alternating with marly limestone, shale and sometimes shelly marly limestone, and reaches up to 60m thickness (Fig. 2.8). However, from the literature the Qishn Formation consists of two parts. The lower part, which is generally sandy, is termed the Qishn clastics and these sandstones are the main reservoir interval in the numerous oil fields of the Masila area (Mills 1992, Redfern and Jones 1995, Ellis *et al.* 1996). The upper part of Qishn Formation is typically a carbonate facies, comprising shallow-water argillaceous shelly limestones and shales, the Qishn carbonates (Mills 1992). The Qishn carbonate sequences are important as they provide the major regional seal for most of the hydrocarbon accumulation in the area (Mills 1992).

2.5 The Harshiyat Formation (Albian-Cenomanian)

The Harshiyat Formation consists mainly of clastic rocks and is distributed throughout the whole area. It conformably overlies the Qishn Formation and consists of a sequence of sandstones with shales forming distinct layers at various levels. Plant remains, now silicified wood, and small rootlets occur throughout the Formation (Fig. 2.9). The Harshiyat Formation contains two well-defined limestone layers which are called the Rays and Sufla members (Beydoun 1964). The two limestone members are exposed in the east end of wadi Hawayrah and they decrease in thickness westward. The Rays member which occurs in the lower part of the Formation, varies from 30m to less than 4m over a strike length of about 10km in the west of wadi Hawayrah (Fig. 2.10). The Sufla member occurs at the upper contact of the Formation and marks the boundary between this Formation and the overlying Mukalla Formation. The Sufla member is not present in the Ydmah area, but it is exposed in wadi Hawayrah about 7km to the north. Here it varies in thickness from 27m in the east and thins gradually along the wadi to the west until it becomes 2m in thickness. These two members are often partially recrystallized to dolomite with a saccharoidal texture obliterating the fossils.

Both members are grey to brown in colour, bedded to semi-massive, coarsely recrystallized dolomitic limestone, sometimes ferruginous, with a reddish brown weathered surface. They are equivalent to the Dhasohis and Maqrat members, respectively, of the Fartaq Formation in the eastern part of the study area. In wadi Kharid the Sufla member contains many fossils of the Rudist bivalve (Fig. 2.11). The Harshiyat Formation is well exposed in the plateau in the Haqab area in the footwall of a major south dipping fault (see sheet III). The clastic Harshiyat Formation has a wide range of colour from red brown to yellow and sometimes the shales are green in colour. The reddish clastic rocks have iron concretions and the whole unit is stained by iron oxides

Fig. 2.3. High intensity of fractures with variable trends in the basement, the conglomerate above is of recent age washed out during flood time,Ydmah area.

Fig. 2.4. Two unconformities: lower one has Cretaceous Qishn Formation (Q) resting on basement (B) and the upper one has Umm er Radhuma Formation resting on the upper Harshiyat Formation (Hu), Ydmah area.

Fig. 2.5. The Qishn Formation is completely recrystallised to dolomite in the Ydmah area.

Fig. 2.6. The conglomerate in the lower part of the Qishn Formation highly fossiliferous.

Fig. 2.7. The Qishn Formation is exposed in a horst at 200m above sea level in wadi Al-Andeep to the east of wadi Bidish.

Fig. 2.8. The Qishn Formation becomes shaly and marly with alternating thin layers of limestone in wadi Shakhawi.

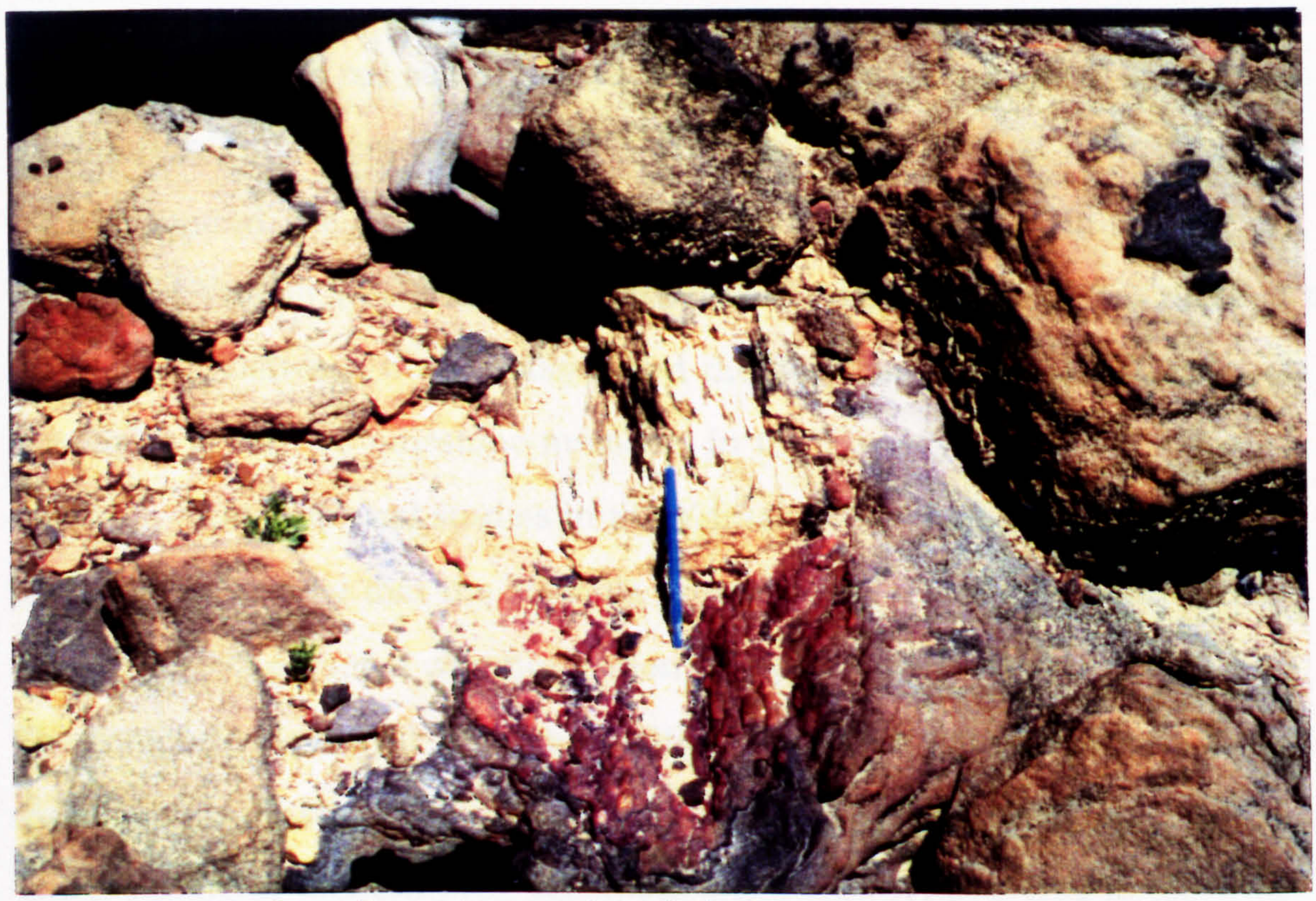

Fig. 2.9. The Harshiyat Formation contains silicified wood in wadi Hawayrah.

Fig. 2.10. Photograph shows the complete section from Umm er Radhuma Formation (UER) through the Mukalla Formation (M) to upper Harshiyat Formation (H_U) with the two limestone members (Rays and Sufla, Ra and S) and the Lower Harshiyat part (H_L) in the footwall of wadi Hawayrah fault in wadi Hawayrah. The limestone members have become very thin in this locality.

to give a very dark red colour. In addition, these clastic rocks have wide variation in grain sizes from granule to silt.

In general, the Harshiyat Formation is well exposed and in the western part in the Ydmah area it attains a thickness in excess of 300m. It is difficult to differentiate between the Harshiyat and the younger Mukalla Formation, especially if the two limestone members in the Harshiyat Formation are missing. Stratigraphical studies in the Ydmah area which represents the Mukalla high, show that the Mukalla Formation is absent (Beydoun 1964, Smewing 1993 personal communication, the present study) (Fig. 2.4).

The complete Harshiyat Formation with the two limestone members is well exposed in wadi Hawayrah (Fig. 2.10) where it is at least 600m in thickness. The exposure of this complete section in wadi Hawayrah is due to footwall

uplift on a major north dipping fault which passes along the main wadi and brings the Umm er Radhuma Formation down against the lower Harshiyat Formation giving a downthrow in excess of 1000m.

The Harshiyat Formation shows lateral changes in sedimentary facies from continental in the west to marine in the east and is the lateral equivalent of the Fartaq Formation in the eastern part of the study area. The Harshiyat Formation is exposed in all main wadis except wadi Araf where only the overlying Mukalla and the Umm er Radhuma Formations are exposed (see sheets I, II, III, VI and V, volume II).

2.6 Fartaq Formation (Albian-Turonian)

The Fartaq Formation consists mainly of limestone and marl with some sandstone beds in the middle of the sequence. The Fartaq Formation is a lateral equivalent of part of the Harshiyat Formation, namely the Sufla member, upper clastic Harshiyat and the Rays member as they gradually change from being dominantly clastic in the west (wadi Hawayrah) to carbonate in the east (wadi Shakhawi) (Fig. 2.2). These three members of the Harshiyat Formation are equivalent to three members (Dhasohis member, Tihayr member and Maqrat member) of the Fartaq Formation (Beydoun 1964). The Dhasohis member occurs in the lower part and consists of marly limestone, although locally it is entirely of rubbly massive limestone and sometime completely recrystallised to dolomite as in wadi Assad (Fig. 2.13). It is equivalent to the Rays member in the western part of the area.

The Tihayr member, which occurs in the middle part of the Formation, is about 100m thick in wadi Al-Rakdoon. This member consists mainly of green and purple shales and an interval of coloured sandstones ranging in colour from pale yellow through red to dark red; sometimes layers of marl and shale have a dark grey colour. An age of Cenomanian-Turonian is recorded by

Wetzel and Morton (cited in Beydoun 1964). It is equivalent to the upper part of the clastic Harshiyat Formation.

The Maqrat member, which represents the top of the Fartaq Formation, and consists of limestone and dolomitic limestone up to 40m in thickness in wadi Assad. In wadi Shakhawi the Fartaq Formation changes to a shaly and marly limestone and the middle part has become entirely a marine facies of shales, marls and shelly limestones.

2.7 The Mukalla Formation (Senonian)

The Mukalla Formation is distributed throughout the whole area. It is exposed mainly in the major wadis where erosion has deeply dissected the fault blocks (see sheets I, II, III, VI, V). It is missing on the Mukalla basement high especially in the Ydmah area, but 7km to the north in wadi Hawayrah, the Mukalla Formation is exposed for a thickness in excess of 450m. The Mukalla Formation conformably overlies the Maqrat member in eastern area and the Sufla member in the western part. It consists of sandstone, with variation of colour ranging from dark red, through red and yellow to grey, with intercalated siltstone and shale. It is barren of fossils and it is difficult to differentiate between the Harshiyat and Mukalla Formations because of the similarity in rock type unless the two limestone members are present in the Harshiyat Formation.

The thickness of the Mukalla Formation in some localities appears to be abnormal; this is due to its repetition by faults which are difficult to detect owing to the similarity of rock type throughout the Formation and the absent of marker beds. For example, in wadi Assad the thickness reaches more than 500m where bedding dips to the north toward a south dipping fault (Fig. 2.12). This fault, which caused the repetition, can be traced to the east side of the wadi where it affects the Umm er Radhuma and Jeza Formations (Fig. 2.12). The

Mukalla Formation includes a rare very thin layer of partially dolomitized limestone known as the Lusp member (Beydoun 1964). The upper part of Harshiyat Formation (Sufla member) and Mukalla Formation are missing in the footwall of the wadi Hamim fault in the Harshiyat-Ydmah area where a local unconformity occurs. However, about 7km to the north, the large escarpment of the wadi Hawayrah fault results in good exposures of the Umm er Radhuma down to the lower Harshiyat Formation. Here the Mukalla Formation is about 500m thick and the Harshiyat Formation contains both its distinct limestone members and it, too, is more than 500m in thickness (Fig. 2.10).

Fig. 2.11. The Sufla member contains fossil Rudists, wadi Kharid.

Fig. 2.12. The Fartaq formation is completely exposed in the footwall of wadi Al-Rakdoon fault in wadi Assad. To the left the Mukalla formation is thicker due to the presence of a south dipping fault which can be traced by faulted down of the Umm er Radhuma and Jeza formation to the right.

2.8 The Umm er Radhuma Formation (Palaeocene)

The Umm er Radhuma Formation represents the Palaeocene transgression and is characterised by very homogeneous sedimentation with only minor changes in facies and thickness. It is of wide distribution over all the margin where it extends to the east into Oman and to the north into Saudi Arabia and Kuwait where the name came from the Umm er Radhuma wells close to the Kuwait border (Henry *et al.* 1935 cited in Agip 1981 unpublished report). To the west of the study area this Formation ranges in thickness between 155m and 250m (Schuppl and Wienholz 1990). Within the study area its thickness has been measured at different localities; for example, at wadi Hawayrah the thickness is 235m, in wadi Assad 180m, in wadi Bidish 240m and in wadi Shakhawi it is thinner at about 100m (Fig. 2.14).

The Umm er Radhuma Formation consists mainly of limestone and, although it is well bedded at the top, it is generally of nodular and semi- bedded limestone (Fig. 2.15). It characteristically forms steep white cliffs which are prominent throughout the whole area and make many areas inaccessible on foot. These scarps are mainly structurally controlled (Fig. 2.16). The contact between the Umm er Radhuma Formation and the underlying Mukalla Formation is unconformable with a transition zone consisting of a 2m to 3m thickness of reddish marly limestone with some fossils and the Sharwayn Formation is missing throughout the area.

In the middle part there is a layer of massive and partially dolomitized limestone of a grey brown colour about 30m to 35m in thickness. This unit is a good marker throughout the area which aids in the determination of the displacement on faults (Fig. 2.17). In the main wadis, the Umm er Radhuma Formation has been eroded to form screes and conglomerate of Recent age (Fig. 2.18). The Umm er Radhuma Formation forms the plateau surface to the north, the top surfaces of the fault blocks and also occurs as inliers on the

coastal plain such as Jabal Dabdab to the east of Ash Shihr city (see sheets I, II, III, VI, V).

2.9 The Jeza Formation (Lower Eocene)

The Jeza Formation conformably overlies the Umm er Radhuma Formation (Fig. 2.19) and it is distributed across the whole area especially toward the plateau in the north although it also occurs sporadically as isolated outcrops along the coastal area (Fig. 2.20). The Jeza Formation comprises alternations of papery, yellow and pink shales with some marls and layers of chalky to crystalline limestone, very commonly silicified, with layers of cherts and occasionally layers of gypsum (Fig. 2.21). The Jeza Formation is very fossiliferous especially with echinoid stems. The most characteristic feature is its occurrence as flat-topped mesa-shaped hills above the extensive outcrops of the Umm er Radhuma Formation. It is easy to distinguish it from the Umm er Radhuma Formation in the field from its geomorphological shape, its rock types and its fossils. Its contact with the overlying Rus Formation is not often seen due to Recent erosion; however, an estimate of its thickness is 150m.

2.10 The Rus Formation (middle Eocene)

The Rus Formation is conformable above the Jeza Formation and consists of bedded to massive gypsum with limestone. The Rus Formation has been eroded from most of the area especially in the southern flank of south Hadhramaut arch, and is now found as sporadic lenses of irregular shape in fault-bounded graben (Fig. 2.22 and 23). It occurs extensively in the plateau north of wadi Shakhawi where its presence can be determined from its characteristic appearance on the satellite images (Fig. 7.6 and see sheet V). The occurrence of the Rus Formation in the flat-lying area parallel to the coast line is rare and here it may be confused with the evaporitic parts of the Shihr

Group.

Fig. 2.13. The Dhasohis member recrystallised to dolomite in wadi Assad.

Fig. 2.14. The Umm er Radhuma Formation has became thinner in wadi Shakhawi.

Fig. 2.15. Typical cliff in the semi-bedded Umm er Radhuma Formation in the Hadhramaut area.

Fig. 2.16. The Umm er Radhuma Formation forms very steep fault scarps which make many places inaccessible.

Fig. 2.17. The marker unit in the Umm er Radhuma Formation which is used as a reference to calculate the vertical displacement. This unit consists of dolomitic limestone with very distinct brown colour within the mainly white colour of the Formation.

Fig. 2.18. The Umm er Radhuma Formation is highly eroded along the main wadis and sometimes leaves screes in many places.

Fig. 2.19. The Jeza Formation conformably overlies the Umm er Radhuma Formation.

Fig. 2.20. The Jeza Formation is highly eroded and sometimes stands as isolated exposures in the flat areas, wadi Hawayrah.

Fig. 2.21. The Jeza Formation sometimes consists of alternating layers of limestones and gypsum. The limestones are highly fractured while the gypsum is stretched and become thin due to its ductility.

Fig. 2.22. The Rus Formation is rarely found in the southern part of the area, but sometimes is preserved in grabens such as the area north of Gayl Bawazir.

2.11 The Habshiya Formation (middle Eocene)

It is difficult to prove the occurrence of the Habshiya Formation which is not exposed in the main plateau of the study area. Small outcrops NE of Ad-Dies town (sheet VI) have been ascribed to this Formation based on their similarity with published descriptions. According to Beydoun (1964), it is conformable on the Rus Formation and consists of grey-green, yellow and pink papery shale and yellow chalky and gypsiferous marls alternating with limestone and chalky limestones (Fig. 2.24). However, the confirmation of this Formation needs more detailed study of fossils to determine its age.

2.12 The Shihr Group (Oligo-Miocene)

The Shihr Group consists of a heterogeneous assemblage of sedimentary rocks including conglomerate, marl, gypsum, limestone, shale and occasionally dolomitic limestone occurring singly or together. The Shihr Group forms most of the flat-lying deposits parallel to the coastline, from Mukalla city eastward to wadi Shakhawi which is restricted to small area. This synrift sediments are classfied into three Formations , the Ghaydah Formation, Taqa Formation and Hami Formation (Haitham and Nani 1990). It rests unconformably on the other Formations and it may be in contact with different Formations, such as the Umm er Radhuma, Jeza, Rus, Habshiya and sometimes even on basement, for example, around Mukalla city (see sheet I).

The Shihr Group represents the syn-rift deposits of the Gulf of Aden and sometimes shows slumping deformation and folding due to slumping particularly in the evaporitic rocks (Fig. 2.25). The Shihr Group is in general tilted gently toward the rift axis; occasionally, it has a very steep dip which is ascribed to proximity to a fault which is obscured by Recent deposits (Fig. 2.26). These rocks show some small asymmetrical folds of both synclines and anticlines which are most likely related to the rotation of fault blocks during

rifting. Most of these folds have subhorizontal to horizontal axes which are parallel to the trend of the Gulf of Aden.

2.13 Pliocene-Recent sediments

The Pliocene sedimentary rocks are mainly exposed in the coast plain. They consist of heterogeneous deposits derived from Cretaceous sedimentary rocks and younger, and occasionally from basement rocks in the western part of the area. The Pliocene sediments have been adequately described by many authors, for example, Little (1925), Von Wissman (1932), Caton-Thompson (1938), Caton-Thompson and Gardner (1939), Wetzel and Morton (1948-1950 cited in Beydoun 1964), Beydoun (1964). Wetzel and Morton (1948-1950 cited in Beydoun 1964) collected fossils from the lower terraces at various localities and noted that these rocks are post Miocene in age and most likely belong to the Pliocene and extending to the Pleistocene. The Pliocene deposits are restricted to the coast plain from the Mukalla area eastward to Qusayr, south of wadi Assad (see sheet I, II, III, IV and V). They overlie the Shihr Group with an angular unconformity showing that the Shihr Group was subjected to erosion and tilting before the Pliocene (Fig. 2.27). These deposits show variations in rock type which indicate the instability of the margin during the deposition of these rocks and which reflect a change in the environment from continental to marine. The Pliocene deposits show that the rifting was still active during the Pliocene and these sedimentary rocks are affected by younger east-west fractures which are parallel to the Gulf of Aden trend and the NE trend of the Alula Fartaq direction which implies that deformation continued after their consolidation.

2.14 River deposits

Many river terraces of Recent age can be seen above the present day drainage levels of the major wadis. They overlie the older rocks from the

Fig. 2.23. The characteristic feature of the Rus Formation is the irregularity shape of its outcrop without any bedding in most places, south wadi Kharid area.

Fig. 2.24. The Habshiya Formation brought against the Rus Formation by north dipping fault, north of Ad-Deis Town.

Fig. 2.25. The Shihr Group shows high deformation and slumping which may be related to early deformation contemporaneous with deposition, east of Tabalah village.

Fig. 2.26. The Shihr Group is in general of gentle dip, but sometimes it has a steeper dip which indicates proximity to a fault, south wadi Kharid.

basement rocks in the western part of the study area and all younger Formations throughout the area. They consist of conglomerates with sand layers, and sometimes are semi-bedded.

2.15 Alluvium deposits

These unconsolidated deposits are the products present day erosion during flash floods. They occurred along all the wadis and consists of all grain sizes from large boulders down to clays.

2.16 Aeolian deposits

Wind-blown sand occurs extensively throughout the coastal plain especially from Fawah eastward to south of wadi Shakhawi.

2.17 Young lavas

The young eruptive rocks have been described by Von Wissman (1932, 1942), Lamare *et al.* 1930, Lamare 1936 and Beydoun (1964). They form part of the Pliocene to Pleistocene Aden volcanic series (Beydoun 1964). These rocks appear in different localities especially in the coast plain around wadi Thowb to the south of wadi Assad and towards Sayhut in the east. Occasionally they are found in the main eastern wadis for example, wadi Bidish and wadi Shakhawi (Fig. 2.28). These eruptive rocks comprise both basaltic cones and flows which extend for variable distances (Fig. 7.19). Such rocks are beyond the scope of current research, but their occurrence may represent valuable information in understanding the younger extension affecting in the area which is going on now associated with the sea floor spreading in the Gulf of Aden.

Fig. 2.27. The unconformable relationship between the Shihr Group and the Pliocene deposits which are nearly always horizontal.

Fig. 2.28. The volcanic flow is on the flat area along the coast plain but sometimes these volcanic flow are occurred inside the main wadis such as the wadi Shakhawi.

CHAPTER 3

REVIEW OF EXTENSIONAL FAULTING

3.1 Introduction

A fault is an approximately plane surface of fracture in a rock body, caused by brittle failure, along which observable relative displacement has occurred between the adjacent blocks. Most faults may be broadly classified according to the direction of slip of adjacent blocks into dip slip, strike slip and oblique slip varieties. The term dip slip fault comprises both normal and reverse faults. Extensional terranes contain a great variety of normal faults formed during deformation which accommodate thinning of the crust.

The review here will focus on extension faults. A normal fault is defined as a fault in which the hanging wall has gone down relative to the footwall and involves lengthening of the crust, commonly causing tilted fault blocks, horsts and grabens. Faults can be classified in different ways depending on the chosen classification, either a genetic or geometrical classification, and the early classification of normal faults was based on their attitude, size and patterns on

maps or cross sections (Billings 1942). Although Anderson (1951) classified faults in terms of stresses, a general and more useful classification is a geometric one where the fault is defined in terms of the sense of movement and the direction of slip (McClay and Ellis 1987).

Faults generally do not persist for great distances and displacement varies systematically along them. In order for regional strains to be accommodated, as displacement on one fault decreases that on an adjacent, often en echelon, fault increases. Often there are well defined zones in which such transfer takes place. Transfer zones are defined by Morley *et al.* (1990) as a coordinated system of deformational features conserving regional extensional strain. They are known also as accommodation zones, relay zones and segment boundaries. These zones are formed due to the changing displacement between individual fault segments. Previous work on the structure of extensional basins identified two main types of transfer zones (i) transfer faults (hard linkage) (Bally 1981, 1982, Gibbs 1984), and (ii) ramps or relay zones (soft linkage) between en echelon fault tip lines (Rosendahl *et al.* 1986, Leeder and Gawthorpe 1987, and Larsen 1988). Recently a wider range of transfer zones has been recognised (Morley 1988, Morley *et al*, 1990, Walsh and Watterson 1991, Peacock and Sanderson 1991)

Continental rifting is the poorly understood thermomechanical process by which the continents break up and new ocean basins form. Rifts do not occur randomly within continents but tend to follow lines of weakness such as orogenic belts, for example, U.S.A. east coast rifted margin (Sawer and Harry 1991), the Gulf of Mexico (Marton and Buffler 1993) and the Gulf of Aden (Laughton *et al.* 1970). Many models have been erected to explain the formation of rifts (Wernicke and Burchfiel 1982, McKenzie 1978, White and Matthews 1980) (Figs. 3.1 and 2) but this study concerns the structural evolution of a small part of the Gulf of Aden rift and is based on small scale mappable structures and hence discussion of these regional models is relevant to the evolution of this Gulf.

3.2 Geometry and classification of extensional faults

The geometrical classifications are obviously less contentious than genetic classifications. They could be based on criteria such as the pitch of the net slip, the attitude of the fault relative to the attitude of the adjacent rocks, the pattern of the faults, the angle at which the faults dip, the apparent movement on the fault, and the type of accommodation structures associated with faults. The shape of the fault surface may play a role in the classification of faults.

Many models have been proposed to explain the geometry and shape of faults, for example, Gibbs (1984), McClay and Ellis (1987), Ellis and McClay (1988), Dula (1991), Trudgill and Cartwright (1994). Recently normal faults have been called extension faults (Wernicke and Burchfiel 1982). However, methods for determining the shape of the fault plane make assumptions about the deformation in the hanging wall and these include constant heave (Verrall 1981), variable-heave (Wheeler 1987), inclined simple shear (White *et al.* 1986, White and Yielding 1991), flexural slip (Davison 1986) and constant-slip (Williams and Vann 1987).

From observations in the Basin and Range province of the western U.S.A., Wernicke and Burchfiel (1982) classified extensional faults, on the basis of the geometry of the fault, into planar non-rotational, planar rotational, and listric faults. Planar non-rotational faults were described by Badley *et al.* (1988) as low displacement faults which accommodate the initial rapid subsidence of rift basins following extensional faulting (Mckenzie 1978, Jarvis 1984). Planar non-rotational faults of large displacement are considered to have low angles of dip (Wernicke 1981 and 1985) (Fig. 3.2).

Planar rotational faults are more commonly recognised. They form tilted terrains in which parallel faults and fault blocks rotate simultaneously. This style of deformation has been termed the "book shelf" (Mandl 1987) or "domino" style, and been applied to numerous extensional provinces since being first described by Ransome *et al.* (1910). The domino fault blocks have internal deformation as has

been demonstrated in analogue models of domino style extension (McClay 1990).

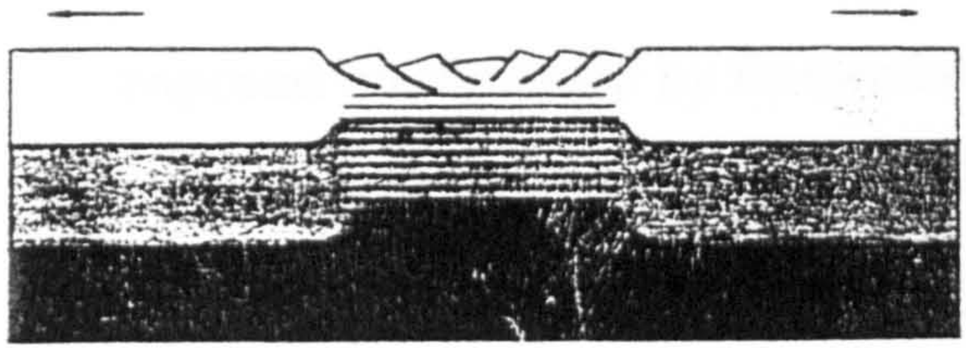

Fig. 3.1. Lithospheric stretching model (after McKenzie 1978)

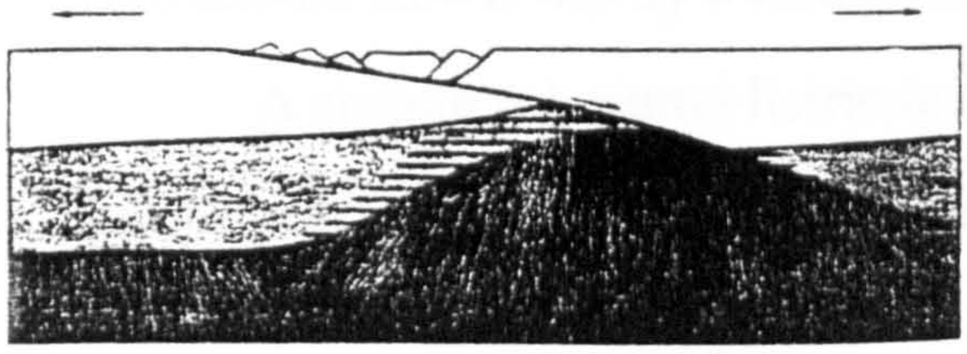

Fig. 3.2. Heterogeneous lithospheric stretching model (after Wernicke 1981)

An important feature of this style of extension is the generation of vertical movement which may be either due to the effect of elastic rebound immediately following fault slip or, in the long term , an isostatic condition (Jackson and Mckenzie 1983, Barr 1987a, 1987b, Jackson *et al.* 1988) and flexural response to the unloading of the footwall (Jackson and Mckenzie 1983, Kusznir *et al.* 1991) and both tilting and vertical movements are observed to accompany movement on active normal faults. These vertical movements involve uplift of the footwall and subsidence of the hanging wall (Jackson *et al.* 1988). The vertical movement decreases with distance from the faults and thus leads to tilting of footwall and hanging wall blocks. The fault consequently rotates about a horizontal axis so that its dip decreases (Jackson *et al.* 1988). However, normal faults rarely occur in

isolation, but are commonly distributed across zones in which several subparallel faults dip in the same direction. Thus a single block is likely to be both the footwall of one fault and the hanging wall of another. The vertical movements imposed on the block by its two bounding faults therefore amount to a torque requiring the block to rotate about a horizontal axis (Jackson *et al.* 1988).

One problem with the rotating domino model is the creation of a space problem at the base of the blocks and the margins of the domino system. Many authors have used basin margins to solve the space problem at the up-dip termination of the domino array (Wernicke and Burchfiel 1982; Barr 1987a and 1987b) and, similarly, Davison (1989) has proposed that domino systems can be terminated down-dip by a listric fault with accompanying rollover.

A simple rotational listric fault occurs by the separation of two blocks on a curved surface. The hanging wall moves down a surface convex toward the footwall strata and the dip of bedding changes toward the footwall where a rollover anticline forms due to the rotation of hanging wall block. Listric faults produce differential tilt between hanging wall and footwall. Thus, a series of imbricate listric fault blocks should display successively steeper tilts as one traverses the blocks in the direction of down throw (Wernicke and Burchfiel 1982). Listric faults have been studied by many workers to show the relationship between hanging wall and footwall deformation, for example, Wernicke and Burchfiel (1982) for the Basin and Range, and Gibbs (1984, 1987) for the North Sea. In these studies interpretation of deep seismic reflection profiling indicates the presence of deep crustal to lithosphere-scale extensional detachments (Allmendinger *et al.* 1983a, Beach 1986, Beach *et al.* 1987). Listric extensional faults are characteristically accompanied by structures such as rollover anticlines and crestal collapse grabens. Listric faults can be classified into two types, simple and complex, according to their accommodation structures (Gibbs 1984). They may be ductile in nature or, more commonly, the internal strains within the rollover

anticlines are wholly or partially accommodated by systems of minor antithetic or synthetic faults (e.g. Bruce 1973, Crans *et al.* 1980, Beach 1984 and Gibbs 1984). At the crest of the rollover anticline a system of contemporaneous antithetic and synthetic faults commonly forms a crestal collapse graben (Merki 1972). The distinction between rotational-planar and listric faults is that planar faults must rotate with bedding, while listric faults may remain fixed, rotation occurring only if the footwall is rotated by structurally lower faults (Wernicke and Burchfiel 1982).

McClay and Scott (1991) demonstrate several examples of similarity between seismic sections and analogue models and show that these models are a powerful tool for understanding the geometric and kinematic development of extensional fault systems. However, these models cannot, as yet, incorporate the isostatic, compaction or thermal effects in natural fault systems.

Complex fault systems with a ramp/flat or "stair case" type geometry have been recognised for many years in regions of contractional tectonics (Dahlstrom 1969, Boyer and Elliott 1982, Suppe 1983). More recently detailed information from seismic data and models has been published on ramp/flat geometry in extensional fault systems (Gibbs 1984, Buchanan and McClay 1991, McClay and Scott 1991) (Fig. 3.3).

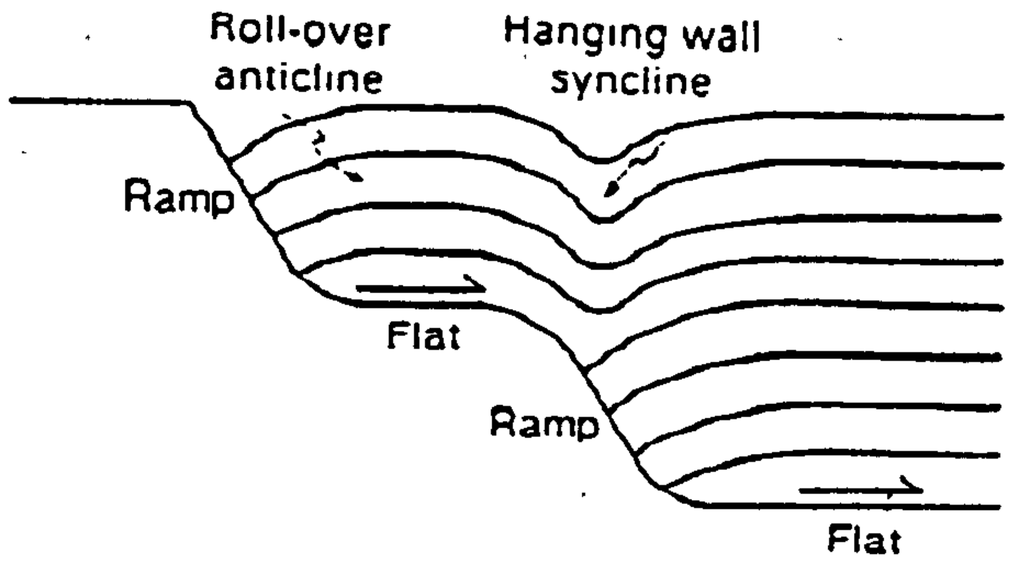

Fig. 3.3. Ramp/flat listric extensional fault model (after Gibbs 1984).

3.3 Accommodation structures in extension region

Accommodation structures such as reverse drag, rollover anticlines and monoclines are associated with extensional faults. Reverse drag is the most common structure associated with most normal faults in many regions and its size depends on the amount of displacement on the faults (Hamblin 1965). The space problems which arise from a listric model can be resolved by the generation of geometrically necessary hanging wall folds and faults. Dula (1991) demonstrates that the relationship between the rollover geometry and the master-fault geometry is dependent upon the dominant deformation mechanism operative in the hanging wall block, and the deformation mechanism will depend upon the rock type and the environment of deformation, including parameters such as lithostatic pressure, fluid pressure, temperature and strain rate. Much research on the origin of rollover folds has focused on the importance of fault shape and the direction of relative motion during hanging wall collapse (White *et al.* 1986, Xiao and Suppe 1992, Groshong 1989, Rowan and Kligfield 1989, Dula 1991, McClay and Scott 1991). Vertical thinning of the rollover on the hanging wall must occur, if there is movement parallel to the bedding planes (Gibbs 1984). The formation of rollover geometry leads to the formation of antithetic or counter faults (Gibbs 1984), with a variety of dip geometries.

All listric extensional fault systems require geometrically necessary hanging wall accommodation structures such as the rollover anticline, found in almost all listric fault systems. For ramp/flat geometries the hanging wall accommodation structures consist of rollover anticlines, associated with the steeping-upwards sections of the detachment surface, and a hanging wall ramp syncline developed above the ramp in major detachment faults (Gibbs 1984, 1987). In addition to rollover anticlines and ramp synclines in complex listric extensional fault systems, internal hanging wall strains are also accommodated by crestal collapse grabens. Small reverse faults have been observed in extensional systems in the North Sea by

Gibbs (1984) who suggested that these may occur above a footwall ramp. Ellis and McClay (1988), in their model experiments, have introduced exciting new insights into the progressive evolution of hanging wall structures developed above listric extensional detachments and observed small reverse faults formed above the crest of the ramp during their experiments. Rollover anticlines with geometrically necessary crestal collapse graben structures are characteristic of the upward steeping segments of listric extensional fault systems.

The degree of hanging wall rotation in the rollover is dependent upon the curvature of the detachment and upon the amount of extension (Ellis and McClay 1988). The constant heave model (Verrall 1981, Gibbs 1983, 1984) also known as the Chevron construction, assumes that fault heave is conserved during deformation. Dula (1991) in his geometric models for constructing master-fault geometry from rollover fold shapes predicts markedly different fault geometries, depending upon the assumed dominant deformation mechanism in the hanging wall. The flattening of the fault reflects an increase in ductility of the rocks with depth (Shelton 1984). Curvature and depth to detachment on the listric fault can be derived from calculating bed length and excess area balance in cross section as well as graphically from the rollover anticlines which are a geometrical and mechanical necessity of listric faulting (Gibbs 1983 and McClay and Scott 1991) (Fig. 3.3).

3.4 Evolution of transfer zones

Transfer zones in extensional regions display a wide range of geometries from discrete fault zones to zones of broad warping (Morley *et al.* 1990). Recently major advances in the understanding of rifts occurred when the concepts of linked fault systems that have been developed in thrust belts were applied to extensional terranes and when large quantities of subsurface information, provided by commercial and academic seismic reflection surveys, were added to field data (e.g.

Burchfiel and Stewart 1966, Wernicke 1981, 1985, Gibbs 1983, 1984, and 1990, Brewer and Smythe 1984, Harding 1984, Ebinger *et al.* 1987, Leeder and Gawthorpe 1987, Peacock and Sanderson 1991, Gawthorpe and Hurst 1993, Destro 1995, Nicol *et al.* 1995). Morley *et al.* (1990) classified the transfer zones into four types, namely, approaching, overlapping, collateral and collinear (Fig. 3.4).

Continental rifts commonly display large-scale structural domains which are largely controlled by the geometry of and interaction among major faults. Such faults generally define either the rift boundary or large horst blocks within the rift. Hence, as faults die out along strike, so do the footwall uplifts. Consequently transfer zones may commonly accommodate not only displacement but elevation differences between adjacent blocks (Ebinger *et al.* 1987, Leeder and Gawthorpe 1987). Gawthorpe and Hurst (1993) demonstrate that the footwall elevation tends to decrease whereas hanging wall elevation tends to increase towards a transfer zone.

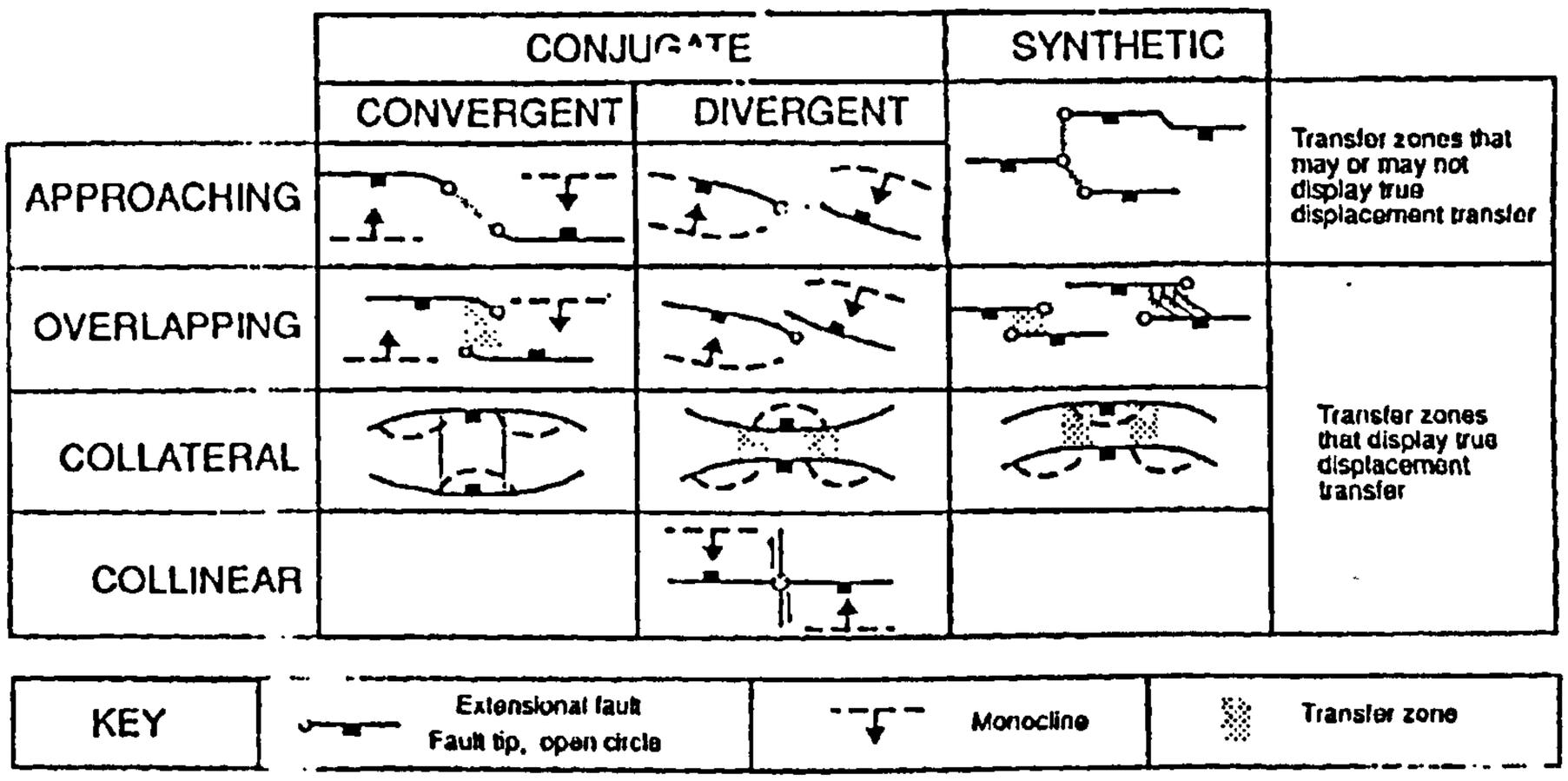

Fig. 3.4. Classification of transfer zones (after Morley 1990).

Peacock and Sanderson (1991) classified fault offsets into (i) displacement-parallel, in which the tip lines of the overlapping faults are parallel to the slip direction, (ii) displacement-normal, in which the tip lines are perpendicular to the

slip direction and (iii) displacement-oblique (Fig. 3.5).

Child *et al.* (1995) classified the overlaps into two types (i) relay zones in which displacement is transferred between the overlapping faults and (ii) non-relay overlaps in which displacement is not transferred and they further defined the mode of overlap in three dimensions as unconnected or linked at a branch-line or branch point (Fig. 3.6). Gibbs (1984) noted that the extensional faults which trend subparallel to the rift are often offset by cross faults that trend at high angles to these faults. These cross faults are termed transfer faults where their formation occurs as an integral part of the extension to allow leakage of strain between extensional faults with different slips. Destro (1995) introduced the new term, release faults, and classified the cross faults into transfer faults (Gibbs 1984) and release faults. In his classification transfer faults form where cross faults connects distinct normal faults and horizontal displacement predominate over vertical displacement. In contrast, release faults form where cross faults, associated with individual normal faults, die out within the hanging wall before connecting to another normal fault (Fig. 3.7). Rosendahl (1987) classified the linkage of the half grabens into families based on their geometries and their relationships. Those half grabens where the adjacent border faults dip toward each other are termed "opposing" and where the border faults have the same dip direction, "similar polarity". Furthermore the opposing half-grabens have been divided into those which are overlapping forming a horst zone that lies below the regional height termed a low relief accommodation zone and those which are non-overlapping forming a high relief accommodation zone (Versfelt and Rosendahl 1989) (Fig. 3.8).

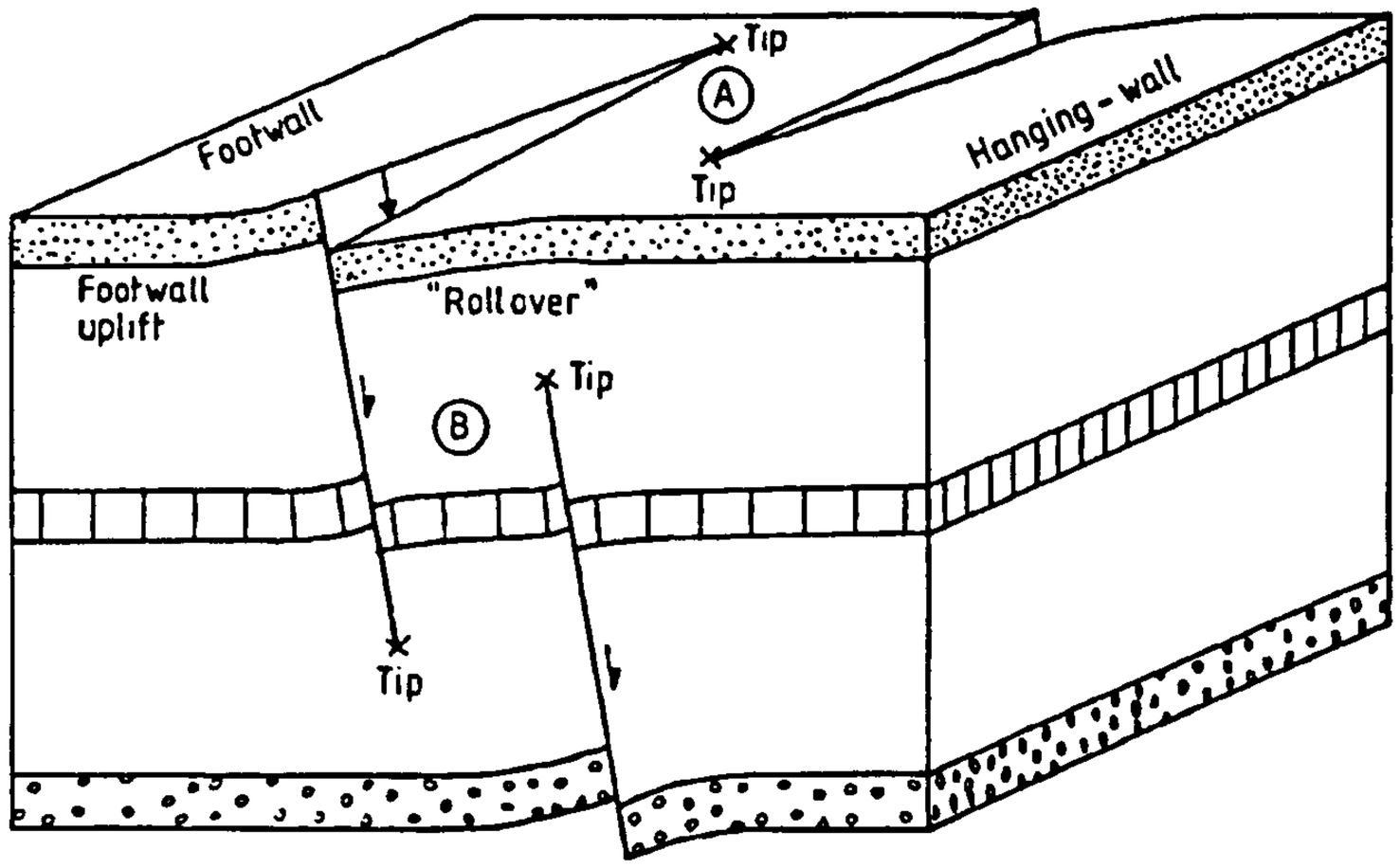

Fig. 3.5. Block diagram of a displacement- normal offset (A) and a displacement-parallel offsets (B) (after Peacock and Sanderson 1991)

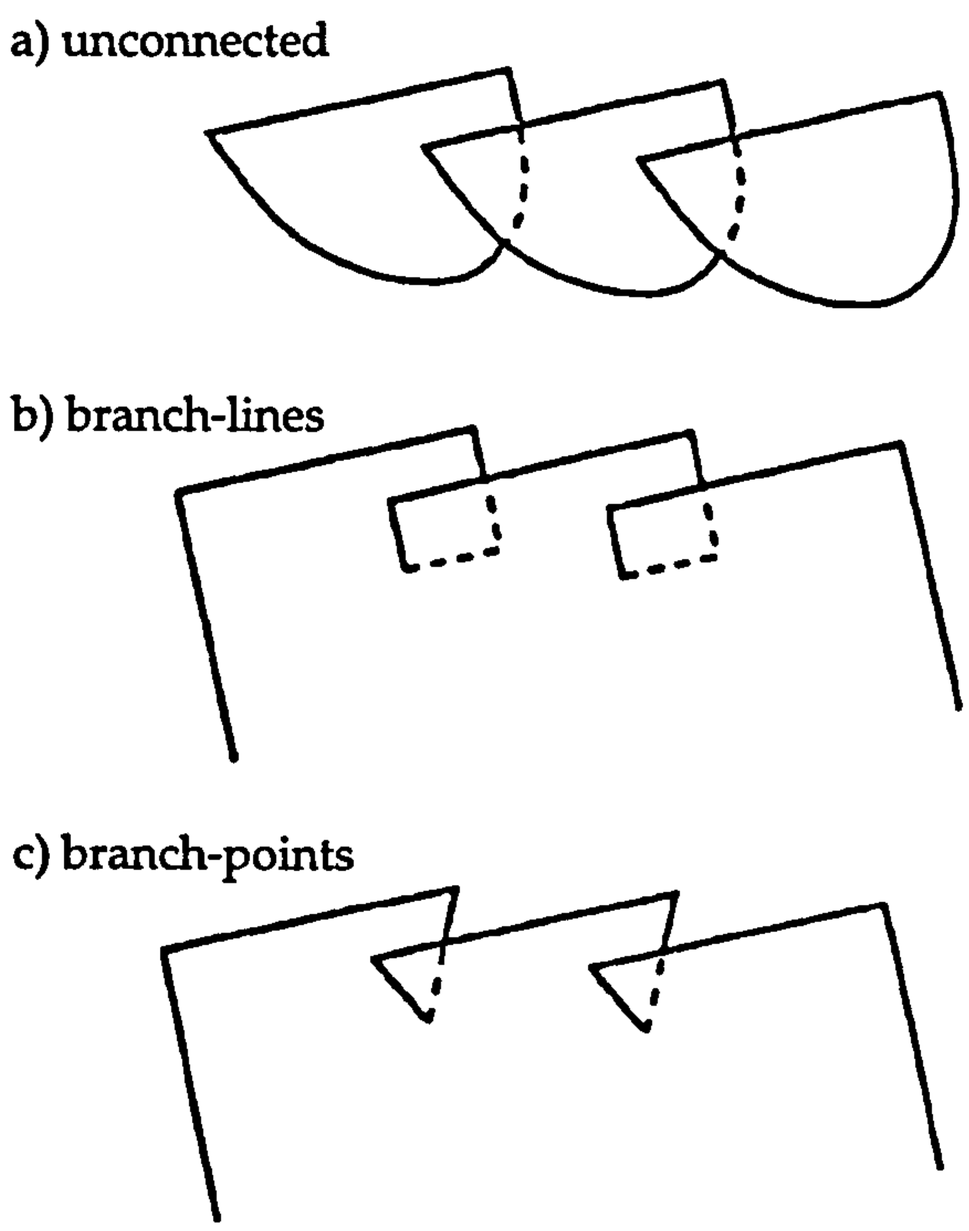

Fig. 3.6. Schematic diagram of the three possible structures underlying a segmented fault zone as seen in map view (a-c) (after Child *et al.* 1995).

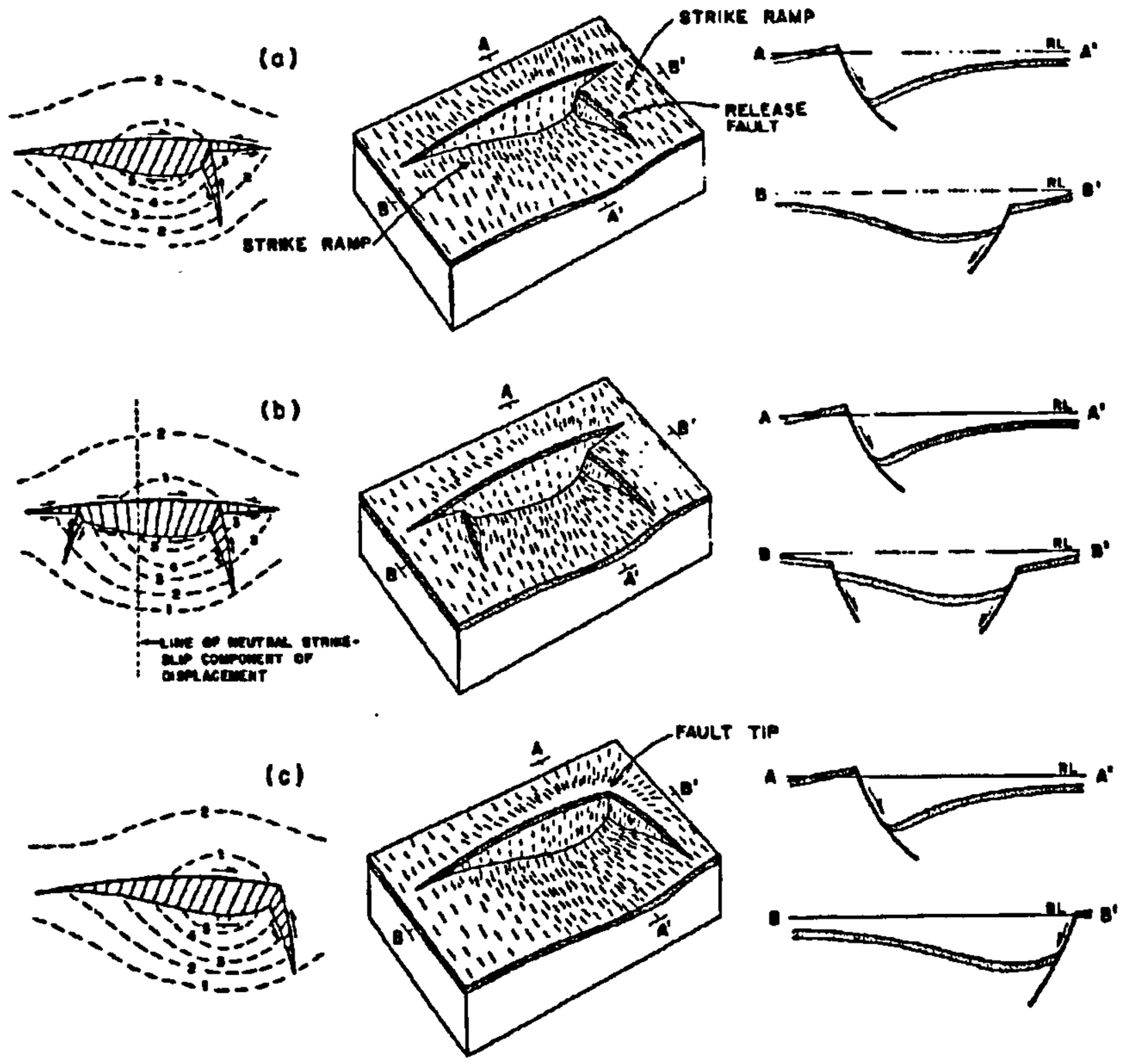

Fig. 3.7 Development of a detached hanging wall relay system (a) detached footwall relay system (b) during propagating extension and break down of the initially symmetrical relay structure (c) shows the release fault formed at the normal fault tips (after Destro 1995).

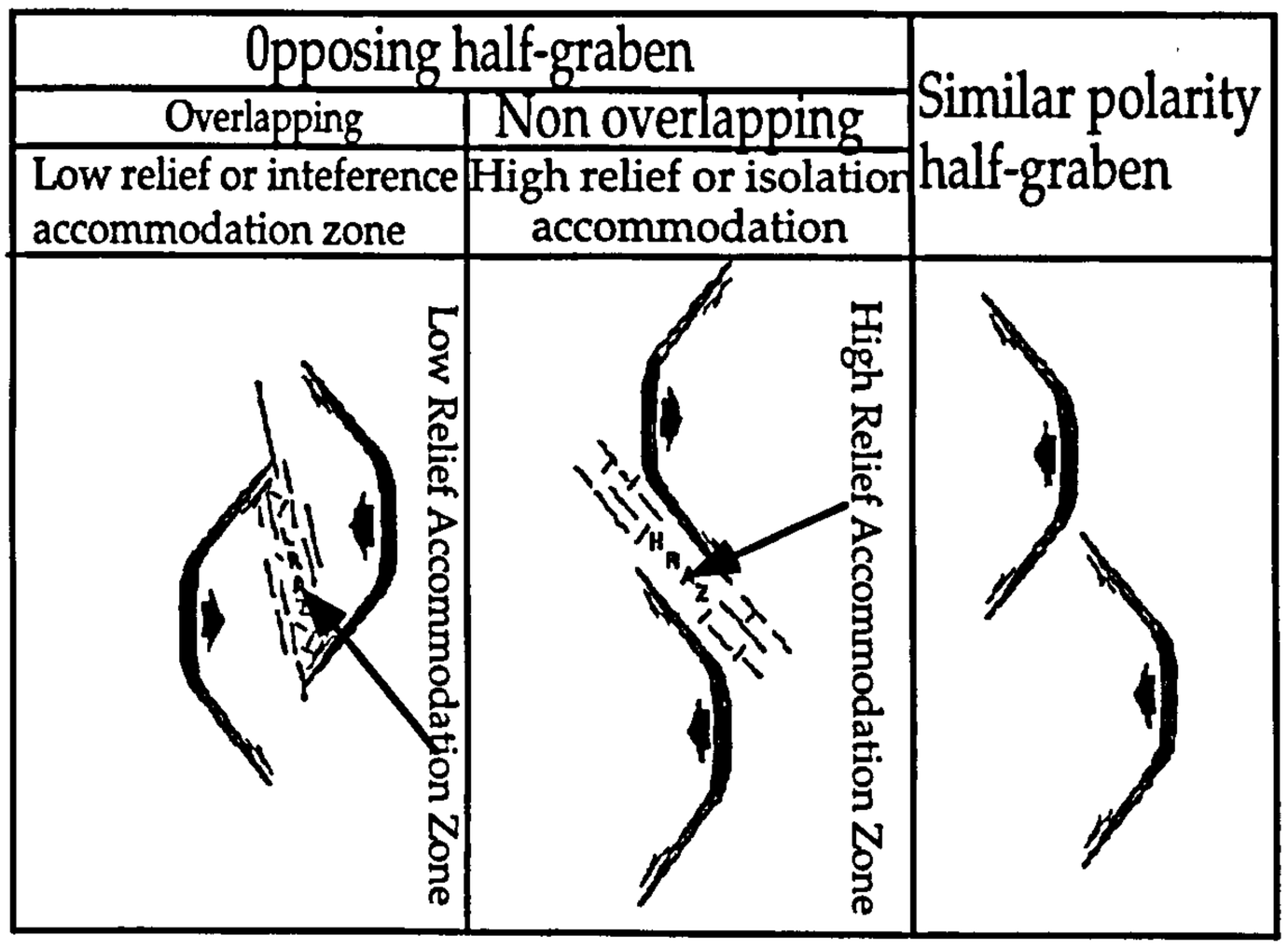

Fig. 3.8. Classification of half graben linkage (after Rosendahl 1987).

A number of models have been erected to explain how extensional faults link together. These can be divided into two groups known as (1) hard linkage where the faults are connected, and (2) those in which fault surfaces are detached

from each other, known as soft linkage. The main elements in the linkage of extensional fault systems are the detachment surface or flat, fault ramps where the dip of the fault surface increases and the transfer fault. The soft-linked faults are formed when the extensional strain is transferred across regions which demonstrate no interconnecting brittle fault structures. They are further divided into arcuate faults which cut across the rift axis and those in which the majority of faults are linear or occur in linear fault zones and are restricted to either one side of the rift or the other (White 1993). Relay structures in a soft-linked system are defined as zones connecting the footwalls and hanging walls of overlapping fault segments (Trudgill and Cartwright 1994). Relay ramps often develop as ephemeral structures eventually becoming breached by hard linkage of the fault segments (Fig. 3.9). Breakdown of ramps by breaching is part of the process of fault growth by segment linkage (Trudgill and Cartwright 1994). To distinguish between hard-linked and soft-linked structures, the definition proposed by Walsh and Watterson (1991), that the hard-linked faults are those in which the fault surfaces are linked on the scale of the map or cross section, is used, while the soft-linked faults are those between which a mechanical and geometrical continuity is achieved by ductile strain of the rock volume between them, rather than by continuity of fault surfaces.

Both hard and soft-linked structures may be divided into synthetic or antithetic types, depending on whether the two faults forming the relay dip in the same or in opposing directions. Trudgill and Cartwright (1994) subdivided hard-linked structures into two types, depending on the pattern of fault breaching; 1) footwall breached relay, developed by hard linkage via the footwall segment, leaving the hanging wall segment as an inactive splay and 2) hanging wall breached relay, developed by hard linkage via hanging wall segment, leaving the footwall segment as an inactive splay (Fig. 3.9).

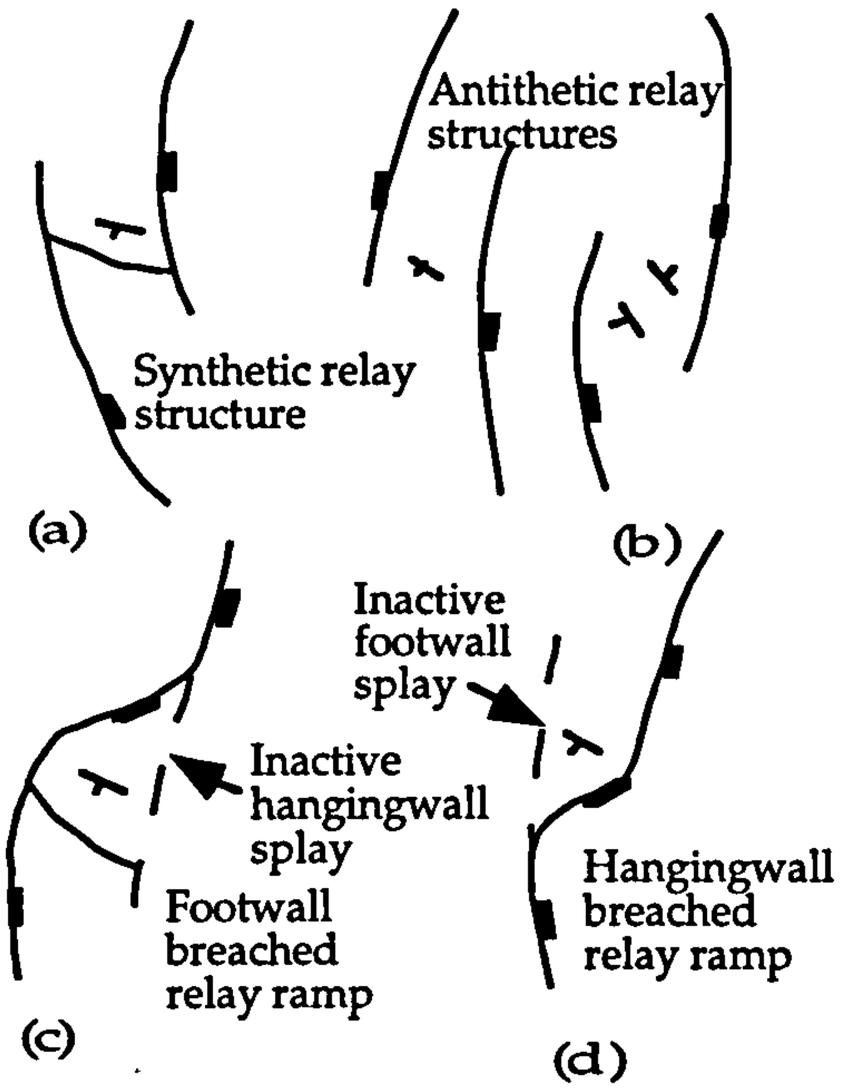

Fig. 3.9. Simple classification of relay zones based on (1) dip direction of the the overlapping fault segments (a) and (b) and (2) offset style of breached relay ramps (c) and (d) (after Trudgill and Cartwright 1994).

3.5 Models of rifting

A number of models have been proposed to explain the evolution of rifts. The most acceptable model which explains lithospheric stretching is the one proposed by McKenzie (1978) for crustal thinning, rifting, and subsidence that predate and accompany continental break-up associated with block faulting due to sudden stretching and the formation of a sedimentary wedge and ultimately the development of a passive continental margin (Fig. 3.1). McKenzie's model assumes homogeneous thinning of the lithosphere. This thinning presumably takes place by faulting and the associated rotation of beds in the upper lithosphere (Coward 1986). This model is more applicable in the evolution of the Gulf of Aden where the similarity of deformation on both sides of the Gulf indicate the pure shear extension. Wernicke (1985) introduced the concept of simple-shear thinning of the entire lithosphere (Fig. 3.2). The main concept of the simple-shear model is that the locus of significant extension in the (brittle) upper crust and in the (ductile) lower crust-mantle lithosphere is offset by low-angle faults or detachment surfaces. Two dominant styles of continental rifting are recognised (1) crevice style rifts (2) arch-volcanic rifts. The crevice style rifts are characterised by initial

graben formation, local uplift of the graben shoulders, and little or no volcanism, while arch-volcanic rifts exhibit an initial doming of the crust, extensive volcanism, and late-stage graben formation (Dunbar and Sawyer 1988). The crevice rifts form in response to regional horizontal stresses, principally derived from the interaction of the lithospheric plates along their edges, whereas arch-volcanic rifts are thought to be the result of mantle convention currents which upwell directly beneath the rift axis. However, Dunbar and Sawyer (1988) propose an alternative working model of continental rifting in which both styles initiate in response to regional horizontal stress. The different surface expressions of the two styles are explained in terms of differences in the mode of failure at different kinds of pre-existing weakness in the continental lithosphere rather than differences in the nature of the driving forces involved. The strong evidence for such stretching comes from crustal thinning and normal fault geometries that indicate large extensions (Bally 1981). Coward (1986) states that the zones of upper and lower lithospheric stretching will be heterogeneous and patchy. This will produce localised uplift and subsequent thermal subsidence within the faulted basins and may explain many of the anomalies between the various stretching estimates made using different techniques (Coward 1986). There seems to be two possible ways in which thinning of the continental lithosphere might occur. First, the whole lithosphere becomes stretched by lateral stresses in the plate, with rifting as the surface expression and consequence of the lithospheric thinning (Girdler and Sowerbutts 1970). Secondly, the lithospheric thinning may be a consequence of the rifting in which the tensional stresses cause brittle fractures which allow hot material to rise from the asthenosphere. Eventually this leads to a large region of thinning as visualised by Brown and Girdler (1980).

Rifts do not occur randomly within continents, but tend to follow orogenic belts and are controlled by local variations in the pre-rift strength of the continental lithosphere (Dunbar and Sawyer 1988). The principal driving

mechanism of plate movement and lithospheric extension governing the evolution of rifts and the break-up of continents is seen in frictional forces exerted by the convecting upper mantle on the base of the lithosphere in combination with deviatoric tensional stresses related to plate boundary processes. Plate interaction plays a major role in the evolution of rifts. On the other hand, geochemical criteria indicate that mantle plumes, rising from the deep mantle, do not appear to play a major role in the evolution of most rift systems (Ziegler 1992), with exceptions of the Cenozoic East Africa rift system (Mohr 1992, Ziegler 1992) and the Mid-Proterozoic midcontinental rift (Cannon and Hinze 1992). Moreover, hot spot activity in conjunction with regional stress fields may have played an important role in the localization and early history of the south Atlantic rift system (Wilson and Guiraud 1992).

Asymmetric detachment models imply that continental extension will result in a highly asymmetric structure on all scales as the middle to lower crust is dragged out from underneath the fracturing and extending upper crust (Lister *et al*. 1986). Gibbs (1984) states that the geometry of extension both in continental aulacogens such as the North Sea and on continental passive margins is not fully understood. The application of simple geometrical models and analogues is therefore of considerable importance in understanding their development.

The McKenzie model of homogeneous lithospheric stretching and the Wernicke model of heterogeneous stretching on a major shear zone of lithospheric scale are end members of a range of crustal extension models (Fig. 3.1). In the McKenzie model the lower lithosphere thins beneath the thinned upper crust, superimposing the thermal subsidence basin on the earlier fault controlled graben. In the Wernicke model the lower lithosphere thins some distance laterally from the thinned upper crust, forming a second sag-type basin separate from the early grabens.

Makris and Henke (1992) have developed a model for the formation of the

Red Sea based on the evaluated geophysical data, which emphasises the key role played by strike-slip faulting during the initial stage of rifting by nucleation of pull-apart basins. The model is in agreement with recent concepts of rifting (White and McKenzie 1989), uplift, magmatism and spreading. Bohannon (1989) proposes models describing the development of the Red Sea and the Gulf of Aden prior to the present period of sea floor spreading, and includes those that use block faulting on steep normal faults, uniform diffuse shear in continental crust and simple shear on large detachment faults, that cut the entire lithosphere and involve detachment faulting, ductile deformation and plutonic inflation (Fig. 3.10).

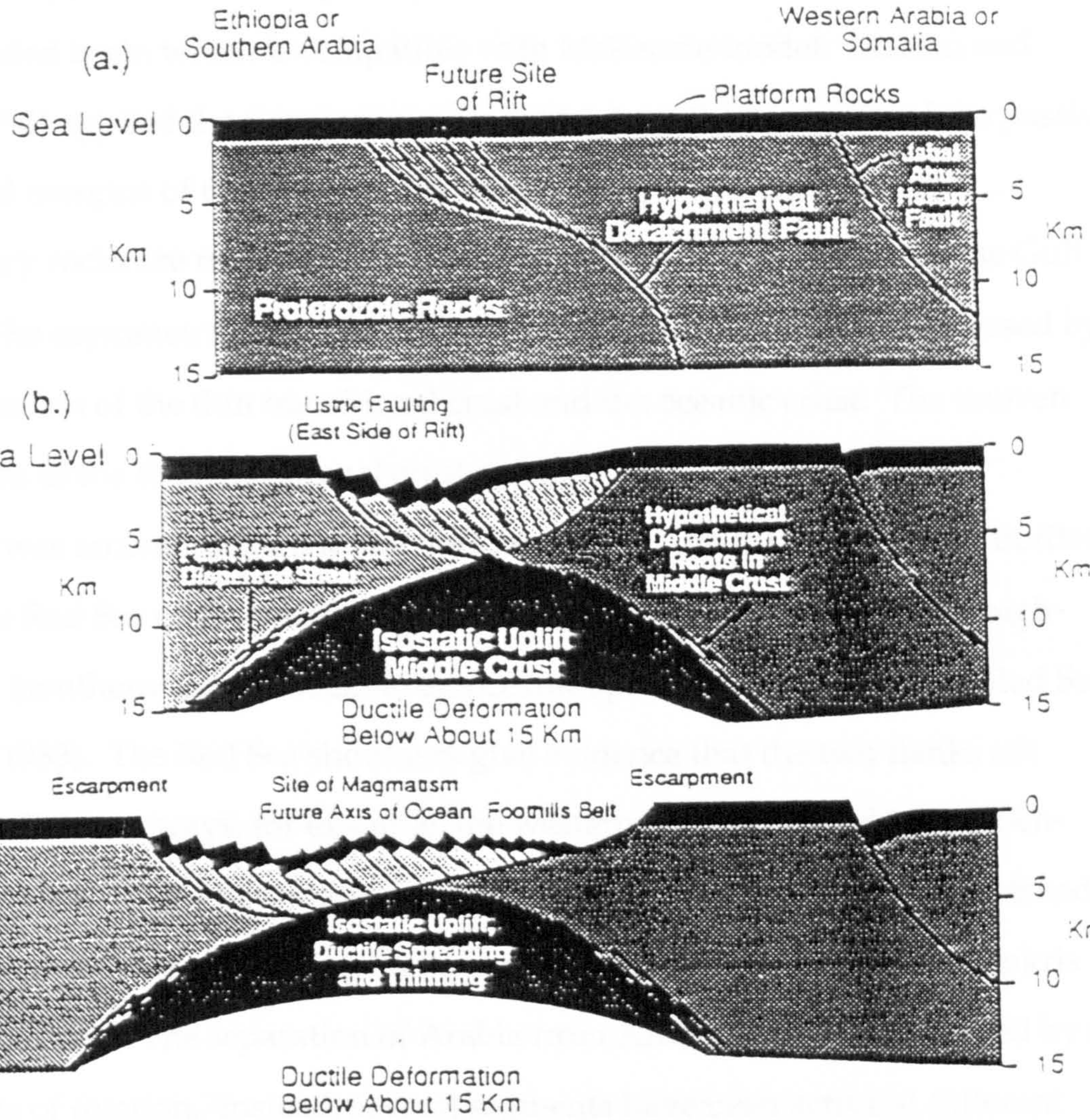

Fig. 3.10. Model for the rift episode in the development of the Red Sea and Gulf of Aden. Three stages are shown starting just prior to rifting and ending prior to the first magmatism in the rift (after Bohannon 1989).

3.6 Discussion of rifts

There are considerable differences of opinion amongst most authors who have written about the evolution of rifting with regard to the location of the ocean-continent transition, and the relative importance of different mechanisms by which rifting has occurred (e.g. continental stretching, sea-floor spreading and the timing of various phases of activity such as age of initiation of separation, continuous separation or periods of quiescence). The asymmetrical distribution of different crustal types of the lithospheric crust gives a lot of variation in the formation of rifts. Coward (1986) notes that the lower lithosphere could extend beneath part of the thinned upper crust and superimpose a thermal subsidence basin on the earlier fault bounded basin which is compatible with McKenzie model. Marton and Buffler (1993) applied the simple-shear model to show the evolution of the passive continental margins of the Mexico basin where sharp differences in the sedimentary rocks are recorded between the south and north margin of the Gulf of Mexico. The asymmetric evolution of the Gulf of Mexico rift is well expressed by the distribution of the thin transitional crust and the oceanic crust. The uneven distribution of the thin transitional crust suggests that much more crustal extension was accommodated in the northern part of the rift (Marton and Buffler 1993). The Red Sea offers one example of the structural transition from a high-strain rift (southern Gulf of Suez) to an oceanic spreading centre (central Red Sea) (Cochran 1983). The Red Sea shoulders give evidence that the two flanks are formed in different ways, for example, the western flank is shaped by wrench-faulting to form a plate boundary, while the eastern flank is floored by stretched continental crust due to uplifting and movement of Arabia from Africa (Makris and Henke 1992). The separation of Arabia from Africa cannot be described by a single pole of rotation. Instead, several segments have been active at different times and with different mechanisms which conflict with the model of anticlockwise rotation (McKenzie *et al.* 1970, Girdler and Styles 1974).

In contrast, the north and south margins of the Gulf of Aden show similar highly attenuated crust and can be matched to a pre-rift geometry (see chapter 8). In addition, the sedimentary rocks on both margins are similar and correlatable and nearly subjected to the same amount of extension. The Gulf of Aden was interpreted by Laughton (1966a) as forming by the separation of Arabia from Africa with a first stage of stretching of continental crust followed, after a hiatus, by sea-floor spreading. The Gulf of Aden developed in the eastern termination of a belt of crust weakness which runs latitudinally from the Guinea Gulf in the west to the Indian Ocean in the east (Fig. 3.11). The Arabian and Nubian plate motion was oblique to this zone of weakness and after the initial stages of rifting, produced basins defined by en echelon WNW fractures in which active clastic sedimentation occurred (Abbate *et al.* 1986).

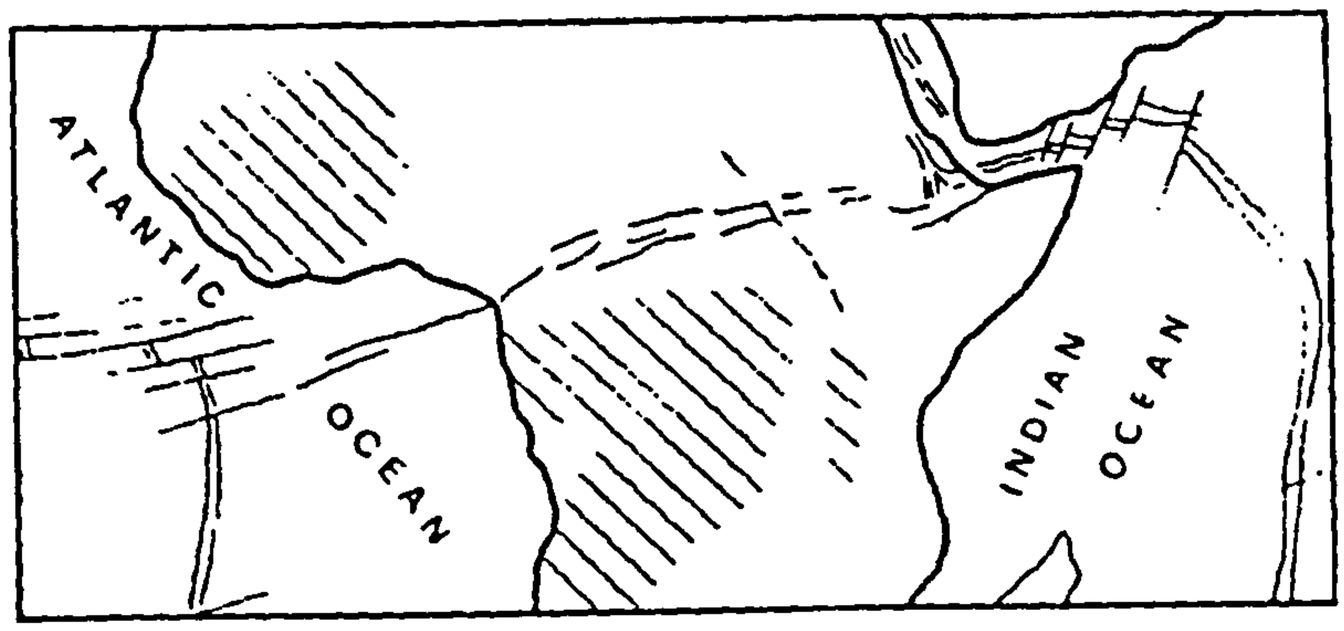

Fig. 3.11. Old lineaments proposed that the Gulf of Aden propagated along it, the hatched areas cratons (after Abbate *et al.* 1986)

Tamsett (1984) states that there were parts of a number of discrete rifts arranged en echelon along a zone of lithospheric weakness during the early opening of the Gulf of Aden which became redundant when transform faults formed and he proposes that the development of a rift with transform faults is similar to that of a spreading centre-transform fault-spreading centre pattern developed in the freezing wax model of Oldenburg and Brune (1975).

The evolution of the rift basins has been ascribed to different mechanisms (Dunbar and Sawyer 1988, Makris and Henke 1992, Cochran 1981). The

subsidence history of a basin is controlled by the mechanisms that create the basins; after a short period of fault-controlled subsidence, passive margin and interior stretched basins subside as a result of thermal re-equilibration (cooling) of the lithosphere and therefore should subside at a rate dependent on the square root of time during the early stage, and exponentially after the lithosphere is thick enough to be affected by mantle convention heat delivery (Parsons and Sclater 1977, McKenzie 1978). Foreland basins on the other hand, subside at a rate dependent on the position, configuration and magnitude of surface and subsurface loads as well as on the flexural rigidity of the lower plate (Beaumont 1981, Fleming and Jordan 1989, Heller *et al.* 1988). Other tectonically controlled basins reflect the particular tectonic processes that lead to their own development.

The analysis of the late Phanerozoic basins of northeast Africa suggests that each of these rift systems records similarities in their structural evolution. All are initiated as a complex arrangement of half-grabens linked by accommodation zones (Bosworth 1993, Morley *et al.* 1990). Northeast Africa underwent repeated phases of regional extension in the late Phanerozoic. In some rift systems, such as the Red Sea, the final phase of continental extension is marked by a shift to high-angle, non-rotational normal faulting. This may represent a fundamental difference between a Basin and Range style of deformation, where repeated generations of detachments develop, and sites of successful oceanic rifting.

3.7 Summary

A number of authors have proposed various fundamental geometries of fault system in extension regions. The most conspicuous structural features that result from extension faults are belts of en echelon faults, tilted fault blocks, horsts and grabens. The accommodation structures associated with extensional regime in different areas show a similarity with each other and with laboratory models.

Accommodation structures such as rollover anticlines, crestal collapse grabens, and ramp synclines in complex listric fault system are formed. The transfer zones in regimes of extension play a role in the shape of faults and the relation between footwall and hanging wall deformation (Morley *et al.* 1990). Transfer zones may commonly accommodate not only displacement but elevation differences between adjacent blocks (Gawthorpe and Hurst 1993). There are two main types of transfer zones where the fault displacements are transferred. Hard linkage where two faults are connected by a fault or soft linkage where the faults are not connected by a brittle structure but strains are transferred through ductile deformation in relay ramps. The geometry of extensional fault system is not fully understood and the application of simple geometrical and analogue models is of considerable importance. The sequential superposition of a number of simple fault elements, with some syn- and post-deformation modification by erosion, sedimentation, compaction and subsidence, can give rise to very complex geometries (Gibbs 1984). The models erected to explain the evolution of the rifts have variations in their formation. Some rifts are associated with volcanic activity during their evolution while in other rifts no evidence has been observed of volcanic activity.

CHAPTER 4

GEOMETRY OF FAULT SURFACES

4.1 Introduction

Many faults seen in seismic reflection sections have a curved shape and they are also often curved in plan view and hence may truly be termed listric. In a theoretical model for listric fault profile shape, Wernicke and Burchfiel (1982) show that the radius of curvature of faults is approximately twice the decollement depth or listric form in profile and concave upwards. Such faults tend to flatten downwards and this results in horizontal movements above a flat-lying detachment or decollement.

Extensional movement on a listric fault generates a rollover anticline in the hanging wall, as originally demonstrated by Hamblin (1965). Gibbs (1983) developed this hypothesis, and showed that thinning and layer parallel stretching of bedding in the rollover is a geometric necessity for the conservation of cross-sectional area. Listric faults that are curved in plan will generate rollover anticlines with curved axial traces in plan view (Gibbs 1984). In a similar fashion, complex hanging wall fold structures will be generated by movement over an irregular fault surface (Gibbs 1984). Using hanging wall

fold geometry, it is possible to predict listric fault shape in detail and to calculate the depth to decollement. This is one of a number of techniques to determine the geometry of faults with depth, in addition to balanced sections and seismic cross sections.

4.2 Models of the geometry of faults

A number of different geometric models, based on different assumptions, have been constructed to determine the fault shape with depth, given the dip of bedding surface and heave or displacement on the fault. These models are based on the assumptions of constant heave, constant displacement, constant bed length, or they use a fixed slip line or inclined simple shear direction (Fig. 4.1).

The constant heave model (Verrall 1981, Gibbs 1983, 1984), also known as the Chevron construction, assumes that fault heave is conserved during deformation. The material points in the hanging wall are assumed to translate a distance horizontally from their initially undeformed position and then displace vertically along vertical slip planes. Deformation of the hanging wall and formation of the anticline are thus accomplished by homogeneous simple shear along vertical shear planes.

The constant displacement model (Coward and Gibbs 1986, Williams and Vann 1987) assumes that each increment of displacement measured along the fault surface is conserved during incremental offset of the hanging wall and that the horizontal and vertical components of displacement paths of material points are parallel in vertical columns within the hanging wall.

Constant bed length is a powerful constraint for constructing and restoring balanced cross sections of many contractional structures (Bally *et al.* 1966, Suppe 1983), and it has been used in some extensional regions (Suppe 1983, Davison 1986, Rowan and Kligfield 1989). The constant bed length model

assumes that the deformation of the hanging wall rollover is accomplished by flexural-slip folding where the bedding planes serve as active slip surfaces.

Williams and Vann (1987) developed the slip line model in which the material points in the hanging wall are assumed to translate along slip lines constructed parallel to the master fault, rather than considering columns in the hanging wall, as in the case for the constant displacement model. The slip line model requires that the dips of individual displacement paths decrease with depth in a comparable vertical column through the hanging wall.

The inclined shear model (White *et al.* 1986, White 1987, Dula 1991) proposes that the material points in the hanging wall are translated parallel to the regional dip line and then shear downward at an angle $\propto$, meassured from the normal to the regional dip line. In this method the geometry of the rollover could be constructed given the fault geometry, the fault heave and the shear angle. In this model the shear angle is estimated either from the orientation of the subsidiary faults or through an iterative process.

Thus, using the geometry of the hanging wall fold, it is possible to predict the listric fault shape in detail and to calculate the depth to decollement. In spite of these efforts there is still some controversy among the structural geologists who deal with these models. For example, Williams and Vann (1987) have amended the Chevron method in two ways, namely, the modified Chevron construction and the slip-line construction, described above. The modified Chevron construction maintains the conservation of displacement along the fault plane and both heave and throw vary continuously with fault dip angle.

Wheeler (1987) shows that both the modified Chevron construction and the slip-line construction produce large area changes and cannot be used quantitatively unless these spurious effects are removed. Wheeler's (1987) modification to include variable heave has initially vertical lines remaining

vertical, but able to move together or apart as the hanging wall moves over a fault surface. These vertical lines retain their length during the deformation. However, if such lines change their relative spacing without a corresponding change of length, then the area of the slab of rock which they bound will increase or decrease. This is a spurious effect of the Williams and Vann (1987) model. In the slip-line model the straight lines perpendicular to the fault in the hanging wall remain straight and perpendicular as they move down the fault plane.

Dula (1991) compares the models and comments on their relative merits (Fig. 4.1). In the absence of confirmatory drill holes or even seismic sections to control the structural interpretations, the constant heave model has been used in the current study. The Chevron construction (Verrall 1981) is a convenient method to constrain the geometry of fault at depth and compared with the other methods it generates a relatively deep detachment (Fig. 4.1). It is very simple to construct the geometry of the fault surface by hand if the attitude of the fault and the dip of bedding in the hanging wall are known and in this study further control is provided by fixes on elevation. The Chevron construction method was selected to calculate the geometry of faults due to its wide acceptable method among many workers and gave good resulted when it is correlated with seismic cross sections

4.3 Methodology

The attitude of bedding of selected rollover anticlines has been measured along traverses perpendicular to the strike of the associated faults. The measurements were made with a Clar compass fixed to an aluminum disc with a diameter of 0.40m (Fig. 4.2). The data collected are distance, measured by pacing, and the dip and dip direction of bedding; an altimeter was used to measure the altitude at the beginning and end of the traverses as an additional

Fig. 4.1. Summary of geometric models for determinig fault shapes from rollover shapes.

MODEL	SLIP LINE	INCLINED SHEAR	CONSTANT DISPLACEMENT	CONSTANT HEAVE	CONSTANT BED LENGTH
CONSTRUCTION	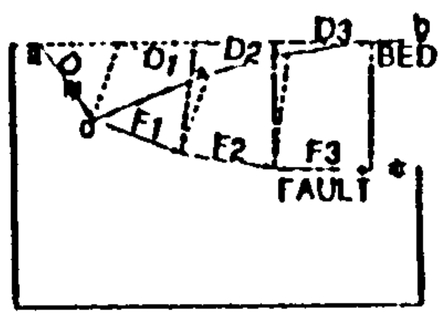	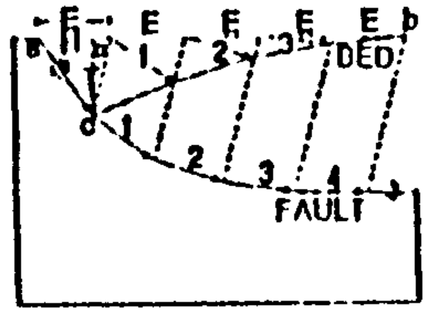	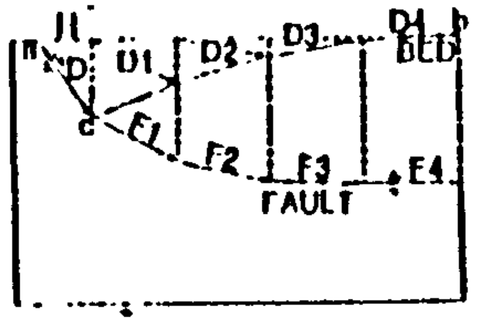	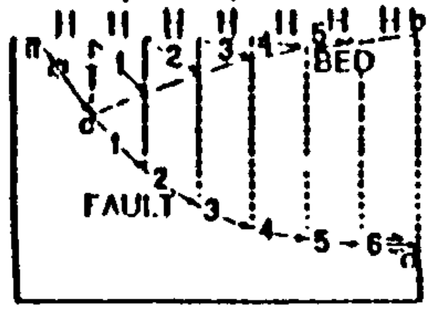	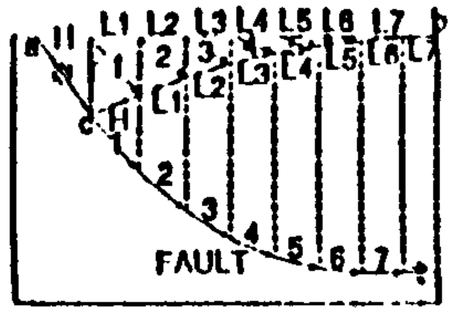
AREA BALANCE PROFILE	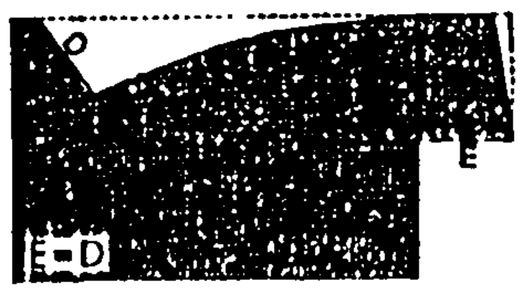	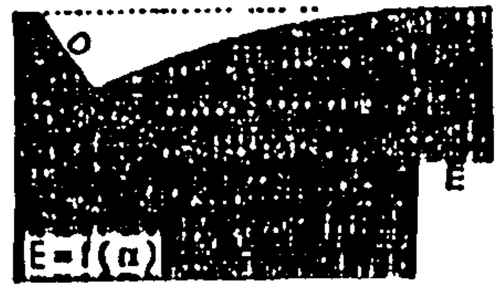	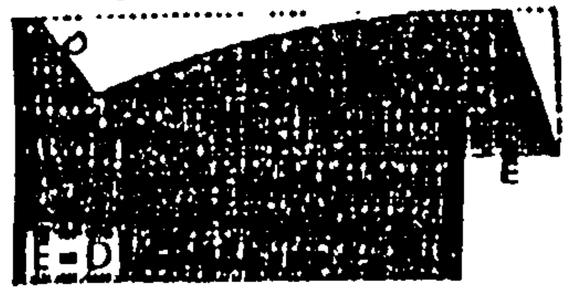	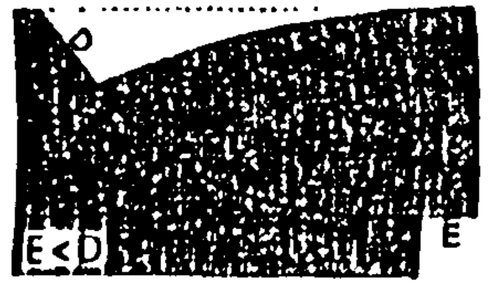	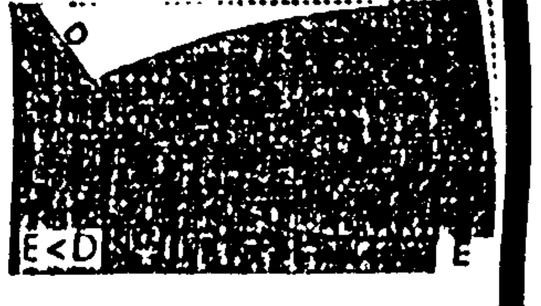
ASSUMPTIONS	Points move parallel to fault	Points move on parallel inclined planes	Constant displacement along fault	Constant horizontal displacement	Constant bed length
	• Plane strain deformation • Footwall relatively undeformed • Deformation by single mechanism • Compaction neglected or corrected				
DEFORMATION MECHANISM	Unspecified Slip Conserved	Simple Shear on Inclined Planes (Subsidiary Faults) Extension Conserved	Unspecified Slip Conserved	Vertical Simple Shear	Bedding-Plane Slip
FOLD STYLE	Unspecified	Similar Folding	Unspecified	Similar Folding	Parallel Folding
DATA REQUIRED	Rollover Shape Displacement	Rollover Shape Fault Heave Shear Angle (α)	Rollover Shape Fault Heave Displacement	Rollover Shape Fault Heave	Rollover Shape Fault Heave
REFERENCES	Williams and Vann (1987)	White et al. (1986) White (1987) Dula 1991	Williams and Vann (1987)	Verrall (1981) Gibbs (1983) This study	Davison (1986)

Fig. 4.2. 0.40m aluminum disk attached to a Clar compass used to even out surface irregularities and give good average values for strike and dip.

constraint on the geometry of the rollover. These data (appendix no. 1) are analysed to give the profile of the hanging wall surface then, by using the constant heave method, the geometry of the fault with depth is constructed (see appendix no. 1).

4.4 Location of traverses

Although the study area is large, some representative areas were selected as representative of the whole area in order to analyse the fault geometry. The main area chosen was the Switchbacks and by focusing the measurements in this area almost all of the faults which were mapped on a scale of 1:23,000 were measured. The field survey, conducted during four field trips, has demonstrated that the Switchbacks is the best location as it displays the typical structural style of the area and, moreover, it is very accessible. The traverses measured in the whole study area are given serial numbers from 1 to 20

(Fig. 4.3). The measurement of the hanging wall surface was accomplished down the dip slopes of a single surface of the Umm er Radhuma Formation in most of the area except in wadi Al-Andeep, to the east of wadi Bidish, where the measurements were on Qishn and Fartaq surfaces (traverse no. 9 and 10 respectively) (Fig. 4.3).

Detailed traverses mainly in the Switchbacks area have been carried out. The hanging wall surface of the same fault was measured at intervals along the strike of the fault to show how the geometry of the fault changes with changes of displacement. The traverses which were measured in the Switchbacks area are numbered as follows: 2, 3, 4, 5, 6, 7, 8, 12, and 13. The remaining traverses have been measured at different localities throughout the area. Traverses nos. 1, 17, 18, 19 and 20 were measured to the east of the Switchbacks north of the Gayl Bawazir area (Fig. 4.3). Traverse no.14 was measured south of wadi Hawayrah in the hanging wall of a fault parallel to the wadi Hamim fault (Fig. 4.3). Traverse no.15 was measured in the hanging wall of a major fault to the east of wadi Araf (Fig. 4.3). Further to the east, traverse no.16 was measured in the Assad area, while the traverses nos. 9, 10 and 11 were measured in the wadi Bidish area at the easternmost area (Fig. 4.3).

4.5 The Switchbacks area

The majority of measured faults sole out in either the Mukalla Formation or deeper in the Harshiyat Formation. However, the two major faults in this area, as would be expected, sole out at greater depth and reach the basement rocks (Fig. 4.4). The traverses which have been measured at the tips of faults show that they sole out at very shallow depth while the traverses across the maximum displacement show that the fault penetrate to greater depth.

Traverse no. 2 has been measured on the hanging wall of the most southerly fault in the Switchbacks area (Fig. 4.4a). Calculation of the fault profile shows that it soles out at a high level in the basement (Fig. 4.4a). The measurement of the dip on the bedding surface indicates rotation of bedding. (appendix no.2 table. 2). The rotation of the hanging wall was observed where the dip at the top of this hanging wall is approximately 0° while at the bottom close to the fault plane it is 30°.

Traverses nos. 3, 4, and 8 were measured on the hanging wall of the largest fault in the Switchbacks area (Figs. 4.4b-d). The calculated fault geometry for all three shows that the fault soles out within basement, with no. 8 in the region of maximum displacement flattening off at the greatest depth (Fig. 4.4c). The dip of bedding ranges from 10° on the top of the hanging wall to 35° in the bottom close to the fault plane (appendix no.2 and tables. 3, 4 and 8).

Traverses nos. 12 and 13 were about 40m apart in one hanging wall near the tip of a fault. The calculated fault shape shows that it soles out rapidly in the top of the Mukalla Formation (Fig. 4.4e and f)). The rotation of the bedding along these traverses is detected from the top of the dip slope of the hanging wall where the dip is 5° and it increases to reach about 23° at the bottom of the hanging wall close to the fault plane (appendix no.2 and tables. 12 and 13).

Traverses no. 5 and 7 are again in the same hanging wall about 1,000m apart with no. 7 being measured at the point of the maximum displacement. Both fault profiles as constructed sole out in the Cretaceous clastic succession with traverse no. 7 giving detachment deep in the Harshiyat Formation and no.5 in the overlying Mukalla Formation (Fig. 4.4g and h) (appendix no. 2 and tables. 5 and 7). Traverse no. 6 was in the hanging wall of small fault. The rotation is very clear in the field and from the measured data (Fig. 4.4i)

(appendix no.2 and table. 6). This fault detaches at a very shallow depth in the upper part of the Mukalla Formation.

The faulting in the Switchbacks area most likely represents accommodation structures in the hanging wall of the major Wadi Hawayrah fault, which has more than 640m vertical displacement (Fig. 6.14).

4.6 Gayl Bawazir Area

Five traverses nos. 1, 17, 18, 19 and 20, were made in an area four kilometres east of the Switchbacks (Fig. 4.3). On traverses no.1 (Fig. 4.3), the calculated shape of the fault shows a flattening out in the upper part of the Harshiyat Formation. The bedding dip in the hanging wall ranges from 3° at the top to 21° close to the fault plane (Fig. 4.4j) (appendix no.2 and table. 1).

On traverses nos. 17 and 18 bedding dip varies from 6° to 28°. The constructed fault flattens out at a shallow depth within the Mukalla Formation (Fig. 4.5a and b, appendix no.2 and table. 17 and 18).

Traverses nos. 19 and 20, recording dip angles from 7° to 33°, (appendix no.2 tabls. 19 and 20) were 200m apart on a fault to the north of the one recorded in traverses no. 17 and 18. Both traverses indicate that the fault detaches approximately in the upper part of the Harshiyat Formation (Fig. 4.5c-d). The results show that the computed geometries of faults in both areas are similar and it is likely that they are represent a similar value of extension (Figs. 4.4e-j and 4.5a-d).

Fig. 4.3. The location of traverses measured throughout the area.

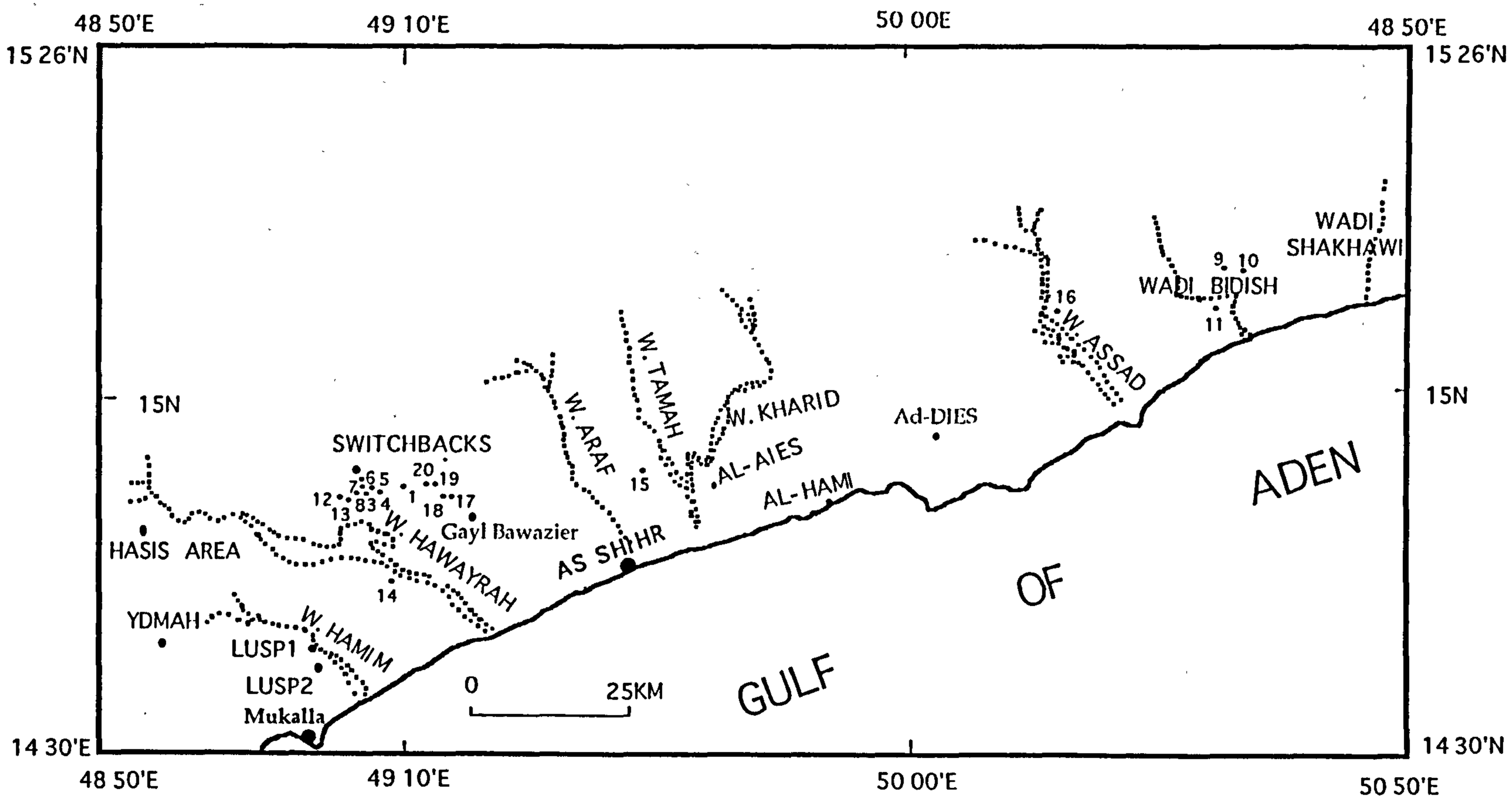

4.7 Additional traverses throughout the whole area

Further traverses were chosen at different sites in order to give a picture of the geometry of faults with depth throughout the whole area. Some 15km south of the Switchbacks traverse no. 14 was measured in the hanging wall of a fault parallel to the wadi Hamim fault which is also the footwall of the wadi Hawayrah fault. The dip of this fault was measured in the field at different localities and ranges between 68° and 74° which is the same as the Hamim fault which brings down the whole sedimentary sequence up to the Umm er Radhuma Formation against the basement rocks (Fig. 4.3 and see sheet I). Construction of the fault shape shows that it remains very steep and soles out at very great depth in the basement block (Fig. 4.5e). The rotation of the hanging wall is obvious from the measured data where the dip ranges between 6° and 29° (appendix no.2 and table. 14).

Another important locality is east of wadi Araf and south of wadi Tamah (Fig. 4.3). Here the hanging wall of a major arcuate fault, has been measured. The rotation of the bedding is recorded at 6° at the top to 23° at the bottom (appendix no.2 table. 15). The analysis shows the fault to be detached at a high level within the basement blocks (Fig. 4.5f). The footwall of this fault stands as discontinuous inliers in the syn-rift deposits throughout the flat area from the Gayl Bawazir area in the west to south of wadi Kharid in the east (see sheet II and III). The fault plane is irregular if taken as a single fault surface, but if it is divided into linear segments then it has a similarity with the footwall of the wadi Hawayrah fault. The footwall of this fault probably represents the hanging wall of another fault to the south where patches of the Jeza and Umm er Radhuma Formations are overlain by the Shihr Group; for example, at Jabal Dabdab to the east of the Ash-Shihr city (see sheet III). South of wadi Assad in the east of the study area where the wadi has cut deeply down through the Formations to give good exposures of the Fartaq and Harshiyat Formations, a

hanging wall bedding surface was measured. Construction of the fault shape shows that the fault detaches at a depth in the upper part of the Jurassic rocks rather than in the basement rocks (Fig. 4.5g). The rotation of the hanging wall is very clear from the field with dips ranging between 4° and 32° (appendix no.2 and table. 16).

According to Haitham and Nani (1993) in reference to the offshore exploration wells drilled in Sarar, Al-Masila area and Qusayr (Agip 1981 unpublished report) immediately south of the study area, the stratigraphic sequence has changed and the Mukalla Formation has become very thin; furthermore the Qishn Formation has become thicker than in the western part of the study area. All the off-shore exploration wells with the exception of the Al-Hami well failed to reach the basement blocks. This fault, therefore probably detaches in the upper part of the Jurassic rocks rather than in basement blocks.

Further east, particularly in wadi Bidish, three traverses, nos. 9, 10 and 11 were measured (Fig. 4.3). No. 11 was measured at the tip of a fault in an area of very complex geology with horizontal slickensides superimposed by very steep slickensides (Fig. 6.4a). The rotation of bedding ranges between 7° and 30° (appendix no.2 and table. 11) and construction of the fault profile shows that it detaches either in the Harshiyat or Qishn Formations (Fig. 4.5h). Traverse no. 9, on a bedding surface of the Qishn Formation, represents the hanging wall of the major fault in wadi Bidish. The rotation of bedding is very clear with dips ranging from 8° to 28° (appendix no.2 and table. 9). This fault detaches at great depth probably in the Jurassic or basement rocks where the stratigraphic sequence is uncertain (Fig. 4.5i). Traverse no. 10 has been taken on a bedding surface of the Fartaq Formation. The fault might detach in the Harshiyat Formation or may even extend into the Jurassic rocks (Fig. 4.5j and appendix no.2 and table. 10).

There are no seismic data available for the subsurface to confirm the geometries of faults as listric faults with detachment in different level of depth and I suggest that the detachment surfaces depend on the displacement on the faults. Where the displacement is maximum the faults detach at great depth and where the displacement is minimum they sole out at shallow depths. This is clear where more than one traverse was measured on the same hanging wall. The rollover anticlines record rotation of bedding around horizontal axes. In addition, rotation around a vertical axis is recorded in the hanging wall of the wadi Hamim fault where the strike varies from east-west (Lusp) to north-south (Harshiyat area) (see sheet I).

4.8 Conclusion

Existing methods for constructing major fault geometries from rollover fold shapes predict markedly different fault geometries, depending upon the assumed dominant deformation mechanism in the hanging wall. Constructed fault shapes for the constant heave method which has been used in this study produced different geometries of fault with depth depending on the vertical displacement on the fault.

However, such surface measurements benefit from subsurface information, such as seismic data, to constrain the geometry and increase the accuracy of the subsurface interpretation. Most of the hanging walls, which have been measured contain rollover anticlines observed in the field, and the rotation of bedding planes down the dip slope of the hanging wall surfaces has been measured. The present study shows that the master faults sole out at great depth while the small faults, which are most likely accommodation faults within the hanging wall, sole out at very shallow depth. From the field evidence and data collected to calculate the geometry of faults it could be said that the majority of large faults sole out at great depth in the basement rocks.

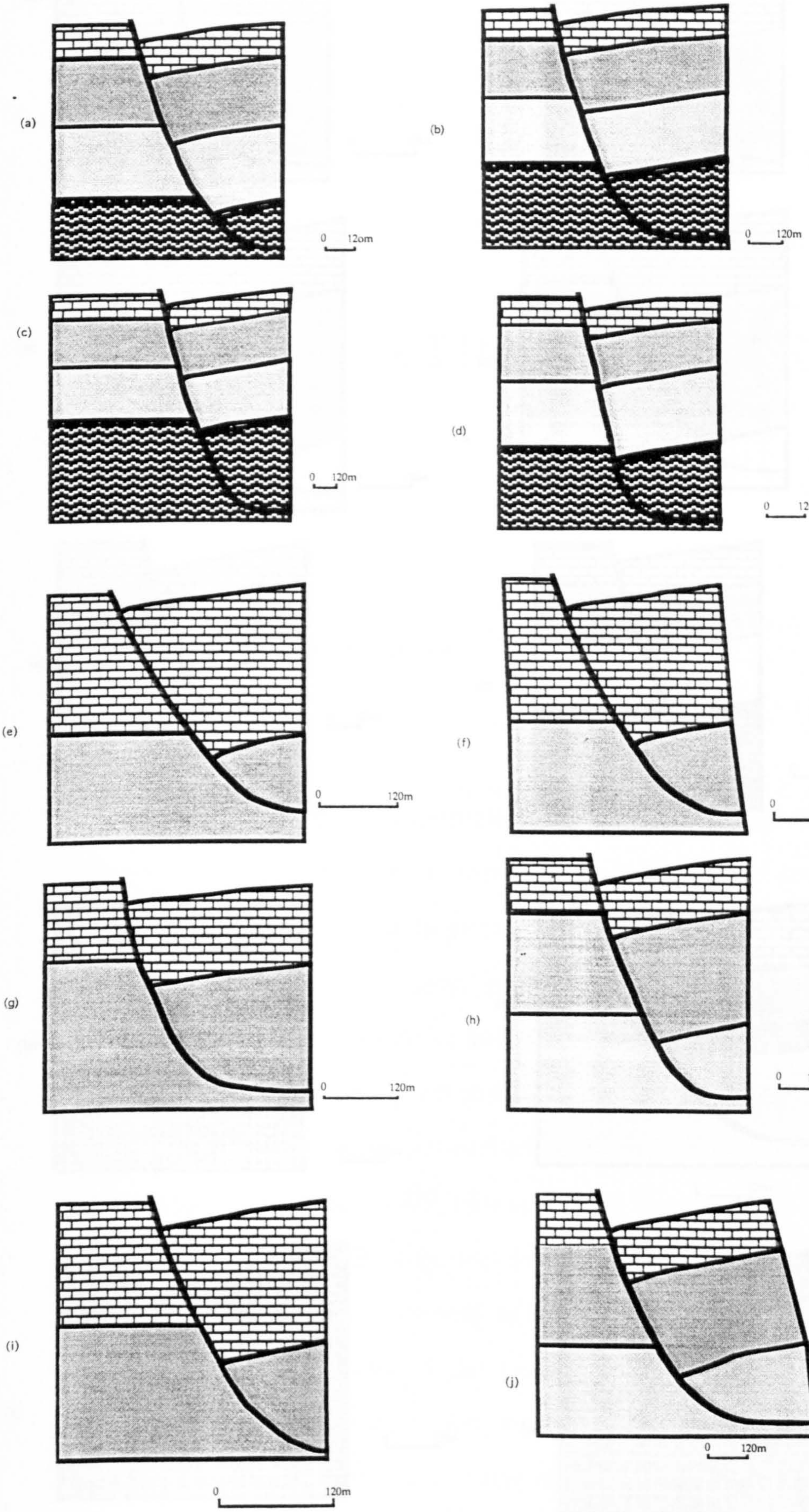

Fig.4.4. The calculation of fault shape with depth in the Switchback area. Vertical and horizontal scales are the same but note that the scale varies from profile to profile.

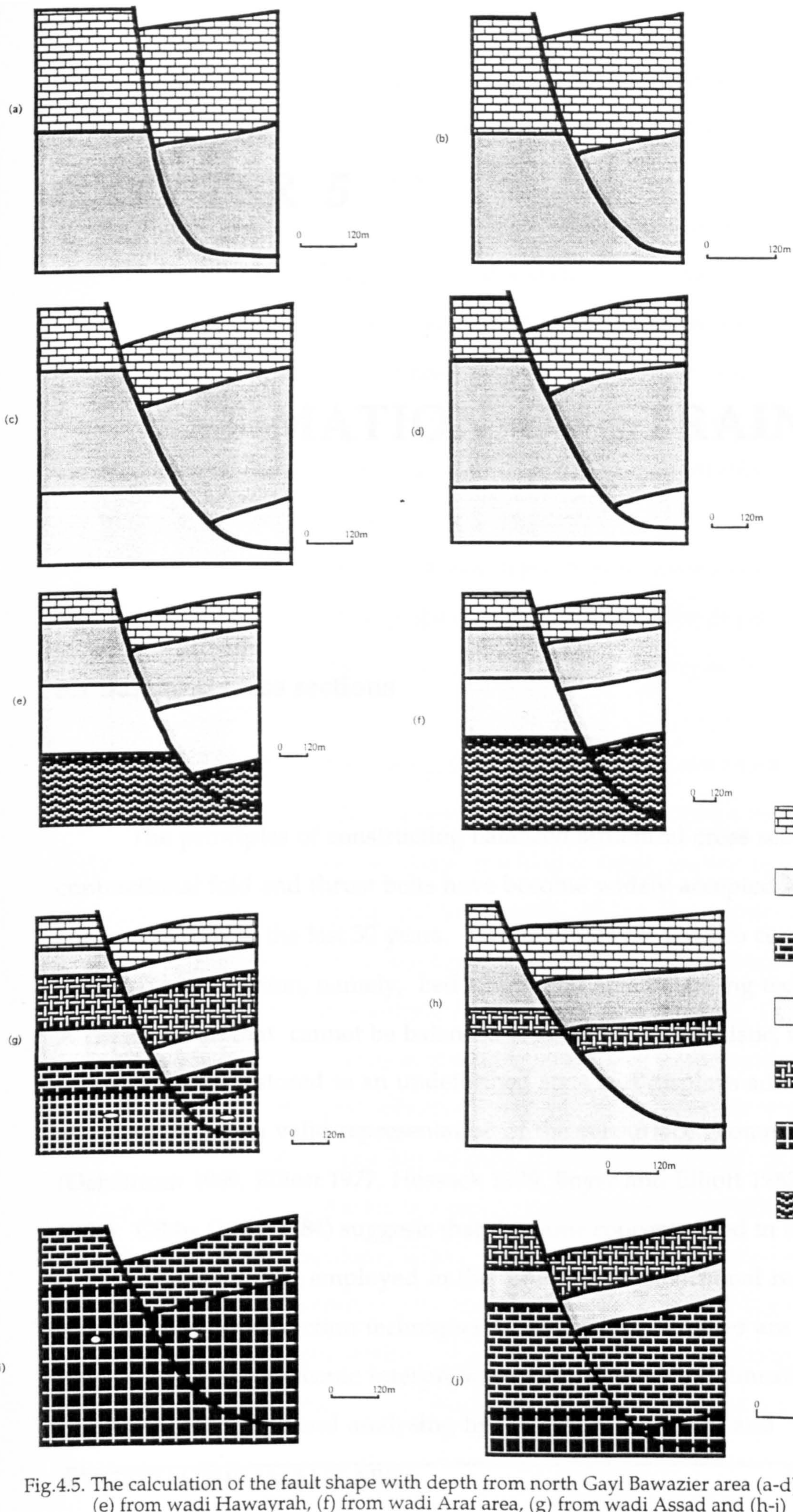

Fig.4.5. The calculation of the fault shape with depth from north Gayl Bawazier area (a-d), (e) from wadi Hawayrah, (f) from wadi Araf area, (g) from wadi Assad and (h-j) from wadi Bidish area. Vertical and horizontal scales are the same, but note that the scale varies from profile to profile.

CHAPTER 5

ESTIMATION OF STRAIN

5.1 Balanced cross sections

5.1.1 Introduction

The principles of constructing balanced structural cross sections in contractional fold and thrust belts have become widely accepted among oil companies during the last 30 years. Two methods are used to construct a balanced cross section, namely, bed length and area balancing techniques. A cross section that cannot be balanced is generally not realistic, whereas one that can be restored to an undeformed state and displays admissible structure may be a valid representation of the subsurface geometry (Dahlstrom 1969, Elliott 1977, Hossack 1979, Boyer and Elliott 1982, Davison 1986). Gibbs (1983, 1984) suggests that the same concepts used in areas of contraction should be employed in the analysis of extensional regimes. The balanced cross section techniques in extensional terranes are powerful tools in evaluating seismic interpretations and precisely delineating reservoir geometries and analysing hydrocarbon migration and

entrapment, particularly where the characteristic extensional structures, such as tilted fault blocks, gravity induced listric growth faults, salt ridges and diapirs are present (Rowan and Kligfield 1989).

Verrall (1981) was first to publish a method for inverting the extensional rollover geometry in an independent half graben to obtain the shape of the fault with depth. His method is based on the assumption of constant heave and models the hanging wall geometry as being the result of vertical simple shear, i.e., vertical slip between adjacent infinitesimally thin segments, by the amount necessary to maintain contact between the base of the hanging wall and the fault (Verrall 1981).

Groshong (1989, 1990) used balanced cross sections in extensional terranes of independent half grabens to restore the pre-fault geometry by a modified version of the technique of Verrall (1981) using oblique simple shear.

Keller (1990) investigated graben tectonics using the assumption of bed length conservation during deformation. He provided a new deformation model for half-grabens in which a listric master fault is proposed to balance hanging wall bed length. His model requires full-grabens and normal faults to segment the hanging wall and may be used for secondary structures but is not valid for regional structures.

A geological cross section should integrate all known subsurface and surface geological data and wherever possible information from off the line of section (Elliott 1983). The line of section should lie parallel to the movement direction so the section can be balanced (Elliott 1983). In a broad classification of cross sections, Elliott (1983) defines four types of sections: 1. Unbalanced section, which is a preliminary investigation of the structures. 2. An unrestorable cross section, which may arise from an unfortunate choice of line of section. 3. A restorable and admissible cross section, i.e.

one containing tectonic structures which conform to certain rules such as extension faults always cut down in the direction of transport. 4. A valid, balanced cross section which integrates various sources of data including that from surface outcrops.

To restore and balance any section, many authors assume no material has been moved into or out of the plane of the cross section (Gibbs 1984a, Rowan and Kligfield 1989). This assumption imposes limitations on the applicability of the techniques; for example, the section must be oriented along the direction of material transport perpendicular to the axis of the rift trough and a section that crosses transfer faults or accommodation zones cannot be restored properly because these involve strike-slip displacement (Gibbs 1984, Bosworth 1985). Many balanced cross sections which have been done by these techniques are based on seismic lines. These sections may contain some errors because there is no outcrop data to constrain the subsurface data and improve the accuracy of the balanced cross sections. For example, the errors could arise from the calculation of depth to the detachment surface.

The localities which were chosen for these cross sections are wadi Hawayrah in the west of the area, the Switchbacks area, wadi Araf, wadi Kharid, wadi Assad, and wadi Bidish in the eastern part of the study area (Fig. 5.1). These are more the accessible wadis where structure and stratigraphy were easily measured.

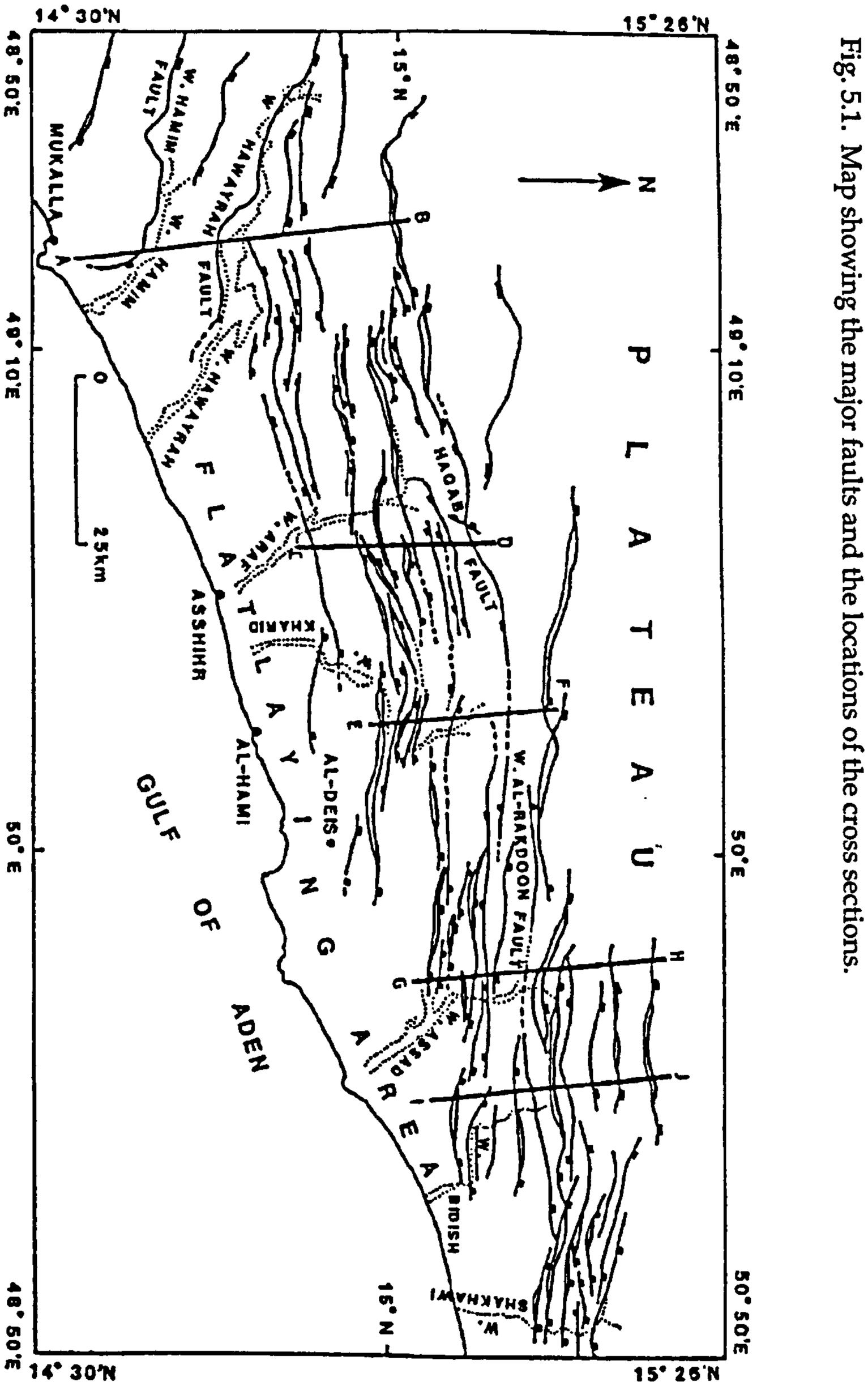

Fig. 5.1. Map showing the major faults and the locations of the cross sections.

In the current study the balanced cross sections have been drawn by using very detailed information collected from the field which is generally very well exposed. The area was mapped at a scale 1:50,000 and outcrop information such as the attitudes of faults and stratigraphic thicknesses was combined with available subsurface well data to construct the sections. In addition, the faults were mapped in detail and their attitudes measured

directly wherever possible. These cross sections are oriented perpendicular to the axis of the Gulf of Aden and in the direction of slip of the main faults. The thicknesses of Formations used in the sections are taken from different sources such as the current study and previous literature either from outcrop or well data.

The extension fractures which have no apparent displacement are not considered during the restoration of these cross sections because they are not mappable. They will, however, have contributed a small amount to the bulk strain. The restoration and balancing of these sections was done manually, so that attention was focused on each fault in turn to avoid cumulative errors which may occur during the balancing of the sections.

5.1.2 Difficulties of balancing cross sections

In the restoration and balancing of cross sections there are certain factors which should be considered. For example, Geiser (1978) criticised the assumption of plane strain in balanced section calculations. The most important difficulty in the balancing of sections is the reduction in area of the section resulting from volume loss during the deformation. It is important to consider the effect of volume loss in balanced section calculations. Lithification volume loss should not affect balanced section calculations, because this process occurs in the early stage of deformation (Hossack 1978).

The most important factor to be considered during balancing is tectonic compaction where there is some evidence that lithified sediments may be compacted further during deformation. Wood (1974) described an increase in density as mudstones are deformed to form slates where the density increases from 2.5 to 2.7-2.85g/cm^3 which is equivalent to a volume reduction of 10%.

Von Plessman (1964) describes the effects of tectonic pressure solution in cleaved rocks, and notes contractions of 20-30% are usual perpendicular to the pressure solution cleavage and may go up to 50%. In permeable rocks such as limestone and sandstone the dissolved material could be removed from the rocks and there will be a corresponding decrease in volume. However, Wood (1974) and Ramsay and Wood (1973) state that the dissolved material may be deposited locally in the area and will therefore not affect the restoration of the section.

5.1.3 The study area

In this area the geometry of faults with depth is constrained by using the constant heave method, also known as the Chevron construction (Verrall 1981, Gibbs 1983) (see appendix no. 1). The method of balanced cross sections is summaries in appendix no. 3. The extensional strain along the 6 cross sections is calculated by restoring them to their original geometry before deformation. Each section will now be described in turn from west to east. All these cross sections have been restored to their undeformed condition and give variable values of extension. These cross sections are enclosed in the second volume, together with maps except the Switchbacks section which is here in the text.

5.1.4 Wadi Hawayrah cross section

This section, representing the western part of the study area, has a length of 47.4 km (Fig. 5.1). This section was selected because of the high quality of stratigraphic detail and structural data and, in addition, its cover sequence is well exposed from the Qishn to the Jeza Formations to enable the relationship of faults in both the basement rocks and the sedimentary cover to be shown. Therefore analysis of the geometry along this section

will give good control on the geometry of the faults with depth. However, this cross section has a very important value from a structural point of view. Its location in the eastern part of the Mukalla high gives information about the faults which formed basins during the Cretaceous and which were rejuvenated in the Oligo-Miocene. The section starts in the Harshiyat area northwest of Mukalla city where the basement rocks are exposed and extends northward to the plateau (see sheet I). Four major faults cross this section line. The most important fault is here called the wadi Hamim fault which has a maximum vertical throw of 1320m where the whole sedimentary sequence up to the Umm er Radhuma Formation has been brought down against the basement.

In the hanging wall contact of the wadi Hamim fault plane, a normal drag fold is formed. This could be interpreted using the model of Xiao and Suppe (1992) which states that a normal drag fold is formed by convex bending along an active axial surface which is parallel to a synthetic fault and has equal dip in the hanging wall. The bedding planes at the fault contact dip north away from the fault and may reach 30° (Fig. 5.2a, see volume II). Normal drag folds are not recorded elsewhere in the study area. The second major fault is named the wadi Hawayrah fault as this wadi has been eroded along the fault. It has a vertical displacement of more than 600m since the Umm er Radhuma Formation has been faulted down against the lower clastic part of the Harshiyat Formation (Fig. 5.2a, see volume II).

The third major fault is at the southern edge of the plateau to the northwest of the Switchbacks area. This fault dips to the south with a vertical throw of more than 350m and together with the Switchbacks fault, plays an important role in the formation of a steep scarp which represents the northern edge of a major graben along this section. The fourth major

fault, at the north end of this cross section, again dips to the north and has a vertical throw of more than 500m bringing the Jeza Formation down against the Mukalla Formation (Fig. 5.2a, see volume II).

The most important structures along this section are the major graben between the wadi Hawayrah fault in the south and the third major fault in the plateau to the north and the horst formed by the third and fourth faults in the plateau. From the wadi Hawayrah fault northward to the plateau, the north and south dipping faults may be regarded as synthetic and antithetic faults respectively of both the wadi Hawayrah and the plateau faults to form a series of half graben and small graben within this major graben (Fig. 5.2a, see volume II).

5.1.5. Restoration of wadi Hawayrah section

This section is the only one in the study area where the basement rocks are exposed at the surface. Hence, some indication of the geometry of faults at the level of the top of basement, may be obtained. The restored section emphasises that the faults penetrate through the basement rocks with steep dips. However, there are some faults with moderate initial dips particularly in the Switchbacks area and in the plateau, which are interpreted to sole out within the cover sequence (Fig. 5.2b, see volume II).

The dip of faults bounding tilted blocks ranges between 55° and 80° and the dip of bedding in the fault blocks varies from 0° to 30°. Most faults cut through the Tertiary and Cretaceous sedimentary rocks and continue down into the basement.

In the Harshiyat area at the south end of this section the dip of the Rays member and the lower Harshiyat Formation is between 20° and 30° to the south which implies that there are further faults to the south of the section line which has caused this rotation. The faults between the wadi

Hamim and wadi Hawayrah faults have very steep dips on the restored section and they are interpreted as resulting from reactivation of old structures of northwest-southeast strike in the basement. For example, the wadi Hamim fault has a 68° dip and the wadi Hawayrah fault has a great thickness of the Mukalla Formation in its hanging wall as a result of rejuvenation during the Cretaceous.

The extension along the Hawayrah section was calculated using bed length balance and gives a value of 7.1%. This amount of extension may be an underestimate since the section crosses two transfer zones in addition to a length of no exposure in excess of 3km in the wadi floor which may conceal some faults. In addition, the numerous small extension fractures are not considered in this estimate.

5.1.6 Switchbacks cross section

The Switchbacks area is the best location for showing the typical structural style in the south Hadhramaut area. The characteristic feature of this area is the en echelon pattern of half grabens (Fig. 5.4). The Switchbacks area stands at more than 900m above sea level and is formed by a nearly vertical south dipping fault (Fig. 5.3a). The geometry of faults in this area has been calculated from the shape of the hanging wall roll-over folds (Fig. 5.5). Four faults in the Switchbacks area sole out at a deep level in the basement but most sole out at shallower levels within the Mukalla and Harshiyat Formations, as already mentioned in chapter 4 (Fig. 5.3a, 5.5 and 4.4). The major south dipping fault which forms the biggest scarp in this area is here called the Switchbacks fault and towards the east displacement is transferred into another major south dipping fault north of Gayl Bawazir town (see sheet II). The Switchbacks fault is antithetic to the wadi Hawayrah fault and has a vertical displacement of more than 250m

(Fig. 5.6). The other faults in the Switchbacks area have throws ranging between 50m and 100m. The dips of faults in the Switchbacks area range between 50° and 84° (Fig. 5.3a). The south dipping fault forms the northern edge of a full graben with the north dipping faults, such as the wadi Hawayrah fault. The ends of the minor faults in the Switchbacks area swing to the northwest towards the Switchbacks fault (Fig. 5.5).

5.1.7 Restoration of the Switchbacks cross section

In this area not only was the geometry of faults and bedding surfaces measured and mapped at a scale of 1:23,000 enlarged from air photographs, but also the exposure scale fractures close to fault tips where the vertical displacement becomes zero were analysed. The result from such a traverse are used to give a more accurate estimate of horizontal extension. One cross sections has been drawn in this area close to and parallel to the wadi Hawayrah section (Figs. 5.3a). This section was drawn after the calculation of the geometry of faults and gives a value of 9.4%. The cumulative extension of small faults on the exposure scale is 3.2%. This is calculated by measuring the horizontal heave along small traverse of 18m, so the total extension in the Switchbacks area is about 12%. Hence, the fractures increase the measured extension by approximately one third. These results from exposure-scale fractures are in accord with those of other studies which conclude that the small scale fractures may result in the underestimation of extension (Kakimi 1980, Marrett and Allmendinger 1990, 1991, Scholz and Cowie 1990, Walsh and Watterson 1991, 1992, Peacock and Sanderson 1994). However, this cross section is not completely restorable as a small excess area occurs, marked by ?, close to the large south dipping fault (Fig. 5.3b). That the cross section does not restore properly to

its pre-deformation geometry is most likely due to horizontal movements recorded in this area.

5.1.8 Wadi Araf cross section

This cross section is constructed along the eastern side of wadi Araf to show the structures at the southern margin of the plateau (Fig. 5.1). The pipe line from the Canadian Occidental Petrolum Company oil field to the shipping terminal at Jabal Addabah, west of Ash Shihr city, has been constructed along wadi Araf. This section has a length of 30.9km and stretches from the coastal plain in the south to the plateau in the north. The dominant structures are alternating full and half graben with two very obvious major grabens along this section. The first major graben is located in the south of this section where the Shihr Group is brought down into contact with the Harshiyat Formation; the second graben, in the middle of the section, is between the wadi Araf fault in the south and the major Haqab fault in the north with a vertical displacement of more than 750m (Fig. 5.7a, see volume II). At the south end there is a basin in which the Oligo-Miocene sediments of the Shihr Group were deposited. There are three major faults each with vertical displacements of more than 400m in this section; at the south end a large north-dipping fault forms a graben with a south dipping fault in the middle of the section which controls the westward branch of wadi Araf and forms a very steep scarp. A third major fault, the Haqab fault, which has the main influence on the geomorphology of this area, forms the southern edge of the plateau at an elevation of more than 2,000m above sea level and has a very steep scarp where most of the stratigraphic sequence from the Jeza at the top to the lower Harshiyat Formation in the bottom is exposed (Fig. 5.7a, see volume II). The dips of

faults along this section range between 72° and 50° and those of bedding planes in the faulted blocks between 4° and 20°.

5.1.9 Restoration of wadi Araf cross section

Only two Formations are exposed along most of this wadi, the Mukalla and Umm er Radhuma Formations. The thickness of this stratigraphic sequence has been derived from comparison with the surrounding areas, information from Watchorn (1993 personal communication) and by field measurement.

With the exception of the fault at the south end of the section, all faults have steep dips. However, the faults in wadi Araf, relative to those in wadi Hawayrah, have slightly less steep dips (Fig. 5.7b, see volume II). Calculation of the geometry of the major fault with depth in the south end of the wadi Araf cross section which shows that, whereas it started at a high angle, it soles out at a low angle at a deep level within basement (Fig. 4.5f). From the cross section (Fig. 5.7b, see volume II), which has been restored, the extension is calculated as 6.7%.

Fig. 5.3. (a) Structural cross section along the Switchbacks area, (b) restored position of faults after line-length balancing. The extension calculated is 9.4%.

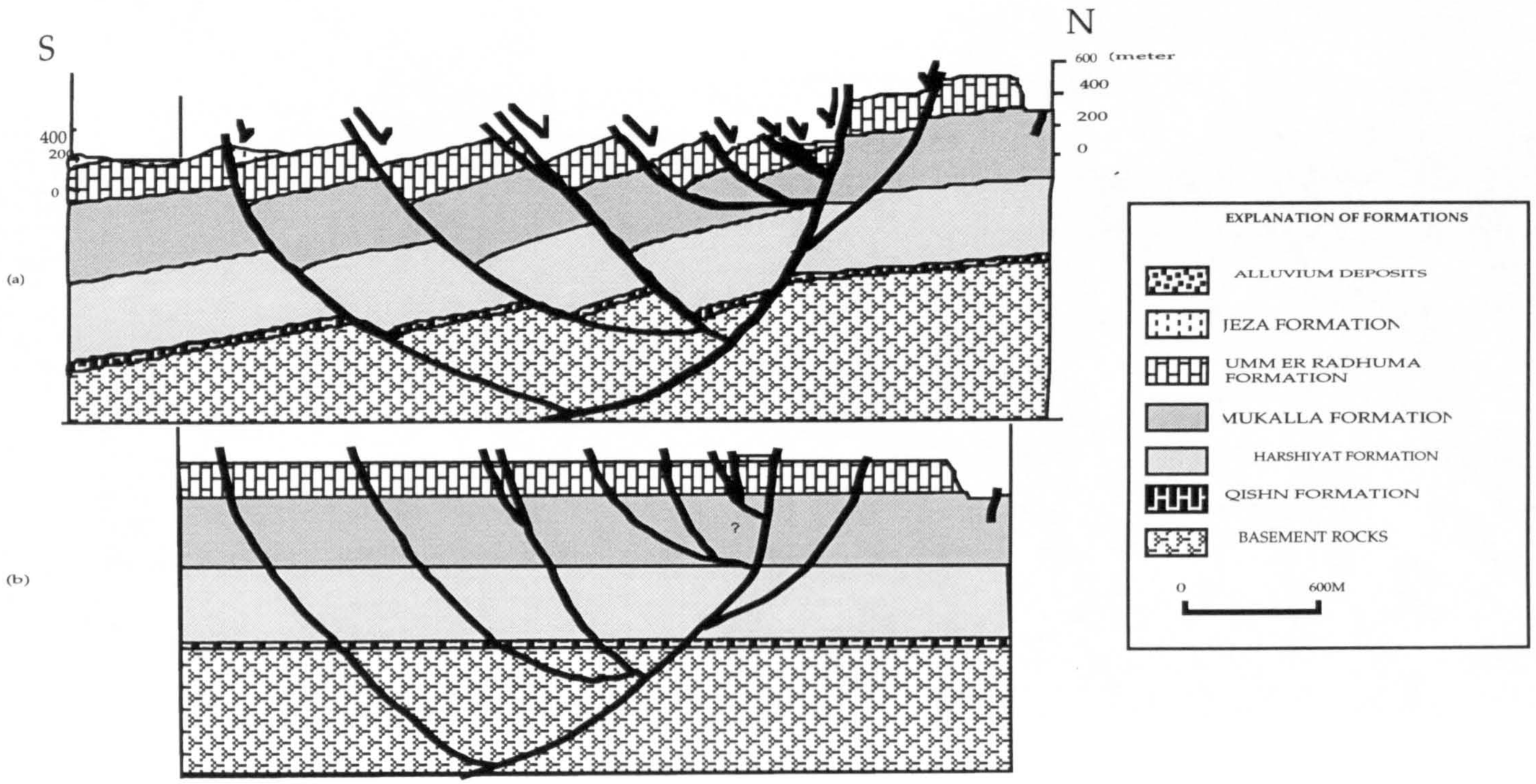

Fig. 5.4. Typical half grabens formed by small north dipping faults whose scarps are seen cutting the Umm er Radhuma formatiom. Looking south from immediately north of the Switchbacks fault toward the scarp of the major north dipping wadi Hawayrah fault.

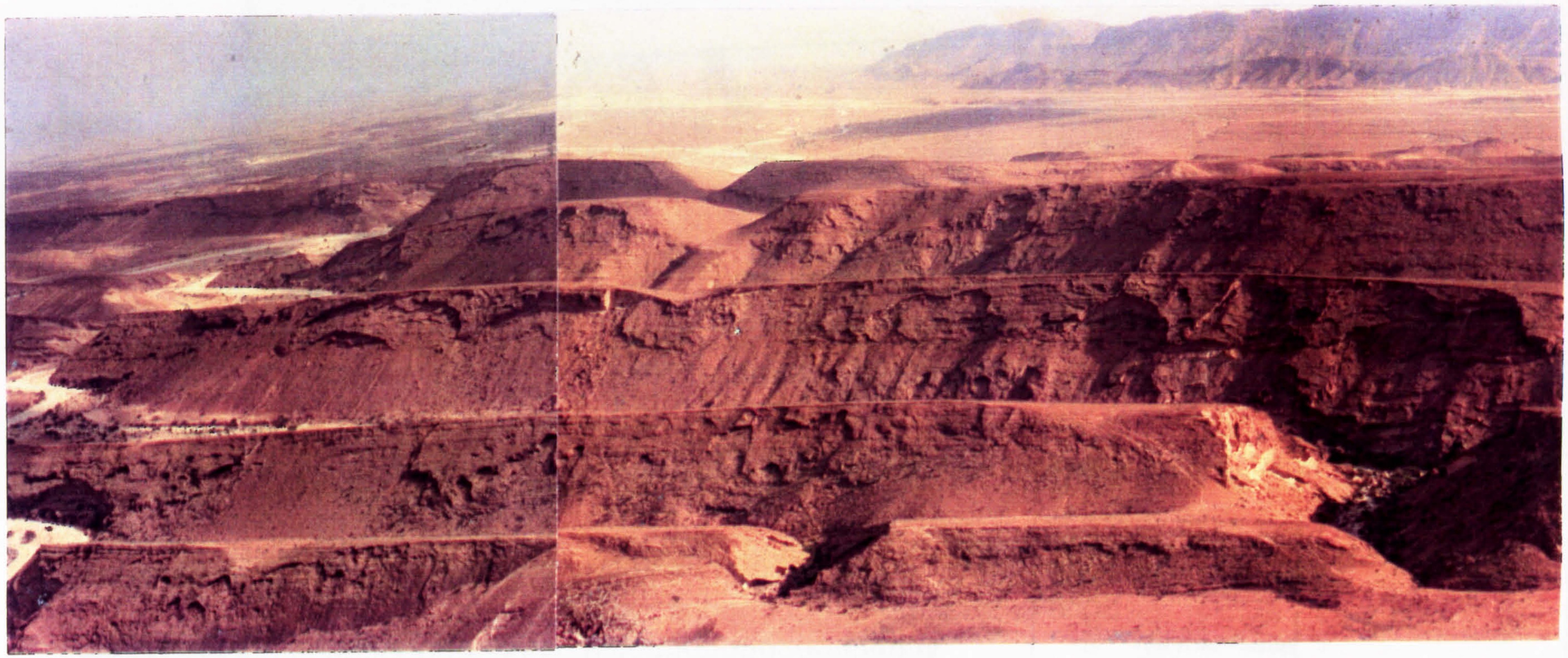

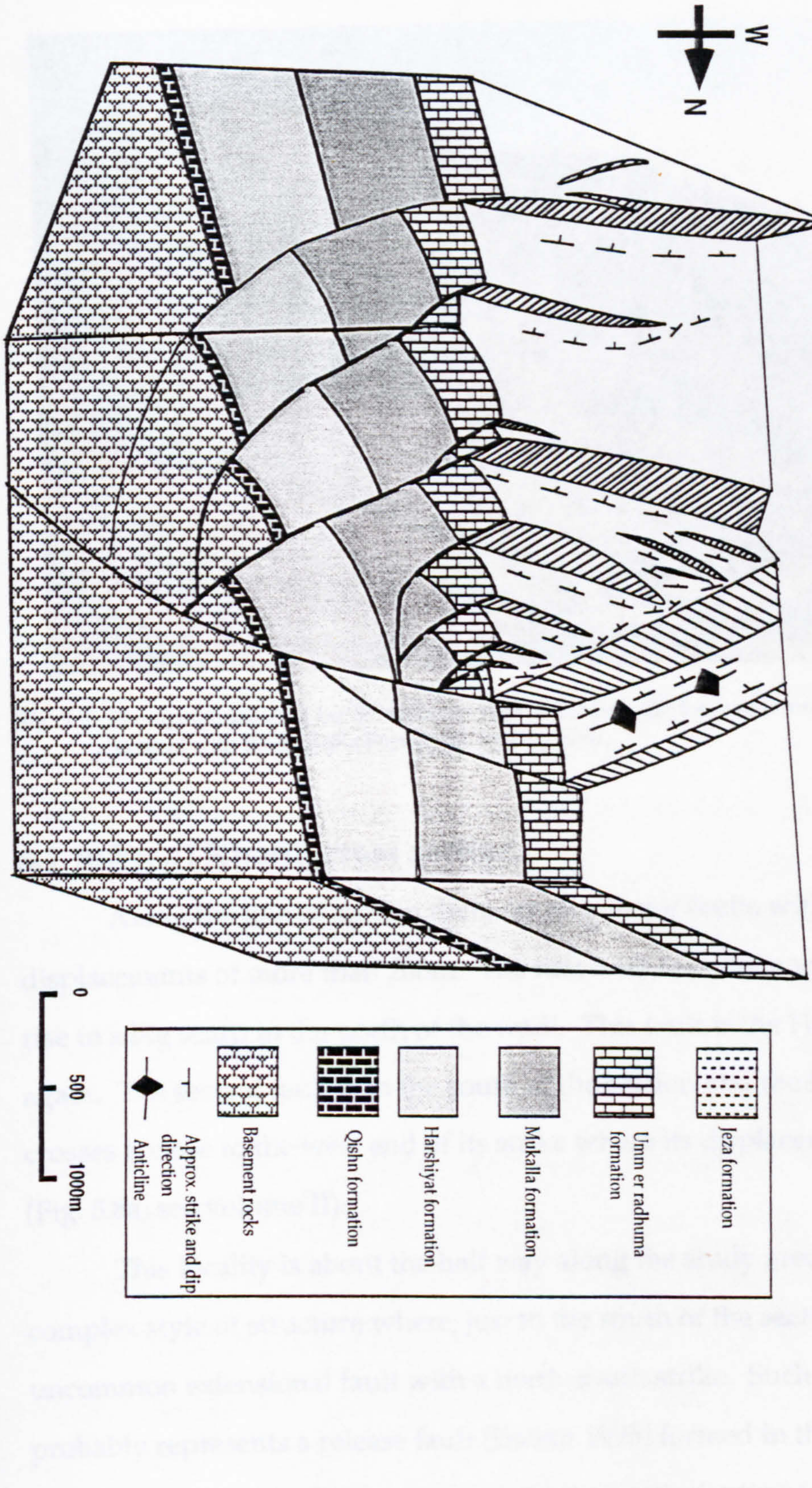

Fig. 5.5. Block diagram showing the the geometry of the faults with depth calculated from shapes of the rollover anticlines, the Switchbacks area.

Fig. 5.6. Photograph showing the Switchbacks fault which brought the Jeza Formation into contact with the Mukalla Formation, looking ENE.

5.1.10 Wadi Kharid cross section

Along the line of section there are two major faults with vertical displacements of more than 200m. The first fault is in the north and gives rise to a big scarp in the north of the wadi. This fault is the Haqab fault again. The second fault is in the south of the section and the line of section crosses it close to the west end of its strike where its displacement is low (Fig. 5.8a, see volume II).

This locality is about the half way along the study area and shows a complex style of structure where, just to the south of the section, there is an uncommon extensional fault with a north-south strike. Such a fault probably represents a release fault (Destro 1995) formed in the hanging wall due to differences in displacement along the north dipping faults (see sheet

IV). In the middle of this section the dip of bedding changes from south to north or becomes nearly horizontal especially in the Umm er Radhuma Formation. Close to faults, the clastic rocks of the Mukalla and Harshiyat Formations have steep dips into the faults giving reverse drag geometry. This change in the dip of bedding is due to the rotation of faulted blocks resulting in the formation of rollover toward south dipping faults where the bedding of Formations is rotated toward the north dipping faults (Fig. 5.8a, and sheet IV see volume II).

The south end of this 26.4km long section is dissected by step faults to form half grabens where the Jeza Formation is faulted down against the Umm er Radhuma Formation and the Pliocene conglomerate is deposited in these half grabens. In the middle of the section there is one major graben with a reverse drag fold associated with the south dipping fault. To the north of this graben the area is uplifted as a horst and the basement occurs at a very shallow depth (Fig. 5.8a, see volume II). This conclusion is confirmed from the offshore Al-Hami well to the south of this wadi where it penetrated the basement with only a thin cover of the Mukalla and Harshiyat Formations (Agip 1981 unpublished report and Haitham and Nani 1993) (Fig. 5.1). In the northern part of the section it is difficult to identify the displacement since the homogeneous clastic rocks of either the Harshiyat or Mukalla Formations occur in both hanging wall and footwall. However, if either of the two limestone members (Sufla and Rays) are present the displacement may be easily estimated. The section extends northward to the plateau where the dip of the bedding planes becomes very gentle and farther to the north nearly horizontal. Here both north and south dipping faults form small grabens (Fig. 5.8a, see volume II).

5.1.11 Restoration of wadi Kharid cross section

The stratigraphy for the balancing of this section is that recorded in the Al-Hami well offshore (Fig. 5.1) to the south of wadi Kharid (Agip 1981 unpublished report, Haitham and Nani 1990, Smewing 1993 personal communication) with additional field observations.

The restored section shows that the faults in this area have moderate dips except those in the plateau which are steeply dipping (Fig. 5.8b, see volume II). In the middle of this section the dip of the faults decreases downward indicating that these faults are listric.

The wadi Kharid section shows that the Mukalla Formation has become thin and this is supported by the subsurface data from the Al-Hami well where the Mukalla Formation is 120m thick (Haitham and Nani 1990). The reduced Mukalla Formation thickness is evidence that the wadi Kharid area and the Al-Hami well are located at the edge of the Mukalla high.

Restoration of this section gives a value of extension of 4.5% (Fig. 5. 8b, see volume II). This low value, compared to the other sections, may be attributed to the difficulty of identifying the trace of faults and their throws through the homogeneous clastic rocks in the middle of wadi where there are no marker beds to show the relative displacements. However, from the measurement of the vertical displacements throughout the study area, four regional transfer zones are identified and wadi Kharid is located in the second from the west and it is most likely that this low value is due to the section line crossing this structure (Fig. 5.8b, see volume II and 6.19).

5.1.12 Wadi Assad cross section

Wadi Assad is the biggest wadi in the eastern part of the study area. The line of this cross section has a length of 53 km and is constructed in the western side of the wadi (Fig. 5.1). This section was chosen to constrain the

geometry and style of structures and in the future it may be compared with the subsurface structures as a seismic line has recently been shot along this wadi. The thicknesses of Formations along this line have been derived from a number of sources (Agip 1981 unpublished report, Haitham and Nani 1993, Smewing 1993 personal communication) and additional field observations.

The Formations exposed in wadi Assad are the Harshiyat Formation represented by a lower clastic sequence at the base which is overlain by the Fartaq Formation with its three subdivisions of Rays member, upper clastic member and Sufla member which together are the lateral equivalent of the upper clastic Harshiyat in the west. Overlying these, are the Mukalla, Umm er Radhuma and Jeza Formations. Here again, the Mukalla Formation is thin and this is confirmed by the subsurface data from the Sharmah and Qusayr off-shore wells (Agip 1981 unpublished report, Haitham and Nani 1990).

The dominant structures along wadi Assad are mainly half grabens formed by north dipping faults with small antithetic faults dipping to the south forming small grabens (Fig. 5.9a, see volume II). On this section the faults with downthrow to the north can be divided into two groups. The first, located at both ends of the section, shows faults with a steep dip which are very obvious in the field but do not have large displacements and so cannot be adequately shown on the section. The second group, located in the middle of the section, have moderate dips (Fig. 5.9a, see volume II). Calculation of the faults' shape at depth from the shape of the roll-over anticlines shows that most faults flatten out at a high level within the Cretaceous or Tertiary sedimentary sequence as has been described in more detail in chapter 4. However, a fault at the southern end of this cross

section has a calculated trajectory which flattens out in the Jurassic rocks (Fig. 4. 5a, see volume II).

Fault segments in the south of the section are tilted with more dip than in the north and indicate that there is rotation by block faulting in this area. However, from the rollover the geometry of a fault in the south of this section is calculated and this confirmed that the fault is curved and soles out at great depth (Fig. 4.5g). In the middle of the section, just east of the line of section, there is a sudden increase in the dip of bedding planes to more than 40°, and this may be attributed to a south dipping fault which results in the repetition of the Mukalla Formation to give an abnormal thickness of more than 500m compared to the surrounding area (Fig. 2.12). This particular area is 1km to the south of Assad Al Jabal village.

The large faults which cross this section are of variable throw with vertical displacements between 200 and 690m. The largest fault is the north dipping wadi Al-Rakdoon fault, which controls the formation of this wadi, with a vertical throw of 690m bringing down the upper part of the Mukalla Formation into contact with the Harshiyat Formation (Fig. 5.9a, see volume II).

The dip of the faults varies between 35° and 80° and bedding planes are in the range from 30° in the south to 6° in the north with are limited areas of dips exceeding 40° (Fig. 5.9a, see volume II). The south dipping faults along the section could represent antithetic structures associated with the large north dipping faults where they sole out at shallow level either in the Mukalla Formation or the Fartaq Formation (Fig. 5.9b). The faults along this section dissect the plateau into fault segments of variable elevation from sea level on the coast to more than 1300m on the plateau (Fig. 5.9a, see volume II).

5.1.13 Restoration of wadi Assad cross section

The restoration and balancing of wadi Assad cross section shows that there are two group of faults along this section. The first group is located at the south of section line with high dips when they are restored to their original position (Fig. 5.9b, see volume II). The second group starts at the middle of section to the north end with slightly less steep dips. However, these faults show initial steep dips (Fig. 5.9b, see volume II). The faults at the northern end of the section, especially in the plateau, have kept or only slightly changed their dips. This is due to bedding in the plateau retaining its original horizontal attitude and, therefore, the faults are observed with their original steep dips (Fig. 5.9a-b, see volume II).

In the middle part of this section, which represents the location of the second group of faults, they become steeper in the restored section and penetrate downward to great depth. In contrast to north dipping faults, the south dipping faults have moderate dip in the restored section and they sole out at shallow depth. This result is supported by the field observations that the faults with downthow to the south are just antithetic structures to the north dipping faults and have low dip (Fig. 5.9b, see volume II). The extension calculated along the line of section is about 9%, and this value represents a high extension in the area (Fig. 5.9b, see volume II).

5.1.14 Wadi Bidish cross section

The section along wadi Bidish, of 43.5 km in length, was chosen to represent the eastern part of the study area (Fig. 5.1). Here the Mukalla Formation has become thinner and the Qishn Formation appears with a considerable thickness of more than 200m (Smewing 1993, personal communication) (Fig. 2.7). Evidence of horizontal slickenside lineations superimposed by dip slip lineations points to a complex evolution of

structures. Some 500m east of wadi Bidish, clastic rocks are underlain by Jeza Formation and overlain by, most likely, the Shihr Group (Fig. 6.3a). The occurrence of these clastic rocks may indicate that a reverse fault passes through this area. This reverse fault is most likely associated with the horizontal movement which is recorded to the south of wadi Bidish itself (Fig. 6.2a).

The thicknesses of Formations used in the construction of this section are from field measurements and from Smewing (1993 personal communication), Agip (1981 unpublished report), and Haitham and Nani (1990). The structures along the line of section are dominantly half graben formed by north dipping faults with some alternating graben and horst between north and south-dipping faults. In the south of the section a south-dipping fault brings the whole Tertiary and syn-rift sequences down into contact with the Umm er Radhuma Formation. Movement on this fault was contemporaneous with deposition of Oligo-Miocene sediments in the hanging wall of this fault (Fig. 5.11a, see volume II).

The stratigraphic Formations exposed in the wadi extend from the Qishn Formation in the bottom to the Jeza Formation on the top on both flanks of the wadi while further to the north, in the plateau the younger Rus and Habshiya Formations are encountered as interpreted from landsat images and air photographs (see sheet V, see volume II). Along this line of section on the western side of the wadi a dolomite layer, at about 600m elevation, is interpreted as part of the Fartaq Formation but, less likely, may belong to the Mukalla Formation in which case it may be the Lusp member, because a thickness of clastic sedimentary rocks lies beneath this dolomite. So, if this dolomite does indeed belong to the Mukalla Formation it implies that the Mukalla Formation has again become thicker in this area.

The faults in the south are of moderate dip and dip increases northward; concomitantly, the dip of bedding is more steep in the south and gradually decreases to the north. There are three major faults along this section with vertical displacements in excess of 200m. The southernmost fault passes along the main wadi and has a maximum displacement of about 270m. The hanging wall of this fault is very complex where the Mukalla Formation is very thin and the bedding planes are rotated to more than 40° (Fig. 5.10). Here the area of the hanging wall most likely was high as a horst during the Cretaceous extensional movements whereas the Mukalla Formation to the south and north of this area has greater thickness. The second fault is in the middle of the wadi and has 230m vertical throw to the south bringing the Jeza Formation down against the Mukalla Formation. The third large fault is located on the plateau at the northern end of the section and has a vertical displacement of 370m to the north. The faults have dips ranging between 55° and 76°.

Fig. 5.10. The bedding of the Mukalla Formation is rotated to more than 40° in the hanging wall of the major north dipping fault.

the faults cut through the Fartaq Formation (Fig. 5.9a see volume II). In general the cross sections display that most faults have steep dips which could have originated from a deep level, inherited from old faults that have the same trend.

In the basement blocks, faults of east-west and NW-SE trend are recorded with slickensides (Fig. 6.23 and 26) and faults and fractures are of similar steep dip in the lower Formations such as Qishn, Harshiyat and Fartaq. The rotation of the fault blocks rarely exceeds about 40°.

The variation in values of extension throughout the area along a strike length of more than 170 km from wadi Hawayrah in the west to wadi Bidish in the east implies that the geometry of extension in the northern margin of the Gulf of Aden is not simple. The study area has only undergone a small amount of extension. The greatest amount of extension is recorded in the eastern part of the area 9% in wadi Bidish, while the lowest value of 4.5% extension is recorded in the middle of the area, in wadi Kharid. Compared to other rift basins low values of extension may be attributed to a number of factors. For example, the area is deformed mainly by half grabens which gives low extension and no major faults of great displacement are observed; the major fault recorded in the area has a maximum displacement of 1320m (Fig. 6.14). On the other hand there are unmappable small faults which are very common and are not considered in the calculation. Also the numerous fractures are not included in the calculation.

Although, the regional transfer zones play a very important role in the value of extension as some of the cross sections passed across these zones which represent the locations of the minimum vertical displacements. Four transfer zones are determined by measuring the vertical displacements of mappable faults throughout the study area.

Although the wadi Hawayrah section crosses the biggest fault in the study area, the calculated extension is still low. This may be attributed to: 1. the highly fractured nature of the basement, 2. the section crossing two transfer zones (Fig. 6.14), 3. a length of greater than 3km of no exposure in the wadi floor which may conceal some faults.

5.2. Estimates of Strain by brittle faulting

The strain depends directly on the geometric moment which is expressed as the product of the average displacement (D) and the surface area (Marrett and Allmendinger 1991). The three dimensional control is rarely sufficient to evaluate the surface area of a fault, therefore, the trace length (L) on maps or cross sections provides the most convenient measure of surface area (op. cit.). Marrett and Allmendinger (1991) state that the measurement of strain in a brittle fault population is lower than the geometrical dimension of the region occupied by the fault population. They explain that the geometry of the sampling domain is of first-order importance for estimating strain in a brittle fault population and further that the geometrical dimensions (s) of the sampling configuration employed to study the strain commonly is lower than the geometrical dimensions (f) of the region occupied by the fault population. For example, the Earth's crust occupies a three-dimensional volume but maps and cross sections provide two-dimensional sampling (s=2), and traverses and boreholes provide one-dimensional sampling (s=1). Since the geometrical dimension of sampling is less than that of the region occupied by a fault population (s<f), the result is an underestimation of the number of small faults present in a region (Marrett and Allmendinger 1991). Furthermore, Nicol *et al.* (1996) state that the geometry of sampling has biases due to spatial variations in fault density, sample-line length, data resolution,

sequence rock type and differences in sampling methodology between or within different data types such as outcrop, coal seam plan and seismic section. The hypothesis that fault populations follow a fractal size distribution is supported by analysis of several data sets from different localities by many authors (Kakimi 1980, Villemin and Sunwoo 1987, Child *et al.* 1990, Marrett and Allmendinger 1991, Walsh and Watterson 1992, Watterson *et al.* 1996, Nicol *et al.* 1996, Clark and Cox 1996, Yielding *et al.* 1996, Cladouhos and Marrett 1996, Fossen and Gabrielsen 1996, Wojtal 1996).

Marret and Allmendinger (1991) propose a method of quantitatively assessing the sampling of brittle fault population based on the conjecture that faults follow fractal (power-law) size distributions. This approach is useful because only two parameters need be evaluated to construct a model (Fig. 5.12a). Plotting fault dimension against displacement shows that there is a near linear relationship between them on a log-log plot (Watterson 1986, Walsh and Watterson 1988, 1990, Marrett and Allmendinger 1991).

The growth model of Walsh and Watterson (1988) demonstrates that the relationship between maximum displacement and fault width is linear over a wide range and has a slope of 2 but the best-fit line to plotted data has a slope of 1.58 (Fig. 5.12b). Their model shows that the data do not lie along a single line. In addition, in the growth fault model the data which do not lie at 45° to the axis of the plot shows a non-linear relationship between displacement and dimension of faults (i.e. an increase in displacement corresponds to a much smaller proportional increase in width (Walsh and Watterson 1988) (Fig. 5.12b).

In this study, 10 traverses were measured in a direction parallel to the cross sections which, together with the sections, provide a representative sample over the whole area (Fig. 5:1 and see appendix 4). For each fault

intersecting this one-dimensional sample line, the vertical displacement was calculated using topographic maps to calculate the elevation difference of the same boundary on both sides of fault or sometimes by calculation from field measurement. There is larger error in assessing the throw of the smaller faults.

The relationship in general is linear at displacements of less than 800 m and at less than 45m the linear relationship breaks down (Fig. 5.12c). Faults with values of displacement less than 45m show a wide range of fault length (Fig. 5.12c). These data collected from the south Hadhramaut area are consistent with the data analysed by many authors in different localities (Kakimi 1980, Villemin and Sunwoo 1987, Walsh and Watterson 1988, 1990, Childs *et al.* 1990, Marrett and Allmendinger 1991, Walsh and Watterson 1992). These authors show that there is a linear relationship between displacement against trace length; however, each area has a different slope of the best fit line to the data. The line of best fit to the Hadhramaut data has a slope of 1.27. The fit to the data is good with displacements varying from 10m to 1320m, for trace lengths between 0.91km and 60km i.e, both vary by over two orders of magnitude.

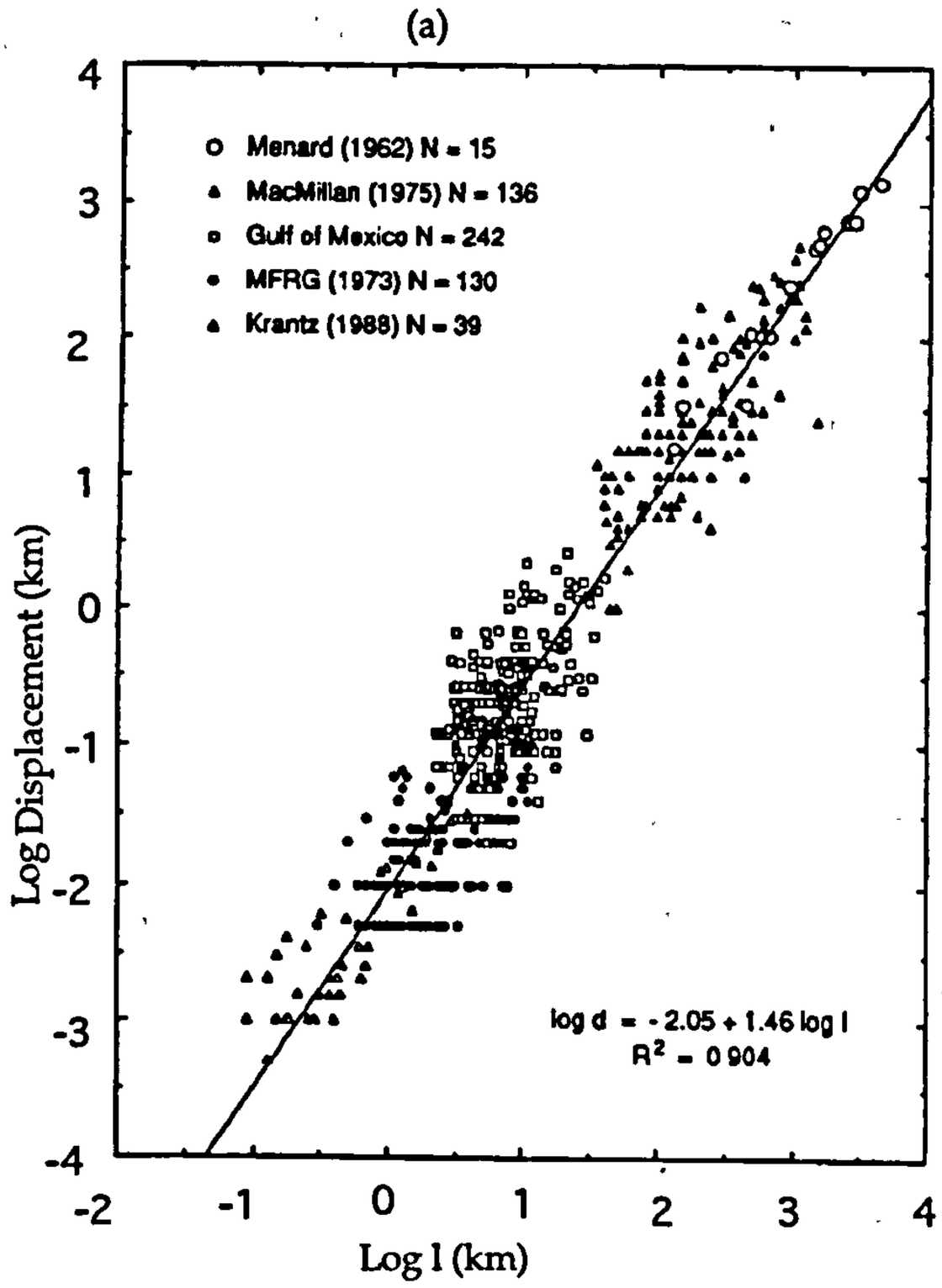

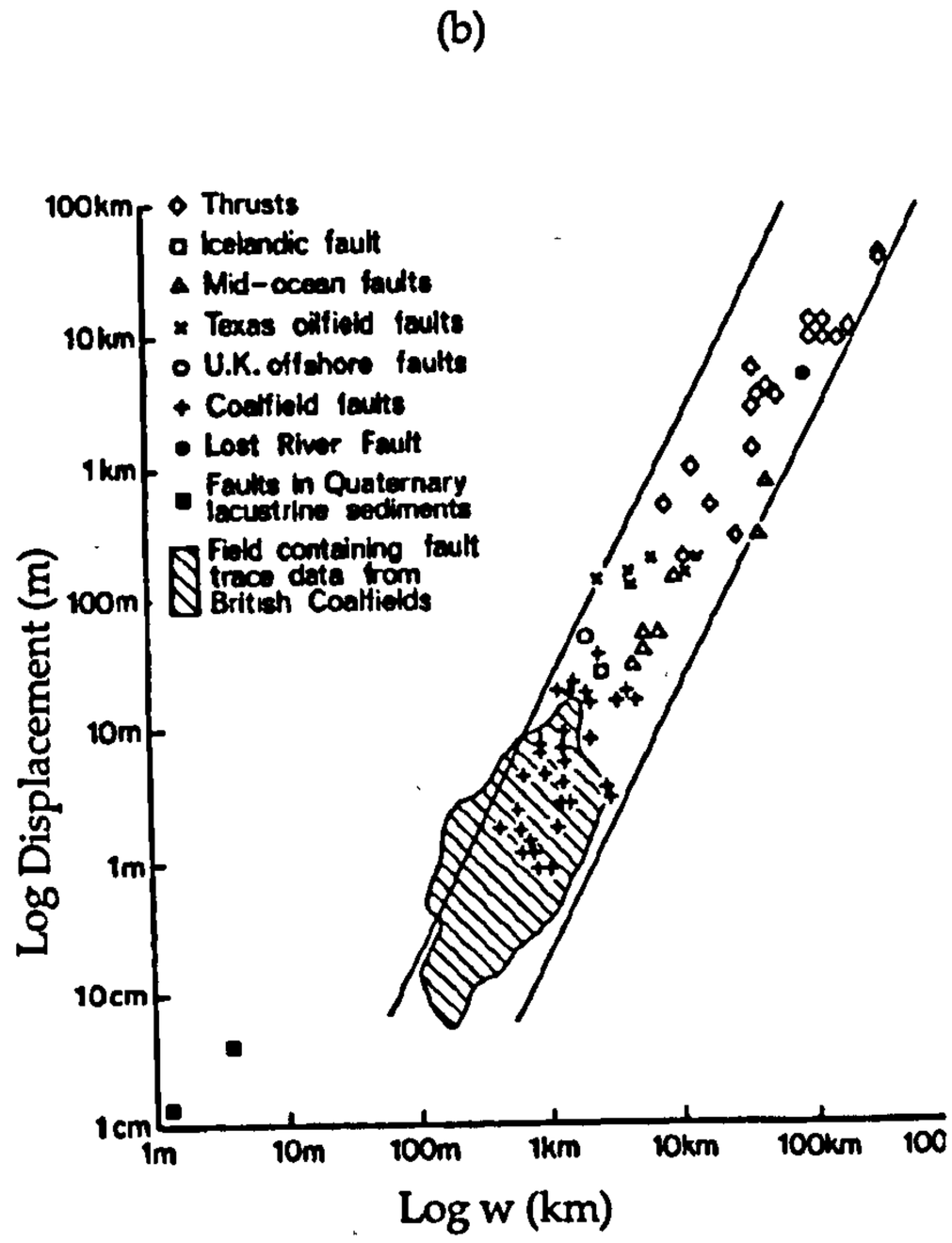

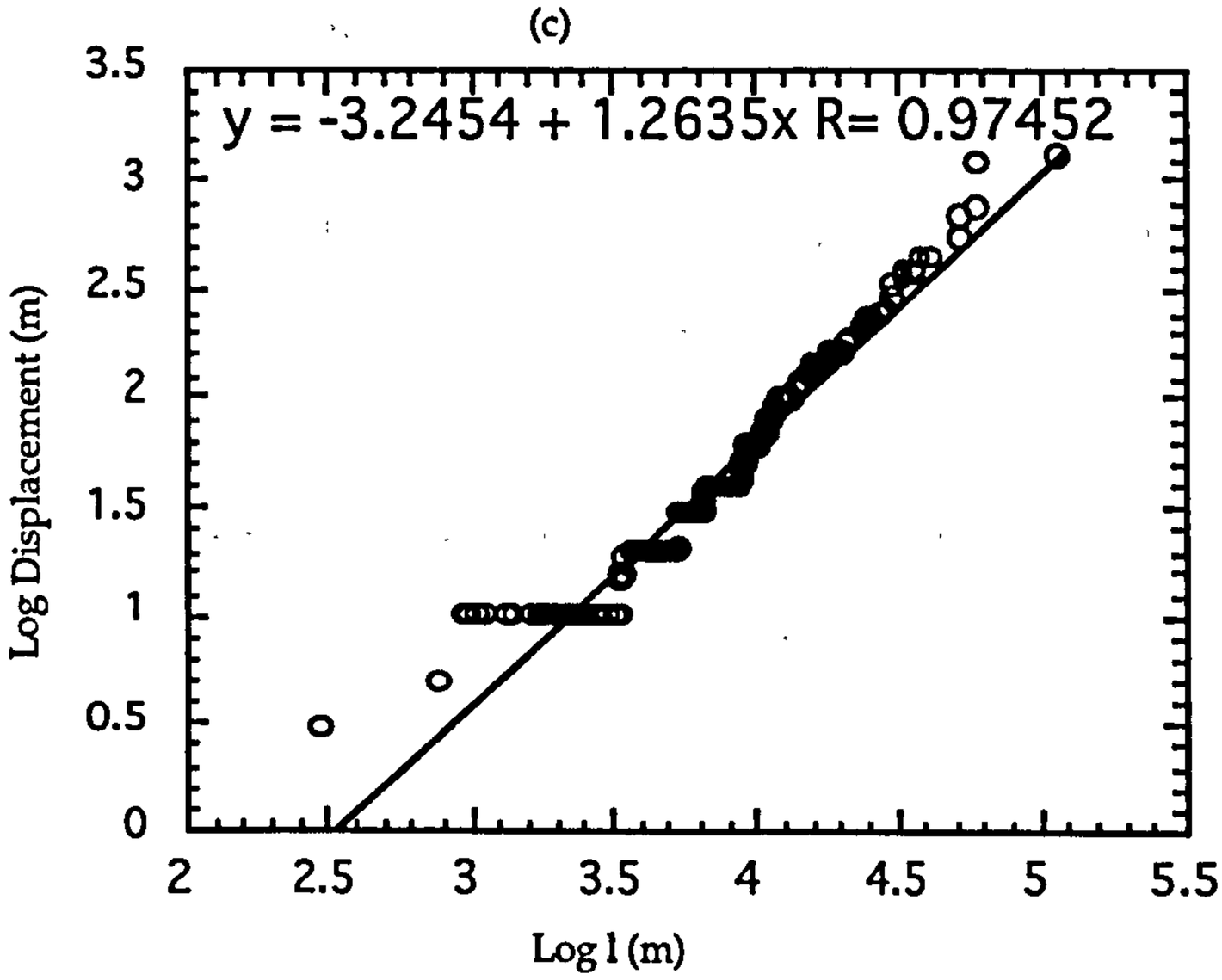

Fig. 5.12. (a) Displacement-trace length data. The line representsthe best fit to the data (after Marrett and Allmendinger 1991) (b) logarithmic plot of width against maximum displacement for faults. Continuous lines have a slope of 2, as appropriate to the growth model (after Walsh and Watterson 1988) (c) displacement-trace length of faults in Hadhramaut area.

5.2.1 Fault displacement populations

The same data which are plotted on the growth fault model may also be plotted on the fault displacement population curve to show the fractal size distribution of the brittle faulting (Fig. 5.13a-b and see appendix 4).The measurement and interpretation of fault displacement have been considered by Childs *et al.* (1990), Heffer and Bevan (1990), Marrett and Allmendinger (1991) and Walsh and Watterson (1992). The fault may be assessed either by maximum displacement or by maximum dimensions. One dimensional samples have been measured along the selected traverses in the area and the displacements are measured at each intersection between the sampling lines of traverses and fault traces of maps. The vertical displacement of 217 faults has been sorted into magnitude order and plotted on a log-log scale against the cumulative number of faults. This gives the fault displacement population curve.

The plotted data coincides with the curve of fault displacement population implying that brittle faulting follows a fractal size distribution. Three distinct segments of the curve can be delineated (Walsh and Watterson 1992) (Fig. 5.13a). The steep right-hand segment of the curve intersects the abscissa at the maximum displacement value of 1320m. This segment is regarded as independent of sampling effect (Walsh and Watterson 1992). However, the field data, particularly from the major faults has been measured with good care and checked in the field so that this relationships is probably due to many of the faults having similar displacements (Fig. 5.13c). The second segment is the central segment of the curve which has an irregular shape and is of variable slope ranging between 0.5 and 1. The central segment represents the mean average of fault size in the southern flank of south Hadhramaut arch with displacements between 40m and 400m. The left-hand segment represents the small faults. Thus

from the fault displacement population curve, the faults in the south Hadhramaut area may be classified into three groups according to their size and displacements.

The first group are the major faults which control the shape and morphology of the northern margin of Gulf of Aden in general and the southern part of the south Hadhramaut area in particular. These large faults, for example, wadi Hawayrah fault, wadi Hamim fault, Haqab fault and wadi Al-Rakdoon fault, have vertical displacements of more than 600m and may reach more than 1300m, as in the wadi Hamim fault (Fig. 5.12c). They form the biggest scarps in the southern part of the south Hadhramaut area and account for the difference of elevation of more than 2000m between the plateau and the coastal plain. This group is not showing well steep segment as in Walsh and Watterson figure due to the lack of reading and repesents by two reading only in the study area.

The second group which includes most of the faults are those of medium size with average displacements between 40m and 400m. This group has controlled the structural style in the area with its half graben and also full graben. The third group are the small faults which are mappable at a scale of 1:50,000 with displacements of between 10m and 40m. However, there are numerous smaller faults which are not mappable on this scale which have been measured and these are analysed together with the mappable faults and discussed below in chapter 6.

In the fault displacement population curve there is an indication of a real decrease in slope for faults with displacements less than 10m. This implies that either the power-law relationship does not apply as suggested by Walsh and Watterson (1992) or there may not be enough data to satisfy that relationship. However, the present data strongly conform with those from other areas (Kakimi 1980, Villemin and Sunwoo 1987, Heffer and

Bevan 1990, Marrett and Allmendinger 1991, Walsh and Watterson 1992) showing that the fault populations do have a fractal size distribution (Figs. 5.13c)

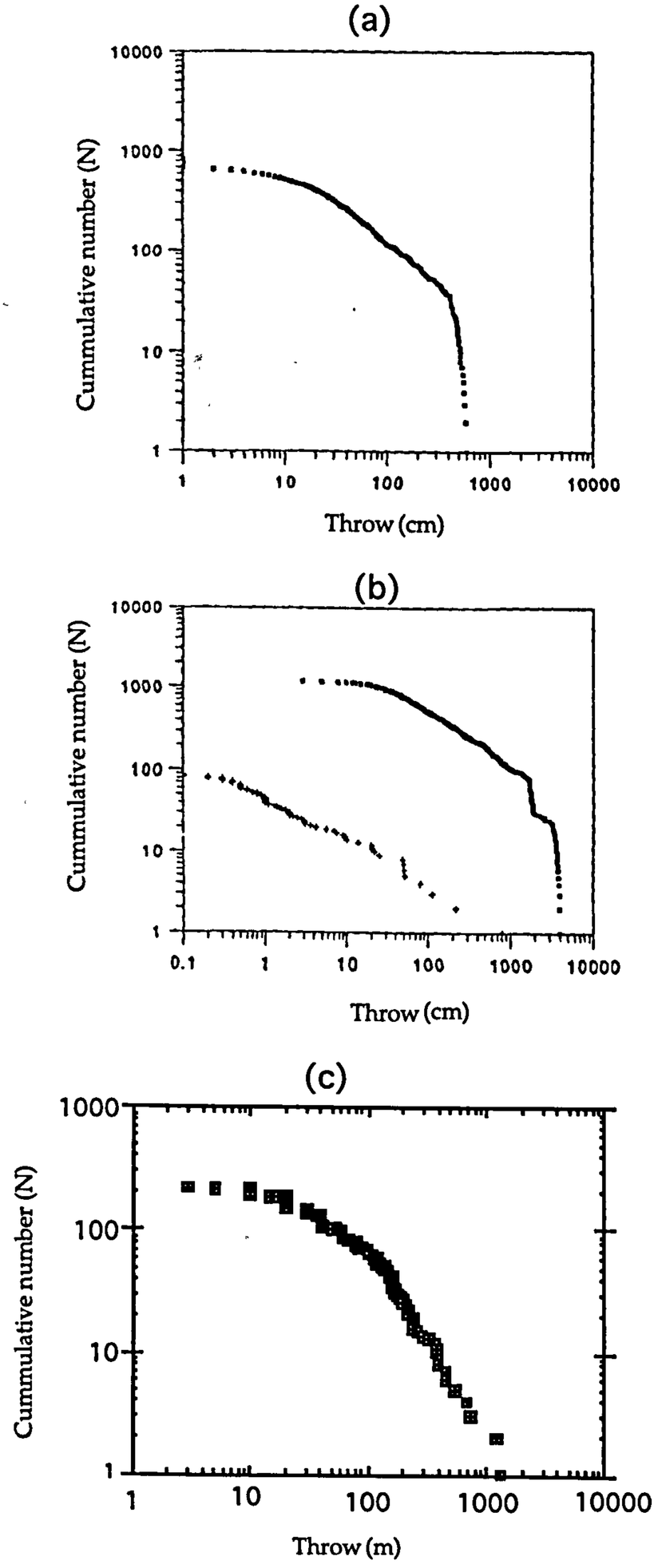

Fig. 5.13 . (a) Fault displacements population curve from seismic reflection data (b) multi-line displacement population curve from mine plan and outcrop data in Britain (after Walsh and Watterson1992) (c) fault displacement population curve from outcrop data in Hadhramaut area.

CHAPTER 6

ANALYSIS OF FAULTS AND FRACTURES

6.1 Introduction

Horst and graben and half-graben systems are the two principal modes of large scale brittle crustal deformation during extensional tectonics. They differ geometrically depending on whether the two faults of a conjugate normal fault set are equally developed (symmetric) or one is selectively formed (asymmetric). Possible theories of faulting, however, do not predict the asymmetry. The Coulomb-Navier criterion for shear failure, for example, can only determine two potential fault planes which are symmetric to the principal stress axes (Jaeger and Cook 1979).

Both continental rifts, for example, the Basin and Range province (Wernicke 1981), North Sea (Ziegler 1982a, White and McKenzie 1988) and mid-ocean ridges (Harper 1985), have a common geometric feature, namely systematic half-grabens with fault asymmetry, nearly equidistant fault spacing and tilting of fault blocks; such characteristics are well simulated in sandbox experiments (Ellis and McClay 1988, Ishikawa and Otsuki 1995).

Most rift basins consists of depressions defined by half-grabens, the polarity of which often changes along strike across transfer zones (Gibbs 1984, Etheridge *et al.* 1985, Rosendahl *et al.* 1992). The structural style of extensional basins depends not only on the orientation of the controlling stress regime relative to the zone of crustal extension (orthogonal or oblique rifting) and the amount of extensional strain but also on the availability of pre-existing basement heterogeneities and on lithological heterogeneties within the sedimentary fill of such basins which can be reactivated by tension (Tron and Brun 1991).

However, during the evolution of a rift the stress regime governing its development can change with time, orthogonal extension may give way to transtensional faulting and even to transpressional deformation, for example, the North sea rift system and the Rhine graben (Illies 1975, 1981).

The underlying craton comprises crystalline rocks of Archaean (Windley *et al.* 1996) to Early Cambrian in age. The platform represents the passive margin of the Palaeozoic Tethys sea (Al-Thour 1992). The Arabian plate has been subjected to several tectonic movements since the late Proterozoic. However, the northern margin of the Gulf of Aden is located in a very active area where ocean floor-spreading is going on now in the Gulf of Aden to the south and in the Red sea to the west, and to the east is the Zagros thrust zone and in the north the Dead Sea rift (Fig. 1.2).

These boundaries represent major tectonic trends and are the most important structural elements, which have controlled the formation of major basins on both the south and north margins of the Gulf of Aden and have affected the distribution of lithologic thicknesses and the geomorphology of its margins. The northern margin of the Gulf of Aden is divided into basins and swells of different age from Early Jurassic to Recent (Fig. 1.3 and see chapter 7).

The structural trends which have controlled the formation of basins are inherited from the ancient Proterozoic trends which have been rejuvenated

during the Early Jurassic and have subsided to give thick sequences of sediments of Jurassic to Late Eocene in age.

The south Hadhramaut area represents part of the northern margin of the Gulf of Aden and consists mainly of sedimentary rocks, these sedimentary cover rocks reach up to 3700m thick (Beydoun 1969). The southern flank of the south Hadhramaut arch, which extends from wadi Hajar in the west for about 350km to Ras Sharwayn in the east comprises the flat-lying southern part of the plateau and the faulted region bordering the coastal plain. The southern flank of the south Hadhramaut arch is subjected to different tectonic trends of extension fractures which may be classified into two types according to their opening. The term fracture is used here for both faults and fractures, faults have displacements of a wide range from less than 10m up to 1300m or more and may be studied on a wide range of scales from outcrop to small-scale map; fractures have no displacement on the scale of observation. Faults are the most important type of fracture in the deformation of this area. These faults are mainly extension faults which have dissected the area into half grabens and sometimes form as conjugate pairs to produce full grabens.

The second class is represented by closed fractures without apparent opening and are of outcrop scale; and these are of at least four trends, though two are dominant. One trend is associated with or parallel to the open fractures and are coincident with the trend of the Gulf of Aden, and the other trend is nearly perpendicular to this first trend.

The fractures will be analysed in two ways. Firstly, the structural pattern, geometry, accommodation structures associated with faults and their relationships based on the mapping field data will be examined. Secondly the data which have been measured on both opening and closed fractures will be analysed to determine the trend of extension.

6.2 Major structures in the northern margin of the Gulf of Aden

6.2.1 Major faults

The northern margin of the Gulf of Aden shows evidence of repeated rejuvenation of old fractures, especially the NW-SE trending fractures of the ancient Najd fault system (Fig. 1.2) (Brown and Jackson 1960). Such rejuvenation resulted in the formation of deep basins in which the basement surface is depressed to an estimated depth of 5-6km, for example, in the Ataq-Balhaf Trough and the Hajar Trough to the west of the study area (Isaev *et al.* 1984). In addition, to the east of the study area, there are other depressions, also with a NW-SE trend, called the Qamar Trough (Iseavs *et al.* 1984), the Aljuf-Marib basin, (Diggens *et al*, 1988 and Al-Thour 1992), and Jeza-Howarrine basin (Ellis *et al.* 1996) (Fig. 1.3).

In general, the northern margin of the Gulf of Aden has been subjected to at least four trends of fractures. These trends can be easily identified and have controlled the deformation of this margin. The Najd (NW-SE) trend which represents the major structures both to the east and west of the study area and is recorded as major rejuvenated extensional faults during Cretaceous time within the area, for example, the wadi Hawayrah fault (see chapter 7). The Gulf of Aden (WSW-ENE) trend is the most dominant in the study area and overprints the older trends. The northeast African North-South to NNE-SSW trend is observed as less common small faults and numerous fractures in the area and the final and youngest trend which is most likely related to the NE-SW Alula-Fartaq transform direction affects all rocks including the syn-rift and Pliocene sediments.

The south Hadhramaut area has many large arcuate faults which can be traced for over 50km and which have vertical displacements of more than 700m. These faults drop the sedimentary sequence down towards the south by over 3000m into the rift of the Gulf of Aden. The curved and discontinuous

nature of the faults here played a role in determining the shape of the margin which may be related to the rotation of the Arabian plate resulting from the greater spreading rate in the Gulf of Aden compared to the Red Sea (Burek 1969) (Fig. 1.3).

The study area is similarly subjected to all these four trends, but the commonest trend occurring in this area is the WSW-ENE (Gulf of Aden) trend. The flat-lying coastal area has been dropped down by successive south dipping faults during the mid-Tertiary rifting, while the plateau is dissected by several extension faults of both synthetic and antithetic nature to form the crestal collapse graben and half graben of the same period. Sometimes full grabens are present and these are arranged in an en-echelon pattern separated by transfer zones (see sheet I, II).

In the study area there are at least four large faults with vertical displacement of more than 600m and with a strike length of over 50km. The Hamim fault, for example, has a maximum throw of more than 1,300m and brings the whole pre-rift sedimentary sequence into contact with metamorphic basement. The strike of this fault is very irregular and its eastern end is rotated around vertical axis of about 80°, the maximum value of the downthrow is in the middle to the south of Lusp village, and decreases westward in the wadi Asfal Al-Ein (Fig. 1.5 and 5.1). Similarly the Hawayrah fault to the north, which is parallel to the Hamim fault, has a throw of more than 700m and may be divided into a number of linear segments. The south dipping Haqab fault brings the Umm er Radhuma Formation down against the clastic lower Harshiyat Formation and also gives a downthrow in excess of 700m. The Wadi Al-Rakdoon fault which passes along the Al-Rakdoon valley and across wadi Assad Al-Jabal is a more or less planar fault and which extends for more than 60km with about 680m vertical displacement.

Both the Hawayrah and Hamim faults are arcuate and are concave to the NE but may be considered as a series of linear segments (Fig. 5.1). The Haqab

fault passes through the plateau parallel to the axis of the south Hadhramaut arch and concave toward the SW. In addition to these major faults numerous faults of variable size and displacements dissect the plateau to give the prominent half grabens. These faults sometimes change their polarity and they are arranged in both right stepping and left stepping en echelon faults. A characteristic property of these faults as a group is that where the displacement becomes a minimum small faults converge toward the major fault as displacement decreases on the major fault and it is transferred to another major fault, a series of small faults form which dissect the relay ramps and arrange in an en echelon pattern. These transfer zones occur therefore, as a series of soft-linkage transfer zones at various scales (Fig. 5.1). Similar transfer zones are recorded in east Africa rift (Morley *et al.* 1990).

6.2.2 Strike slip faults

It is not easy to recognise strike slip faults in this area due to the intensive dissection of the region by extension faults related to the rifting of the Gulf of Aden. However, from field observations there is strong evidence of strike slip faulting, especially in wadi Bidish, wadi Shakhawi, wadi Assad in the east and the Switchbacks area. In all of these areas horizontal slickensides are observed but no offset of markers can be identified from the geological mapping, or from field observation (Fig. 6.1a-b and 2a-b).

In wadi Bidish there is a major north dipping fault whose hanging wall is very complex. Here the Mukalla Formation is very thin and this is interpreted as a high during sedimentation of the Mukalla Formation. However, to the east of wadi Bidish clastic rocks underlain by limestone are exposed (Fig. 6.1a-b) and are interpreted to be the Mukalla Formation, which has been brought in by strike slip faulting although the position of the fault is not clear. Here, horizontal slickensides occur on a steeply dipping fault (Fig. 6.2a).

Further evidence for horizontal movement occurs in wadi Shakhawi and wadi Al-Masila where small thrust faults are recorded within the Umm er Radhuma Formation and the Qishn Formation respectively (Figs. 6.4a-b).

6.2.3 Folds

In general, the northern margin of the Gulf of Aden was subjected to compressional uplift during late Eocene time to form a series of alternating anticlines and synclines which are arranged in an en echelon style such as the Dhufar-Huqf arch to the east (Saint-Marc 1978), the coastal range arch to the west (DGME 1986) and the north and south Hadhramaut arches (Beydoun 1964, Burek 1969) (Fig. 1.3). To the west of the study area the Ataq-Balhaf and Hajar troughs are separated by a narrow compressional uplift, the Al-Aswad ridge (Iseavs *et al.* 1984) (Fig. 1.3). In addition to the regional major folds there are small folds associated with faults, the most common being monoclinal folds. In the coastal plain there are several anticlines and synclines of considerable size whose formation may be related to faulting after the deposition of the Oligo-Miocene sediments. The axial traces of these folds in the coastal plain are parallel to the axes of the south and north Hadhramaut arches with approximately subhorizontal plunges (see sheet I, II, and VI). Several monoclines occur as accommodation structures with the extensional faulting which will be described below in this chapter.

6.3 STRUCTURAL PATTERNS

A number of distinct areas that exhibit different patterns of extensional faulting can be defined within the fault system in the south Hadhramaut arch. Three localities in the southern flank were selected to show the patterns, geometries of faults and their relationships with transfer zones in the area; these are the Hasis area in the western part of study area, the Switchbacks area and the Al-Madi area to the west of wadi Araf. In addition some other localities

will be considered to show the variation of fault relations along the strike of the arch (Fig. 1.3).

The Hasis area is characterised by a graben bounded by steep conjugate faults (Fig. 6.6a). The graben between these conjugate faults is asymmetrical since the displacements on these faults are not equal. The relationship of the faults in the Hasis area is shown in (Fig. 6.6b). The conjugate faults are complex and similar to those which have recently been classified into simple and complex conjugate faults (Nicol *et al.* 1995). The Hasis structure is one of a number of subparallel graben lying in the western part of the study area. This graben is bounded by asymmetrical conjugate normal faults with vertical offsets of 200m along the north boundary while the southern boundary consists of several small half graben with vertical offsets ranging from 50 to 100m. Both of these faults splay toward the west and
east on subsidiary faults associated with small graben (see sheet I). It is apparent that these much smaller scale graben occur in all parts of the study area. In the Hasis area, the relay structures between adjacent en echelon faults are characterised by both soft and hard-linkages.

Half-graben have recently been recognised as the basic rift geometry (Rosendahl 1987, Bosworth 1985, 1987, Ebinger*et al.* 1984) and this geometry is well displayed in the cross sections of this and the Switchbacks area (Fig. 6.7a). The Switchbacks areas consists of a series of step faults to give half grabens as the dominant style of structure in this area
(Fig. 6.7b). In addition, two full graben are arranged in an en echelon pattern (Fig, 6.7a and 8). The half graben are bounded on one side by the main border fault zone, the throw of which is greater than the throw on the top of the hanging wall due to the rotation of the hanging walls near the scarps of faults. This asymmetrical subsidence of faulted blocks creates an increase in subsidence towards the border faults. However, the half grabens in the Switchbacks area are of a small scale compared to the other half grabens in the area and are most

likely controlled by major south dipping faults which result in the subsidence of all half graben in its hanging wall to more than 250m. Its footwall is uplifted to give the top of the Switchbacks a height of 900m above sea level. The full graben in this area lie in a transfer zone with alternating ridges and basins (see sheet I, volume II). The ridges represent the footwall of divergent faults, while the grabens are formed as result of conjugate convergent transfer zones. These two full graben are asymmetrical, formed by asymmetrical conjugate convergent faults (Figs. 6.7a and 8). The Al-Madi area represents the most important change in the polarity of faults in the southern flank of south Hadhramaut arch. Here, a major full graben is formed by two conjugate faults namely the Haqab fault to the north and the Araf fault to the south. These two faults are very distinct structures in the plateau where very steep scarps have been formed (Fig. 6.9a). The subsided block is segmented by a number of both synthetic and antithetic faults to form alternating horsts and grabens within the major full graben (Fig. 6.9b). This graben is located on the axis of the south Hadhramaut arch where the dip of the stratigraphic sequence in the footwall of the Haqab fault changes to the north (see sheet II and III, volume II).

Other fault geometries occur but are not common. For example, faults with a linear, rather than arcuate outcrop occur on the plateau to the north of Wadi Hawayrah. The faults in this area are characterised by overlapping synthetic transfer faults with opposing dips. The transfer zones are formed parallel to the strike to give strike ramps between two overlapping synthetic faults as, for example, at the Switchbacks, Haqab and Hasis areas. In the plateau to the north of wadi Hawayrah and the Switchbacks area another style of relay structure occurs. Here the linear faults are linked by strike relay ramps parallel to the strike of the faults and forming soft-linked transfer zones, for example, zones A and B in (Fig. 6.10). Throughout the area the relay segments are broken up by minor faults such as the zones indicated by C and D in (Fig. 6. 9). Some

faults are strongly curved, for example, west of Ydmah, and are often of short strike length (Fig. 6.11).

6.3.1 TRANSFER ZONES

Transfer zones form important structural elements in extensional regimes, accommodating displacement changes between fault segments. Transfer zone geometry is related to the extension direction, the displacement, dip polarity, overlap and overstep of fault segments (Gawthorpe and Hurst 1993). Relay structures are considered to form where offset listric fault traces, or two en echelon strands in map view, curve into a single low angle or subhorizontal fault at depth (Larsen 1988). A relay ramp is the structure between the two tip lines of the offset faults connecting the hanging wall and footwall blocks. In map view, relay structures may be arranged in different patterns from random to symmetrical and en echelon. The dip of bedding in the relay ramp follows the curvature of faults at their tips. In a propagating relay system the hanging wall block can also be detached from the footwall block by fault migration parallel to the relay ramps, see, for example, Larsen (1988) (Fig. 6.12). Where the two initial faults in their central part have been offset towards the hanging wall block, the deformation will continue on these two faults to join up making one major fault. The displacement along the strike of this major fault shows a variation with minimum throw where these two fault join up (Fig. 6.13).

Relay structures occur in extensional regimes at relatively low strains (Larsen 1988) while high strains result in the formation of transfer faults connecting the two faults (Gibbs 1984). The transfer zones in the southern part of the south Hadhramaut arch display a wide range of geometries from discrete fault zones to zones of more complex structures with local contractional deformation. However, the soft-linkage transfer zones in which a relay ramp occurs between the en echelon fault tips are the most common (Fig. 5.1). The

most characteristic feature of the faults is their arcuate shape and common soft-linked transfer zones (Fig. 5.1). Transfer faults similar to those described by Gibbs (1984) are recorded in the western part of the area (see sheet I). In addition, small faults of north-south trend have been mapped at a scale of 1:50,000 particularly in the wadi Hawayrah area which could be referred to as release faults. They occur in the hanging wall of the wadi Hawayrah fault and in the hanging wall of wadi Hamim fault and most likely represent reactivation of an old basement trend (see sheet I). Throughout the area small north-south faults, too small to be recorded on the maps, are observed. Mappable north-south faults occur in wadi Hawayrah, south wadi Kharid and in wadi Shakhawi.

The best classification of transfer zone geometry is by Morley *et al.* (1990) which is based on the relative dips of the fault boundaries and the degree of overlap of fault terminations (Fig. 3.4). The faults in the south Hadhramaut area are arranged en echelon with both right-stepping and left-stepping patterns (Fig. 5.1). The relationship of these extensional faults in the study area with their accommodation structures such as relay zones (soft-linkage), release faults (Destro 1995), hanging wall rollover folds and antithetic faults will now be described. The faults in this area are characterised by overlapping synthetic transfer faults with opposing dips (Fig. 5.1). The transfer zones are formed parallel to the strike to give strike ramps between two overlapping synthetic faults as, for example, at the Switchbacks, Haqab and Hasis areas. In the plateau to the north of wadi Hawayrah and the Switchbacks area another style of linear relay structure occurs and this is characteristic of linear fault segments formed by synthetic normal faults (Fig. 6.10). The most common relay structure in this locality is the strike relay where the faults transfer parallel to the strike of faults, a second characteristic of the faults is soft-linkage and, finally, a constant

a)

b)

Fig. 6.1. (a) Horizontal slickensides on a steep fault surface by the roadside in the Switchbacks area, (b) grooving on a fault, Switchbacks area.

a)

b)

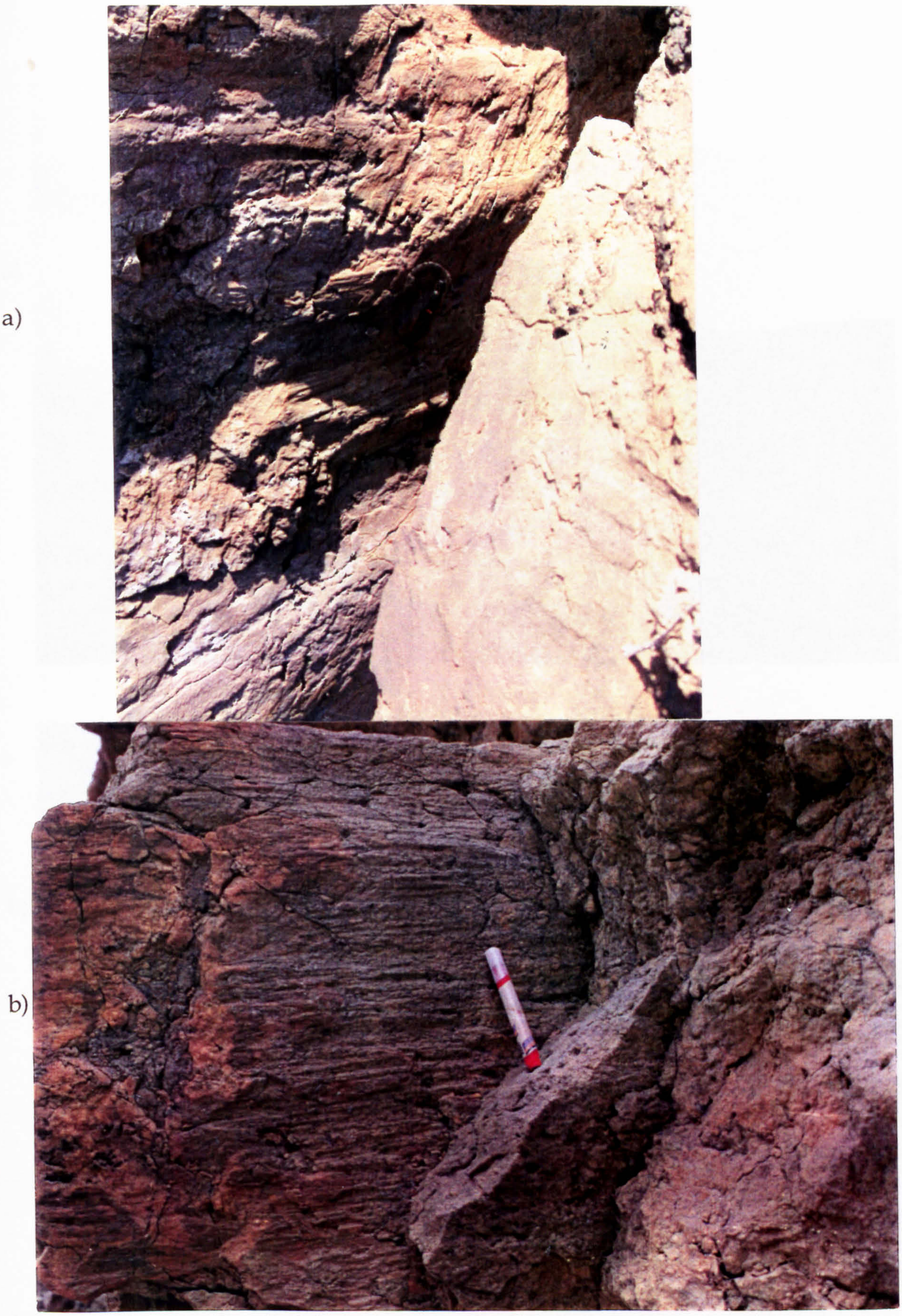

Fig. 6.2. (a) Slickensides in both horizontal and vertical directions on a fault surface in wadi Bidish, (b) horizontal slickensides on a fault surface in wadi Shakhawi.

a)

b)

Fig. 6.3. (a) Clastic sedimentary rocks and dolomite of the Mukalla Formation (m) overlies the Jeza Formation (J), (b) shows the Mukalla Formation (M) underlies the Shihr Group (Sh), east wadi Bidish.

a)

b)

Fig. 6.4. (a) Low angle fault affecting the Umm er Radhuma Formation in wadi Shakhawi, (b) thrust fault in wadi Al-Masila.

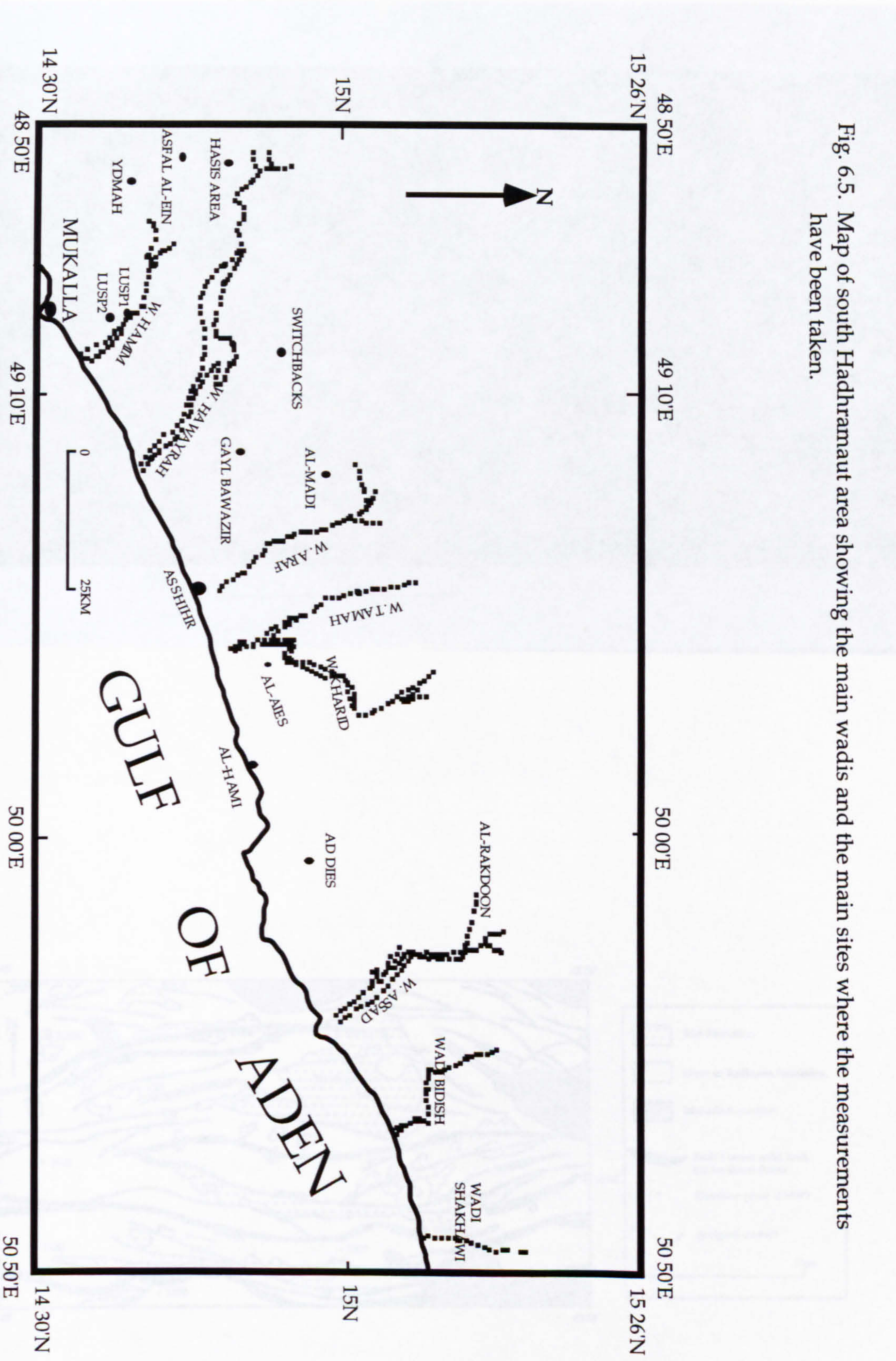

Fig. 6.5. Map of south Hadhramaut area showing the main wadis and the main sites where the measurements have been taken.

a)

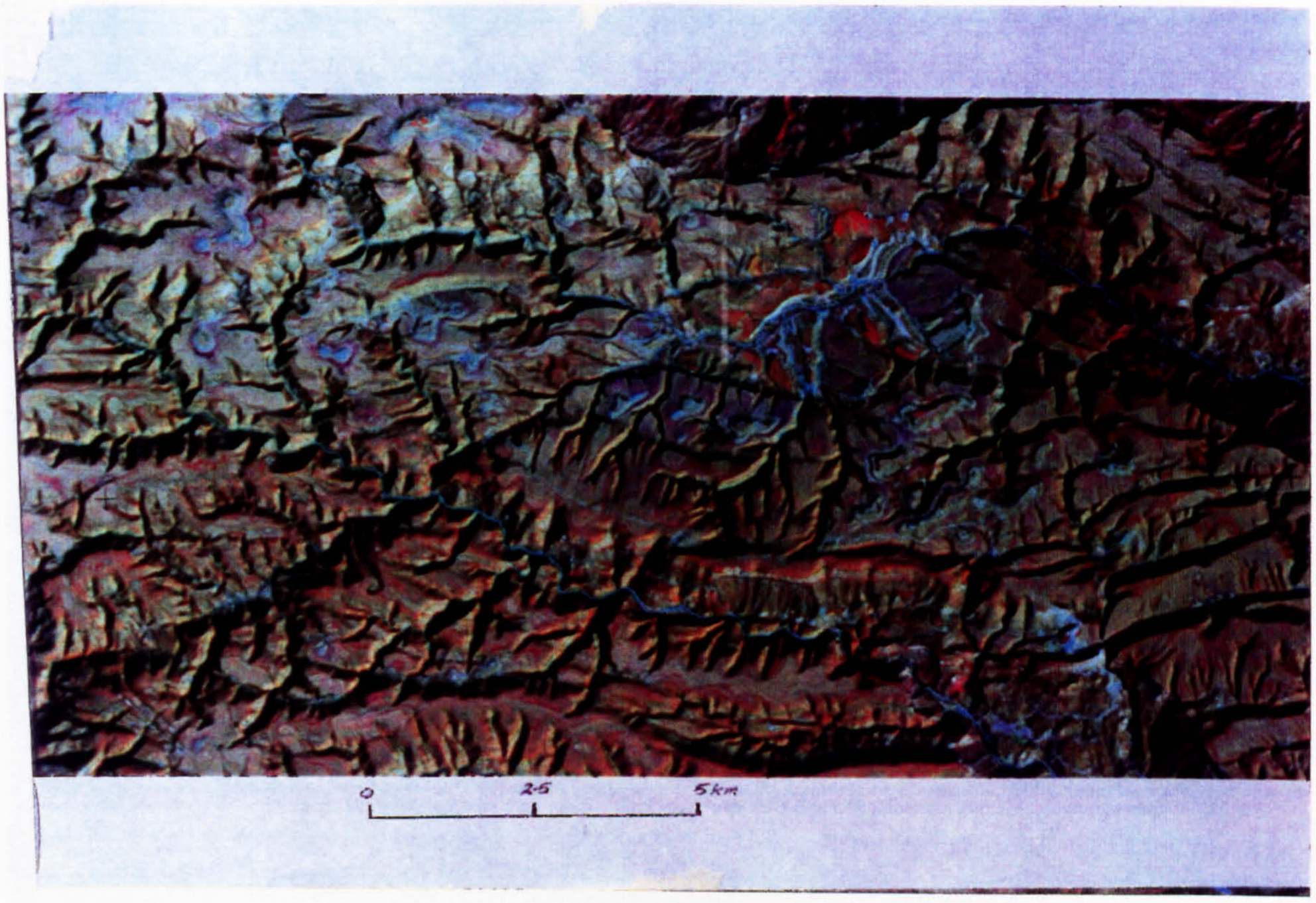

b)

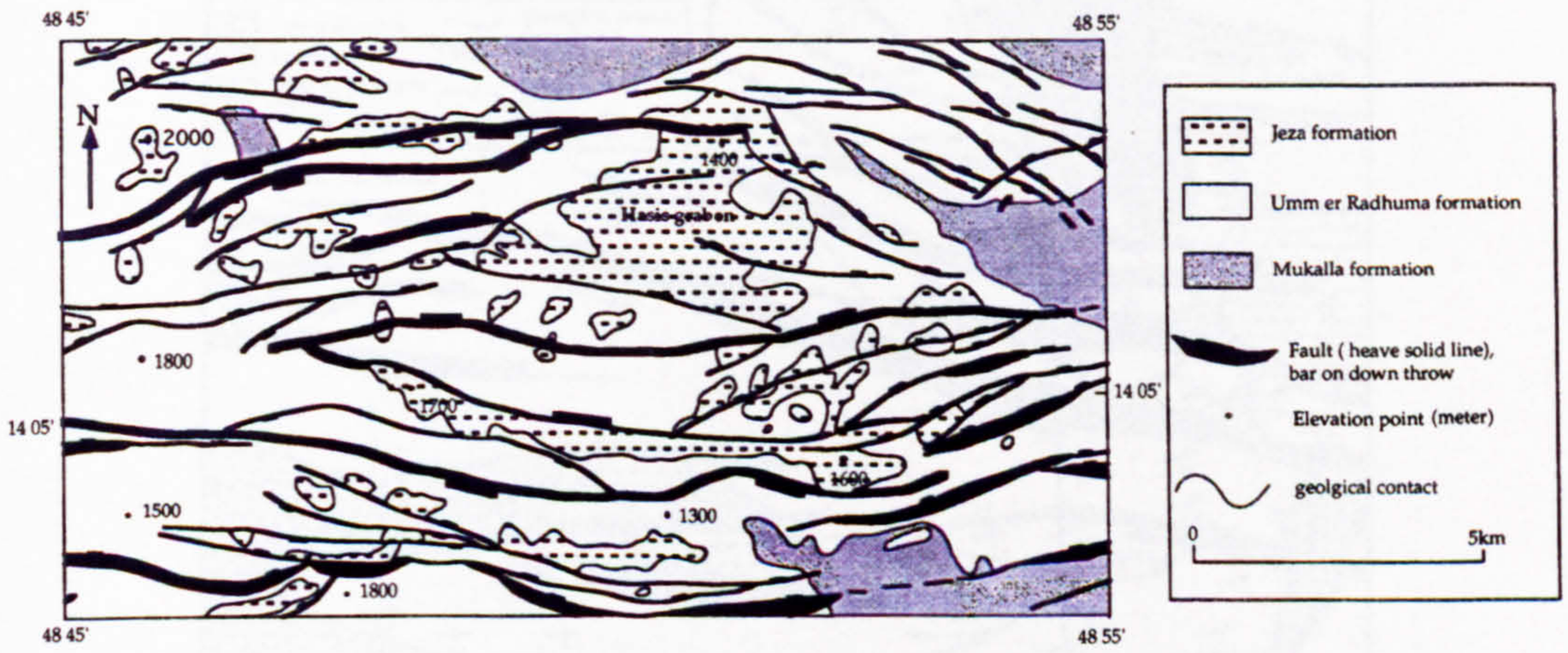

Fig. 6.6. The Hasis graben is recognised by the presence of the Jeza Formation faulted down between conjugate faults. The faults in this area are connected by both soft and hard-linkage transfer zones. The margins of the graben are dissected by parallel faults to form a series of terraces from the plateau into the centre of the graben. (a) Landsat image. (b) Geological map based on Landsat interpretation and field mapping.

a)

b)

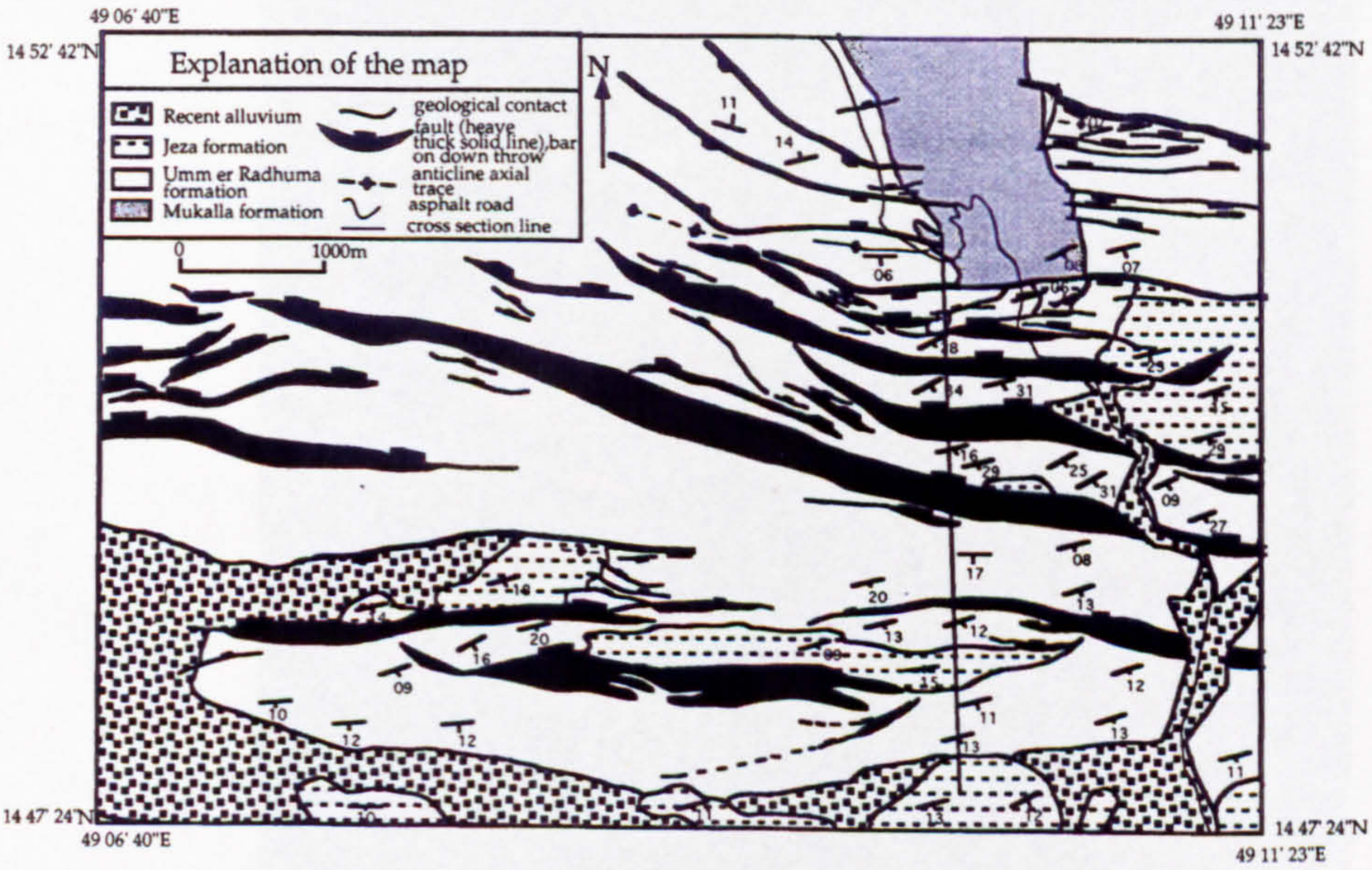

Fig. 6.7. (a) Oblique air photograph looking north to the Switchbacks (top centre) showing the dip slopes of the Umm er Radhuma Formation forming a series of half grabens, (b) structural geological map of the Switchbacks area.

Fig. 6.8. Graben formed by asymmetrical conjugate faults in the Switchbacks area, looking ENE. Note the resistant Umm er Radhuma Formation (u) of nodular limestone forming the very steep cliffs.

a)

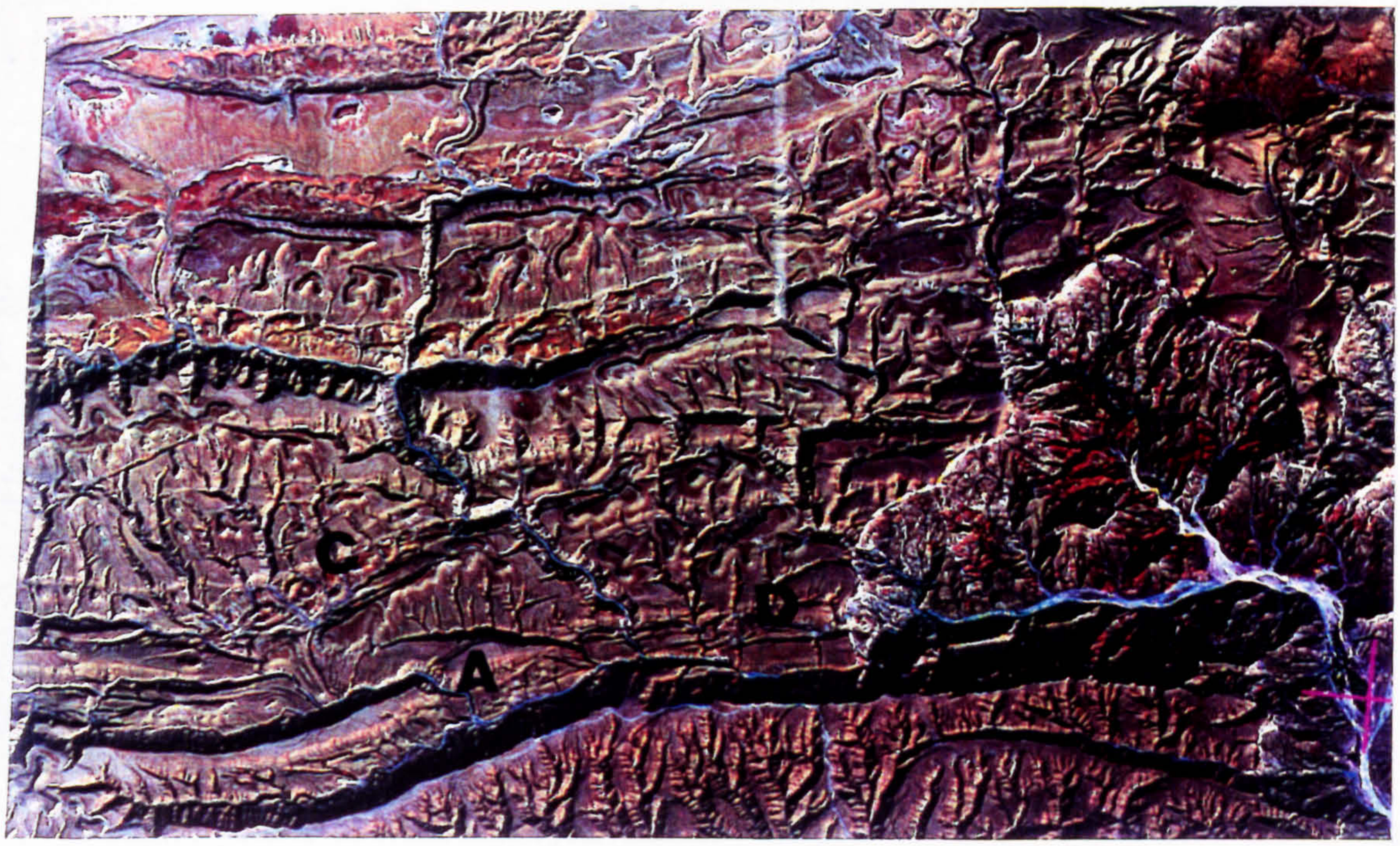

b)

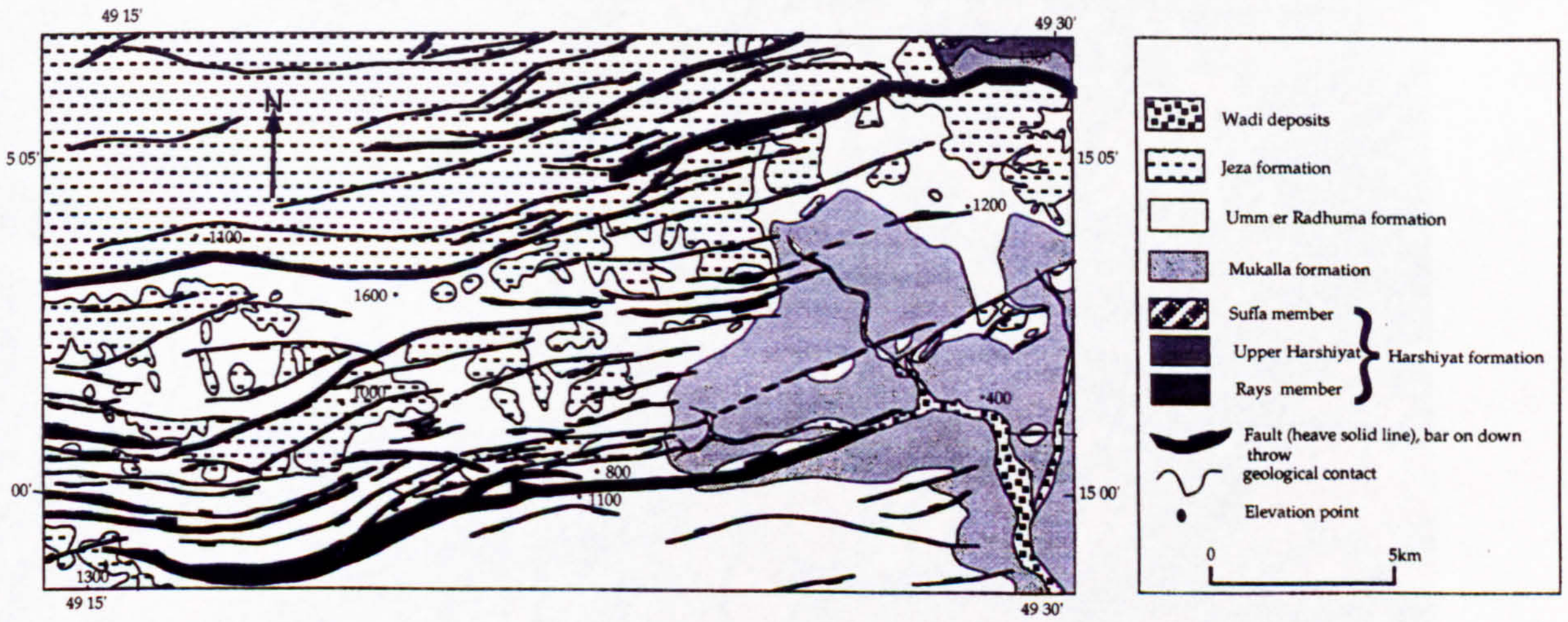

Fig. 6.9. (a) Asymmetrical Al-Madi-Haqab graben and the soft-linkage transfer zone (A) (satellite image), the width of image covers 48km. (b) Structural geological map of the Al-Madi-Haqab graben showing the Jeza Formation occurring within the graben. The down faulted block is dissected by small faults to form a series of small horsts and grabens with soft-linkage transfer between faults (C and D).

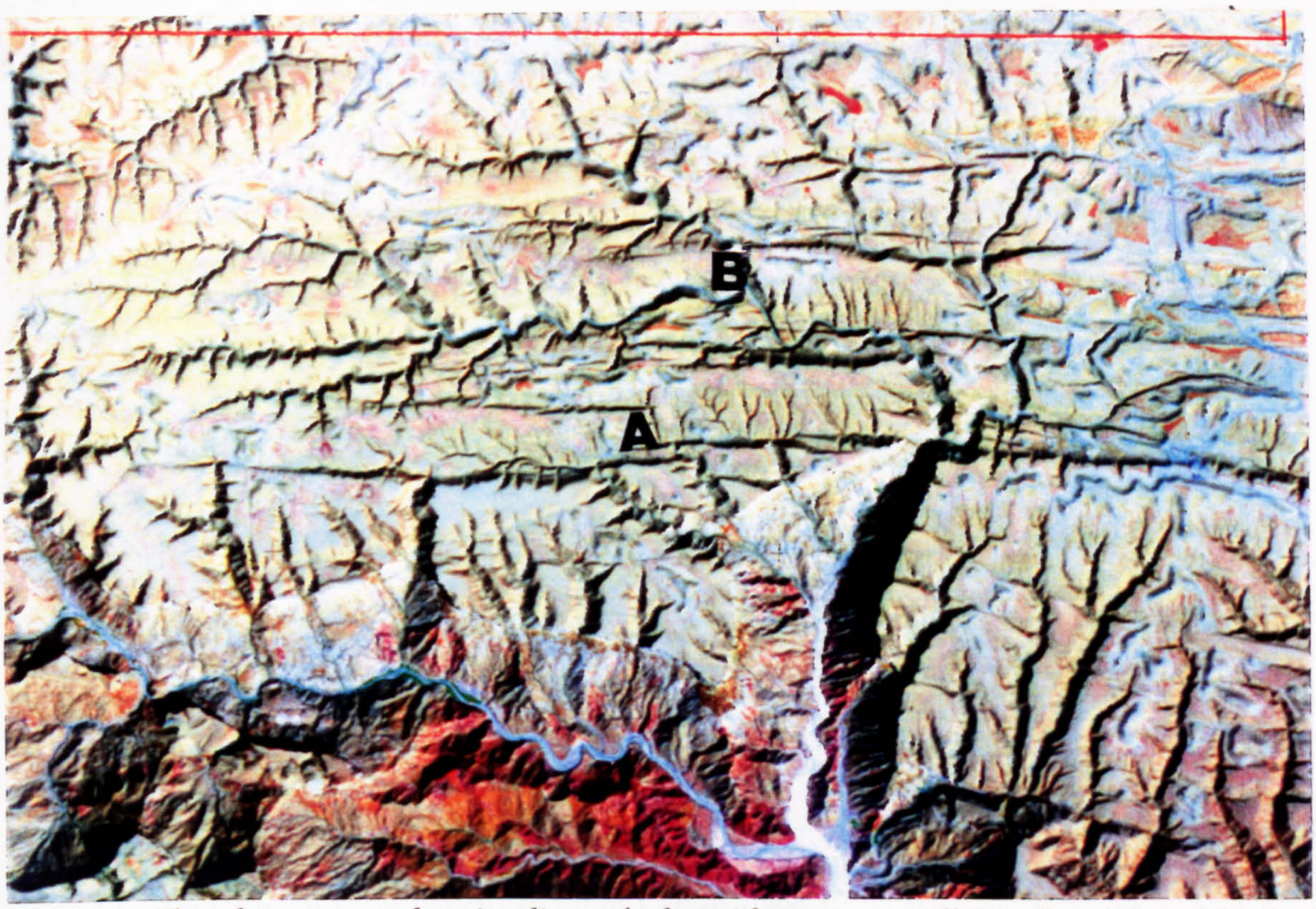

Fig. 6.10. The plateau area showing linear faults with ramps parallel to the strike of faults (A and B), north of wadi Hawayrah (satellite image). The short dimension of this image covers 15km.

Fig. 6.11. Half-graben and curved faults west of the Ydmah area (satellite image). The short dimension of this image covers 15km.

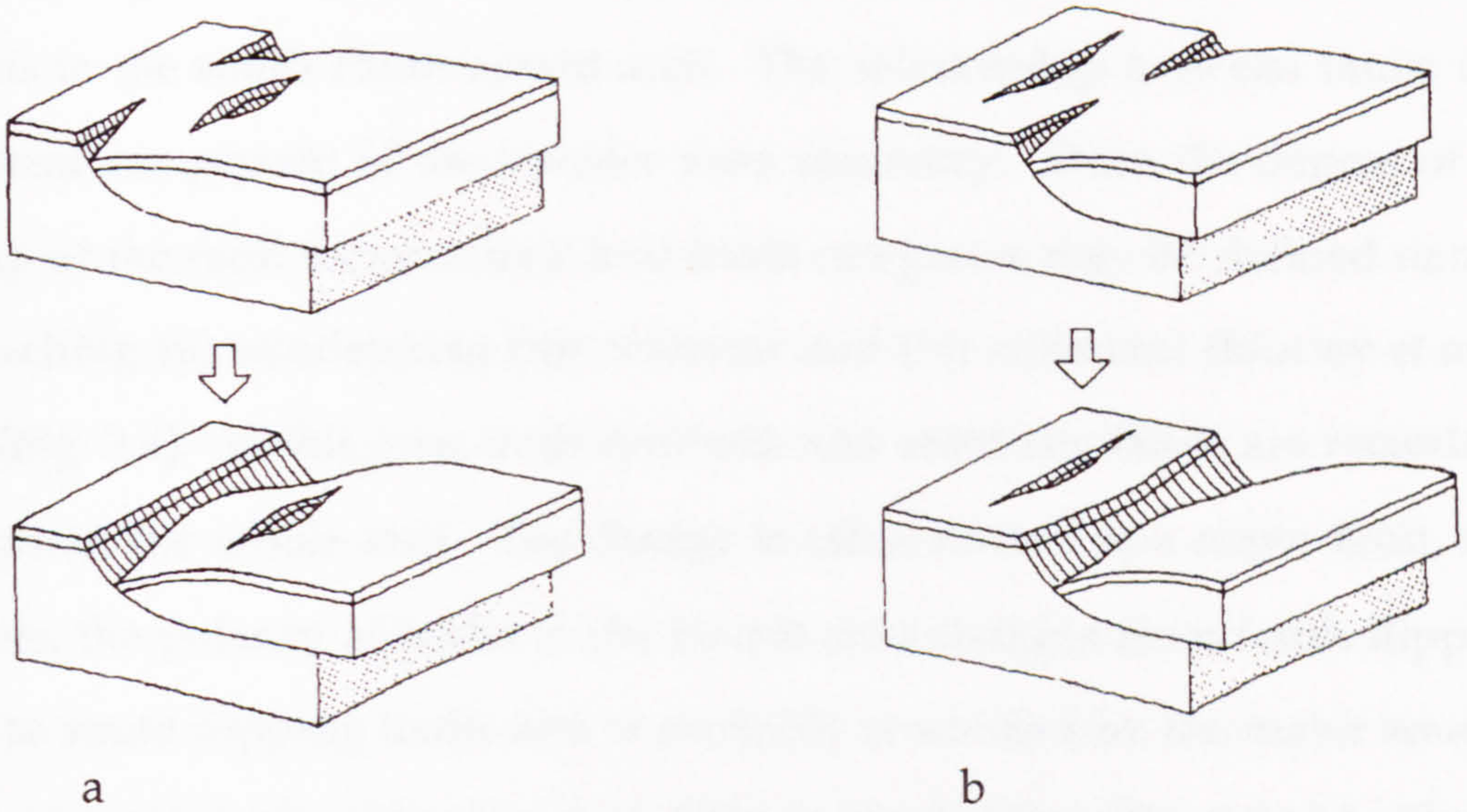

Fig. 6.12. Development of a detached hanging wall relay system (a), and a detached footwall relay system (b) during propagating extension and break-down of the initially symmetrical relay structures (after Larsen 1988).

Fig. 6.13. Small fault formed parallel to the relay ramps where two faults join up to form one fault similar to a detached footwall relay system (cf. Fig. 6.12b), north Gayl Bawazir area, looking SW.

feature in the study area is the relay segments broken up by minor synthetic faults (Fig. 6.9 and 12). Antithetic faults, recorded in this area, form full grabens with those synthetic faults. This style of structure is associated with half grabens in the south Hadhramaut arch. The relationship between faults is an important component of the transfer zone geometry. From the degree of overlap of the fault terminations four basic categories may be defined namely (i) approaching (ii) overlapping (iii) collinear and (iv) collateral (Morley *et al.* 1990) (Fig. 3.4). In this area, both synthetic and antithetic faults are recorded throughout the whole area. The change is often related to a major fault, for example, the polarity of faults in the Haqab area changes from north dipping faults to south dipping faults and is probably controlled by the major south dipping Haqab fault with more than 600m vertical offset (Fig. 6.9a-b). The Haqab fault forms a big asymmetric graben with the Araf fault and gives the same style of structure as in the Hasis area. Both convergent and divergent transfer faults (Morley *et al.* 1990) have been mapped in the study area. The conjugate pattern is described as convergent where the hanging walls move toward one another and divergent where the faults dip away from each other (Nicol *et al.* 1995).

The vertical displacement of mappable faults in the study area has been estimated throughout the whole area along 10 traverse lines, five of which coincide with the section lines while the other five are parallel to and spaced between them (Fig. 5.1). The values have been contoured with a 200m interval and the presence of regional transfer zones is indicated by the zones of lower displacement and offset of the areas of high values. Consequently, four such transfer zones occur in the south Hadhramaut arch (Al-Kotbah and Allison 1995) (Fig. 6.14). The first transfer zone starts from the tip of the wadi Hamim fault at its east end and extends northward to the plateau. The second zone coincides with wadi Kharid and is confirmed by the balanced section along this wadi which gives a value of extension of 4.5% which is the lowest value in the

study area. The third zone to the west of wadi Assad nearly coincides with wadi Shazwah and the fourth zone represents the eastern part of the area between wadi Assad and wadi Bidish.

6.3.3 Accommodation structures

Accommodation structures associated with the extensional faults in the south Hadhramaut area included monoclinal folds recorded throughout the area on a local scale. Occasionally, major faults transfer into monoclinal folds of considerable size at their tips (Fig. 6.15 and 16).

Rollover anticline folds represent the most important structures associated with extensional faults and occur in the hanging wall of most faults (Fig. 6.17 and 18). They are of small scale throughout the whole area. These folds are formed due to internal deformation of the hanging wall as it slips along a concave upwards fault surface. Normal drag fault is associated with the wadi Hamim fault in the west of the area but is much less common than reverse drag. In the Switchbacks area reverse drag is found where the Jeza Formation changes its dip from south to north forming a rollover around the south dipping faults resulting in the formation of the Switchbacks scarp. In the Al-Madi area, the Umm er Radhuma Formation in the hanging wall is rotated by more than 20° (Fig. 6.17).

Sometimes tight folds are found in the Jeza and Mukalla Formations but these structures are not common and may be related to syn-sedimentary deformation and may be evidence of extension fault movement before the mid-Tertiary rifting of the Gulf of Aden (Figs. 6.19 and 20). These folds are recorded in the south of wadi Shakhawi where horizontal movement has been identified.

Reverse faults occur on a small scale, especially in wadi Shakhawi and wadi Al-Masila where a low angle thrust faults occur (Fig. 6.4a-b and 21). In

addition small reverse faults are recorded in the Harshiyat Formation in wadi Hawayrah and wadi Kharid.

Rollover structures are also associated with crestal collapse grabens and relative rotation of the layering in the hanging wall may reach 30° such as in wadi Bidish and wadi Hawayrah where the actual dip of layering reaches 50° (Figs. 5.10 and Fig. 6.22).

Release faults (Destro 1995) are recorded in the area where the transfer faults are formed in the hanging wall of individual faults, for example, in the south of wadi Kharid, and in the hanging wall of wadi Hawayrah fault (see sheet I and VI). Antithetic faults are characterised by crestal collapse faults in the hanging walls and these structures are very dominant associated with synthetic faults to form grabens of different sizes in the study area. Moreover, the hanging walls of the major faults are dissected by these antithetic faults as accommodation structures.

6.4 Geometrical analysis of faults and fractures

Detailed analysis of faults and fractures has been carried out to deduce their geometry and relation to the rift axis. The strike and dip of fault and fracture planes were measured using a Clar compass. More than four hundred and seventy fault planes were measured particularly along the main wadis and sometimes in the plateau as access allowed. More than 90% of the faults cutting across the main wadis have been measured. In addition, more than nine hundred fractures were measured. Most of the fractures have the same trend as the major faults and the other fractures are nearly perpendicular to that trend. It is often difficult to trace fault planes in the clastic sedimentary rocks, for example, the Mukalla Formation, and fewer faults were measured from the clastic sequences compared to the harder, resistant carbonates.

The main wadis (Fig. 6.5) are separated by inaccessible rugged plateau where no measurements have been taken. However, these wadis provide

Fig. 6.14. Contour map of vertical displacement of faults throughout the area. Values have been taken from field measurements along the main wadis and from maps. The transfer zones are determined by the low values of displacement and are numbered from 1 to 4. Contours are in metres with a 200m interval.

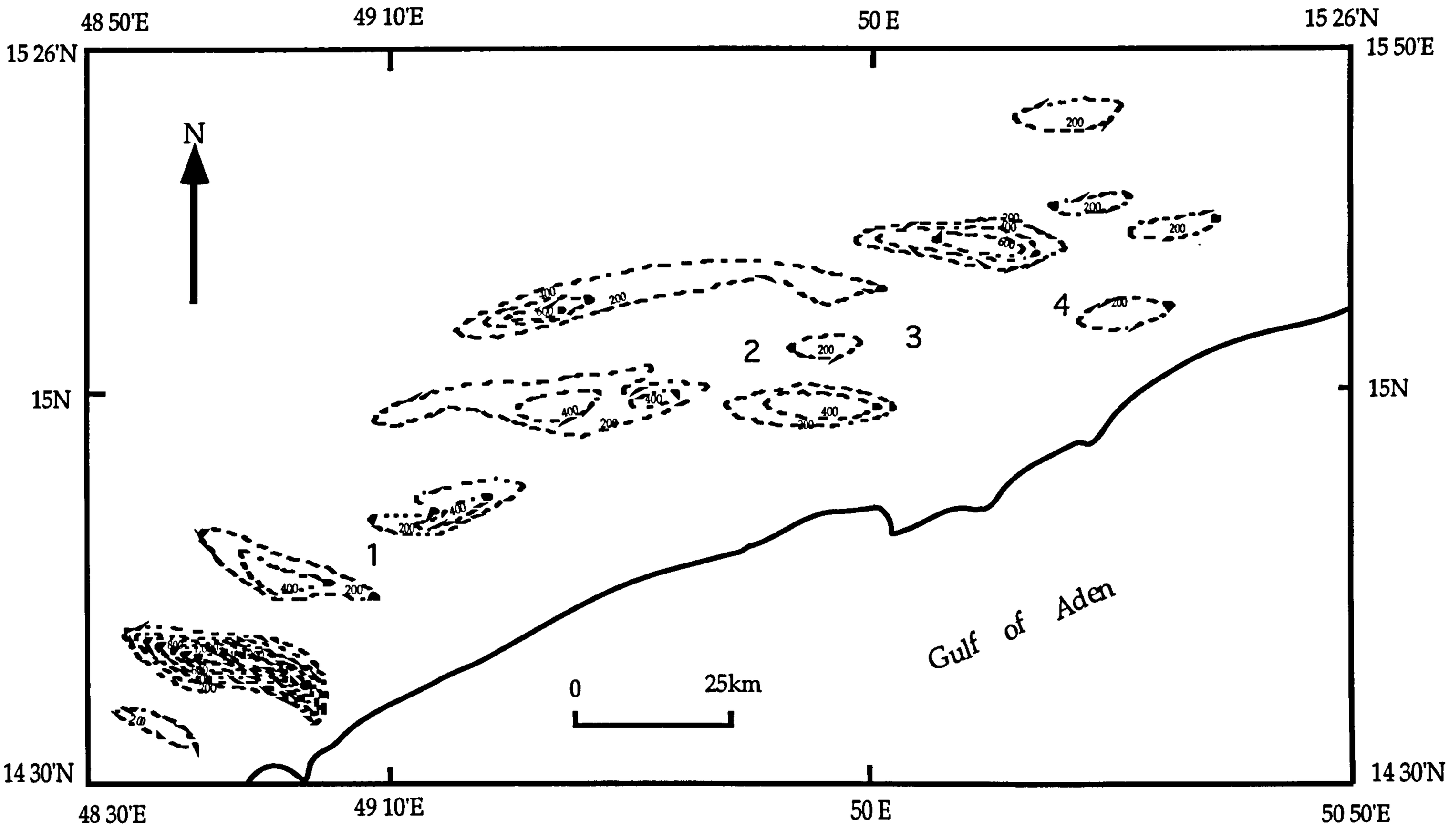

Fig. 6.17. Rollover anticline showing the rotation of the hanging wall bedding toward the fault, Al-Madi area, looking WSW. The dip increases from 8° on the right to 50° at the left near the fault scarp.

Fig. 6.18. Rollover anticline showing the rotation of the Jeza bedding (J) in the hanging wall to the right toward the fault scarp (U) at the left, Switchbacks area.

Fig. 6.19. Folds in Jeza Formation interpreted as forming above a reverse fault, north of the town of Ad-Deis, looking ESE.

Fig. 6.20. Deformation of the Harshiyat Formation in wadi Shakhawi interpreted as being associated with strike slip movement which is recorded in this area.

Fig. 6.21. Photograph showing small reverse fault in the Harshiyat Formation, wadi Shakhawi.

Fig. 6.22. The Umm er Radhuma Formation has been rotated to dip at 40° in the hanging wall of major north dipping fault, in wadi Hawayrah, looking NW.

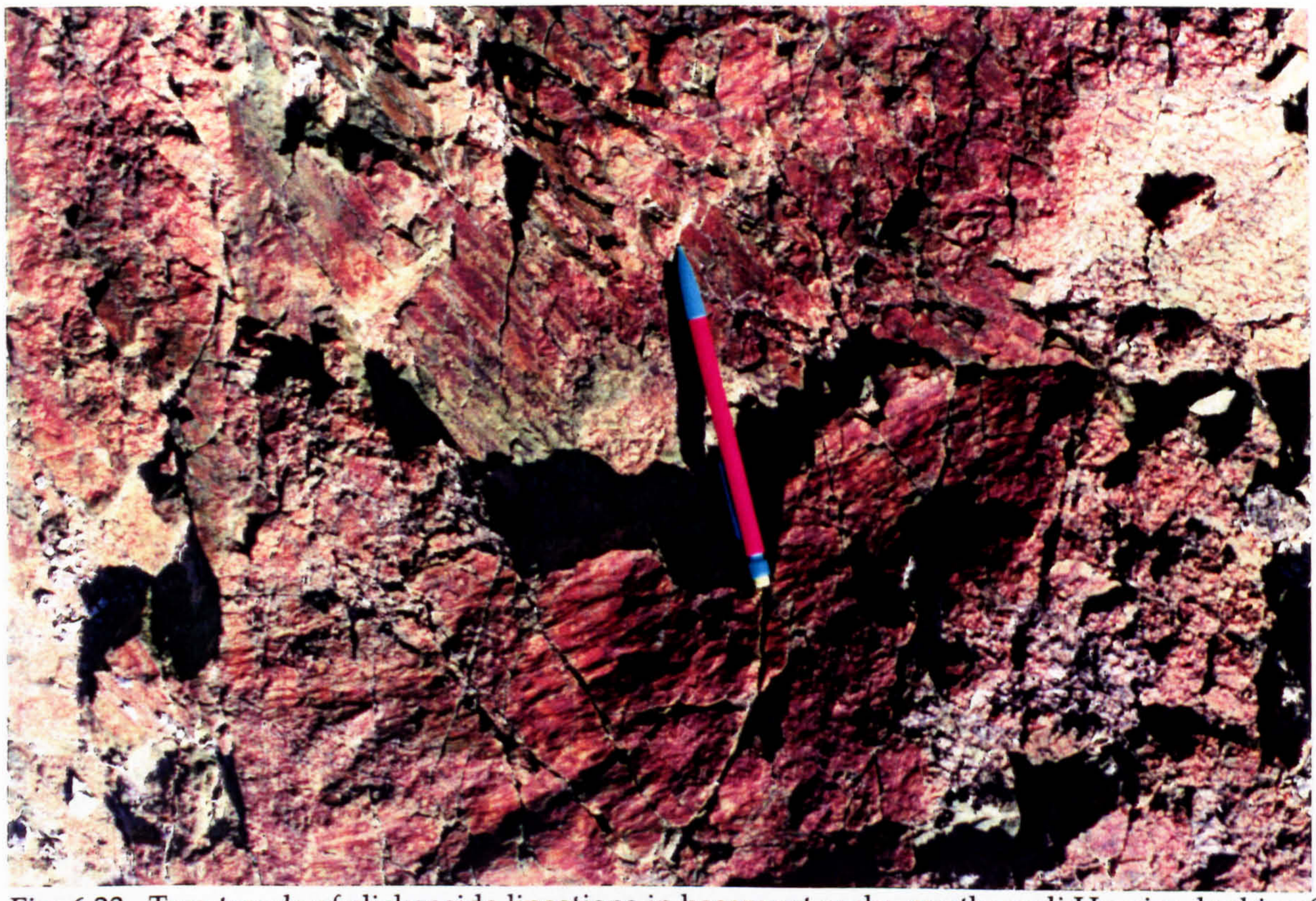

Fig. 6.23. Two trends of slickenside lineations in basement rocks, south wadi Hamim, looking S.

Fig. 6.24. Various sets of fractures with dips from steep to low angle in basement rocks in wadi Mahanea to the south of Lusp area, looking N.

Fig. 6.25. High intensity of fracturing in basement rocks in the lower part; these fractures do not affect the sedimentary cover in the upper part, Ydmah area, looking SW.

a representative sample of the whole area. Wherever possible localities for measurement were sited in adjacent areas of different lithological Formations. The plotting of faults and fractures as poles in both scatter and contour diagram has been done by using the Fabric, version 1.8, programme (Starkey 1977) and Stereonet, version 4.6 (Allmendinger 1993)

6.4.1 Faults and fractures in basement rock

The basement rocks are exposed in a limited area in the Harshiyat-Ydmah area. It is beyond the scope of the present study to carry out a thorough analysis of fracture in the basement rocks. The aim here is to relate trends in

the basement to those in the sedimentary cover. Twenty three faults and more than 90 fractures were measured in an area some 4km long and less than 1km wide. The fault planes are showed a wide range of distribution with a slightly more dominant trend as north dipping faults (Fig. 6.26a-b). At least one trend of fault planes with slickensides is recorded in the basement rocks which do not affect the sedimentary cover and are therefore pre-Cretaceous (Fig. 6.23). The fault planes recorded in the basement rocks have a wide range of dips, some less than 45°. In addition, intense fracturing of variable trends and dip are also found. In general the fractures have a steeper dip than the faults (Fig. 6. 25 and 28).

The dominant trends of fractures are ESE-WNW and NE-SW and their formation is either synchronous with rifting of the Gulf of Aden or later in the Pliocene. However, of the fractures in the basement rocks, at least three trends could have been rejuvenated during the rifting, namely, the ESE-WNW, the NW-SE trend and the north-south trend (Fig. 6.26d-e). The steeply dipping younger ESE-WNW trend in the basement rocks can be easily distinguished from the older, shallower trends (Fig. 6.24 and 25).

The steep faults and fractures coincide strongly with trends, particularly those which are parallel to the rift axis and the Fartaq-Alula fracture, observed in the cover sequence. These fractures have very steep dips which may indicate that are originated from great depth. However, it is still difficult to confirm that they are rejuvenated and inherited from the older trends. The low angle faults and fractures are not recorded in the younger sedimentary cover.

The fractures show a variable orientation with high frequency of west-east to WSW-ENE trend less dominant (Fig. 6.26d-e) with steep dip and north-south trend with some fractures of moderate dip and then NE-SW trend. This wide variation in fracture trends and angle of dip is attributed to the basement rocks having been subjected to tectonic movement over a large period of

geological time. This distribution of faults and fractures in the basement rocks is not totally duplicated in the overlying sedimentary sequences.

6.4.2 Slip movement in basement rocks

Seven fault planes with slickensides have been measured and they display two main dominant trends of extension faults. The NNE-SSW extension was accompanied by an oblique slip component and similarly the NW-SE extensional trend is accompanied by an oblique component. The NE-SW trend has mainly dip slip movement. The most dominant trends of extension are NNE-SSW and WNW-ESE (Fig. 6.26c).

6.4.3 Faults and fractures in Ydmah-Hawayrah area

In the Ydmah-Hawayrah area, measurements were taken in a number of different localities. Fractures from the Qishn Formation in the Ydmah area show three main trends (Fig. 6.27a-b). Two trends are parallel to the dominant extension faults (i.e. ESE-WNW and NE-SW) while the third trend is NW-SE and is most likely due to the upward propagation of basement fractures. The faults in the Qishn Formation on the other hand show a more random distribution but with a high frequency of the ESE-WNW to E-W strike trend with steep angles of dip. North-south and NW-SE faults are recorded in this area but not common (Fig. 6.27c-d). The NW-SE faults formed a steep half graben basin during the Oligo-Miocene extension when the Shihr Group was being deposited and may extend eastward along the coast plain beneath the Shihr Group.

In the Lusp-Ydmah-Hawayrah areas, fractures were measured from different localities and different stratigraphic Formations, namely, Lusp 1, Lusp 2, Ydmah and wadi Hawayrah area (Fig. 6.5). In these four localities the majority occur in an ESE-WNW trend with a subsidiary NE-SE and NW trends (Fig. 6.27f-g). Those fractures of NW-SE strike may be inherited from the

basement (cf Fig. 6.27f-g). These areas show a similarity with those from the basement rocks which may imply that some old faults and fractures are rejuvenated, where they show wide range of strike (Fig. 6.27a-b, and f-g). Most of these extension fractures, particularly those with NW strike, are associated with the wadi Hawayrah fault. North-south fractures recorded in wadi Hawayrah are likely reactivated from the basement rocks which are very near to the surface in wadi Hawayrah since the Harshiyat Formation is exposed in the footwall of wadi Hawayrah fault.

In the Switchbacks area, the fault planes have become more restricted to a NW-SE strike with wide fluctuation due to curvature at their tips as they approach the south dipping east-west faults (Fig. 6.28a-b). The faults in the Switchbacks show an alternating change of polarity from north to south dipping faults. However, the north dipping faults are more dominant. In this locality the north-south faults have a steep dip. In this area, two trends of extension fractures are observed; those with an ESE-WNW strike and a large angular fluctuation and, less commonly, those of NE-SW trend (Fig. 6.28d-e) and all fractures have steep dip. There is a strong E-W orientation of fractures adjacent to a NW-SE fault plane. Either, the fractures prevailed are not contemporaneous with faulting or there is a component of strike-slip motion (Fig. 6.28f-g).

In the Switchbacks area, measurements were taken from around a fault tip where the vertical displacement is less than 1m to show the relation with the main faults. The plot of fracture data shows that most of the fractures at the tip of the fault do not follow the strike of the fault. These fractures most likely belong to a younger stage of extension. However, some fractures do follow the strike of the fault which swings toward the NW (Fig. 6.28f-g). The Hawayrah area, from Lusp in the south to the Switchbacks in the north, shows that the old trends of fractures in basement rocks are recorded throughout with the exception of the Switchbacks area. The most likely interpretation is that the

Switchbacks area is stratigraphically much higher above the basement than areas south of wadi Hawayrah which are very close to the basement rocks which are exposed at the surface.

6.4.4 Slip movement in Ydmah -Hawayrah area

Since the faults and fractures from the different localities in the Ydmah, Lusp and wadi Hawayrah area show a similar pattern of extension with exception of the Switchbacks location, the data on slickenside lineations are combined together and those of the Switchbacks kept separate. The slip movement indicates NW-SE extension, with a less dominant direction of extension of NE-SW. The slip movement consists of dip slip with oblique component although horizontal movement is also recorded (Fig. 6.27e).

6.4.5 The slip movement in the Switchbacks area

The Switchbacks locality is represented by a few measurement of slickenside lineations of dip slip and horizontal slip. Horizontal slip directions have not been recorded in the published literature previously. This movement affects Umm er Radhuma Formation and all older Formations. The Switchbacks area shows only one trend of extension in a direction NW-SE. However, the horizontal movement is very obvious from both field observation (Fig. 6.1a-b) and from the plot of slickenside lineations (Fig. 6.28c).

6.4.6 Faults and fractures in wadi Araf-wadi Tamah area

In this area 33 faults have been measured mainly within the Umm er Radhuma but also in the Mukalla Formation. The dominant strike trend of these faults is NW-SE and they have alternating polarity of north and south dipping faults (conjugate faults) (Fig. 6.29a-b). Forty five fractures were also measured in these wadis (Fig. 6.29d-e). Two trends are indicated, the first has a dominant strike of ESE-WNW with high angle of dip. This trend coincides

with the faults in the wadi Araf-Tamah area. Comparison of fault and fracture plots shows that the strike of the fractures follows the strike of the faults. The second trend is less common with strike of nearly NE-SW and with steep to moderate angle of dip.

6.4.7 Slip movement in wadi Araf-wadi Tamah area

Six faults with slickensides were measured in this area. Mainly dip slip is indicated with the extension direction of NW-SE and become close to north-south with slight rotation to the NE. This rotation is supported by the rotation of fractures in this area and are of steep angles of dip (Fig. 6.29c).

6.4.8 Fault and fractures in Wadi Kharid

Wadi Kharid has been eroded more deeply than adjacent wadis to expose the Harshiyat Formation. The measurements here are taken from the Harshiyat, Mukalla and Umm er Radhuma Formations. Thirty two faults have been measured along the wadi for a distance of 15km to the plateau. The southern part of wadi Kharid is more complex and north-south faults are recorded which are uncommon in the area as mappable faults except in wadi Hawayrah and wadi Shakhawi. The dominant faults are east-west and of steep to moderate dip (Fig. 6.30a-b). Less common is the NE-SW trend.

Seventy fractures were measured in wadi Kharid and they show a wide range of distribution around the two main trends of ESE-WNW strike and NE-SW strike (Fig. 6.30d-e). The fractures generally, have a steep dip with very some fractures of moderate angle of dip and rarely low dip. The other trend is the NE-SW trend and has steep angle of dip at the tip of a fault in the south of wadi Kharid, fractures were measured and show a wide range of strike values. These fractures very strongly follow the curvature of the fault toward the NE (Fig. 6.30f-g).

6.4.9 Slip movement in wadi Kharid

The dominant displacement component is dip slip with some oblique movement and a main NW-SE extension direction is evident with less common extension in a NE-SW direction (Fig. 6.30c).

(a)

n=23

contour 1 2 3 4

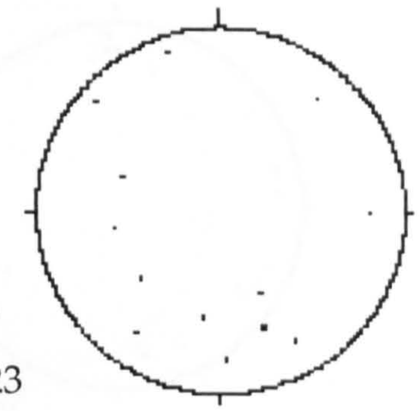

(b)

n=23

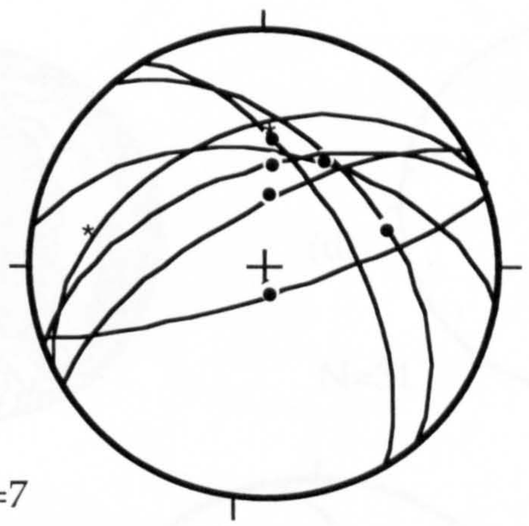

(c)

n=7

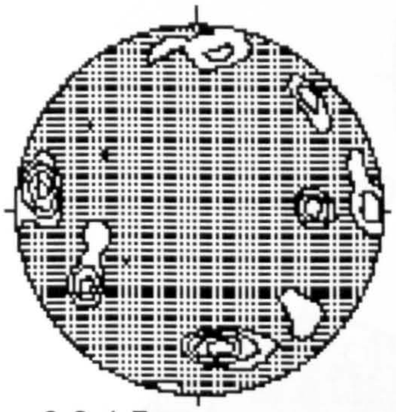

(d)

n=97

contour 2 3 4 5

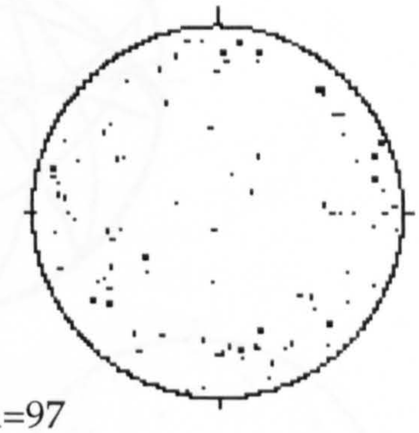

(e)

n=97

Fig. 6.26. Lower-hemisphere equal area projection of faults and fractures in basement rocks, (a-b) poles of faults in basement (c) slip sense of faults, and the star indicates the oblique slip, (d-e) contour and scatter of fractures in basement rocks. Contours are in points per 1% area and have been generated using the computer programe Fabric, version 1.8 (Starkey 1977). In the contour diagram the area of empty space, or the area of values below the lowest contour, is cross-hatched. The contour values are given below the diagram.

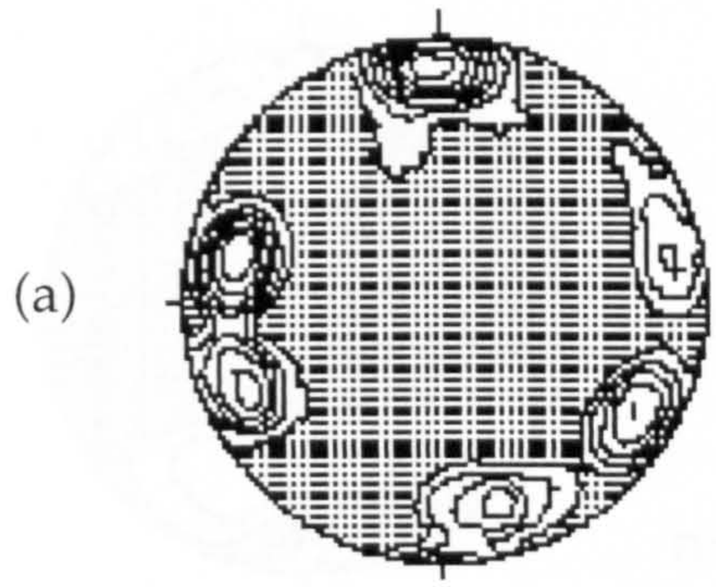

Fig. 6.27. (a-b) Contoured and scatter plots of fractures in Ydmah area (c-d) contour and scatter plots of faults in wadi Hawayrah area (e) slip motion of faults in wadi Hawayrah, the star indicates oblique to horizontal slip (g-h) contours and scatter plot of poles of fractures in Lusp-Hawayrah areas.

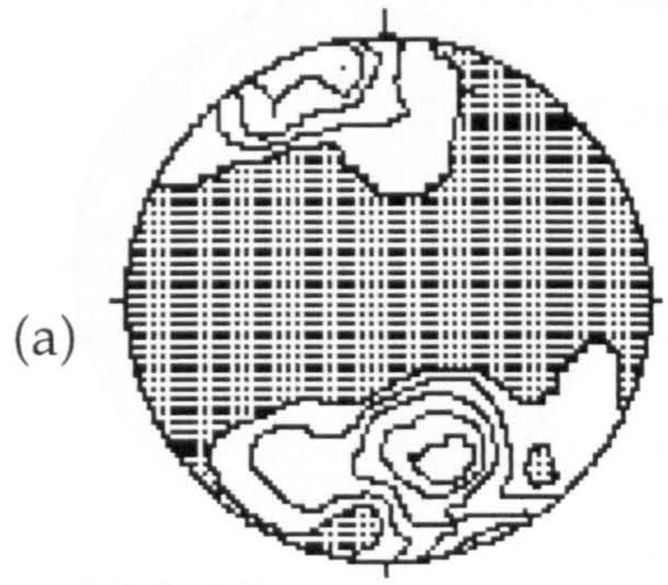

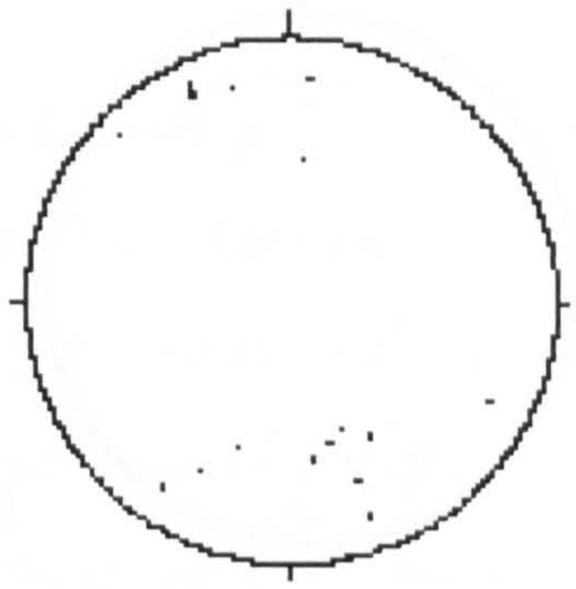

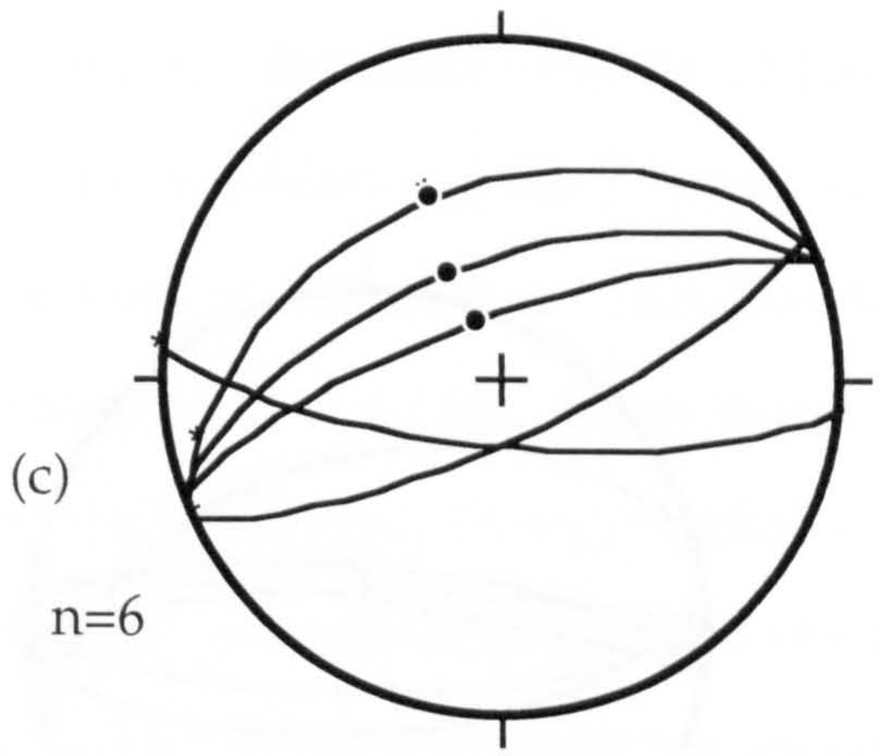

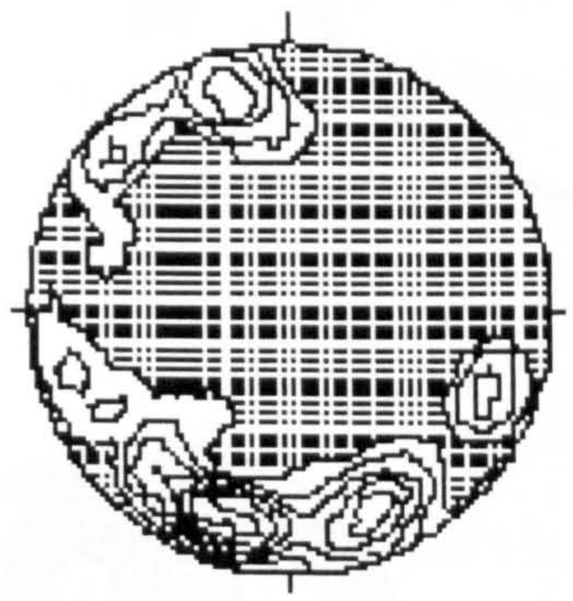

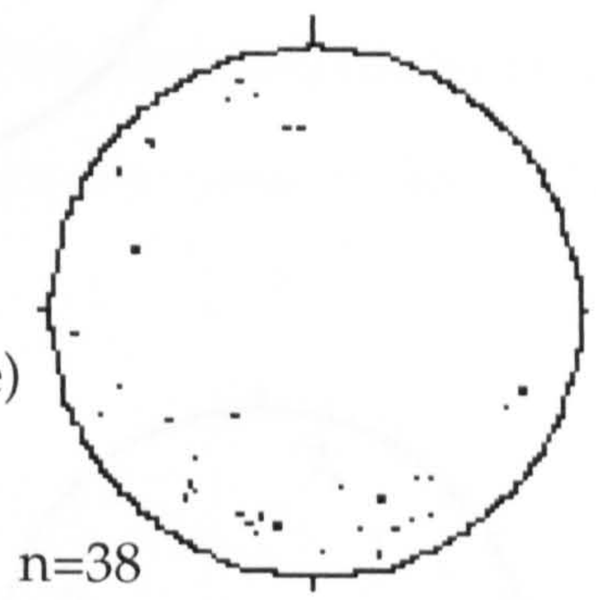

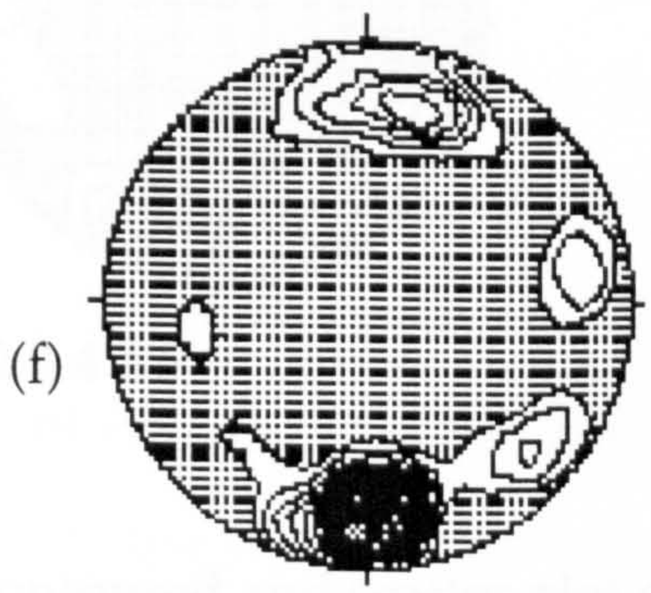

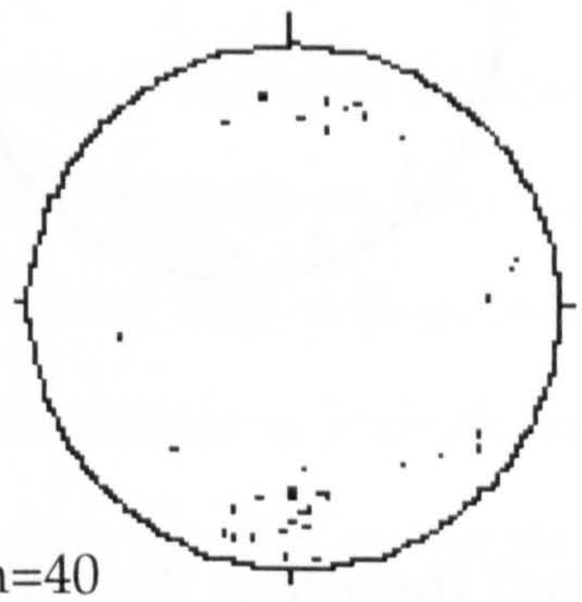

Fig. 6.28. (a-b) Contoured and scatter plots of faults in the Switchbacks area (c) slickenside lineation on faults in the Switchbacks area, the star indicates horizontal slip, two lineation readings were measured on one fault plane (d-e) contoured and scatter plot of fractures, (f-g) contoured and scatter plot of fractures which have been measured at the tip of a fault in the Switchbacks area.

(a)

n=33

contour 1 2 3 4 5 6 7 8

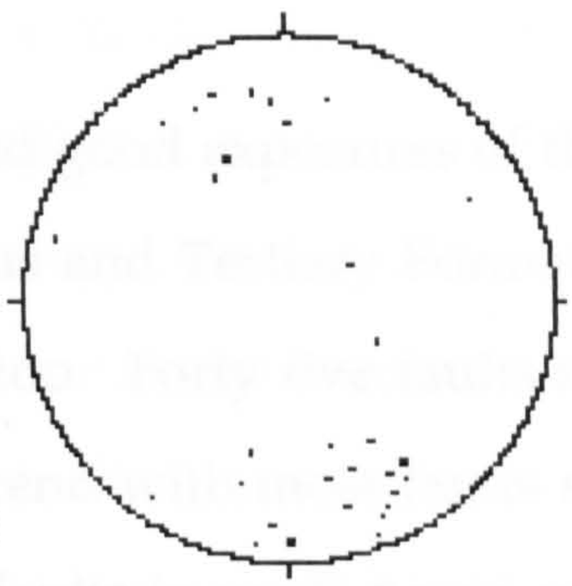

(b)

n=33

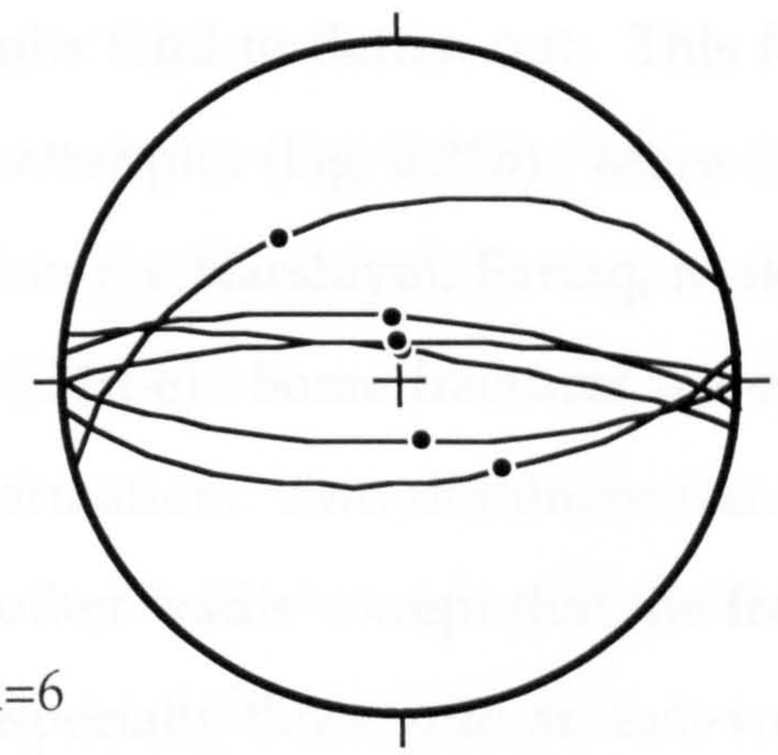

(c)

n=6

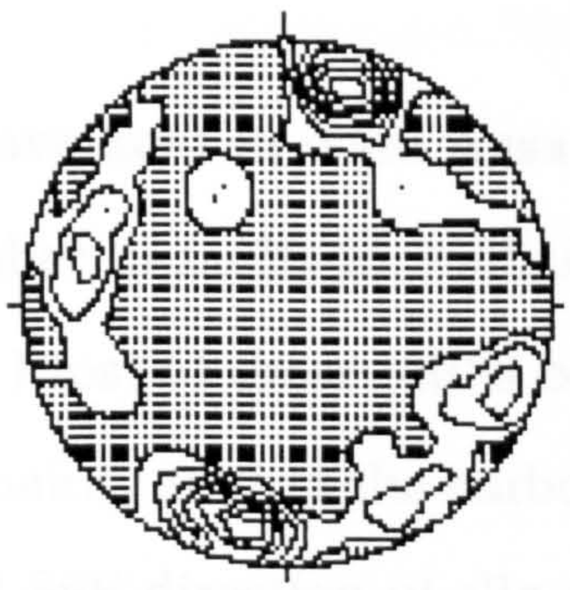

(d)

n=45

contour 1 2 3 4 5 6

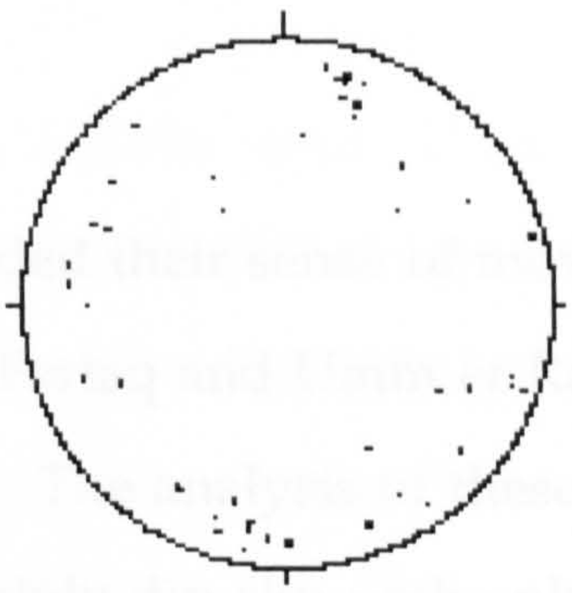

(e)

n=45

Fig. 6.29. (a-b) Contoured and scatter plot of faults in wadi Araf-wadi Tamha area, (c) slip direction of faults (d-e) contoured and scatter of fractures in Araf-Tamha area.

6.4.10 Faults and fractures in wadi Assad

In wadi Assad, deep erosion has provided good exposures of the stratigraphic sequence of most of the Cretaceous and Tertiary Formations from the Harshiyat in the bottom to the Jeza on the top. Forty five faults measured along the main wadi, show a very consistent trend with most faults striking E-W, with steep to moderate dips. The strike of faults in wadi Assad vary from WSW-ENE to east-west (Fig. 6.31a-b). The moderate dip of faults may be attributed to the deep erosion of wadi exposing the Mukalla and Harshiyat Formations in which the faults tend to flatten out. This feature is clear in the field and observed on the scatter plot (Fig. 6.31b). More than 140 fractures in wadi Assad were measured in the Harshiyat, Fartaq, Mukalla and Umm er Radhuma Formations (Fig. 6.31d-e). Some fractures were of low dip particularly in the Fartaq Formation. Two dominant trends are apparent and are similar to trends in the other wadis except that the fractures in wadi Assad have a wider range of dip especially those with an east-west strike. These trends are east-west and NNE-SSW.

6.4.11 Slip movement in wadi Assad

A number of faults in wadi Assad recorded their sense of movement in slickensides. Most of these faults occur in the Fartaq and Umm er Radhuma Formations mainly within the carbonate rocks. The analysis of these faults gives a NNW-SSE direction of slip which is mainly dip slip with only a slight oblique component (Fig. 6. 5c). The horizontal movement is also observed in wadi Al-Rakdoon to the west of wadi Assad affecting the Fartaq Formation.

6.4.12 Faults and fractures wadi Bidish

Wadi Bidish is one of the most complex areas. Here the Mukalla Formation is very thin in the hanging wall of a major north dipping fault which is the structural control on the main wadi at its southern end. Thirty

faults have been measured along the wadi (Fig. 6.32a-b). They retain the common ENE-WSW trend but swing more to the NE compared with those in adjacent wadi Assad. The faults are of steep to moderate angle of dip.

Seventy three fractures from the whole stratigraphic sequence from the Qishn Formation to the Umm er Radhuma Formation were measured (Fig. 6.32d-e). The orientation diagram shows a wide variation in strike direction of the fractures with one maximum in the NE-SW direction.

6.4.13 Slip movement in wadi Bidish

Slickenside lineations were observed on fifteen normal faults in wadi Bidish. The main movement is dip slip in approximately a north-south direction (Fig. 6.32c). Some faults have a component of oblique slip. Horizontal movement is again recorded and the subhorizontal slickensides are overprinted by steeply pitching slickensides implying that the faults were reactivated as normal faults (Fig. 6.2a).

6.4.14 Faults and fractures wadi Shakhawi

Wadi Shakhawi is in the easternmost part of the area. Thirty normal faults have been measured and most of them have an ESE-WNW strike with steep to moderate dip (Fig. 6.33a-b). The faults have a slight clockwise rotation compared to those in wadi Bidish and they have a much more limited fluctuation in strike.

The fractures which were measured in wadi Shakhawi were mainly from Qishn and Fartaq Formations with some from the Umm er Radhuma Formation. More than 20 fractures were measured and they are similar in trend to those in the other eastern wadis (Fig. 6.33d-e). There are two trends; those with an east-west strike and a smaller population with a NNE-SSW strike.

6.4.15 Slip movement in wadi Shakhawi

As indicated by slickensides, movement in wadi Shakhawi is characterised by more than one slip direction. Dip slip movement is dominant but oblique slip is also evident. Horizontal movement is also recorded and appears to be older than the dip slip component (Fig. 6.33c). Although the faults record the same north-south extension as in the other wadis, there is locally an easterly directed extension especially associated with faults of north-south trend.

6.4.16 Shihr Group

Some attention was paid to the syn-rift deposits (Shihr Group) and more than 40 fractures were measured from a locality in the Al-Aies area, NE of Ash Shihr city and south of wadi Kharid. Analysis of these fractures shows that the main trends evident in the pre-rift Formations continue in these syn-rift deposits. The main set has a strike of NE-SW with a wide fluctuation and with steep dips. ENE-WSW fractures are less common in this area (Fig. 6.33f-g)

6.5 Bedding analysis

The south Hadhramaut arch consists of an asymmetrical anticlinal fold with a gently dipping northern flank and a southern flank of steeper and variable dip. The southern flank is highly dissected by extensional faults and the large variation in dip is due to tilting of fault blocks. Large fault scarps up to 600m high are concentrated in this part. The altitude of bedding was measured throughout the area. For analysis the data were grouped into four areas, namely, wadi Hawayrah, wadi Araf-Kharid, wadi Assad and wadi Bidish-Shakhawi. The orientation diagrams and rose diagrams of the dip direction suggest that there is a slight swing in strike from west to east.

In wadi Hawayrah the main dip direction of bedding is to the SSE with a restricted range of dip direction (Fig. 6.34a-b). The wadi Kharid area, including

wadi Araf and wadi Tamah, shows that the dip of bedding has a wide distribution, with some bedding planes dipping north due to the tilting of fault blocks towards south-dipping faults, particularly in wadi Kharid. However, the dominant trend of dip direction in this area is to the south (Figs. 6.36c-d). In wadi Assad, the dip direction of bedding planes has swung towards the SSW (Figs. 6.36e-f). In the easternmost part of the area the dip direction returns to due south similar to the average in wadi Kharid (Figs. 6.36g-h).

6.6 Conclusion

From the analysis of faults in the south Hadhramaut area, it is concluded that there is one dominant trend of faults with a narrow range of strike from ESE-WNW to ENE-WSW. The extension direction in this area is north-south to NNW-SSE. The fractures show a larger number of sets although there are two main trends in strike, namely ESE-WNW and NE-SW. The first direction follows the dominant trend of the faults, while the second extension trend is related to that the off-shore fracture zones. The faults display a swing in strike from ESE-WNW the western part through east-west in the middle to ENE-WSW in the east (Figs. 6.29a-b, 31a-b, 32a-b, 33a-b, 34a-b and 35). The slip movement of the extensional faults is mainly dip slip with oblique component movement. Moreover, a horizontal movement older than the rifting is recorded where it is overprinted by the younger very steep dip slip.

The analysis of bedding planes very strongly support the swing of the northern margin of the Gulf of Aden which could be related to strike slip movement affected in the margin. The dip direction of bedding in the west in wadi Hawayrah area is toward the SE (Fig. 6.34b), then it rotates to the west to become due south in Araf-Kharid area (Fig. 6.34d) and in wadi Assad more rotation to the west where the dip direction is to SW (Fig. 6.34f), while in the east in the Bidish-Shakhawi area it dips south to SE (Fig. 6.34h) similar to the dip direction in wadi Hawayrah area

(a)

n=32
contour 1 2 3 4 5 6 7

(b)

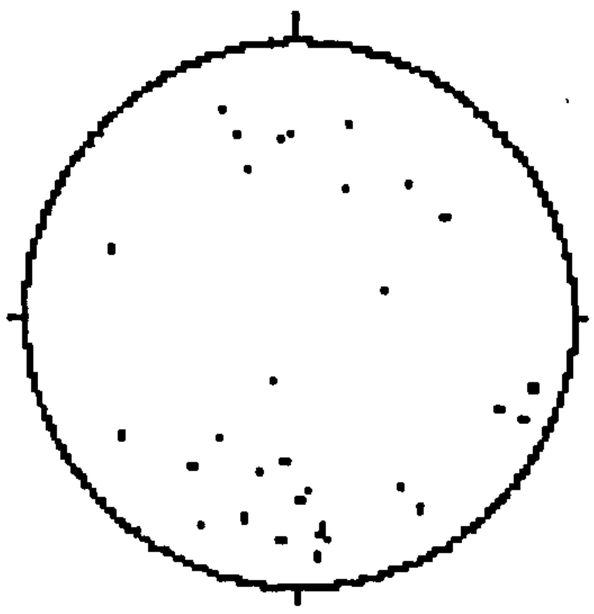

n=32

(c)

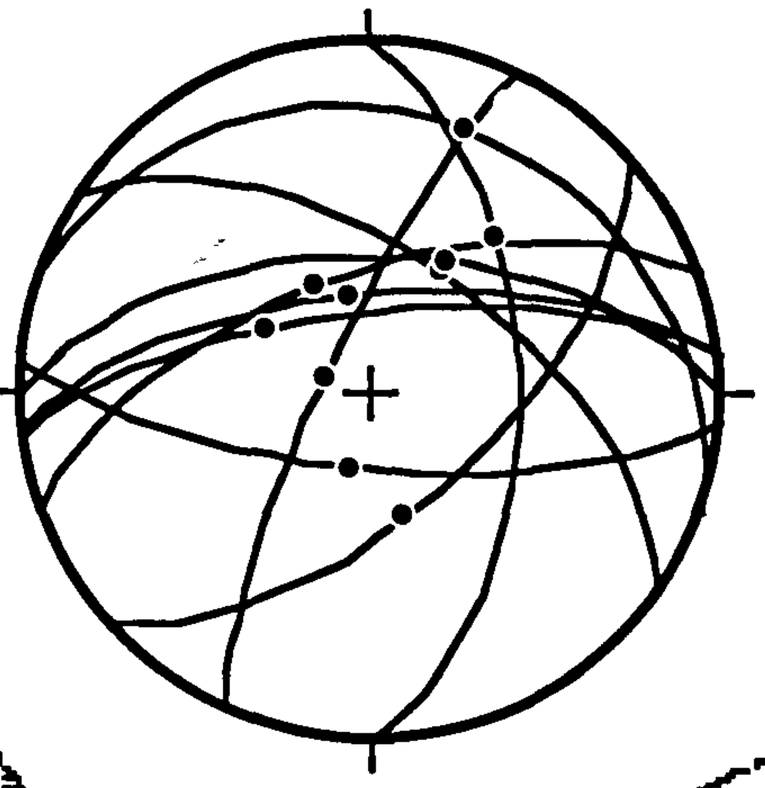

n=12

(d)

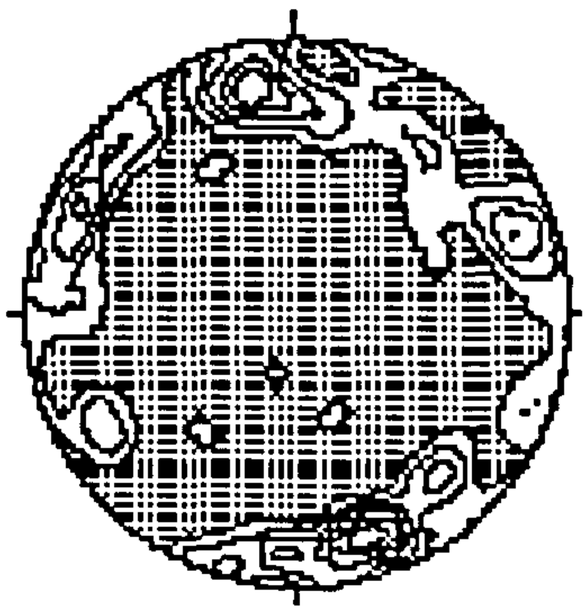

n=70
contour 1 2 3 4 5 6

(e)

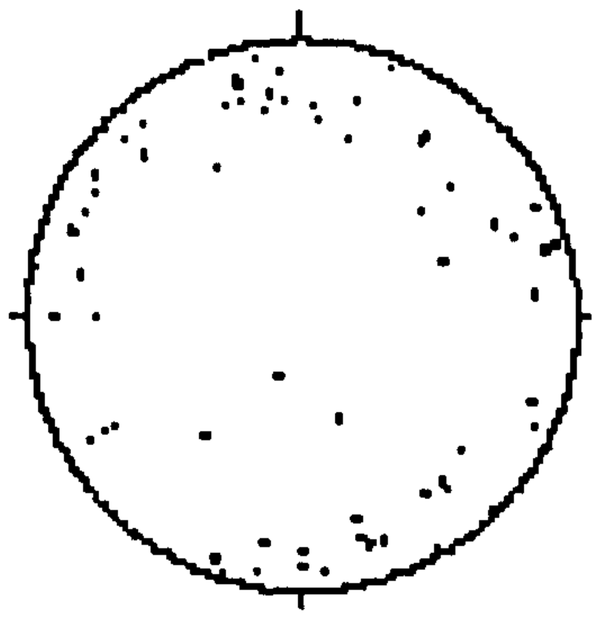

n=70

(f)

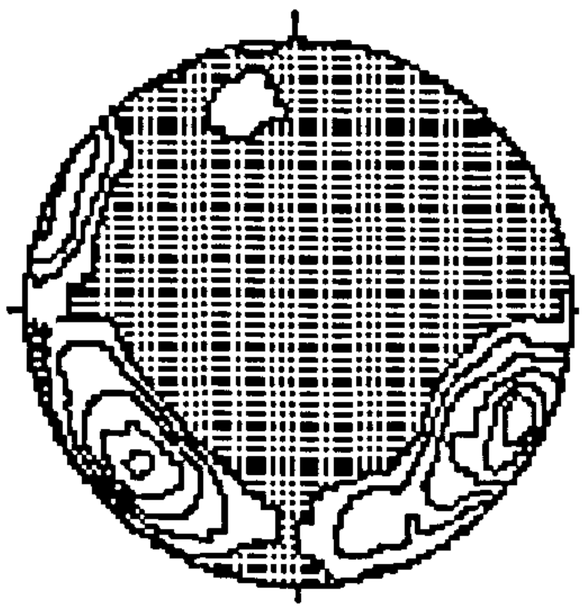

n=20
contour 1 2 3 4 5 6

(g)

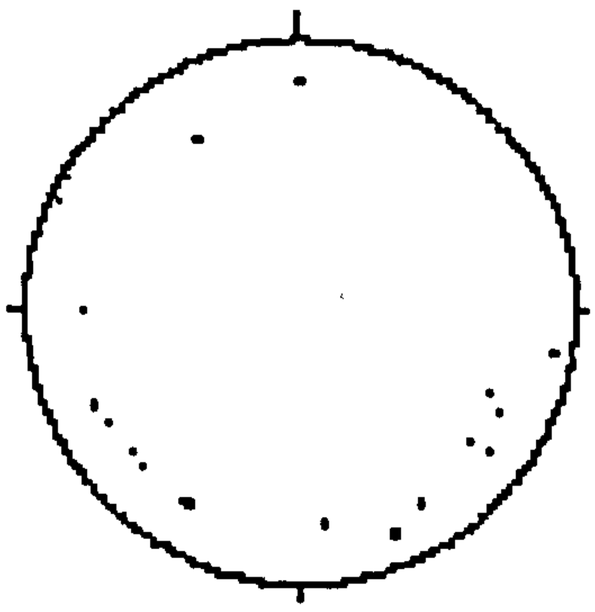

n=20

Fig. 6.30. Plot of faults and fractures in wadi Kharid areas (a-b) contour and scatter plots of faults in wadi Kharid area (c) slip motion of faults wadi Kharid, (d-e) contour and scatter of fractures in wadi Kharid and (f-g) fractures measured at the tip of a fault in south wadi Kharid.

(a)

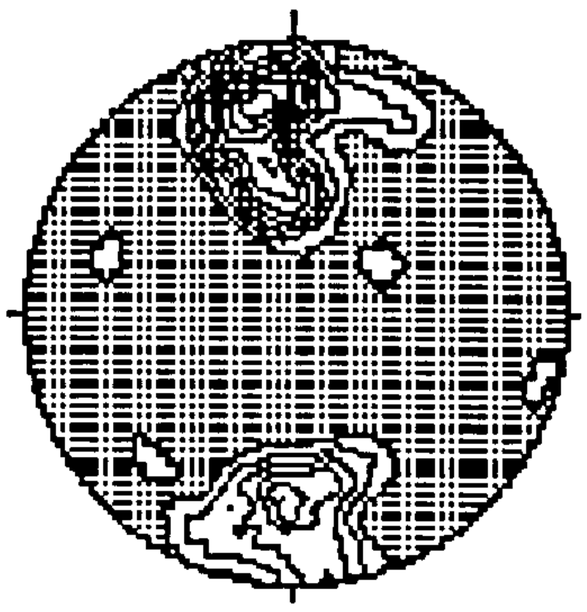

n=45
contour 1 2 3 4 5 6 7 8

(b)

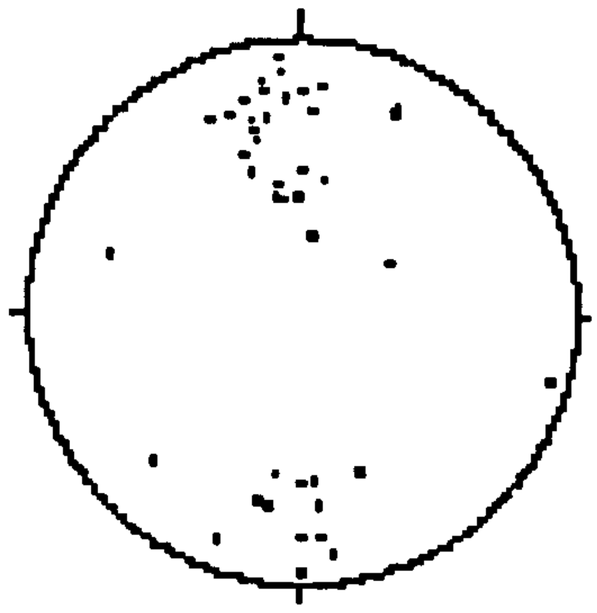

n=45

(c)

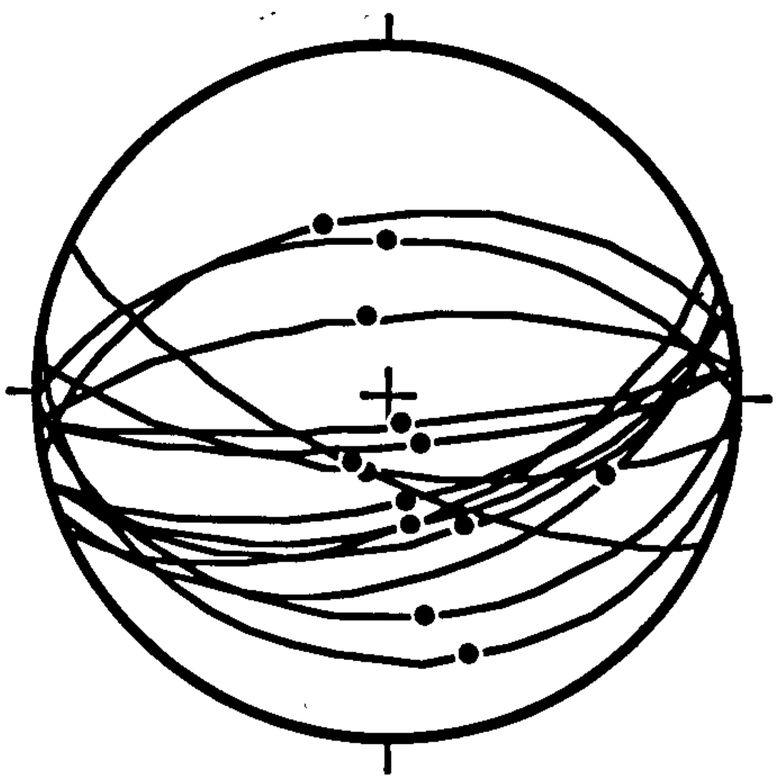

n=14

(d)

n=149
contour 2 3 4 5 6 7 8 9

(e)

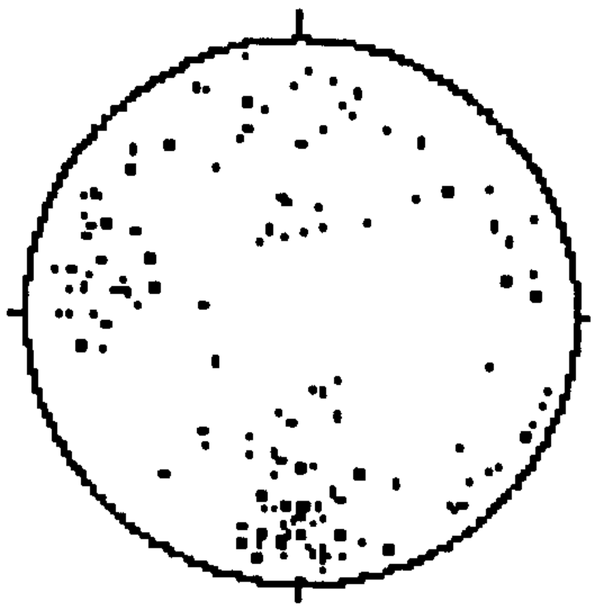

n=149

Fig. 6.31. (a-b) Contour and scatter plot of faults in wadi Assad, (c) slip of motion of faults, (d-e) contour and scatter of fractures in wadi Assad.

(a)

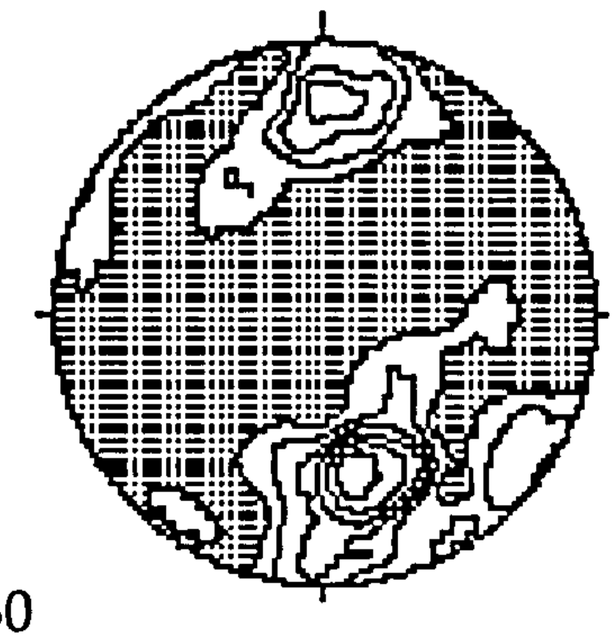

n=30
contour 1 2 3 4 5 6

(b)

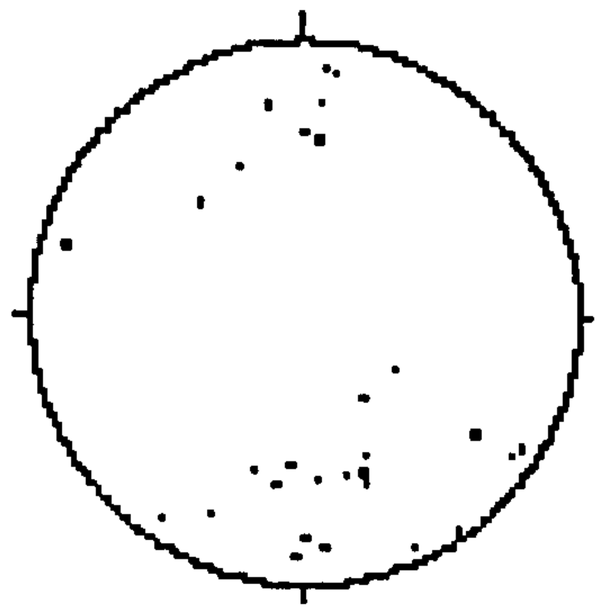

n=30

(c)

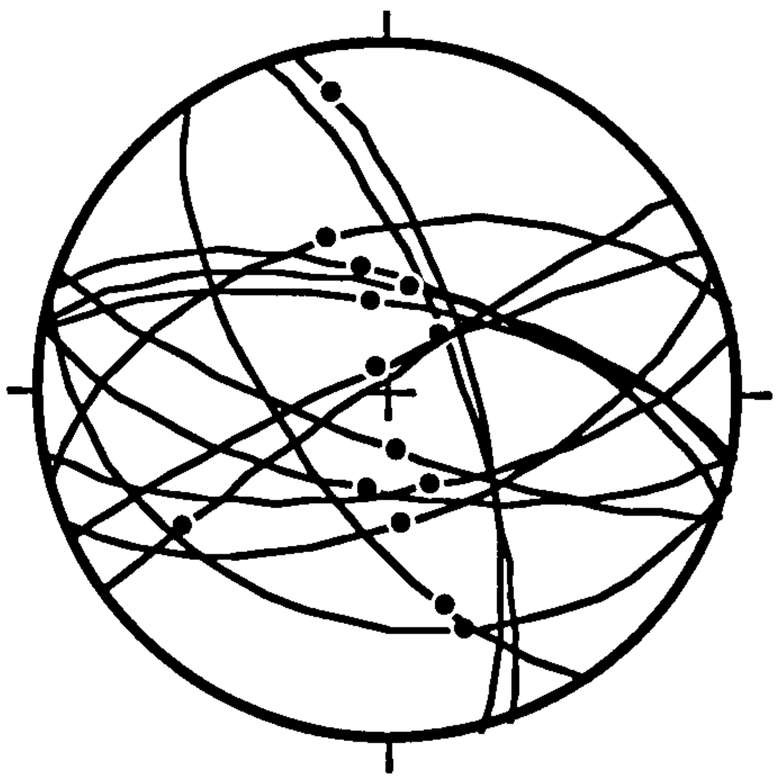

n=15

(d)

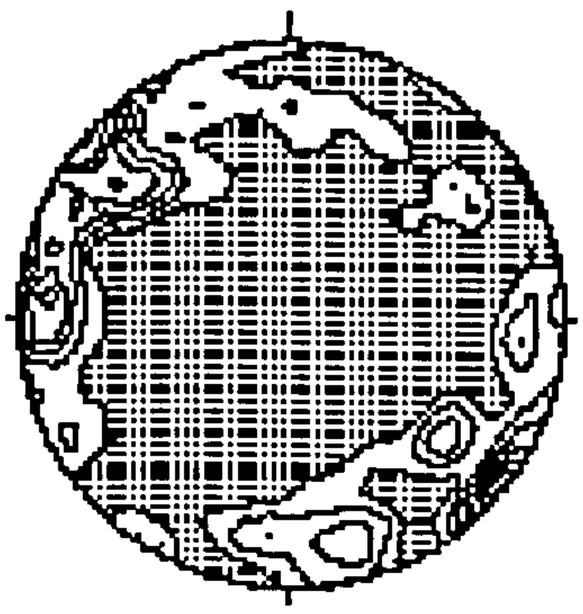

n=73
contour 1 2 3 4 5

(e)

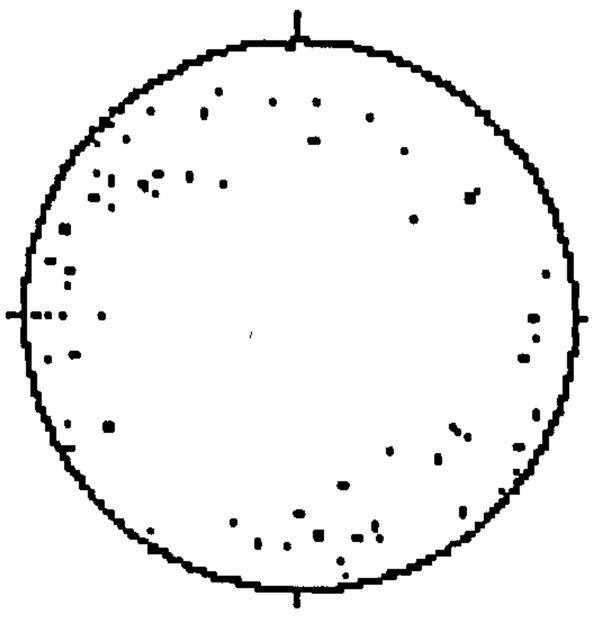

n=73

Fig. 6.32. (a-b) Contour and scatter plot of faults in wadi Bidish (c) slip motion of faults, (d-e) contour and scatter plot of fractures in wadi Bidish.

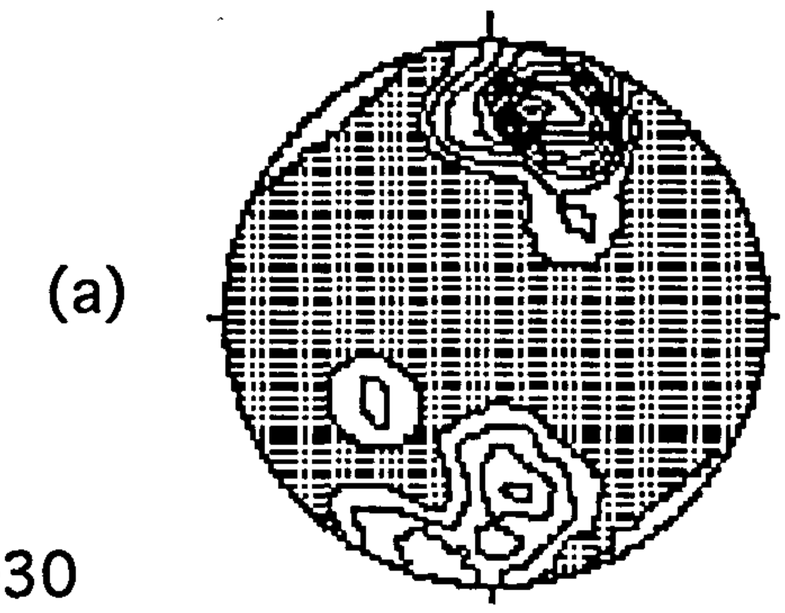

(a)

n=30

contour 1 2 3 4 5 6 7 8

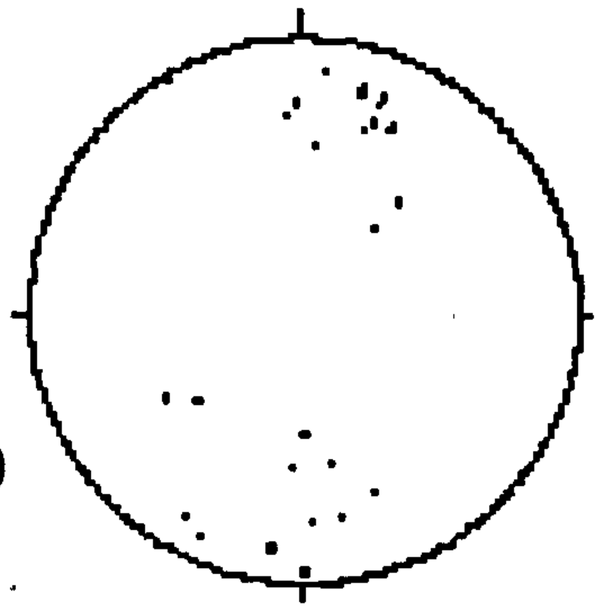

(b)

n=30

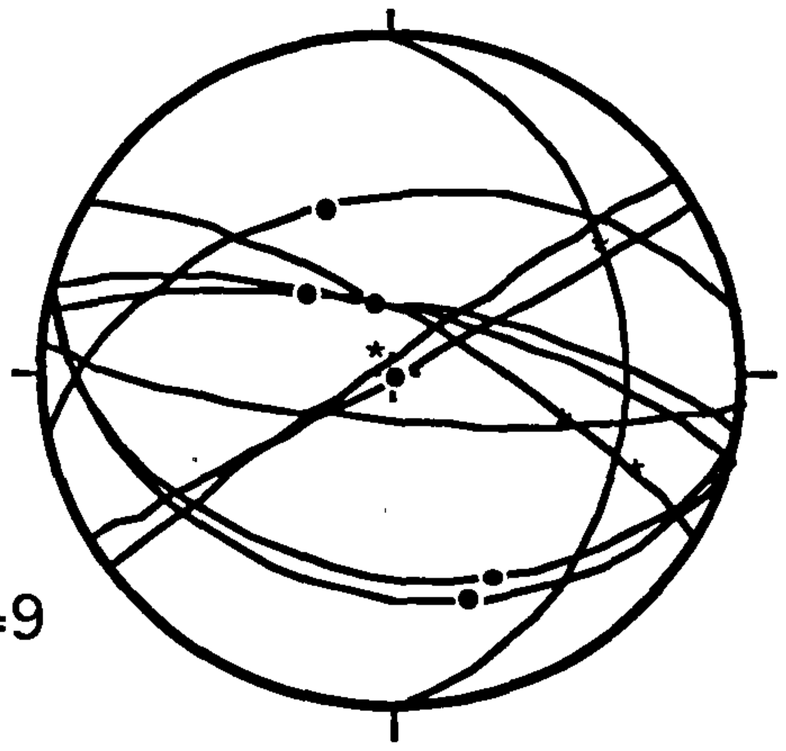

(c)

n=9

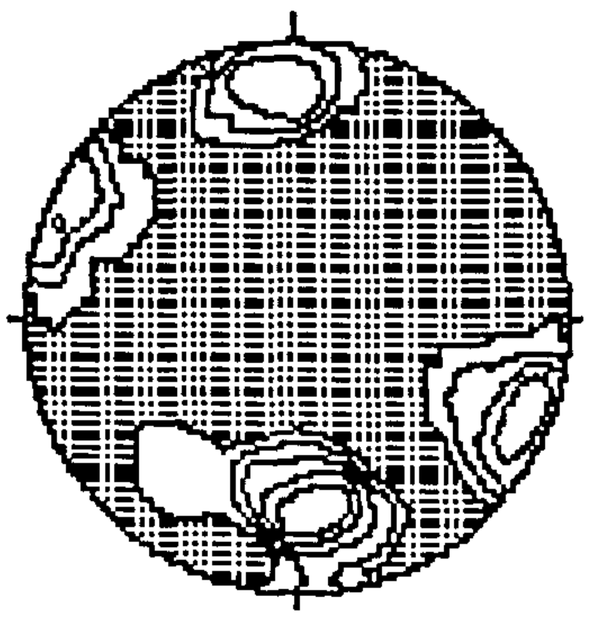

(d)

n=22

contour 1 2 3 4 5 6 7 8 9 10

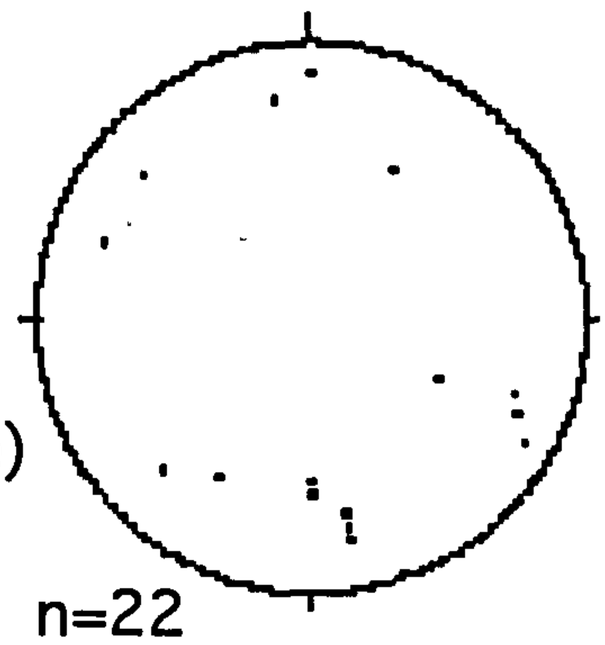

(e)

n=22

(f)

n=41

contour 1 2 3 4 5 6 7

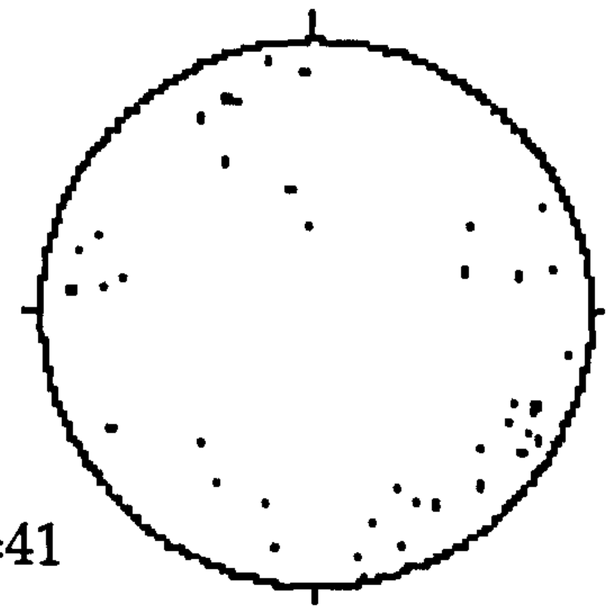

(g)

n=41

Fig. 6.33. (a-b) Scatter plot of faults in waid Shakhawi and (c) slip of motion of faults, (d-e) contours and scatter of fractures in wadi Shakhawi, (f-g) contoured and scatter plots of fractures measured the Shihr group.

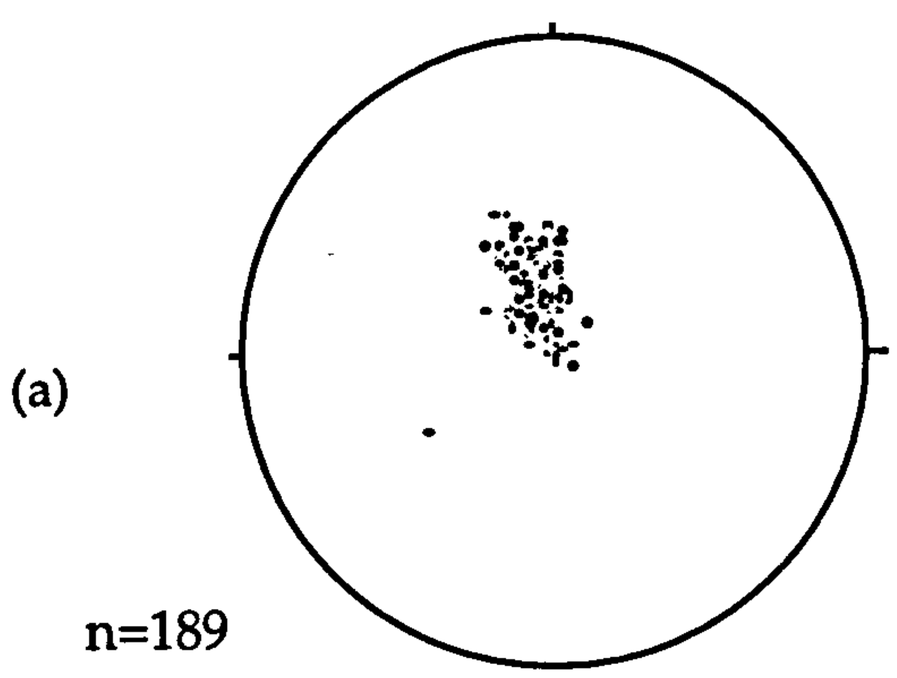

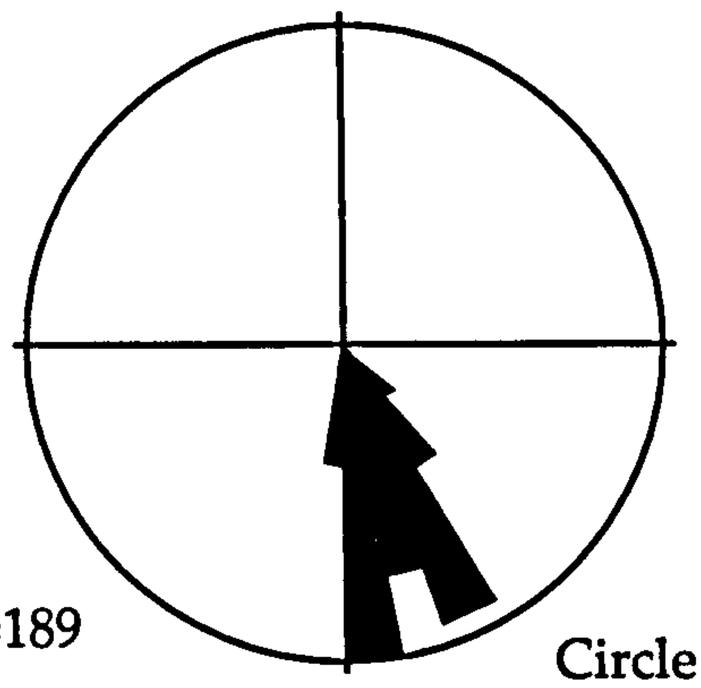

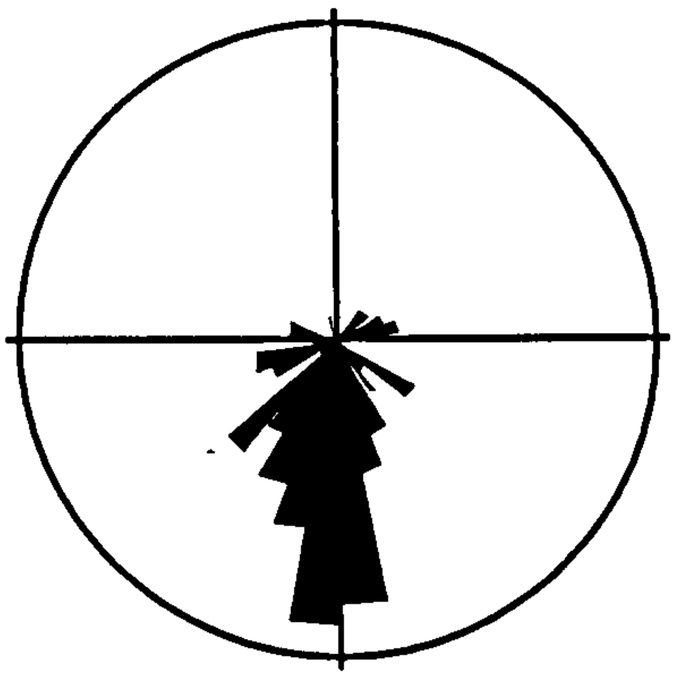

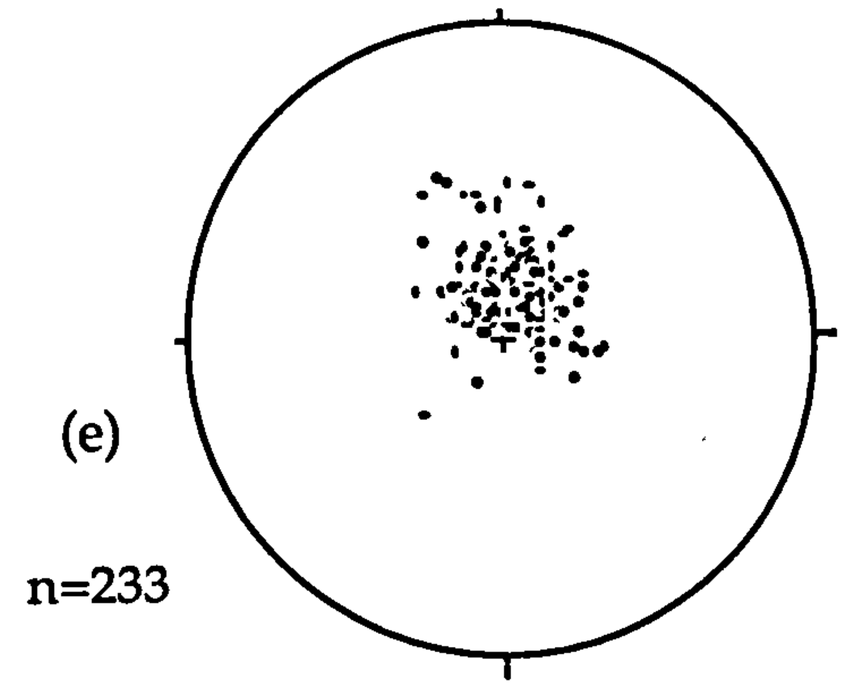

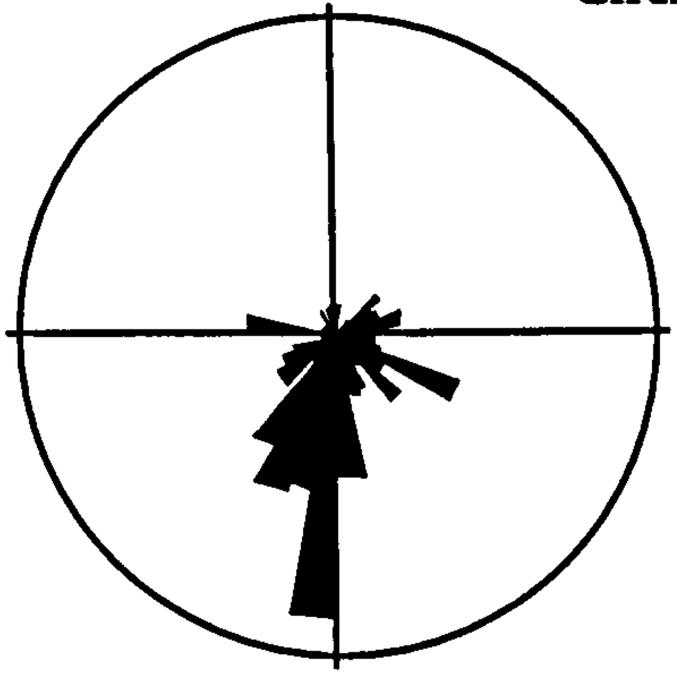

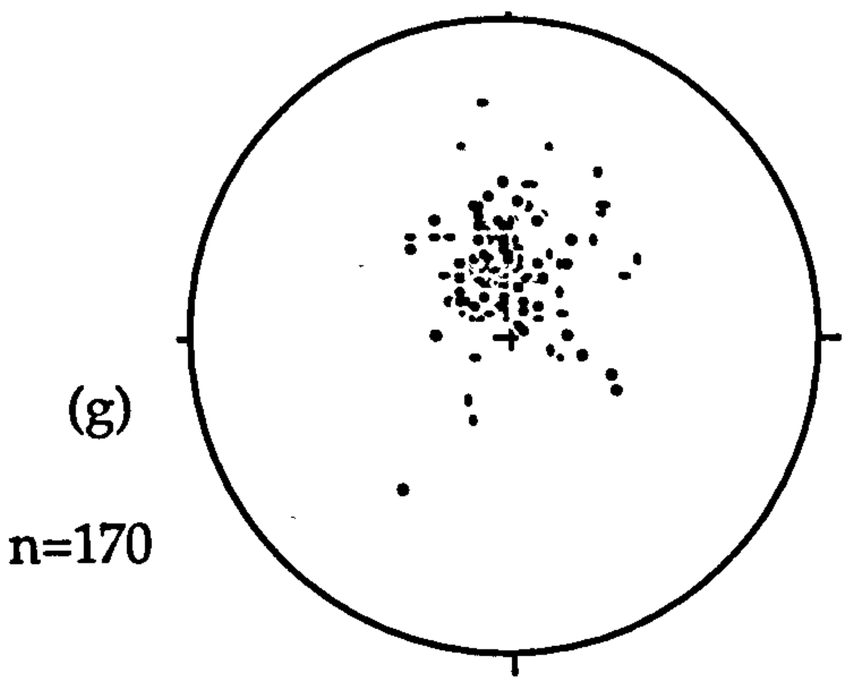

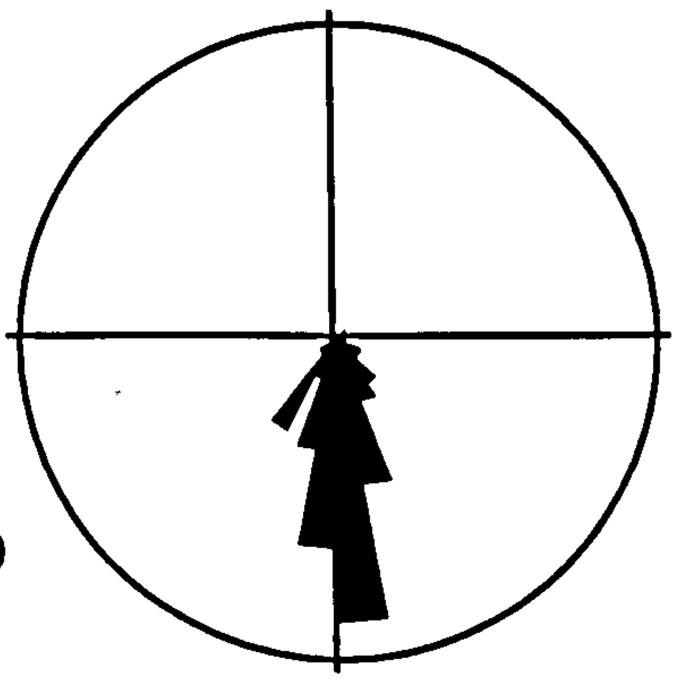

Fig. 6.34. (a-b) (a-b) Bedding planes in Hawayrah area, (c-d) bedding planes in Araf-Kharid area, (e-f) bedding planes in wadi Assad area and (g-h) bedding planes in wadi Bidish-Shakhawi area, a c e and g are orientation diagrams poles to bedding, b d f and h are rose diagrams of dip direction.

CHAPTER 7

GEOLOGICAL EVOLUTION

7.1 Introduction:

The northern margin of the Gulf of Aden encompasses a vast area both offshore and onshore and extends from Bab-Almandab in the west to Dhufar in the east (Fig. 1.1). Its geology is known only from limited field geological studies of certain parts. The margin consists of a crystalline basement of Late Precambrian to Cambrian age overlain by sedimentary rocks of Jurassic to Recent. Here the basement rocks are considered only so far as they may influence the development of younger structures.

Recently, Redfern and Jones (1995) defined three main basins formed in the northern margin of the Gulf of Aden whose formation as interior rifts was related to rejuvenation of the old Najd trend during Jurassic and Cretaceous times. These basins become progressively younger from west to east according to the age of their sedimentary rock; the western Marib-Shabwa Basin is filled dominantly by Jurassic rocks whilst the eastern Shabwa Basin and Sirr-Sayun Basin exhibit a progressively younger, early Cretaceous fill. The third basin known as the Hadhramaut-Jeza basin is located in the east of the margin and is the youngest basin wholly filled by Cretaceous deposits (Fig. 7.1). However, the

formation of the Hadhramaut-Jeza basin was most likely initiated on major conjugate extensional faults in the Jurassic with continuing movement during the Cretaceous since an off-shore well indicates the presence of a very thick Cretaceous section in excess of 4,000m (Richardson *et al.* 1995). These extensional faults are well observed in the study area. Cretaceous extensional faults have been recorded in the study area in outcrop and are compatible with subsurface structures (Paul 1990, Bott *et al.* 1992, Redfern and Jones 1995). Movement on these extension faults has resulted in the formation of Cretaceous basins such as the wadi Hawayrah basin and the Hadhramaut-Jeza basin (Fig. 7.1).

In addition to the geological mapping of the area (sheets I to V), analysis of more than 470 faults and 900 fractures concludes that at least five tectonic sets are represented and allows the tectonic evolution of the area to be described. The first was recorded in the basement rocks and most likely occurred during Precambrian times as the faults only affect the basement rocks and were later filled by younger dykes which do not intrude the cover sequence. The extension faults have a north-south strike parallel to the Mukalla high (Fig. 7.2).

The second set is recorded outside the borders of the study area from surface and subsurface, for example, in the Shabwa basin (Jungwirth and As-Saruri 1990), the Marib basin and the Hadhramaut-Jeza basin (Fig. 7.1) (Paul 1990, Diggens *et al.* 1988). This stage represents the most important movement other than the Oligo-Miocene affecting the margin and relates to Jurassic rifting and the formation of basins with considerable thicknesses of Jurassic rocks. These faults are recorded in the study area as rejuvenated faults during Cretaceous time to give thick deposits of the Harshiyat and Mukalla Formations (Fig. 7.3). Examples are the wadi Hamim fault, wadi Hawayrah fault and wadi Al-Madi fault (see sheet I and II, see volume II).

The third stage is not very common in the margin but it is recorded in the area in a few localities and has resulted in the formation of local unconformities in the Cretaceous succession. Some faults acted as growth faults, for example, extension faults in wadi Habeth in the uppermost part of wadi Assad affected the Fartaq Formation; the Mukalla Formation is missing in the footwall and thick in the hanging wall; a local unconformity occurs between the Fartaq Formation and the Umm er Radhuma Formation (Fig. 7.4)

Cretaceous extension faults of WNW-ESE strike resulted in the formation of local highs and unconformities as indicated by the absence of the Mukalla Formation and the variation in thickness of the Mukalla Formation throughout the south Hadhramaut area. The Cretaceous sedimentary rocks from the Qishn Formation at the base to the Mukalla Formation are of mixed marine and continental environments with mainly clastics in the west changing to carbonates in the east (Fig. 2.2 and Fig. 7.5).

The fourth stage is not obvious on the margin, but it has been confirmed during the field work that the margin has been subjected to horizontal movement in the Palaeocene and perhaps extending into the Middle Eocene. The evidence for this movement is overprinted by very steep slickensides relating to the Oligo-Miocene rifting (Fig. 7.6). The complexity of this horizontal movement increases in the east where a thrust fault is recorded in wadi Al-Masila and a reverse fault in wadi Shakhawi (Figs. 6.4b and 6.21). This horizontal movement is recorded by horizontal slickenside lineations in different localities. The horizontal lineations are later overprinted by those of the Oligo-Miocene extensional faulting (Figs. 7.6 and Fig. 6.2a).

The fifth stage represents the main period of extension which has caused the dissection of the plateau and is associated with the Oligo-Miocene rifting of the Gulf of Aden. This stage has generally obscured all the older tectonic movements due to its intensity particularly in the southern part of the margin

(Fig. 7.7). A later, post Pliocene, phase of extension, which can be differentiated from the fifth extensional stage, is recognisable by its affect on the Pliocene deposits (Fig. 7.8).

This extension follows the Oligo-Miocene trend which is related to the ocean floor spreading in the Gulf of Aden. In addition, another direction of extension follows the trend of the offshore fracture zones, i.e. NE-SW strike (Fig. 7.9).

Faults controlling the NW-SE trend are parallel to the Najd fault system which is recorded in the basement rocks in Saudia Arabia (Brown and Jackson (1960) and in the Al-Bayda area (Al-Kotbah 1992) as well as in the study area (Al-Kotbah and Allison 1995). In addition to the north-south trend (Hijaz) the old movement recorded in the basement rocks and the NW-SE trend (Najd), another trend in a WSW-ENE direction follows the trend of the Gulf of Aden and was probably initiated as strike slip faults along old weaknesses in the eastern part of Gondwana before separation of Somalia from the Arabian plate (Laughton *et al.* 1970). This trend was reactivated in Palaeocene times when it affects the sedimentary rocks of Jurassic to Palaeocene age in different localities and may even extend up to the Eocene.

The Palaeocene represents a period of quiescence on the northern margin of the Gulf of Aden and probably in the whole of the Arabian platform and even Somalia when the extensive and uniform nodular limestone of the Umm er Radhuma Formation was deposited (Beydoun 1964). During the early Eocene or middle Eocene, the northern margin was subjected to contractional movements which affected all sedimentary units from the Qishn to the Habshiya Formation and resulted in the formation of the south and north Hadhramaut arches with the intervening Jeza syncline (Burek 1969, Beydoun 1964, DGME 1986, Jungwirth and As-Saruri 1990) (Fig. 1.3). Other arches and

synclines formed along the margin to the north; the amplitude of these folds increases to the north and they become very tight in the south (Burek 1969).

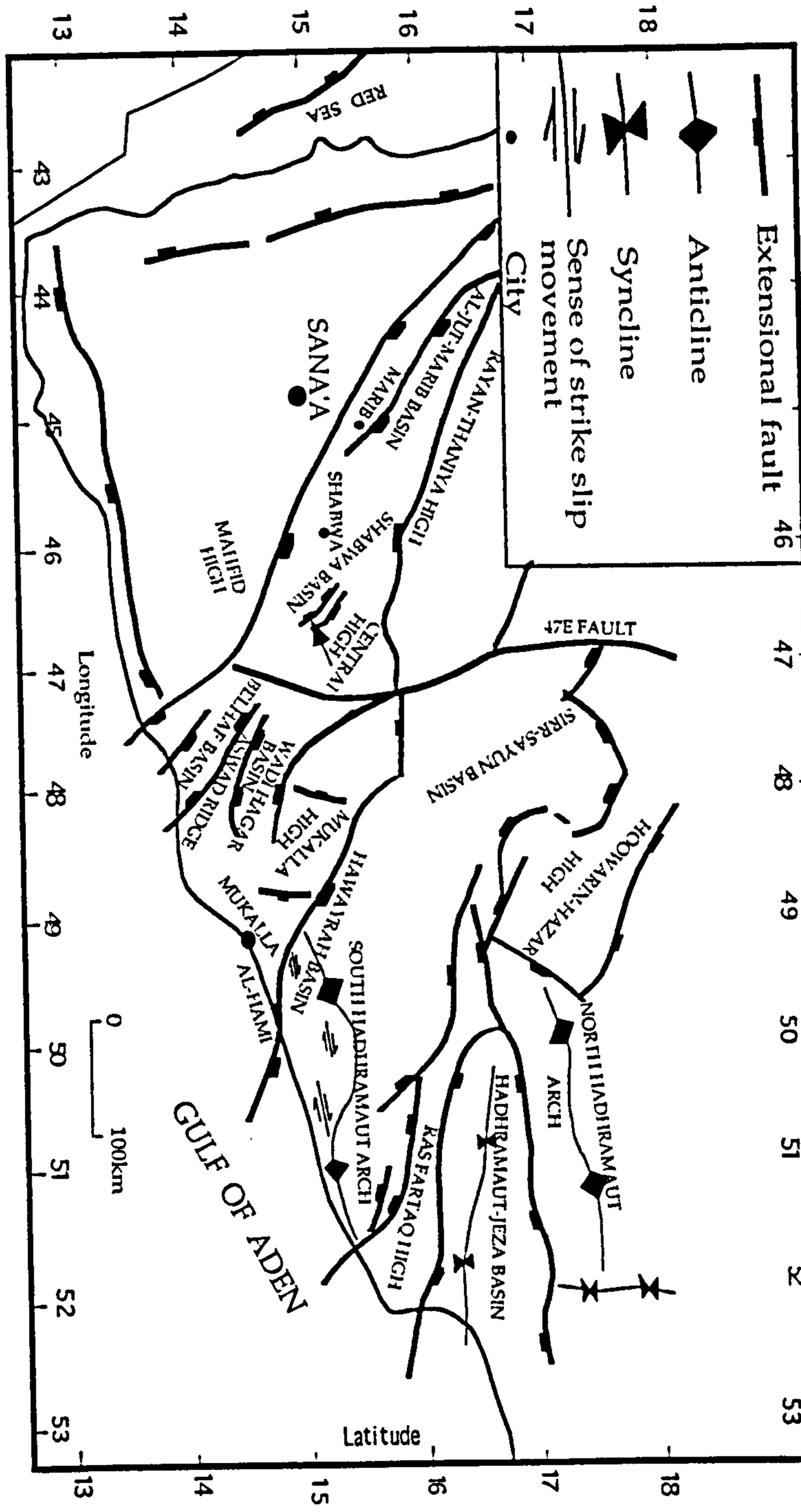

Fig. 7.1. Main basins of the northern margin of the Gulf of Aden (after Redfern *et al.* 1995) and the present study.

Table. 7.1. Summary of tectonic events.

Age	Tectonic event	Description
Early Proterozoic	Hijaz cycle	Reactivated Hijaz structures recorded in south Hadhramaut area by the presence of the Mukalla-Hoowarin high. With absence of the Jurassic rocks confirmed from the outcrop and subsurface data. In addition, north-south faults recorded in the area have the same trend as of the Hijaz orogen.
Proterozoic-Cambrian	Najd movement	Najd fault system trend; reactivation of Najd structures played an movement play an important role in the formation of many basins during the Jurassic time (e.g. Shabwa-Belhaf basins) and were rejuvenated again during the Cretaceous to form the Hadhramaut-Jeza basin.
Palaeocene	Strike slip movement	Strike slip movement occurred in the area at the end of Palaeocene and extended to Eocene
Post Middle Eocene	Alternating series of anticlines and synclines	At the end of Middle Eocene the margin was subjected to a contractional stage which affected all rocks older than the Habshiya Formation.
Oligo-Miocene	Rifting of the Gulf of Aden	Extension stage which represents the most obvious event seen today in the northern margin of the Gulf of Aden.
Pliocene	Volcanic activity	The volcanic activity affected the margin from Bab-Almandab in the west to the Qishn in the east. These basaltic lavas flow mainly along wadis.

The Oligo-Miocene sedimentary rocks of the northern margin of the Gulf of Aden occur on a narrow and discontinuous coastal belt especially between Mukalla and Sayhut. They extend offshore and are encountered in offshore wells drilled by Agip (see sheet VI). The Oligo-Miocene deposits are the synrift rocks with a heterogeneous nature comprising carbonates, sandstones, shales, conglomerates and evaporites.

At the end of the Miocene a period of uplift occurred and resulted in the peneplanation of the Shihr Group, before another stage of extensional faulting started relating to a second stage of sea floor spreading in the Gulf of Aden (Matthews 1967). The resulting subsidence allowed the deposition of the Pliocene deposits unconformably on the syn-rift Shihr Group. During the Pliocene volcanic activity occurred along the coastal plain from Bab-Almandab in the west to the Qishn area in the east.

A summary of the tectonic movements affecting the northern margin is shown in table 7.1.

7.2 Basement structure

In the study area the basement rocks are exposed in a limited area in the Harshiyat-Ydmah area. Fractures and lineaments have been mapped from air photos, satellite images and field work (see sheet I).

Further west, fracture trends, such as NNE-WSW and NW-SE, in addition to the trend of WSW-ENE which is parallel to the Gulf of Aden, have been recorded by many authors (Beydoun 1964, Greenwood and Bleackley 1967, and Al-Kotbah 1992). Recently Redfern and Jones (1995) state that the north-south structural grain was offset by conjugate wrench faults of the NW-SE (Najd) trend and NE-SW (Hadhramaut) trend. The left-lateral Najd trend was dominant and is considered to have controlled the later (600-540Ma) formation of the Arabian infra-Cambrian salt basins, as small pull apart basins, under a

generally extensional regime (Greenwood *et al.* 1980, Husseini and Husseini 1990). The regional effect of these three principal orientations of Precambrian basement grain (Hajaz, Najd and Hadhramaut trends) across the Arabian craton is extensive, and they have exerted a strong control on subsequent tectonics. These structural lineaments are observed in the Harshiyat-Ydmah area (Fig. 7.2). Some trends, including some with low angles of dip, are only recorded in the basement rocks and do not occur in the sedimentary cover (Fig. 7.10). A thin layer of conglomerate of the Qishn Formation rests unconformably on the basement in the Ydmah area (Fig. 7.11). A large gap of geological time from the Cambrian to the Lower Cretaceous is missing in this area which acted as a high controlled by the old basement structures.

North-south fractures are very common in the basement rocks and have wide range of dip from high to low angle. Most of fractures of this trend are extensively developed in the basement rocks and some fractures are filled by dykes implying east-west extension (Fig. 7.2 and 12). Subsequently, some fractures have been reactivated and have affected the sedimentary cover (see sheet I). To the northwest of Ydmah, a reactivated north-south fault continues upward through the Qishn Formation with small offset (Fig. 7.13). Shallow pitching slickensides on the fault planes indicate that strike slip motion of the Precambrian age is recorded in the basement rocks which is probably the same trend affected in the sedimentary cover during the Palaeocene (Fig. 7.14); however, most of the old fractures have been reactivated during the Jurassic and Cretaceous time and onward.

Fig. 7.2. Dyke in basement intruded along north-south fracture, Ydmah area.

Fig. 7.3. Thick sequence of Cretaceous rocks of the Mukalla and Harshiyat Formations, wadi Hawayrah. Prominent layer in middle of sequence is the Sufla member and the a row pointed to it.

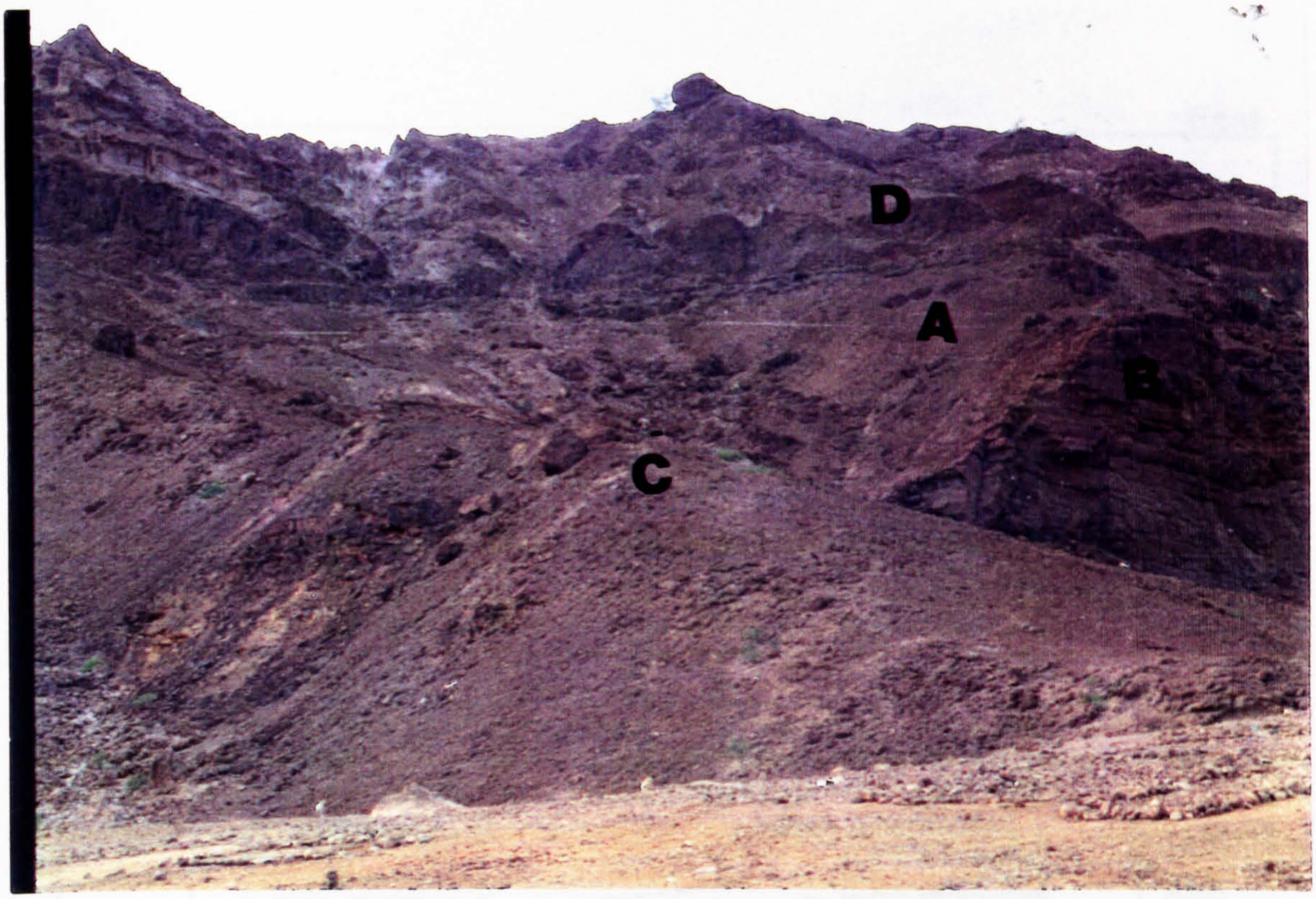

Fig. 7.4. Cretaceous extensional fault (A) cutting the Fartaq Formation (B) and Mukalla Formations (C) but not the Palaeocene Umm er Radhuma Formation (D), wadi Assad.

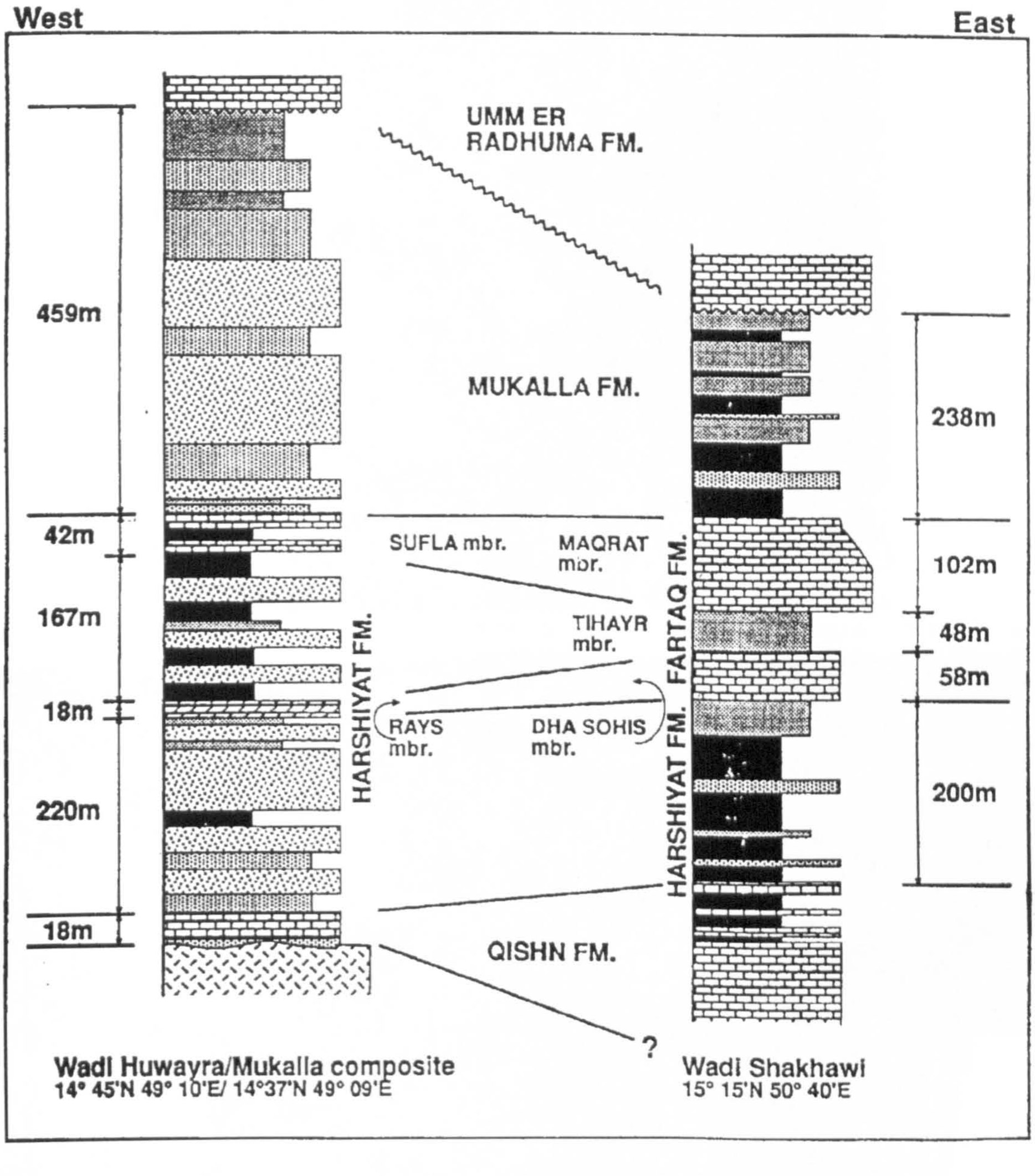

Fig. 7.5. Stratigraphy of the Tawilah Group, Hadhramaut Province (after Watchorn 1995).

Fig. 7.6. Older horizontal and younger vertical slickensides on a fault surface, wadi Bidish.

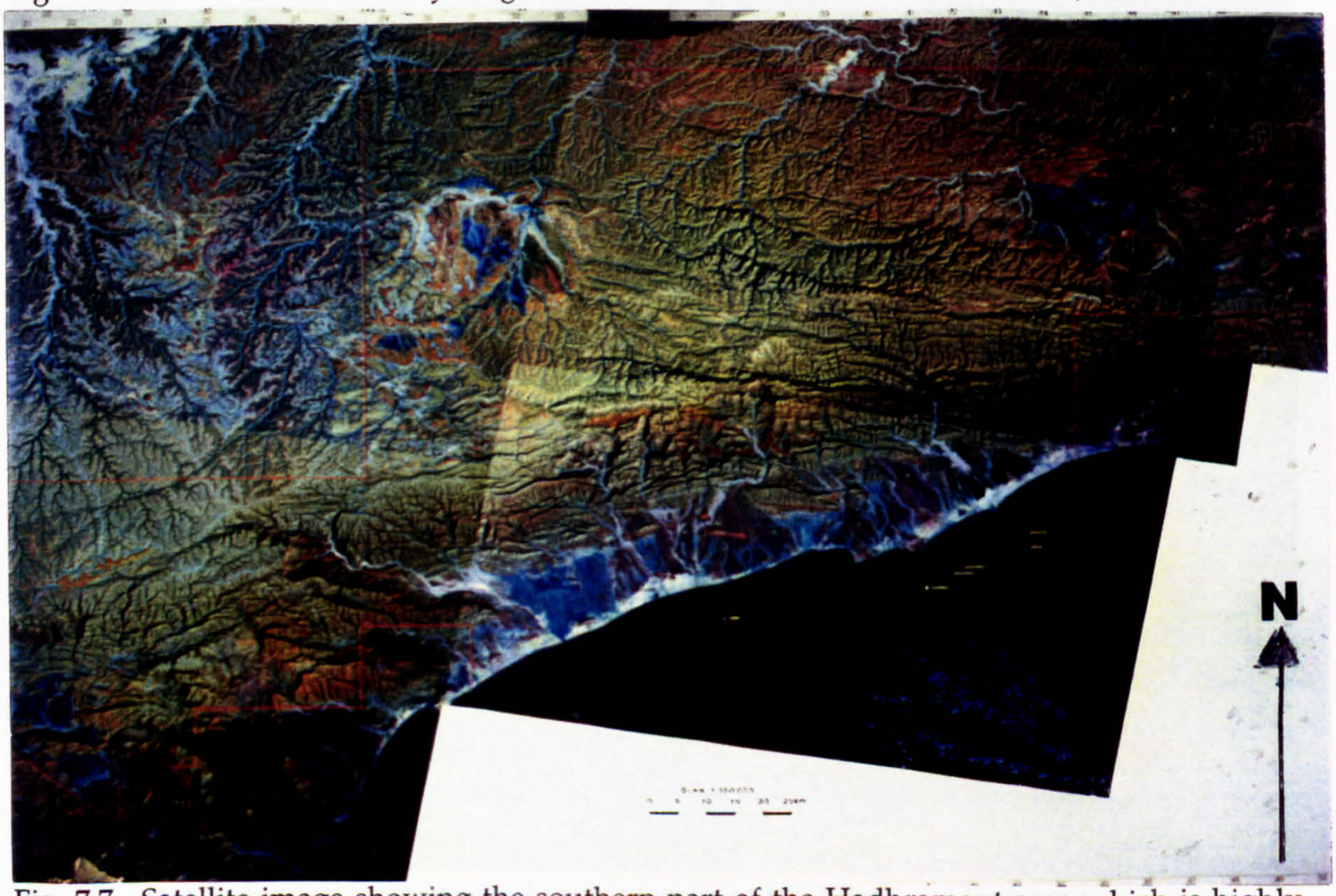

Fig. 7.7. Satellite image showing the southern part of the Hadhramaut area which is highly dissected by the Oligo-Miocene extensional faults.

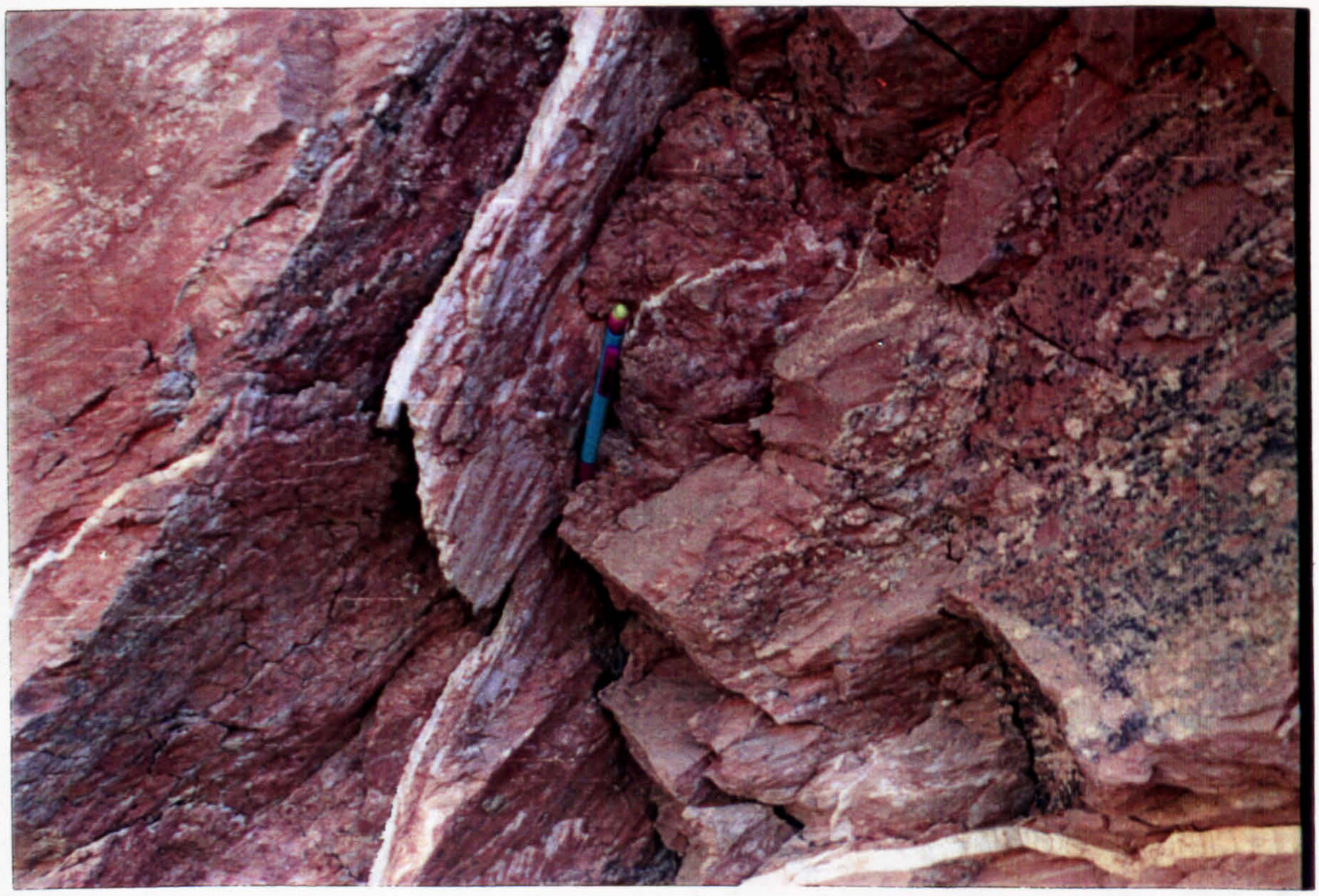

Fig. 7.8. Fault with oblique slickensides cutting the syn-rift Shihr Group rocks, north of Al-Hami area.

Fig. 7.9. The Shihr Group is subjected to two trends of fractures, Ad-Deis area.

Fig. 7.10. Fractures within basement showing variation in dip. Note especially the low angle fractures, wadi Mahanea to the south of Lusp village.

Fig. 7.11. Unconformity between the basement rocks and the Cretaceous Qishn Formation in the Ydmah area.

Fig. 7.12. Unconformity showing a high intensity of fractures in the basement rocks in the lower part and fewer fractures in the sedimentary cover in the upper part, Ydmah area, looking SW.

Fig. 7.13. Contact between the basement rocks (B) and the Qishn Formation (Q). Steep younger fault affects both rocks. Wadi Asfal Al-Ein, northwest of the Ydmah area, looking S.

Fig. 7.14. Oblique slickenside lineations in basement rocks, south wadi Hamim.

7.3 Jurassic structures

The exploration for hydrocarbons in Yemen has provided a geological framework for the evolution of the northern margin of the Gulf of Aden. Subsurface data has allowed the delineation of high areas during the Jurassic and the corresponding basins. The thickness of Jurassic rocks varies from one basin to another. Four Formations make up the Amran Group in the southern part of Yemen; they are the lower Shuqra Formation, the middle Madbi Formation and the upper Naifa Formation with a transitional Sabatain Formation (Beydoun 1964).

Tectonic movement in Jurassic times resulted in the formation of immature rift basins in which a thick sequence of Jurassic carbonates were

deposited as potential source and reservoir rocks of petroleum in several localities such as the Marib, Shabwa and Jeza basins.

Rapid subsidence of these Jurassic basins allowed up to 6 km depth of sediment to accumulated (Diggens *et al.* 1988, Al-Thour 1992 and Jungwirth and As-Saruri 1990). The structural elements controlling these basins were either reactivated Palaeozoic faults, or new structures formed during the Mesozoic (Beydoun 1981 and 1988) (Fig. 7.1).

During the middle and upper Jurassic, the thermal sag phase led to a marine transgression with the deposition of the extensive pelagic carbonates of the Shuqra, Madbi, Naifa Formations and evaporate Sabatain Formation (Beydoun 1969).

From a synthesis of previous data and current fieldwork it can be concluded that the western part of the study area was positive during the Jurassic as all Formations of that age are missing on the highs and also in the Al-Hami off-shore well which penetrated through the Tertiary and Cretaceous rocks directly into basement (Agip 1981 unpublished report, Haitham and Nani 1990).

7.4 Cretaceous structures

The Cretaceous sea level was unstable with alternating transgressions and regressions which is evident from the presence of three layers of limestones intertonguing with mainly clastic rocks of a continental environment indicated by silicified wood in the Harshiyat Formation (Fig. 2.8). Extension during the Cretaceous formed faults which cut the Cretaceous rocks but do not affect the Umm er Radhuma and younger Formations (Fig. 7.4). Thick sequences of Cretaceous rocks in some localities are probably attributed to growth faults. For example, in wadi Hawayrah the Mukalla and Harshiyat Formations reach more than 1,000m in the hanging wall of wadi Hamim fault

(Fig. 7.3) and in the AlFalk IX well more than 1200m of Cretaceous is encountered (Paul 1990). This well is located in the centre of the Hadhramaut-Jeza basin which formed during the Jurassic and whose development continued into the Cretaceous.

During the Cretaceous, the northern margin of the Gulf of Aden still belonged to the Tethyan domain (Al-Thour 1992, Platel and Roger 1989) with extensive middle-shelf carbonate sedimentation in a shallow warm sea allowing the development of Rudist biotopes. In the study area during the early Cretaceous, most of this area was uplifted and any Jurassic rocks were eroded away or, alternatively, this area was a high even during the Jurassic and continuing into the Lower Cretaceous. In the Ydmah-Harshiyat area where the basement rocks are exposed, part of the Mukalla-Hoowarin high subsided and the sea transgressed during Barremian-Aptian times to deposit the lower Qishn Formation.

The Cretaceous succession starts with the Qishn Formation in which a highly fossiliferous basal conglomerate, which includes some fragments of the basement rocks, is overlain by the Qishn limestone as the sea became deeper and clastic input decreased. From the end of the Aptian, through the Albian-Cenomanian period deposition was mainly of continental deposits with intertonguing arms of limestones which die out in the west of the area. The source of these clastic rocks is probably the basement rocks or, less likely, the pre-Cretaceous rocks which were high in the central part of Yemen. During this period the margin was subjected to three stages of intermittent subsidence which resulted in the formation of shallow calm water in the western part becoming deeper to the east.

The late Cretaceous was a time when continued movement on active faults formed deep marine basins in the east, such as the Hadhramaut-Jeza basin, while in the west continuous regression of the sea formed the thick

sequences of the Harshiyat and Mukalla Formations as continental clastic deposits of braided rivers which may be correlated with the Tawilah clastics in western Yemen (Al-Subbary 1995). The shallow marine facies in the west grades eastward to relatively deep marine facies resulting in the formation of lateral changes to mainly shales and marls alternating with thin layers of limestones in the east (Fig. 2.2).

The Mukalla Formation is well defined and conformable with Harshiyat-Fartaq Formations and it is very difficult to differentiate between the Harshiyat and Mukalla Formations if the two limestone members (Rays and Sufla) are not present (Fig. 7.3). During the deposition of the Mukalla, there is strong evidence to suggest that the margin was subjected to extension. The extensional faults of the Cretaceous have strikes parallel to the axis of the Gulf of Aden (Fig. 7.4). Horizontal movements on these Cretaceous faults may support the hypothesis that there is an old weakness trending parallel to the present rift axis (Fig. 8.1). The Mukalla Formation is distributed throughout the margin with local changes in its thickness which may be attributed to either the differential elevation of block faulting during the Cretaceous extension stage or, less likely, to partial erosion.

In the study area deposits of Maastrichtian age, the Sharwayn Formation, are not recorded whereas it occurs further east outside the study area. Within the Mukalla high the Qishn Formation is very thin while to the east of the Al-Hami well it becomes thicker as shown in the Sharmah and Sarrar wells and wadi Shakhawi (Fig. 7.5). The offshore wells show that the Jurassic rocks occur in subsurface and they confirmed that the Jurassic basins are structurally controlled. These structures are reactivated during the Cretaceous to give thick deposits in the margin such as the wadi Hawayrah basin and Hadhramaut-Jeza basin.

7.5 Palaeocene-Eocene structures

The northern margin of the Gulf of Aden was flooded during the Palaeocene to form a shallow marine platform where the homogeneous Umm re Radhuma Formation was deposited all over the margin and extending north to cover all Yemen, Saudi Arabia, Oman, United Arab Emirate and extends northeast further to Iraq. It has a nearly constant thickness varying slightly between 200m and 250m in thickness.

The transgression of the sea continued during the early Eocene when the Jeza Formation was formed. The Jeza Formation consists of shales and marls and indicates deeper water conditions. In its upper part, evaporites and limestones indicate a minor regression. During the middle Eocene the sea became restricted and a thick sequence of evaporites, the Rus Formation, were deposited. These evaporites are widely distributed throughout most of the eastern part of the northern margin particularly in the plateau and they extend north into Saudi Arabia.

The Rus Formation is significant as a cap rock and seal of the pre-Shihr Group rocks. During the late middle Eocene, in a further transgressive stage, the Habshiya Formation was deposited consisting of alternating limestone with papery shales, both highly fossiliferous. The Habshiya Formation is conformable with the Rus Formation in most of the northern margin, but in some localities shows a distinct change from evaporites to shales and marls, indicating a possible time break, for example, in south eastern Mahra the Habshiya Formation overlies either the Jeza or the Umm er Radhuma Formation (Beydoun 1964).

Structurally, the margin was uplifted at the end of the middle Eocene and no late Eocene sediments have been deposited. The significant tectonic movement during Palaeocene to Eocene times, are horizontal movements affecting the whole area. This event affects the Umm er Radhuma and older

Formations and probably extends to the Eocene deposits, but this has not been confirmed (Fig. 7.6). This horizontal movement is recorded in different places, for example, in the Switchbacks area, in south wadi Bidish, at Al-Mahdith a place famous among the bedu for its hot springs which are used for treatment and in wadi Shakhawi (Fig. 7.6 and Fig. 6.2b). This movement is clearly older than the rifting because the horizontal slickensides associated with this movement are everywhere overprinted by very steep slickensides which are related to the Oligo-Miocene syn-rift faults (Fig. 7.6 and Fig. 6.2a-b).

By the end of the middle Eocene, this area was subjected to contractional movement resulting in the formation of alternating anticlines and synclines along the margin, for example, the coastal range arch in the west, offshore syncline, south and north Hadhramaut arches, Jeza syncline and Dhufar-Haqf arch in the east (Fig. 7.1).

The amplitudes of folds formed during the Eocene decrease northward and die out gradually and increase to very tight southward to the Gulf of Aden (Burek 1969). In the study area the major regional structures are the Mukalla high and the south Hadhramaut arch even though the geomorphology of the area is related to the intensity of extensional faults. The structures formed during the various events all tend to have an en echelon pattern whether they are the broad arches or closely-spaced extensional faults. This pattern is most likely due to rotational strains affecting the margin. The northern margin of the Gulf of Aden has this structural property that the tectonic movements of different ages are arranged in en echelon patterns, for example, the contractional movement of Eocene time forming the alternating anticlines and synclines have this pattern then the Oligo-Miocene extension faults show this property. So the structural pattern is probably related to one source of major forces which controlled their formation.

Beydoun (1995) has recently changed his opinion on the existence of the south Hadhramaut arch. The basis of his new interpretation is subsurface data, available since his initial field work, which indicates that there is no evidence for this arch.

7.6 Oligo-Miocene structures

The Oligo-Miocene history of the northern margin of the Gulf of Aden was dominated by faulting during the major extensional stage and is associated with the opening of the Gulf of Aden and oceanic floor spreading along the Sheba ridge (Fig. 7.7). The structures which formed during this period are mainly extensional faults associated with subsidence of fault blocks from the coastal plain and the offshore basins. This basin has a thick sequence of syn-rift sediments, the Shihr Group, which exceeds 2000 m (Agip 1981 unpublished report).

The extensional faults have dissected the entire northern margin of the Gulf of Aden and have resulted in an increase in dip of bedding in the southern part of the margin close to the coastal plain. This change in the dip is due to rotation of the faulted blocks. To the north, the intensity of extensional faulting decreases.

The extensional faults are very obvious in the satellite images which were used as base maps during the field work and mapping. The maps are dominated by the faults related to the Oligo-Miocene extension for which values have been computed for a number of cross sections (see chapter 5) (see sheet, I, II, III, IV, and V, in volume II).

These Oligo-Miocene structures are mainly half-grabens and sometimes, full graben. Full graben are arranged in an en echelon style similar to the style of folds (Fig. 7.7). This en echelon pattern may be related to structures underneath the sedimentary cover or to strike slip fractures of the trend of

those offsetting the Sheba ridge. The regions where displacement is transferred from one major structure laterally to another are transfer zones in which the values of extension are lower than elsewhere (Fig. 6.14) (Al-Kotbah and Allison 1995).

At the end of the Shihr Group deposition, the northern margin was uplifted and a short period of erosion took place since there is an unconformity between the Shihr Group and the Pliocene deposits (Fig. 7.15). The Shihr Group is affected by local asymmetrical folds. Most of the fold axes plunge gently toward the east while some are horizontal (see sheet, I, II, and III).

7.7 Pliocene-Recent structures

The Pliocene deposits consist of sedimentary rocks from various environments such as marine, river, alluvium and wind dunes. These different environments indicate that the margin during Pliocene times was unstable. The Pliocene deposits are not thick and are found sporadically along the coastal plain and in the floors of the bigger wadis. They may be seen to overlie unconformably all other stratigraphic units. The conglomerate deposits of the Pliocene-Recent are varied from well bedded to unbedded with different grain sizes and the source rocks can be easily identified as the formations seen today in the plateau.

Structurally, the Pliocene deposits are in most places nearly horizontal, and only rarely are these rocks tilted (Fig. 7.16). No major extensional faults are recorded in the Pliocene deposits, but they are affected by two dominant fracture trends which coincide with the Gulf of Aden trend and the Alula-Fartaq fracture (Fig. 7.17 and 7).

After the deposition of the Pliocene-Recent deposits the northern margin of the Gulf of Aden was affected by volcanic activity which formed lava flows on the coastal plain at different localities along the main wadis such as in

wadi Thowb to the west of wadi Assad, wadi Bidish, wadi Shakhawi in the eastern part of the study area and on the flat area along the coast plain and in the Qusayr-Sayhut area to the east (Fig. 7.18).

More recently, the northern margin of the Gulf of Aden has been uplifted slightly and Recent marine sediments now stand more than 80-100m above sea level; this stage of uplift is probably still active (Fig. 7.19).

Fig. 7.15. Angular unconformity between the Shihr Group below and the Pliocene deposits in the Ad-Deis area to the south of wadi Kharid, looking east.

Fig. 7.16. Pliocene deposits dipping to the north due to the rotation towards a fault plane, south wadi Bidish, looking east.

Fig. 7.17. Pliocene conglomerates affected by extensional fractures, wadi Bidish.

Fig. 7.18. Lava spreads in south wadi Assad overlying the Shihr Group and Pliocene deposits, oblique air photograph.

Fig. 7.19. Coast plain about 100m above sea level showing the Umm er Radhuma Formation occurring as an inlier, south wadi Kharid, looking SW.

CHAPTER 8

REGIONAL IMPLICATIONS

8.1 Introduction

The northern and southern margins of Gulf of Aden which are now 300 km apart, are stratigraphically and structurally comparable, with the Jurassic to Middle Eocene succession able to be matched across the Gulf (Beydoun 1964, 1970, Abbate *et al.* 1974, Abbate *et al.* 1986, Bruni and Fazzuoli 1976, 1980 and Bosellini 1989). In the northern margin Precambrian basement occurs along the coast from Abyan in the west to Mukalla in the east and is connected to the main mass of Precambrian rocks which make up the central plateau of Yemen. In the north of Somalia the Precambrian basement occurs as a discontinuous chain along the coastal margin (Bosellini 1989). The present thesis deals with the structural elements in the south Hadhramaut area and is regarded as the first detailed structural study on the sedimentary rocks of Cretaceous to Recent in age. The distribution of different stratigraphic Formations and the major structures are considered to be correlatable with those in the western part of Yemen, in Oman and also with those in the southern margin in northern Somalia. However, the break-up of Gondwanaland during the Late Permian resulted in extension and rifting. Separation of the former fragments of the northeast margin of

Gondwanaland from Arabia occurred during the Triassic (Beydoun 1991, Redfern and Jones 1995, Janssen *et al.* 1995). The southeast Arabian margin (Oman, Somalia and Yemen) was closely involved in this activity, as the Afghan and Central Iran blocks had originally been sandwiched between Arabia and India and are believed to have moved eastward along major transform faults during the early Triassic. These movements maintained the uplifted attitude of the Somalia and Yemen area, which was further supported by updoming, prior to Indian-Arabian rifting.

During this period, transgression across the shallow shelf deposited the terrestrial to transitional marine basal Kohlan sandstone (Early-Middle Jurassic) and the shallow-marine Shukra carbonates (Oxfordian to lower Kimmeridgian) over a wide area. These deposits are thought to have largely accumulated in incipient intracratonic sags, developed between highs such as the Hoowarin, Mukalla, Mahfid and Rayan-Thaniya highs, all of which remained essentially free of Jurassic sediments (Redfern and Jones 1995) (Fig. 7.1).

The Cretaceous sediments are of wide distribution throughout Yemen and extend to Somalia and east Africa. In the study area these rocks consist of clastics in the west and change laterally into carbonates in the east. The equivalent rocks in north Somalia show the same variation from west to east.

The Oligo-Miocene deposits are of local distribution and restricted to borders of the Gulf of Aden (Beydoun, 1964, 1966, 1970, Bruni and Fazzuoli 1976, Bosellini 1989). The Oligo-Miocene extensional faults on both margins show the same structural style.

8.2 Precambrian

Since cratonization of the Arabian-Nubian shield at the end of the Proterozoic much of it has remained subaerial and of low relief, on the northern border of Gondwanaland (Almond 1986). The basement rocks which are uplifted

today in central Yemen to more than 2,000m above sea level most likely represent the source rocks of clastic rocks in both sides of the Gulf.

However, the major faulting affecting north Somalia is the WNW to NW trend which is predominant and can be traced from the onshore to the continental rise (Abbate *et al.* 1986). This trend in pre-drift reconstruction can be matched a cross the Gulf (Abdel-Gawad 1970). Abbate *et al.* (1986) assumed that the Gulf of Aden nucleated and developed in this belt of crustal weakness, and the fault patterns of the initial deformation (rifting) and of the successive continental dismembering and drifting were determined both by the ENE trend of the belt and by the NNE direction of the Nubian and Arabian relative plate motion.

A peneplanation of the Precambrian rocks occurred between the Cambrian and the middle Jurassic in most of the margin. Strong differential vertical movement resulted in the formation of the Mukalla-Hoowarin high where the Jurassic sequence is missing; its north-south orientation probably resulting from Jurassic reactivation of faults of the Hijaz trend (Beydoun 1969, Brown and Coleman 1972).

In some places Cambrian clastic rocks are found in the northern margin such as Ghabar Group to the west of Mukalla and Murbat Formation close to the Salalah in Oman, these clastic rocks are slightly metamorphosed (Beydoun 1964), and they are not recorded in the study area even from subsurface data. Many workers interested in the margin never mentioned any evidence of the presence of Cambrian to Palaeozoic sediments with exception of the Ghabar Group (Beydoun 1964, 1969, Greenwood and Bleackley 1967) and this view was reiterated by Beydoun and Greenwood (1968) and Murbat Formation to the east in Dhufar (Beydoun and Greenwood 1968). The southeastern part of the Arabian plate, particularly the Hadhramaut area, was positive during the Palaeozoic and continued until the end of Jurassic time. Consequently, this area was affected by north-south tectonic movement resulting in the uplifting of most of the south Hadhramaut area, as shown by the absence of Jurassic rocks along the strike of the

Mukalla-Hoowarin high and confirmed by subsurface data from Hawarim, Tarfayt and Shu'ayt wells (Beydoun 1969) and the Al-Hami well in the study area.

8.3 The Jurassic

The northern margin of the Gulf of Aden was dissected by many major faults to form several Jurassic basins. These faults are rejuvenated from the old Najd tectonic movement of NW trend. These Jurassic basins have been described throughout the northern and southern margins by many authors (Beydoun 1964, 1966, 1970, Bruni and Fazzuoli 1976, Abbate *et al.* 1986, Bruni and Fazzuoli 1980, Diggens *et al.* 1988, Bosellini 1989, Jungwirth and As-Saruri 1990, Redfern and Jones 1995 Ellis *et al.* 1996). Continuity of structural features, including faults or fracture belt trends and block-faulted highs or basins with the added presence or absence of Jurassic sediments on some localities on both sides of the Gulf, provide the best geological support for the recent separation to form the Gulf of Aden (Beydoun 1970). The Jurassic basins extend from the northern to the southern margin, for example, the Belhaf-Berbara basin and Al-Masila-Al-Medo basins (Bott *et al.* 1992) and the highs can also be traced on both sides such as the Mukalla-Erigavo high (Bruni and Fazzuoli 1980). However, the Jurassic fault trend is recorded in the study area as reactivated structures of the old trend (Najd fault system), for example, the wadi Hawayrah fault and the Al-Madi fault (see sheet I and II). These faults were rejuvenated during the Cretaceous as growth faults resulting in great thicknesses of Cretaceous succession in many hanging walls. Bruni and Fazzuoli (1980) suggest that two major Jurassic fault systems were active, the NNE-SSW and NNW-SSE. These two trends are recorded in the Hadhramaut area. The NNE-SSW trend is most likely older than the Jurassic and probably controlled the formation of highs on both margins of the Gulf. I suggest that these highs were elevated during the Jurassic and no deposition took place. These highs continued to be subaerial intil the early Cretaceous when both

margins were covered by the sea. However, more subsurface data is needed to evaluate the development of these highs. To the west of the study area in the Marib-Al-Juf basin two types of extensional faults are interpreted from seismics as a moderate to steep-dipping set of extensional faults which define the margins of several sub-basins (Diggens *et al.* 1988). These faults involve the basement and do not flatten out within the upper 8 km of the crust; and the moderate to gentle-dipping set of extensional faults which sole out within the lower part of the Jurassic rocks, both sets with dips ranging between 35° and 75° (Diggens *et al.* 1988). The dip of faults in Marib-Al-Juf basin are comparable with the major faults in the Hadhramaut area. However, the calculation of the geometry of the major faults with depth in the study area shows that they dip steeply to a great depth in the basement. The structural features of Jurassic time show that the region was dominated by normal faulting with moderate amounts of salt movement, these salt domes forming pillows rather than piercement structures (Paul 1990). The Jurassic rocks are encountered from outcrop and subsurface to the east and west of the area, for example, at Alfalk IX well and wadi Al-Masila. However, the presence of Jurassic deposits is restricted to the area of down faulting associated with rapid subsidence to form deep basins. Consequently, the study area probably was high during this time or, less likely, the Jurassic deposits were eroded away early in the lower Cretaceous since a thin Jurassic sequence, for example in the Hadhramaut-Jeza basin, is overlain by thick Cretaceous deposits (Paul 1990, Bott *et al.* 1992).

8.4 Cretaceous

During the early Cretaceous the northern margin and particularly the south Hadhramaut area was covered by a marine transgression. In the Senonian, the margin suffered extension with the formation of growth faults with East-West to WNW-ESE strike which is recorded in the clastic rocks of the late Cretaceous. The differential elevation on these faults caused high and low areas to form . The highs

and lows are today reflected in the presence of great thicknesses or thin sequences of the Cretaceous Formations and the presence of local unconformities (Fig. 7.5). Beydoun (1966) attributed these local uplifts to a general uplift of the Hadhramaut area during this time; however, I consider that they are due to the differential elevation by extensional faults during the Cretaceous. Cretaceous deposits provide more direct support for the proposition that the south and north margins of the Gulf of Aden were connected. These deposits show a clear change in a westerly direction from predominantly calcareous to predominantly arenaceous facies, and in the correlation of identifiable limestone tongues across the present gulf (Beydoun 1966, 1970, Bosellini 1989, Luger *et al.* 1990). Luger *et al.* (1990) state that the northern part of Somalia underwent subsidence during the Aptian to Cenomanian when marine carbonates in the east interfingered with continental clastic in the west; this is comparable with a similar stratigraphic sequence in the study area where three layers of carbonates interfinger with clastic rocks in the western part and change gradually to carbonate in the east (Fig. 2.2).

During the Cretaceous the post Jurassic erosion surface was tilted gently down toward the east and the Cretaceous marine transgressions advanced up this gentle slope from the east (Beydoun 1966). The Tawilah Group consists of a siliciclastic-dominated sequence that crops out over a large area in the western and central part of Yemen. Age determinations range from late Cretaceous to Eocene (Davison *et al.* 1994). This variation in the Cretaceous rocks might be referred to the long transport distance and the western part was very close to source rocks. The Cretaceous of coastal Yemen shows many similarities with the coeval succession of northern Somalia. West of the study area the Cretaceous rests unconformably on different Jurassic terrain, the contact being generally marked by a thin conglomerate with little or no angular discordance. In the study area in the Mukalla high, the Cretaceous rests unconformably on a peneplaned basement, while to the east it lies on the upper Jurassic.

8.5 Palaeocene-Eocene

The Palaeocene Umm er Radhuma Formation is of regional distribution over most of the Arabian plate (Jones and Racey 1994). It consists mainly of carbonates throughout the study area and shows uniform distribution with only very slight changes in thickness, but to the west, in central and western Yemen, the Medj-zir Formation, of equivalent age, is mainly of shallow marine clastic rocks (Al-Subbary 1990, Davison *et al.* 1994). These rocks have been subjected to horizontal movements which occurred before rifting and have not previously been reported in the literature. These movements are overprinted by the steep slickensides related to the rifting. This movement was concentrated in the eastern part of the area where the field evidence is most abundant. The distribution of the Palaeocene rocks throughout the whole of Yemen indicates that the northern margin of the Gulf of Aden was uplifted more rapidly in the west than in the east. This stage of uplift probably started early in the Palaeocene and continued contemporaneous with the development of the Hadhramaut arches. The observations suggest that the development of the Somalia plateau was similar to that of its counterpart in the Hadhramaut area, and that the geanticlinal arches on both sides of the Gulf of Aden were due to regional compression acting normal or oblique to the Gulf axis in the west and to the old lines of weakness on Dhufar-Kuria Muria and Socotra trends in the east (Beydoun 1966, Abbate *et al.* 1986). To the east in Dhufar the stratigraphic sequence continues with variation in the Rus Formation where it consists of extensive gypsiferous beds in Hadhramaut area and become marls, mudstone and chalky limestones (Hawkins *et al.* 1981). In the northern part of Somalia the main Red Sea faulting occurred at the end of the middle Eocene; in the southwest Hadhramaut strong faulting on the same trend occurred before the Oligocene and Miocene (Beydoun 1966). In the Early Eocene, thickness variations again reflect progressive development of the Hadhramaut arches and the maximum development of evaporites (Rus Formation) occurred in

the intervening gentle syncline trough of the Hadhramaut-Jeza basin with greater thickness in the east than in the west (Beydoun 1966, Jungwirth and As-Saruri 1990). The Habshiya Formation in the west is thin and sandy suggesting that the geanticlinal uplift with an eastward plunge was continuing (Beydoun 1970). The progressive development of the Hadhramaut arches as geanticlinal warping led to final emergence in the upper Eocene (Beydoun 1966). Similarly the equivalent arches on the southern margin of the Gulf of Aden are recorded in the northern part of Somalia (Beydoun 1966). The uplifting of both south and north margins is most likely related to the development of the Afro-Arabian dome (Almond 1986).

8.6 Oligo-Miocene

The most recent rifting and opening phase in the history of Gondwanland started in the late Eocene and led to the development of the Gulf of Aden, Red Sea and East African rift system (Rosendahl *et al.* 1992, Janssen *et al.* 1995). The north and south margins of the Gulf of Aden during the Oligo-Miocene were subjected to extensional faulting. These extensional faults formed due to stretching of the continental crust a cross the Gulf. The major faults observed in the Hadhramaut area have maximum displacements of about 1300m and of 300m on the other side of the Gulf in northern Somalia (Abbate *et al.* 1993). The structural features on both sides of the Gulf show the same characteristic arcuate shape of faults with a dominant half graben style (Abbate *et al.* 1986, Abbate *et al.* 1993). Some old trends are rejuvenated, for example, the Hawayrah basin in the study area which has been formed by rejuvenation of a Cretaceous WNW extensional fault. The basins in the Hadhramaut area have similar stratigraphic sequences of the same age as the basins in north Somalia, for example, the Daban basin. The major structures in the study area are very strongly correlatable with those on the southern margin (Fig. 8.1). For example, the wadi Hamim, wadi Hawayrah and Haqab faults, as the major structures in the area are characterised by their arcuate shape and this

pattern is recorded in the northern part of Somalia in faults such as the Auradu and Dagah Shabel faults. East-west and NE-SW trends which are recorded in northern Somalia and in Dhufar area, also occur in the study area particularly the east-west trend while the NE trends are recorded as fractures. The east-west trend is parallel to the Sheba ridge segments, while the NE fault in north Somalia, the fractures in the study area and faults in Dhufar area are parallel to the transform faults (Laughton *et al.* 1970, Platel and Roger 1989).

The Dhufar area represents the continuation of the Hadhramaut to the east of the southern part of Yemen. Dhufar comprises two large structural domains; a broad monoclinal plateau tilted gently to the north with large grabens in its southern part and the complex coastal belt, traversed by normal faults related to the episodes of extension during rifting of the Gulf of Aden (Platel and Roger 1989).

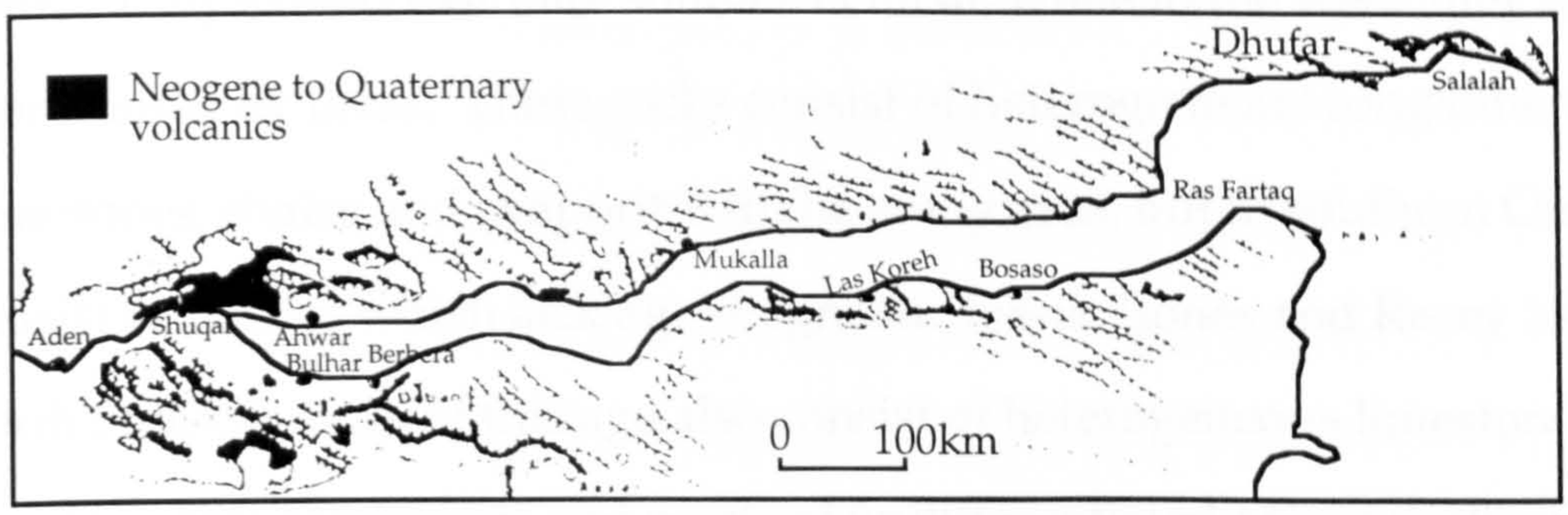

Fig. 8.1. Generalised structural features of the Gulf of Aden continental margins restored to pre-separation position. Neogene to Quaternary volcanics added (after Beydoun 1970 and Merla *et al*. 1979).

The structural patterns in the study area continue east into the Dhufar area, and the swing of the strike of faults also continues into Dhufar to become NW-SE (Fig. 8.1). The Dhufar area is more complex than the south Hadhramaut area since another direction of east-west contraction has resulted in the formation of north-south folds (Platel and Roger 1989).

The western part of Yemen was volcanically active during the Oligo-Miocene, intermittently between 30 and 19 Ma. (Capaldi *et al.* 1986). No sedimentary rocks have been recorded during this time except local continental deposits, a huge volume of volcanic extrusive rocks, with their peaks reaching an elevation of 3666m above sea level, are attributed to plume heating (Davison *et al.* 1994). The northern margin was uplifted by the end of the Miocene. Emergence of the margin is indicated by an unconformity between the syn-rift deposits and the Pliocene deposits. This unconformity also occurs in the northern part of Somalia (Bosellini 1989).

8.7 Pliocene-Recent

The younger sequences are limited to the present coastal areas and show evidence of minor local extension (Beydoun 1964, Abbate *et al.* 1986, Bosellini 1989). They extend east into southern Oman, while to the west they are mainly represented by lavas. These rocks consist of heterogeneous conglomerates, limestones, shales and evaporites in the study area, but in southern Oman they consist of clastics which lack age-diagnostic fossils (Jones and Racey 1994). In north Somalia rocks of this age also consist of heterogeneous limestones, conglomerate sandstones and marls of undifferentiated Miocene-Pliocene in age (Bosellini 1989). The Pliocene deposits imply that the environment is restricted locally even in the study area which is indicative of the instability of sea level during the Pliocene. However, both south and north margins are affected by volcanic activity in the post-Pliocene and these younger deposits have been uplifted to more than 80m above sea level in the Hadhramaut area (Fig. 7.20).

CHAPTER 9

CONCLUSIONS

9.1 Summary of the results

The study area consists mainly of sedimentary rocks with very limited outcrops of basement rocks in the western part, in the Harshiyat-Ydmah area. The stratigraphic sequence excluding the basement rocks ranges in age from Jurassic to Recent. The thickness of different stratigraphic Formations varies from west to east and is attributed to tectonic movements affecting the northern margin. Consequently, some Formations are missing in places and this is reflected in unconformities. Detailed mapping and structural field analysis of faults and fractures from the southern part of the south Hadhramaut area have been produced using satellite images and air photographs as base maps. The major result of this work is the preparation of five maps at scale of 1:50,000 with the exception of the wadi Shakhawi area in the east which was mapped at a scale of 1:100,000. These maps show the relationships of the dominant extensional faults and the different lithologic Formations in the area. In addition, measurements of more than 470 faults and 900 fractures were analysed and this has led to the reconstruction of the tectonic evolution of this part of the northern margin of the

Gulf of Aden from the Precambrian to Recent. Five main tectonic events have been recognised. These movements mainly affect the sedimentary cover.

The first was recorded in the basement rocks and occurred during the Precambrian when these North-South faults were later filled by younger dykes which belong to the basement. These Precambrian extension faults have a north-south strike parallel to the Mukalla high (Fig. 7.3).

The second event is recorded outside the borders of the study area from surface and subsurface, for example, in the Shabwa basin, the Marib basin and the Hadhramaut-Jeza basin (Fig. 7.2). This stage represents the second most important movement after the Oligo-Miocene affecting the margin and relates to Jurassic rifting and the formation of basins with considerable thicknesses of Jurassic rocks. These faults are recognised in the study area as rejuvenated faults during Cretaceous time responsible for this thick deposits of the Harshiyat and Mukalla Formations. Examples are the wadi Hamim fault, wadi Hawayrah fault and wadi Al-Madi fault (see sheet I and II).

The third stage is not very profound but is recorded in different localities and resulted in the formation of local Cretaceous unconformities and sometimes growth faults. For example, extension faults in wadi Habeth in the upper part of wadi Assad affected the Fartaq Formation and the Mukalla Formation, missing in the footwall is thick in the hanging wall. Thus a local unconformity occurs between the Fartaq Formation and the Umm er Radhuma Formation (Fig. 7.5). These Cretaceous extension faults have a WNW-ESE strike and result in thickness variations of the Mukalla Formation throughout the area.

The fourth tectonic event of horizontal movement is also not common on the margin, but has been confirmed during the field work. The movements are Palaeocene to Middle Eocene in age.

The fifth stage is represented by dominant extension which has highly dissected the margin and is associated with rifting in the Gulf of Aden. This stage

has largely obscured all the old tectonic movements due to its intensity throughout the margin and particularly the southern part (Fig. 7.7). A further stage of post Pliocene extension is going on now which can be differentiated from the fifth extensional stage by its effect on the Pliocene deposits (Fig. 7.9). This extension follows the direction of the Oligo-Miocene trend. In addition, another common trend of numerous fractures follows that of offshore fractures, such as the Alula-Fartaq fracture (Fig. 1.3).

The Palaeocene represents a period of quiescence on the northern margin of the Gulf of Aden and probably in the whole of the Arabian platform and even in Somalia before rifting, when the extensive and uniform nodular limestone of the Umm er Radhuma Formation was deposited. During the early Eocene and by the end of the middle Eocene, the northern margin was subjected to contractional movements which affected all sedimentary units from the Qishn to the Habshiya Formation and resulted in the formation of the south and north Hadhramaut arches with the intervening Jeza syncline. Other arches and synclines formed along the margin to the north and their amplitude increases to the north (Burek 1969, Beydoun 1964, Chabman 1984, Jungwirth and As-Saruri 1990).

The horizontal movement has been convincingly confirmed and is documented for the first time. Horizontal slickenside lineations in a number of localities are overprinted by steep slickensides related to the Oligo-Miocene extension.

The Oligo-Miocene deposits, the Shihr Group, are synrift rocks and are of a heterogeneous nature comprising carbonates, sandstones, shales, conglomerates and evaporites. They occur on a narrow and discontinuous coastal belt especially between Mukalla and Sayhut and are also encountered in offshore wells.

At the end of the Miocene a small period of uplift occurred and resulted in the peneplanation of the Shihr Group which was followed by extensional faulting related to the second stage of sea floor spreading in the Gulf of Aden (Matthews

1968). A period of subsidence resulted in the deposition of the Pliocene deposits unconformably on the (syn-rift) Shihr Group. During the Pliocene, the margin was experienced to volcanic activity along the coastal plain from Bab-Almandab at the western end to the Qishn area in the east. Occasionally, igneous rocks such as the volcanic flows in wadi Al-Masila, the Sayhut and Assad areas were extruded.

Existing methods for constructing major fault geometries from rollover fold shapes predict markedly different fault geometries, depending upon the assumed dominant deformation mechanism in the hanging wall. Constructed fault shapes using the constant heave or Chevron model showed that different faults penetrated to various depth depending on their vertical displacement.

Many hanging walls are accompanied by rollover anticlines and the rotation of faulted blocks can be determined by measuring the dips of the bedding planes down the dip slope of the hanging wall surfaces. The present study shows that the master faults sole out at great depth while the small faults, which are most likely accommodation faults, sole out at shallow depth within the clastic rocks of the cover sequence. The major faults extended deep into basement and are probably rejuvenated from the old lineaments in the area.

Balanced cross sections show that the faults tend to be very steep in the western part of the study area, for example, wadi Hawayrah (Fig. 5.2a-b), and change gradually toward the east where the faults have more moderate to steep dips, for example, in wadi Assad and particularly in the middle of the section where the faults cut through the Fartaq Formation (Fig. 5.9a-b). In general, the cross sections show that most of the faults have steep dips and they could have originated from a deep level as inherited structures from old faults with the same trend in the basement blocks (Fig. 6.26). The rotation of faulted blocks rarely exceeds about 40°.

The variation in values of extension throughout the area along a strike length of more than 170 km from (wadi Hawayrah in the west to wadi Bidish in the east) implies that the geometry of extension in the northern margin of the Gulf of Aden is not simple. The study area has only undergone a small amount of extension. The greatest amount of extension is recorded in the eastern part of the area, in wadi Bidish , which excluded the small fractures 9% and with considering the small fractures was 12% in the Switchbacks area while the lowest value of 4.5% is recorded in the middle of the area, in wadi Kharid. This low value of extension may be attributed to a lack of major faults of great displacement. The largest fault recorded in the area has a maximum displacement of 1320m (Fig. 6.14). Small unmappable faults are not recorded in the calculation although they are very common, not have the numerous fractures been taken into account. The wadi Kharid cross section, where the lowest value is recorded, most likely represents a transfer zone. The lower value of extension in the wadi Hawayrah section where the major fault is recorded may be attributed to 1) the section crossing two transfer zones, or 2) more than 3 km of no exposure in the wadi floor which may conceal some faults. The characteristic structures of half graben in the south Hadhramaut area are well illustrated on the cross sections. Some sections display syn-rift basins which have been infilled with Oligo-Miocene sediments, for example, wadi Hawayrah basin and south of wadi Araf basin.

In this study, 10 traverses were measured in a direction parallel to the cross sections which, together with the sections, provide a representative sample of structures over the whole area (Fig. 5.1). For every fault along the one-dimensional sample line, the vertical displacement was calculated using topographic maps to calculate the elevation difference of the same boundary on both sides of the fault or sometimes by extrapolating the dip of bedding planes

and sometimes by direct field measurement. There is greater error in assessing the throw of the smaller faults.

The relationship in general is linear but at displacements of 10m, 20m, 30m, and 45m the linear relationship breaks down (Fig. 5.12). At these values of displacement, the faults have a wide range of strike length. The data collected from the south Hadhramaut area are consistent with the data analysed by many authors in different localities (Kakimi 1980, Villemin and Sunwoo 1987, Walsh and Watterson 1988, 1990, Childs *et al.* 1990, Marrett and Allmendinger 1991, Walsh and Watterson 1992). The line of best fit to these data has a slope of 1.27. The fit to the data is good with displacements varying from 10m to 1320m and the trace lengths between 0.91 km to 60 km.

The extensional faults in the study area could be classified into three groups according to their size and dimensions, the first group are the major faults which control the shape and morphology of the northern margin of Gulf of Aden in general and the southern part of the south Hadhramaut area in particular. These major faults, for example, wadi Hawayrah fault, wadi Hamim fault, Haqab fault and wadi Al-Rakdoon fault, have vertical displacements of more than 600m and sometimes reach more than 1300m, as in the wadi Hamim fault (Fig. 6.14). They form the largest scarps in the area and account for the difference of elevation of more than 2000m between the plateau and the coastal plain.

The second group, which includes most of the faults, are those of medium size with average displacements between 40m and 400m. This group has also contributed to the present shape and morphology of the area and show the characteristic style of structures in the area namely half grabens and less commonly, full graben. The third group are the smallest faults which are mappable at a scale of 1:50,000 and have displacements of between 10m and 40m. However, there are numerous smaller faults which are not mappable on this scale which have been measured and analysed together with these mappable faults and

are discussed in chapter 6. The faults display a swing in strike from ESE-WNW the eastern part through east-west in the middle to ENE-WSW in the west.

From the analysis of both faults and fractures, it is concluded that there is one dominant trend of faults with a range of strikes from ESE-WNW to ENE-WSW. The extension direction in the southern part of Hadhramaut area is of NNW-SSE to north-south. The fractures belong to two main trends, namely NE-SW and ESE-WNW.

Formation of the fractures is related to different stages of tectonic movement. In most areas two or three main trends occur. In different areas different trends are dominant. For example, in wadi Hawayrah the ESE-WNW trend is of less common while the NE-SW and NW-SE are the dominant.

9.2 Conclusions

1. The major faults penetrated to great depth in the basement, while the small faults are detached at shallow depth in the clastic rocks of either the Mukalla or Harshiyat Formations.

2. Five tectonic events from Precambrian to Recent in age are recorded in the area, all accompanied by extensional deformations.

3. The dominant extension is related to the rifting of the Gulf of Aden during the Oligo-Miocene.

4. Another phase of extension continues to the present resulting in two dominant directions of fractures, the first parallel to the extensional faults of east-west to ENE-WSW strike and the second parallel to the strike of the off-shore ridges such as the Alula-Fartaq fracture zone.

5. Horizontal movement is strongly recorded and the field evidence shows that this movement is older than the rifting.

6. The low values of extension calculated of from the balanced cross sections implies that large faults with major displacements are not observed.

7. The structural style in the area is characterised by half grabens and the accommodation structures associated with these are rollover anticlines, monoclines and small antithetic and synthetic faults.

8. Mapping the vertical displacements of the faults shows four transfer zones which are approximately parallel to the fracture zones off-shore.

9. There is a swing in strike of structures from WSW-ENE in the west through east-west in the middle to ESE-WNW in the east.

9.3 Recommendation for further work

The area has potential for hydrocarbon occurrence with suitable source, reservoir and sealing units. The maps prepared in this study are a comprehensive record of the surface geology and the sections provide an initial interpretation of sub-surface structure. Future work will be the correlation with subsurface data from seismic surveying and wells when they become available.

References

Abbate, E., Bruni, P. and Sagri, M. 1993. Tertiary basins in the Northern Somalia continental margin: Their structural significance in the Gulf of Aden rift system, *Geoscientific Research* in Northeast Africa 291-294.

Abbate, E., Bruni, P., Fazzuoli, M. & Sagri, M. 1986. The Gulf of Aden continental margin of Northern Somalia: Tertiary sedimentation, rifting and drifting. *Mem. Soc Geol. It.* **31,** 427-445.

Abbate, E., Ficcarelli, G., Pirini Raddrizzani, C., Salvietti, A., Torre, D. & Turi, A. 1974. Jurassic sequences from the Somali coast of the Gulf of Aden. *Riv. It. Paleont. Stratigr.* 80, 409-478

Abdel-Gawad, M. 1970. Interpretation of satellite photographs of the Red Sea and Gulf of Aden. *Phil. Trans. Roy. Soc. Lond.* Ser. A, 267, 23-40.

Agip. 1981. Exploration data (surface geology, subsurface well results) for Agip permit areas in the Gulf of Aden region. (former, PDR Yemen, unpublished report).

Al-Kotbah, A. M. & Allison, I. 1995. Extension faulting of the northern margin of the Gulf of Aden, Hadhramaut area, Yemen Republic (abstract). In: Rift sedimetation and tectonics in the Red Sea-Gulf of Aden region. conference, Sana'a.

Al-Kotbah, A. M. & Allison, I. 1995. Fault geometry of the rift margin of the Gulf of Aden, Yemen Republic (abstract). 26th. Ann. Meeting. TSG. Cardiff U.K.

Al-Kotbah, A. M. 1992. Structural studies on the basement rocks, Abas area, Al-Bayda district, Yemen Republic. unpublished M.Sc. thesis, University of Sana'a, 161p.

Al-Subbary, A. 1995. Stratigraphy and Sedimentology of the Cretaceous to early Tertiary Tawilah Group of western Yemen, unpublished Ph.D. thesis, University of London, 309p.

Al-Thour, K. 1992. Stratigraphy and Sedimentology and Diagenesis of the Amran Group (Jurassic) of the region to the west and north-west of Sana'a Yemen Republic unpublished Ph.D. thesis, University of Birmingham, England, 293p.

Allmendinger, R. W. 1993. Stereonet version 4.6, a plotting program for orientation data for the Macintosh. Cornell University, New York.

Allmendinger, R. W., Ramos, V. A., Jordan, T. E., Palma, M. & Isacks, B. L. 1983b. Paleogeography and Andean structural geometry, northwest Argentina. *Tectonic* s **2**, 1-16

Allmendinger, R. W., Sharp, S. W., Von Tish, D., Serpa, L., Kaufman, S., Oliver, J. & Smith, R. B. 1983a. Cenozoic and Mesozoic structure of the eastern Basin and Range Province, Utah from COCORP seismic reflection data. *Geology* **11**, 532-536.

Almond, D. C. 1986. Geological evolution of the Afro-Arabian Dome. *Tectonophysics* **131**, 301-332

Anderson, E. M. 1951. The dynamics of faulting. Oliver and Boyd, Edinburgh.

Badley, M. E., Price, J. D., Rambechdahl, C. & Agdestein, T. 1988. The structural evolution of the northern Viking graben and its bearing upon extensional modes of basin formation. *J. Geol. Soc.* **145**, 455-472.

Bally, A. W. 1981. Atlantic-type margin. In: Geology of passive continental margins, (edited by Bally, A. W., Watts, A. B., Grow, J. A., Manspeezer, W., Bernoulii, D., Schreiber, C. & Hunt, J. M.).*Am. Assoc. Petrol. Geol. Bull.* Education Course note Series **19**, 1-148.

Bally, A. W. 1982. Musings over sedimentary basin evolution. *Phil. Trans. R. Soc. Ser.* A, **305**, 325-328.

Bally, A. W., Gordy, P. L. & Stewart, G. A. 1966. Structure, seismic data, and orogenic evolution of southern Canadian Rocky Mountains. *Bull. Can. Petrol. Geol.* **14**, 337-381.

Barr, D. 1987a. Lithospheric stretching, detached normal faulting and footwall uplift. In: Continental extensional tectonics. (edited by Coward, M. P., Dewey, J. F., & Hancock, P. L). *Spec. Publ. Geol. Soc. Lond.* **28**, 75-94.

Barr, D. 1987b. Structural/stratigraphical models for extensional basins of half-graben type. *J. Struct. Geol.* 9, 491-500.

Beach, A. 1984. The structural evolution of the Witch Ground Graden. *J. Geol. Soc.* 141, 621-628.

Beach, A. 1986. A deep seismic reflection profile across the northern North Sea. *Nature* 323, 53-55.

Beach, A., Bird, T. & Gibbs, A. 1987. Extensional tectonics and crustal structure: deep seismic reflection data from the northern North Sea Viking graben. In: Continental Extensional Tectonics. (edited by Coward, M. P., Dewey, J. F., & Hancock, P. L.). *Spec. Publ. GeoL. Soc.* 28, 467-478.

Beaumont, C. 1981. Foreland basins. *Geophys. J. R. Ast. Soc.* 65, 291-329.

Beydoun, Z. R. &. Greenwood, J. E. W. 1968. Aden Protectorate and Dhufar. In: Lexique Stratigraphique International (edited by. L. Dubertret), III, Asie, CNRS, Paris, fasc. 128p.

Beydoun, Z. R. 1964. The stratigraphy and structure of the eastern Aden Protectorate. *Overseas Geol. Miner. Resour. Bull. Suppl.* 5, HMSO London, 107p.

Beydoun, Z. R. 1966. Eastern Aden Protectorate and part of Dhufar. In: Geology of Arabian Peninsula. *U. S . Geol. Surv. Prof. Pap.* No. 460H,

Beydoun, Z. R. 1969. Note on the age of the Hadhramaut arch. *Overseas Geol. Miner. Resour.* 10, 236-240.

Beydoun, Z. R. 1970. Southern Arabia and northern Somalia: comparative geology. *Phil. Trans. R. Soc. Lond. ser.* A, 267, 267-292.

Beydoun, Z. R. 1981. Some open questions relating to petroleum prospects in Lebanon. *J. Petrol. Geol.* 3, 304-314.

Beydoun, Z. R. 1988. The petroleum resources of the Middle East : Regional geology and petroleum resources. *Scientific Press*, U.K. 292P.

Beydoun, Z. R. 1991. Arabian plate hydrocarbon geology and potential: A plate tectonic approach. *Am. Assoc. Petrol. Geol. Stud. Geol.* no. 33, 77p.

Beydoun, Z. R., Bamahmoud, M. O. & Nani, A. S. O. 1993. The Qishn formation, Yemen: lithofacies and hydrocarbon habitat. *J. Marine Petrol. Geol.* **10**, 364-372.

Billings, M. P. 1942. Structural geology (first edition). Sir Isaac Pitman & Sons Ltd. London 473p.

Bohannon, R. G. 1989. Style of extensional tectonism during rifting, Red Sea and Gulf of Aden. *J. Africa Earth Sci. & Mid. East* 8, 589-602.

Bosellini, A. 1989. The continental margins of Somalia: Their structural Evolution and sequence stratigraphy. *Memorie di scienze geologche* **XLI**, 373-458.

Bosworth, W. 1985. Geometry of propagating continental rifts. *Nature* **316**, 625-627.

Bosworth, W. 1987. Off-axes volcanism in the Gregory rift, East Africa: implications for models of continental rifting. *Geology* **15**, 397-400.

Bosworth, W. 1993. Structural style and tectonic evolution of the rift basins of northeast Africa. Geoscientific Research in North Africa (edited by Thorweihe & Schandelmeier), Balkema, Rotterdam.

Bott, W. F., Smith, B. A., Oakes, G. S., Sikander, A. H. & Ibraham, A. I. 1992. The tectonic framework and regional hydrocarbon prospectivity of the Gulf of Aden. *J. Petrol. Geol.* **15**, 211-243.

Boyer, S. E. & Elliott, D. 1982. Thrust systems. *Am. Assoc. Petrol. Geol. Bull.* **66**, 1196-1230.

Brewer, J. A. & Smythe, D. K. 1984. MOIST and the continuity of crustal reflector geometry along the Caledonian-Appalachian orogen. *J. Geol. Soc. Lond.* **141**, 105-120.

Brown, C. & Girdler, R. W. 1980. Interpretation of east Africa gravity data and its implications for the breakup of the continents. *J. Geophysical Res.* 85, 6443-6455.

Brown, G. F. & Coleman, R. G. 1972. Tectonic framework of the Arabian Peninsula. *24th Int. Geol. Congr.* Montreal 3, 300-305.

Brown, G. F. & Jackson, R. O. 1960. The Arabian Shield. *21st. Int. Geol. Congr.* Copenhagen 9, 69-77.

Bruce, C. 1973. Pressured shale and related sediment deformation: mechanism for development of regional contemporaneous faults. *Am. Assoc. Petrol. Geol. Bull.*. **57**, 878-886.

Bruni, P. & Fazzuoli, M. 1977. Sedimentological observations on Jurassic and Cretaceous sequences from northern Somalia, preliminary report. *Boll. Soc. Geol. It.* **95**, 1571-1588.

Bruni, P. & Fazzuoli, M. 1980. Mesozoic structural evolution of the Somali coast on the Gulf of Aden. *Acc. Naz. Lincei.* Atti dei Convergni no. **47**, 193-207.

Bruni, P. A. F., M. 1986. Mesozoic structural evolution of the Somali coast on the Gulf of Aden. *Boll. Soc. Geol. It.* 192-207.

Bruni, S. P. & Fazzuoli, M. 1976. Sedimentology observations on Jurassic and Cretaceous sequences of northern Somalia. *Boll. Soc. Geol. It.* **95**, 1571-1588.

Buchanan, P. G. & McClay, K. R. 1991. Sandbox experiments of inverted listric and planar faults systems. *Tectonophysics* **188**, 97-115.

Buck, W. R. 1988. Flexural rotation of normal faults. *Tectonics*. **7**, 959-973.

Burchfiel, B. C. & Stewart, J. 1966. The pull apart, origin of Death Valley, California. *Geol. Soc. Am. Bull.* **77**, 439-442.

Burek, P. J. 1969. Structural effects of sea-floor spreading in the Gulf of Aden and Red sea on the Arabian Shield. In: Hot Brines and Recent Heavy Metal deposits in the Red sea (edited by Degens, E. T. & Ross, D). Springer Verlag, Berlin-Heidelberg, 59-70.

Cannon, F. W. & Hinze, W. J. 1992. Speculation on the origin of the North America Midcontinent rift. *Tectonophysics* **213**, 49-55.

Capaldi, G., Chisa, S., Civetta, L., La Volpe, L., Manetti, P., Orsi, G. & Piccardo, G. B. 1986. Magmatic and tectonic activities in north Yemen during Tertiary and Quaternary times. *Mem. Soc. Geol. It.* **31**, 375-393.

Caton-Thompson, G. & Gardner, E. W. 1939. Climate, irrigation, and early man in Hadhramaut. *Geog. J.* **93**, 18-38.

Caton-Thompson, G. 1938. Geology and archaeology of Hadhramaut, southwest Arabia, preliminary notes on Lord wakefield Expedition. *Nature* **142**, 139-142.

Child, C. ,Watterson, J. & Walsh, J. J. 1995. Fault overlap zones within developing normal fault systems. *J. Geol. Soc. Lond.* **152**, 535-549.

Child, C., Walsh, J. J. & Watterson, J. 1990. A method for estimation of the density of fault displacements below the limits of seismic resolution in reservoir formations. In: North Sea Oil and Gas Reservoirs II (edited by The Norwegian Institute of Technology). Graham & Trotman, London, 309-318.

Cladouhos, T. T. & Marrett, R. 1996. Are fault growth and linkage models consistent with power-law distributions of fault lengths?. *J. Struct. Geol.* **18**, 281-293.

Clark, R. M. & Cox, S. J. D. 1996. A modern regression approach to determining fault displacement-length scaling relationships. *J. Struct. Geol.* **18**, 147-152.

Cochran, J. R. 1981. The Gulf of Aden: Structure and Evolution of a Young Ocean Basin and Continental Margin. *J. Geophysical Res.*. **86**, 263-287.

Cochran, J. R. 1983. Model for development of Red Sea. *Am. Assoc. Petrol. Geol. Bull.* **67**, 41-69.

Coward, M. P. & Gibbs, A. D. 1986. Structural interpretation with emphasis on extensional tectonics. *Joint Assoc. Petrol. Expl. Courses* (U.K.), 49.

Coward, M. P. 1986. Heterogeneous stretching, simple shear and basin development. *Earth. Planet. Sci. Lett.* **80**, 325-336.

Crans, W. Mandl, G. & Haremboume, J. 1980. On theory of growth faulting, a geomechanical delta model based on gravity sliding. *J. Petrol. Geol.* **2**, 265-307.

Dahlstrom, C. D. A. 1969. Balanced cross-sections. *Can. J. Earth Sci.* **6**, 743-757.

Dahlstrom, C. D. A. 1970. Structural geology in the Eastern margin of the Canidian Rocky Mountains. *Bull. Can. Petrol. Geol.* **18**, 332-406.

Davison, I. 1986. Listric normal fault profiles: calculation using bed-length balance and fault displacement. *J. Struct. Geol.* **8**, 209-210.

Davison, I. 1989. Extensional domino fault tectonics: kinematics and geometrical constraints. *Annales Tectonicae* **3**, 12-24.

Davison, I., Al-Kadasi, M., Al-Khirbash, S., Al-Subbary, A., Baker, J., Blakey, S.,Bosence, D., Dart, C., Heaton, R., McClay, K., Menzies, M., Nichols, G., Owen, L. & Yelland, A. 1994. Geological evolution of the southeastern Red Sea rift margin, Republic of Yemen. *Geol. Soc. Am. Bull.* **106**, 1474-1493.

Destro, N. 1995. Release fault: A variety of cross fault in linked extensional fault system, in the Sergipe-Alagoas Basin, NE Brazil. *J. Struct. Geol.* **17**, 615-629.

DGME (Department of Geology and Mineral Exploration) 1986. Geological survey and prospecting in the Haban-Mukalla area, Regional Geology (former south Yemen). *Final report* , **1**, 167-269, unpublished.

Diggens, J. N. Dixon, R. J. Downie, R. A. Harris, J. P. Jakubowski, M. Lucas, P. M. Matthews, S. J. Southwood, D. A. & Ventris, P. A. 1988. A geological model for the evolution of the Marib-Al-Juf Basin, Yemen Republic.: Robertson Research International Limited **1**, Report no. 6216/IIb, project no. RRPC/878 IIB/40018 (Unpublished report).

Dula, W. F. 1991. Geometric models of listric normal faults and rollover folds. *Bull. Am. Assoc. Petrol. Geol.* **75**, 1609-1625.

Dunbar, J. A. & Sawyer, D. S. 1988. Continental rifting at pre-existing lithospheric weaknesses. *Nature* **333**, 450-452.

Ebinger, C. J., Crow, M. J., Rosendahl, B. R. & Fournier, J. Le. 1984. Structural evolution of Lake Malawi, Africa. *Nature* **308**, 627-629.

Ebinger, C. J., Rosendahl, B. R. & Reynolds, D. J. 1987. Tectonic model of the Malawi rift, Africa. In: Sedimentary basins within the Dead Sea and other rift zones. (edited by Ben-Avrham, z).*Tectonophysics* **141**, 215-235.

Elliott, D. 1977. Some aspects of the geometry and mechanics of thrust belts, part 1. Eight Annual Seminar. *Can. Soc. Petrol. Geol.* University of Calgary, 95p.

Elliott, D. 1983. The construction of balanced cross sections. *J. Struct. Geol.* **5**, 101.

Ellis, A. C., Kerr, H. M., Cornwell, C. P. & William, D. O. 1996. A tectono-stratigraphic framework for Yemen and its implications for hydrocarbon potential. *Petrol. Geoscience* **2**, 29-42.

Ellis, P. G. & McClay, K. R. 1988. Listric extensional fault systems results of analogue model experiments. *Basin Research* , **1**, 55-70.

Etheridge, M. A., Branson, J. C. & Stuart-Smith, P. G. 1985. Extensional basin-forming structures in Bass Strait and their importance for hydrocarbon exploration. *J. Aust Petrol. Expl. Assoc.* **25**, 344-361.

Flemings, P. B. & Jordan, T. E. 1989. A synthetic stratigraphic model of foreland basin development. *J. Geophysical Res.* **94**, 3851-3866.

Fossen, H. & Gabrielsen, R. H. 1996. Experimental modelling of extensional fault systems by use of plaster. *J. Struct. Geol.* **18**, 673-687.

Gawthorpe, R. L. &. Hurst, J. M. 1993. Transfer zones in extensional basins: Their structural style and influence on drainage development and stratigraphy. *J. Geol. soc. Lond.* **150**, 1137-1152.

Geiser, P. 1978. Gravity tectonic removal of cover of Blue ridge anticlinorium to form Valley and ridge Province: Discussion. *Bull. Geol. Soc. Am.* **89**, 1429-1430.

Geukens, F. 1966. Geology of the Arabian Peninsula, Yemen. *U. S. Geol. Surv.* Professional paper 506-B, 23P.

Gibbs, A. D. 1983. Balanced section constructions from seismic sections in areas of extensional tectonics. *J. Struct. Geol.* **5**, 153-160.

Gibbs, A. D. 1984. Structural evolution of extensional basin margins. *J. Geol. Soc. Lond.* **141**, 609-620.

Gibbs, A. D. 1987. Linked tectonics of the Northern North Sea basin. In: Sedimentary Basins and Basin Forming Mechanisms. (edited by Beaumont, C. & Tankard, A. J.). *Can. Soc. Petrol. Geol. Mem.* **12**, 163-171.

Gibbs, A. D. 1990. Linked fault families in basin formation. *J.* Struct. *Geol.* **12**, 795-803.

Girdler, R. W. & Sowerbutts, W. T. W. 1970. Recent geophysical studies of the rift system in East Africa. *J. Geomagnet. Geoelect* **22**, 153-163.

Girdler, R. W. & Styles, P. 1974. Two stage Red Sea floor spreading. *Nature* **247**, 1-11.

Girdler, R. W. & Styles, P. 1978. Seafloor spreading in the western Gulf of Aden. *Nature* **271**, 615-617.

Greenwood, J. E. G. & Bleackley, D. 1967. Aden Protectorate. In: Geology of the Arabian Peninsula. *U. S. Geol. Surv.* Professional paper 560-C.

Greenwood, W. R., Anderson, R. E., Fleck, R. J. & Schmidt, D. C. 1980. Precambrian geological history and plate tectonic evolution of the Arabian Shield. *Saudia Arabia Dir. Gen. Res. Bull.* **24**, 35p

Groshong, R. H. 1990. Unique determination of normal fault shape from hanging-wall bed geometry in detached half grabens. *Eclogae Geol. Helv. 83* , 455-471.

Groshong, R. H. J. 1994. Area balance, depth to detachment, and strain in extension. *Tectonics* **13**, 1488-1497.

Groshong, R., H. 1989. Half-graben structures: Balanced models of extensional fault-bend folds. *Geol. soc. Am. Bull.* **101**, 96-105.

Haitham, F. M. &. Nani, A. S. O. 1990. The Gulf of Aden Rift: hydrocarbon potential of the Arabian sector. *J. Petrol. Geol.* **13**, 211-220.

Hamblin, W. K. 1965. Origin of reverse drag on the downthrow side of normal faults. *Geol. Soc. Am. Bull.*, **76**, 1145-1164.

Harding, T. P. 1984. Graben hydrocarbon occurrences and structural style. *Am. Assoc. Petrol. Geol. Bull.* **68**, 333-362.

Harland, W. B., Armstrong, R. L., Cod, A. g., Craig, L., Smith, A. & Smith, D. G. 1990. Geological time scale, Cambridge University press, Cambridge, U.K.

Harper, G. D. 1985. Tectonics of slow spreading mid-ocean ridge and consequences of a variable depth to the brittle/ductile transition. *Tectonics* **4**, 395-409.

Hawkins, T. R., Hindle, D. & Strugnell, R. 1981. Outlines of the stratigraphy and structural framework of southern Dhofar (Sultanate of Oman). *Geol. Mijnbouw* **60**, 247-256.

Heffer, K. J. &. Bevan, T. G. 1990. Scaling relationships in natural fractures - data, theory and applications. *Soc. Petrol. Eng.*. paper No. 20981, 362-376.

Heller, P. L., Angevine, C. L., Wilson, N. S. & Paola, C. 1988. Two-phase stratigraphic model of foreland-basin sequences. *Geology* **16**, 501-504.

Hossack, J. R. 1978. The correction of stratigraphic sections for tectonic finite strain in the Bygdin area, Norway. *J. Geol. Soc. Lond.* **135**, 229-241.

Hossack, J. R. 1979. The use of balanced cross sections in the calculation of orogenic contraction: a review. *J. Geol. Soc.. Lond.* **136**, 705-711.

Hudson, R. G. S. 1954. Jurassic stromatoporoids from southern Arabia. Paris, Mus. natl. d'Histoire nat. *Notes et Me'm. Sur le Moyen-Orient* **5**, 207-221.

Husseini, M. I. & Husseini, S. I. 1990. Origin of the infracambrian salt basins of the Middle East. In: Classic Petroleum Provinces. (edited by Brooks, J.). *Spec. Publ. Geol. Soc. Lond.* **50**, 279-292.

Illies, J. H. 1975. Recent and paleo-interpolate tectonics in stable Europe and Rhine-graben rift system. *Tectonophysics* **29**, 251-264.

Illies, J. H. 1981. Mechanism of graben formation. *Tectonophysics* **73**, 249-266.

Isaev, E. N., Samoilyuk, V. V., Isaeva, I. V. & Chuprov, A. I. 1984. Anomalous magnetic field of the (former) south Yemen, Explanatory notes to the maps of 1:500,000 and 1:100,000 scale (unpublished report).

Ishikawa, M.& Otsuki, K.1995. Effects of strain gradients on asymmetry of experimental normal fault system. *J. Struct. Geol.* **17**, 1047-1053.

Jackson, J. A. & McKenzie, D. P. 1983. The geometrical evolution of normal fault systems. *J. Struct. Geol.* **5**, 471-482.

Jackson, J. A. 1987. Active normal faulting and continental extension. In: continental extensional tectonics (edited by Coward, M. P., Dewey, J. F. & Hancock, P. L.). *Spec. Publs geol. Soc. London.* **28**, 3-17.

Jackson, J. A., White, N. J., Garfunkel, Z. & Anderson, H. 1988. Relations between normal fault geometry, tilting and vertical motions in extensional terrains: an example from the southern Gulf of Suez. *J. Struct. Geol.* **10**, 155-170.

Jaeger, J. C. & Cook, N. G. W. 1979. Fundamentals of rock mechanics. Chapman and Hall, London.

Janssen, M. E., Stephenson, R. A. & Cloetingh, S. 1995. Change in plate motions and their control on the subsidence of rifted in the Africa plate. *Geoscientific Research in Northeast Africa* 185-188.

Jarvis, G. T. 1984. An extensional model of graben subsidence-the first stage of basin evolution. *Sedimentary Geology* **40**, 13-31.

Jones, R. W. &. Racey, A. 1994. Cenozoic stratigraphy of the Arabian Peninsula and Gulf, Micropalaeontology and Hydrocarbon Exploration in the middle East.(edited by. M. D. Simmons), Chapman & Hall, London, 273-307.

Jungwirth, J. & As-Saruri, M. 1990. Structural evolution of the platform coveron southern Arabian Peninsula (former, P. D. R. Yemen). Z. *Geol. Wissenschaft* **18**, *Berlin*, 505-514.

Kakimi, T. 1980. Magnitude-frequence relation for displacement of minor faults and its significance in crustal deformation. *Bull. Geol. Surv. Japan* (Chishitu Chosasho Geppo) **31**, 225-237.

Keller, P. 1990. Geometric and kinematic model of bed length balanced structures. *Eclogae Geol. Helv.* 83, 473-492.

Kusznir, N. J. & Ziegler, P. A. 1992. The mechanics of continental extension and sedimentary basin formation: A simple-shear/pure-shear flexural cantilever model. *Geol. Soc. Am. Bull.* **215**, 117-131.

Kusznir, N. J., Marsden, G. & Egan, S. S. 1991. A flexural-cantilever simple-shear/pure-shear model of continental lithosphere extension: applications to the Jeanne d' Arc Basin, Grand Banks and Viking Graben, Northern Sea. In: The geometry of normal faults,

(edited by Roberts, A. M., Yielding, G., & Freeman, B.). *Spec. Publ. Geol. Soc. Lond.* **56,** 41-60.

Lamare, P. 1936. Structure geologique de l'Arabie. Paris and Lie'ge Libraire Polytechnique Ch. Beranger, 63p.

Lamare, P., Base, E, D., Maurice, A. & Teilhard de Chardin, P. 1930. Studes ge'ologique en Ethiopie, Somalie, et Arabic meridionale. *France Mem. new ser.* **6,** 1-83.

Larsen, P. H. 1988. Relay structures in a Lower Permian basement-involved extension system, East Greenland. *J. Struct. Geol.* **10,** 3-8.

Laughton, A. S. 1966a. The Gulf of Aden. *Phil. Trans. R. Soc. Lond. ser.* A, **259,** 150-171

Laughton, A. S., Whitemarsh, R. B. & Jones, M. T. 1970. The evolution of the Gulf of Aden. *Phil. Trans. R. Soc. Lond. Ser.* A, **267,** 22-266.

Leeder, M. R. & Gawthorpe, R. L. 1987. Sedimentary models for extensional tilt-block/half-graben basins. In: Continental extensional tectonics (edited, by Coward, M. P., Dewey, J. F. & Hancock, P. L.). *Spec. Publ. Geol. Soc. Lond.* **28,** 139-152.

Lister, G. S., Etheridge, M. A. & Symonds, P. A. 1986. Detachment faulting and the evolution of passive continental margins. *Geology* **14,** 246-250.

Little, O. H. 1925. The geography and geology of Mukalla (southern Yemen). *Egypt Geol. Surv.* Cairo, 250p.

Luger, P., Hendriks, F., Arush, M., Bussmann, M., Kallenbach, H., Mette, W. & Strouhal, A. 1990. The Jurassic and the Cretaceous of northern Somalia: Preliminary results of the sedimentologic and stratigraphic investigations. *Berliner Geowiss. Abh.* A, **120,** 571-594.

Makris, J. & Henke, C. H. 1992. Pull-apart evolution of the Red Sea. *J. Petrol. Geol.* **15,** 127-134.

Mandl, G. 1987. Tectonic deformation by rotating parallel faults: the bookshelf mechanism. *Tectonophysics* **141,** 277-316.

Marrett, R. & Allmendinger, R. W. 1990. Kinematic analysis of fault-slip data. *J. Struct. Geol.*. **12,** 973-986.

Marrett, R. & Allmendinger, R. W. 1991. Estimates of strain due to brittle faulting: sampling of fault populations. *J. Struct. Geol.* **13**, 735-738.

Marton, G. & Buffler, R. T. 1993. Application of simple-shear model to the evolution of passive continental margins of the Gulf of Mexico basin. *Geology* **21**, 495-498.

Matthews, D. H. 1966. The Owen fracture zone and the northern end of the Carlsberg ridge. *Phil. Trans. R. Soc. Lond.* Ser. A, **267**, 172-197.

Matthews, D. H., Williams, C. & Laughton, A. S. 1967. Mid-ocean ridge in the mouth of the Gulf of Aden. *Nature* **215**, 1052-1053.

McClay, K. R. & Ellis, P. G. 1987. Analogue models of extensional fault geometries. In: continental extensional tectonics. (edited by Coward, M. P., Dewey, J. F. & Hancock, P. L.). *Spec. publ. Geol. Soc. Lond.* **28**, 109-125.

McClay, K. R. & Ellis, P. G. 1987. Geometries of extensional fault systems developed in model experiments. *Geology* **15**, 341-344.

McClay, K. R. & Scott, A. D. 1991. Experimental models of hanging wall deformation in ramp-flat listric extensional fault systems. *Tectonophysics* **188**, 85-96.

McClay, K. R. 1990. Deformation mechanics in analogue models of extensional fault systems. In: deformation mechanics and reology. (edited by Knipe, R. J.). *Spec. Publ. Geol. Soc. Lond.* **54**, 445-454.

McKenzie, D. P. 1978. Some remarks on the development of sedimentary basins. *Earth planet. Sci. Lett* **40**, 25-32.

McKenzie, D. P., Davies, D. & Molnar, P. 1970. Plate tectonics of the Red Sea and east Africa. *Nature* **226**, 243-248.

Merki, P. 1972. Structural geology of Cenozoic Niger delta. In: African geology. (edited by Dessauviagie, T. F. & Whiteman, A. J.). Ibadan University, 247-266.

Merla, G., Abbate, E., Azzaroli, A., Bruni, P., Canuti, P., Fazzuoli, M., Sagri, M. & Tacconi. P. 1979. A geological map of Ethiopia and Somalia.

Mills, S. J. 1992. Oil discoveries in the Hadhramaut: how Canadian OXY scored in Yemen: *Oil Gas J.* 49-52.

Millson, J. A., Mercadier, C. G., Livera, S. E. & Peters, J. M. 1996. The Lower Palaeozoic of Oman and its context in the evolution of a Gondwana continental margin. *J. Geol. Soc. Lond.* **153**, 213-230.

Mohr, P. 1992. Nature of the crust beneath magmatically active continental rifts. In: geodynamics of rifting, volume II. Case history studies on rifts, north and south America and Africa. (edited by Ziegler, P. A).*Tectonophysics* **213**, 269-284.

Morley, C. K. 1988. Extension, detachments and sedimentation in continental rifts (with particular reference to east Africa).*Tectonics* **8**, 1175-1192.

Morley, C. K., Nelson, R. A., Patton, T. L. & Munn, S. G. 1990. Transfer Zones in the East Africa Rift System and Their Relevance to Hydrocarbon Exploration in Rifts. *Am. Assoc. Petrol. Geol. Bull.* **74**, 1234-1253.

Nicol, A., Walsh, J. J. & Gillespie, P. A. 1996. Fault size distribution - are they really power law ?. *J. Struct. Geol.* **18**, 191-197.

Nicol, A., Walsh, J. J. Watterson, J. & Bretan, P. G. 1995. Three-dimensional geometry and growth of conjugate normal faults. *J. Struct. Geol.* **17**, 847-862.

Oldenburg, D. W. & Brune, J. N. 1975. An explanation for the orthogonality of ocean ridges and transform faults. *J. Geophys. Res.* **80**, 2575-2585.

Parsons, B. & Sclater, J. 1977. An analysis of the variation of ocean floor bathymetry and heat flow with age. *J. Geophys. Res.* **82**, 803-827

Paul, S. K. 1990. Yemen (former People's Democratic Republic of Yemen):: In: Classic Petroleum Provinces (edited by J. Brookes). *Spec. Publ. Geol. Soc. Lond.* **40**, 329-339.

Peacock, D. C. P. & Sanderson, D. J. 1991. Displacements, segment linkage and relay ramps in normal fault zones. *J. Struct. Geol.* **13**, 721-733.

Peacock, D. C. P. & Sanderson, D. J. 1994. Strain and scaling of faults in the chalk at Flamborough Head, U.K. *J. Struct. Geol.* **16**, 97-107.

Platel, P. J. &. Roger, J. 1989. Geodynamic evolution of Dhofar (Sultanae of Oman) Cretaceous and Tertiary in relation with the Gulf of Aden opening. *Bull. Soc. Geol. France Ser.* 8, **5**, 253-263.

Ramsay, J. G. & Wood, D. S. 1973. The geometric effect of volume change during deformation process. *Tectonophysics*, **16**, 263-277.

Ransome, F. L., Emmons, W. H. & Garrey, G. H. 1910. Geology and ore deposits of the Bullfrog District, Nevada. *U.S. Geol. Surv. Bull.* 407, 1-130.

Redfern, P. &. Jones, J. A. 1995. The interior rifts of the Yemen - analysis of basin structure and stratigraphy in a regional plate tectonic context. *Basin Research* **7**, 337-356.

Richardson, S. M., Bott, W. F., Smith, B. A., Hollar, W. D. & Bermington, P. M. 1995. A new hydrocarbon "play" area offshore Socotra Island, Republic of Yemen. *J. Petrol. Geol.* **18**, 5-28.

Rosendahl, B. R. 1987. Architecture of continental rifts with special reference to east Africa. *Annual Review of Earth and Planetry Science* **15**, 445-503.

Rosendahl, B. R., Kilembe, E. & Kaczmarick, K. 1992. Comparison of the Tanganyika, Malawi, Rukwa and Turkana rift zones from analysis of seismic reflection data. *Tectonophysics* **213**, 235-256.

Rosendahl, B. R. Reynolds, D. Lorber, P. Burgess, C. McGill, J. Scott, D.Lambiase, J. & Derksen, S. 1986. Structural expressions of rifting: lessons from Lake Tanganyika. In: Sedimentation in the east Africa Rifts, (edited by Frostick, L. E.), *Geological Society Special Publication* **25**, 29-43.

Rowan, M. H. & Kligfield, R. 1989. Cross section restoration and balancing as aid to seismic interpretation in extension terranes. *Am. Assoc. Petrol. Geol. Bull.* **73**, 955-966.

Saint-Marc, P. 1978. Arabian Peninsula. In: The Phanerozoic geology of the world part II. (edited by Moullade, M. & Nain, A. E. D.). Amsterdam, 435-462.

Sawer, D. S. & Harry, D. L. 1991. Dynamic modelling of divergent margin formation, application to the U. S. Atlantic margin. *Marine Geology* **102**, 29-42.

Scholz, C. H. &. Cowie, P. A. 1990. Determination of total geologic strain from faulting using slip measurements. *Nature* 346, 837-839.

Schuppel, D. & Wienholz, R. 1990. The development of the Tertiary in the Habban-Al-Mukalla area, Yemen. Z. *Geol. Wiss.* 18, 523-528.

Shelton, J. W. 1984. Listric Normal Fault: An Illustrated Summary. *Am. Assoc. Petrol. Geol. Bull.* 68, 801-815.

Starkey, J. 1977. The contouring of orientation data represented in spherical projection. *Can. J. Earth Sci.* 14, 268-177.

Suppe, J. 1983. Geometry and kinematics of fault-bend folding. *Am. J. Sci.* 283, 684-721.

Tamestt, D. &. Searle, R. 1988. Structure and development of the Midocean Ridge Plate Boundary in the Gulf of Aden: Evidence From GLORIA side Scan Sonar. *J. Geophysical Res.* 93, no. B4, 3157-3178.

Tamestt, D. &. Searle, R. 1990. Structure of the Alula-Fartaq Fracture Zone, Gulf of Aden. *J. Geophysical Res.* 95, no. B2, 1239-1254.

Tamsett, D. 1984. Comments on the development of rifts and transform faults during continental breakup; example from the Gulf of Aden and northern Red Sea. *Tectonophysics*, 104, 35-46.

Tron, V. &. Brun, B. J. 1991. Experiments on oblique rifting in brittle-ductile systems. *Tectonophysics* 188, 71-84.

Trudgill, B. & Cartwright, J. 1994. Relay-ramp forms and normal-fault linkages, Canyonlands National Park, Utah. *Geol. Soc. Am. Bull.* 106, 11143-1157.

Verrall, P. 1981. Structural interpretation with application to North Sea problems, Courses notes No. 3. *Joint Assoc. Petrol Expl.* London.

Versfelt, J. &. Rosendahl, B. R. 1989. Relationship between pre-rift structure and rift architecture in Lake Tanganyika and Malawi, East Africa. *Nature* 337, 354-357.

Villemin, T. & Sunwoo, C. 1987. Distribution logarithmique self-similaire des rejets et des longeurs de failles: example du Bassin Houllier Lorrain. *C. r. Acad. Sci. Paris* 305,

1309-1312

Von Plessman, W. 1964. Gesteinlosung, ein Hauptfaktor beim Schieferungsprozess. *Geol. Mit. Aachen*. 4, 69-82.

Von Wissmam, H. 1932. Ubersich uber Aufbau und Oberflachen-gestaltung Arabiens. *Berlin, Zeitschr. Gesell. Erdkunde*, no. 9-10, 335-357.

Von Wissman, H., Rathjens, C. & Kossmat, F. 1942. Beitrage zur Tektonic Arabiens. *Geol. Rundsch*. 33, 221-353.

Walsh, J. J. & Watterson, J. 1990. New methods of fault projection for coalmine planning. *Proceeding of the Yorkshire Geol. Soc. Lond.* 48, part 2, 209-219.

Walsh, J. J. & Watterson, J. 1991. Geometric and kinematic coherence and scale effects in normal fault systems. *Spec. Publ. Geol. Soc. Lond.* 56, 193-203.

Walsh, J. J. & Watterson, J. 1992. Population of faults and fault displacement and their effects on estimates of fault-related regional extension. *J.Struct. Geol.* 14, 770-712.

Walsh, J. J. &. Watterson, J. 1988. Analysis of the relationship between displacements and dimensions of faults. *J. Struct. Geol.* 10, 239-247.

Watchorn, F. 1995. Regional sedimentary evolution of the Tawilah group, Hadhramaut province, Yemen (abstract). In: Rift sedimetation and tectonics in the Red Sea-Gulf of Aden region. conference, Sana'a.

Watterson, J. 1986. Fault dimensions, displacements and growth. *Pure & Appl. Geophys* 124, 365-373.

Watterson, J., Walsh, J. J., Gillespie, P. A. & Easton, S. 1996. Scaling systematics of fault sizes on a large-scale range fault map. *J. Struct. Geol.* 18, 199-214.

Wernicke, B. & Burchfiel, B. C. 1982. Modes of extensional tectonics. *J. Struct. Geol.* 4, 105-115.

Wernicke, B. 1981. Low-angle normal faults in the Basin and Range province: nappe in an extending orogenic. *Nature* 291, 645-648.

Wernicke, B. 1985. Uniform sense normal simple shear of the continental lithosphere. *Can. J. Earth Sci.*. 22, 108-125.

Wheeler, J. 1987. Variable-heave models of deformation above listric normal faults: the importance of area conservation. *J. Struct Geol.* 9, 1047-1049.

White, M. J. 1993. Physical modelling and analysis of the geometries and kinematics of orthogonal and oblique rift systems. Unpublished Ph.D. thesis, University of London, U.K.

White, N. & McKenzie, D. P. 1988. Formation of the "Steer's head" geometry of sedimentary basins by differential stretching of the crust and mantle.*Geology* 16, 250-253.

White, N. 1987. Constraints on the measurements of extension in the brittle upper crust. *Norsk. Geol. Tidssker.* 67, 269-909.

White, N. J. & Yeilding, G. 1991. Calculated normal fault geometries at depth: theory and examples. In: The geometry of normal faults (edited by Roberts, A. M. Yielding, G. & Freeman, B.). *Spec. Publ. Geol. Soc. Lond.* 56, 897-909.

White, N. J., Jackson, J. A. & McKenzie, D. P. 1986. The relationship between the geometry of normal faults and that of the sedimentary layers in their hanging walls. *J. Struct Geol.* 8, 393-413.

White, R. S. & Matthews, D. H. 1980. Variations in oceanic Upper crustal structure in a small area of the northeastern Atlantic. *Geophys. J. Roy. Astron. Soc.* 61, 401-435.

White, R. S. & McKenzie, D. P. 1989. Magmatism at rift zones and the generation of volcanic continental margins and flood basalt. *J. Geophys. Res.*. 94, 7685-7729.

Williams, G. &. Vann, I. 1987. The geometry of listric normal faults and deformation in their hanging walls. *J. Struct. Geol.* 9, 789-795.

Wilson, M. & Guiraud, R. 1992. Magmatism and rifting in western and central Africa, from late Jurassic to Recent times. *Tectonophysics* 213. 203-225.

Windley, B. F., Whitehouse, M. J. & Ba-Battat, M. A. O. 1996. Early Precabrian gneiss terranes and Pan-African island arcs in the Yemen: Crustal accretion of the eastern Arabian Shield. *Geology* 24, 131-134.

Wojtal, S. F. 1996. Change in fault displacement populations correlated to linkage between faults. *J. Struct. Geol.* 18, 265-279.

Wood, D. S. 1974. Current views of the development of slaty cleavage. *Ann. Rev. Earth Sci.* **2,** 369-401.

Xiao, H. & Suppe, J. 1992. Origin of Rollover. *Am. Assoc. Petrol. Geol. Bull.* **76,** 509-529.

Yielding, G., Needham, T. & Jones, H. 1996. Sampling of fault populations using sub-surface data: a review. *J. Struct. Geol.* **18,** 135-146.

Ziegler, P. 1992. Geodynamics of rifting and implications for hydrocarbon habitat. *Tectonophysics* **215,** 221-253.

Ziegler, P. A. 1982a. Faulting and graben formation in western and central Europe. *Phil. Trans. R. Soc. Lond.* Ser. A, **305,** 113-143.

Ziegler, P. A. 1983. Crustal thinning and subsidence in the North Sea. *Nature* **304,** p561.

Appendix no. 1

Construction of fault profile at depth from rollover anticline

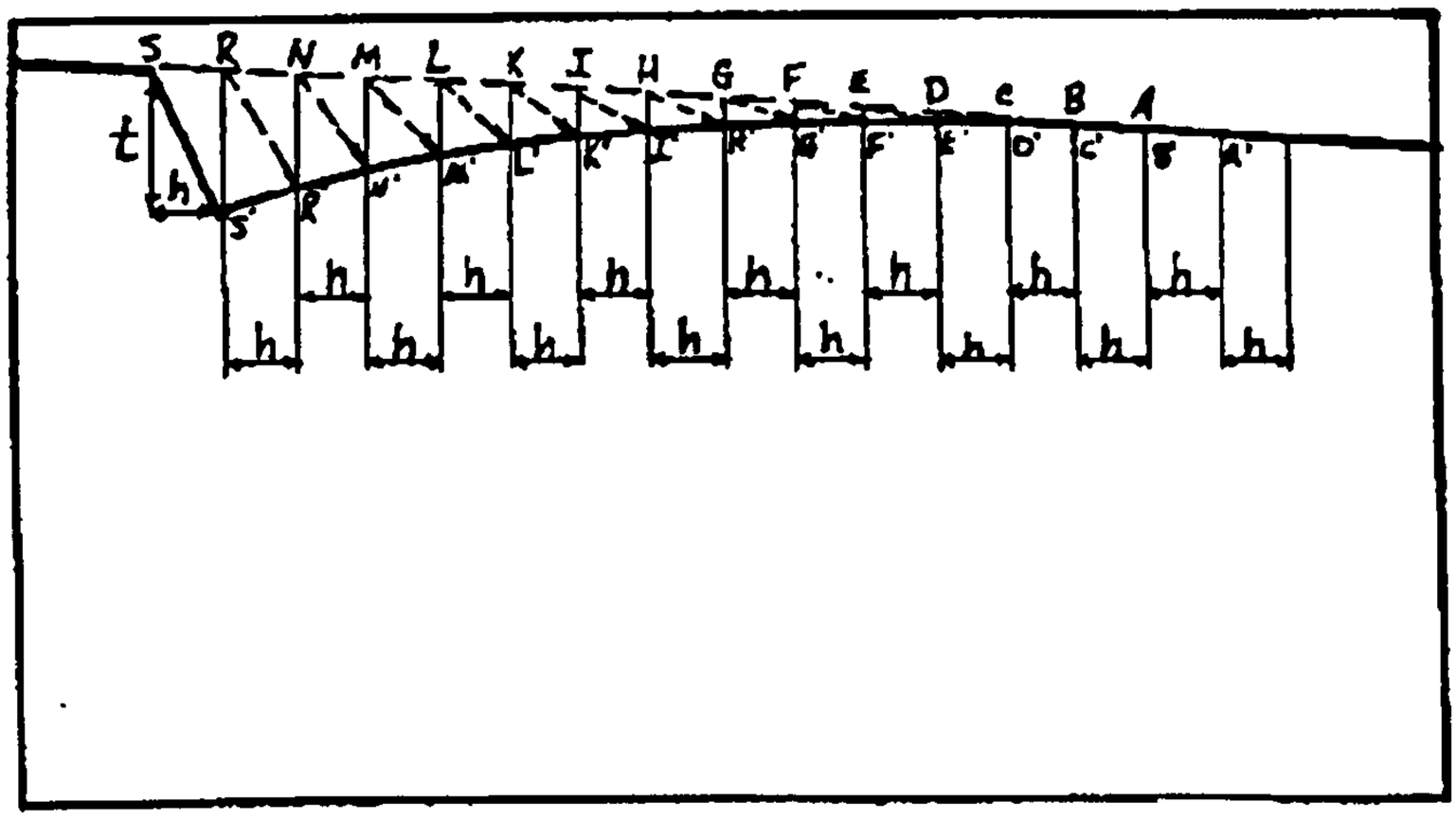

a. Roll-over profile

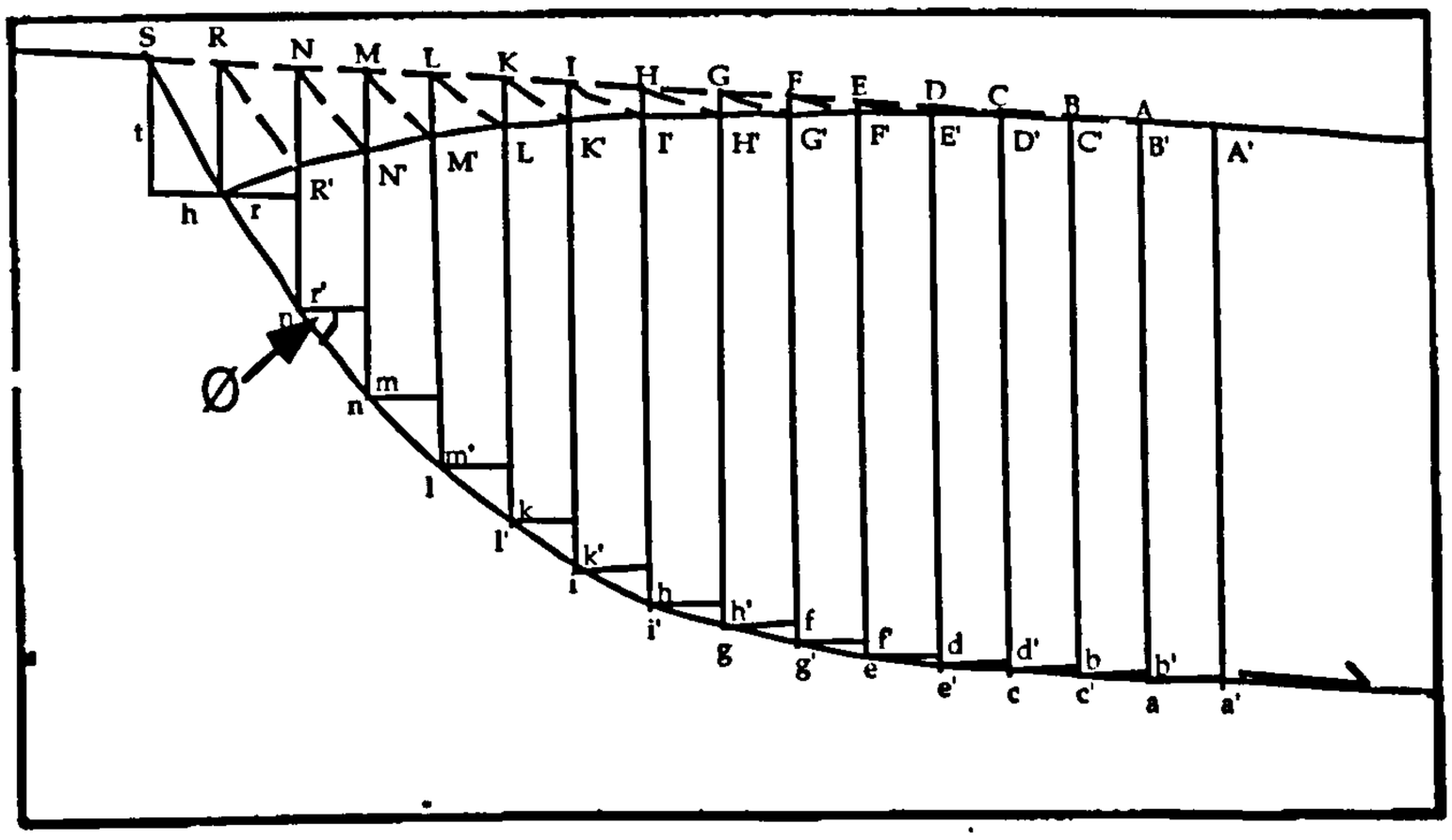

b. Fault shape

Method:

1. Project the regional dip from the footwall cutoff, S to the top of the hanging wall A. Construct vertical lines through S and S' . The horizontal distance between these lines gives the heave, h.
2. Lay out a grid of vertical lines (A, B, C, etc.) separated by heave h (Fig. a).
3. Construct lines SS', RR' etc which represent the resultant vectors of heave and throw.
4. Move line RR' vertically down until point N.
5. Move line NN' vertically down until point N continuous with point R' and repeat for all other vectors.
6. The curved shape of the fault is the continuous line SS', RR' etc.

Appendix no.2

Field data for calculation of shape of rollover anticline.

A. dip of bedding measured every 20 paces down bedding surface of rollover anticline.

B. distance from arbitrary starting point to fault.

C. horizontal distance calculated by trigonometry; C = B cos A.

D. vertical distance calculated by trigonometry; D = B sin A.

E. horizontal distance from fault $E = \sum_{1}^{n} C - \sum_{1}^{x} C$

F. altitude of each measurement based on altimeter reading at point 1 and vertical distance from column D.

G. vertical distance of each station from start point.

H. altitude corrected by a factor obtained by noting altimeter reading at end point H_n compared to calculated altitude at end point Fn

TABLE 1

A	B	C	D	E	F	G	H	I
dips	metres	horizontal	vertical	distance	height	vert. dist.	height corr.	factor corr.
3	0	0	0	539.1	410	0	410	-0.9
5	19.8	19.7	1.7	519.4	408.3	-1.7	408.5	
7	16.2	16.1	2.0	503.3	406.3	-3.7	406.7	
12	19.8	19.4	4.1	484.0	402.2	-7.8	403.1	
13	16.2	15.8	3.6	468.2	398.5	-11.5	399.8	
18	18	17.1	5.6	451.0	393.0	-17.0	394.9	
16	18	17.3	5.0	433.7	388.0	-22.0	390.5	
17	19.8	18.9	5.8	414.8	382.2	-27.8	385.4	
24	16.2	14.8	6.6	400.0	375.6	-34.4	379.5	
18	16.2	15.4	5.0	384.6	370.6	-39.4	375.1	
18	19.8	18.8	6.1	365.8	364.5	-45.5	369.7	
18	18	17.1	5.6	348.7	359.0	-51.0	364.7	
25	18	16.3	7.6	332.3	351.3	-51.0	364.7	
20	18	16.9	6.2	315.4	345.2	-64.8	352.5	
24	18	16.4	7.3	299.0	337.9	-72.1	346.0	
24	18	16.4	7.3	282.5	330.5	-79.5	339.6	
22	18	16.7	6.7	265.9	323.8	-86.2	333.6	
21	18	16.8	6.5	249.0	317.4	-92.6	327.9	
23	18	16.6	7.0	232.5	310.3	-99.7	321.6	
16	18	17.3	5.0	215.2	305.4	-104.6	317.2	
18	18	17.1	5.6	198.1	299.8	-110.2	312.3	
20	18	16.9	6.2	181.1	293.6	-116.4	306.8	
19	18.9	17.9	6.2	163.3	287.5	-122.5	301.4	
11	17.1	16.8	3.3	146.5	284.2	-125.8	298.5	
20	18.9	17.8	6.5	128.7	277.8	-132.2	292.7	
21	17.1	16.0	6.1	112.8	271.6	-138.4	287.3	
18	18.9	18.0	5.8	94.8	265.8	-144.2	282.1	

19	18	17.0	5.9	77.8	259.9	-150.1	276.9	
15	18	17.4	4.7	60.4	229.9	-180.1	250.3	
19	18	17.0	5.9	43.4	224.1	-185.9	245.1	
21	16.2	15.1	5.8	28.2	218.3	-191.7	240.0	

TABLE 2

metres	dip	horizontal	vertical	distance	height	vert. dist.	height corr.	factor corr.
0	0			608.4	320	0	320	0.75
18	2	18.0	0.6	590.4	319.4	-0.6	320.5	
18	0	18.0	0.0	572.4	319.4	0.0	320.0	
18	10	17.7	3.1	554.7	316.2	-3.8	317.2	
18	8	17.8	2.5	536.9	313.7	-6.3	315.3	
18	12	17.6	3.7	519.3	310.0	-10.0	312.5	
18	8	17.8	2.5	501.4	307.5	-12.5	310.6	
18	13	17.5	4.0	483.9	303.4	-16.6	307.6	
18	18	17.1	5.6	466.8	297.9	-22.1	303.4	
18	21	16.8	6.5	450.0	291.4	-28.6	298.6	
18	9	17.8	2.8	432.2	288.6	-31.4	296.5	
18	16	17.3	5.0	414.9	283.7	-36.3	292.8	
18	16	17.3	5.0	397.6	278.7	-41.3	289.1	
18	11	17.7	3.4	379.9	275.3	-44.7	286.5	
18	11	17.7	3.4	362.2	271.8	-48.2	283.9	
18	13	17.5	4.0	344.7	267.8	-52.2	280.9	
18	17	17.2	5.3	327.5	262.5	-57.5	277.0	
18	15	17.4	4.7	310.1	257.9	-62.1	273.5	
18	11	17.7	3.4	292.4	254.4	-65.6	270.9	
18	20	16.9	6.2	275.5	248.3	-71.7	266.3	
18	19	17.0	5.9	258.5	242.4	-77.6	261.9	
18	16	17.3	5.0	241.2	237.4	-82.6	258.2	
18	14	17.5	4.4	223.7	233.1	-86.9	255.0	
19.8	15	19.1	5.1	204.6	228.0	-92.0	251.1	
21.6	38	17.0	13.3	187.6	214.7	-105.3	241.2	
28.8	17	27.5	8.4	160.0	206.2	-113.8	234.9	
14.4	14	14.0	3.5	146.1	202.8	-117.2	232.3	
14.4	21	13.4	5.2	132.6	197.6	-122.4	228.4	
14.4	16	13.8	4.0	118.8	193.6	-126.4	225.4	
16.2	19	15.3	5.3	103.5	188.4	-131.6	221.5	
21.6	14	21.0	5.2	82.5	183.1	-136.9	217.6	
16.2	11	15.9	3.1	66.6	180.0	-140.0	215.3	
18	12	17.6	3.7	49.0	176.3	-143.7	212.5	
27	7	26.8	3.3	22.2	173.0	-147.0	210.0	

TABLE 3

dips	metres	horizontal	vertical	distance	height	vert. dist.	height corr.	factor corr.
7	0	0	0	412.2	290	0	290	-0.72
9	18	17.8	2.8	394.4	287.2	-2.8	288.0	
11	18	17.7	3.4	376.8	283.7	-6.3	285.5	
14	18	17.5	4.4	359.3	279.4	-10.6	282.3	
16	18	17.3	5.0	342.0	274.4	-15.6	278.7	
17	18	17.2	5.3	324.8	269.2	-20.8	274.9	
17	18	17.2	5.3	307.6	263.9	-26.1	271.1	
23	19.8	18.2	7.7	289.3	256.2	-33.8	265.5	
21	16.2	15.1	5.8	274.2	250.4	-39.6	261.3	
20	19.8	18.6	6.8	255.6	243.6	-46.4	256.4	

29	16.2	14.2	7.9	241.4	235.7	-54.3	250.7	
25	18	16.3	7.6	225.1	228.1	-61.9	245.2	
27	18	16.0	8.2	209.1	220.0	-70.0	239.2	
32	18	15.3	9.5	193.8	210.4	-79.6	232.3	
34	18	14.9	10.1	178.9	200.4	-89.6	225.0	
23	18	16.6	7.0	162.3	193.3	-96.7	219.9	
14	18	17.5	4.4	144.9	189.0	-101.0	216.8	
25	19.8	17.9	8.4	126.9	180.6	-109.4	210.7	
24	19.8	18.1	8.1	108.8	172.5	-117.5	204.9	
21	16.2	15.1	5.8	93.7	166.7	-123.3	200.6	
23	16.2	14.9	6.3	78.8	160.4	-129.6	196.1	
25	18	16.3	7.6	62.5	152.8	-137.2	190.5	
31	18	15.4	9.3	47.0	143.5	-146.5	183.8	
19	16.2	15.3	5.3	31.7	138.3	-151.7	180.0	

TABLE 4

dips	metres	horizontal	vertical	distance	height	vert. dist.	height corr.	factor corr.
9	0	0	0	268.2	250	0	250	-0.62
19	18	17.0	5.9	251.2	244.1	-5.9	246.4	
11	18	17.7	3.4	233.5	240.7	-9.3	244.3	
24	18	16.4	7.3	217.1	233.4	-16.6	239.7	
26	18	16.2	7.9	200.9	225.5	-24.5	234.9	
22	18	16.7	6.7	184.2	218.8	-31.2	230.7	
35	18	14.7	10.3	169.5	208.4	-41.6	224.3	
30	18	15.6	9.0	153.9	199.4	-50.6	218.8	
22	18	16.7	6.7	137.2	192.7	-57.3	214.6	
29	18	15.7	8.7	121.4	184.0	-66.0	209.2	
27	18	16.0	8.2	105.4	175.8	-74.2	204.2	
22	18	16.7	6.7	88.7	169.0	-81.0	200.0	
31	18	15.4	9.3	73.3	159.8	-90.2	194.3	
30	18	15.6	9.0	57.7	150.8	-99.2	188.7	
22	18	16.7	6.7	41.0	144.0	-106.0	184.5	
27	16.2	14.4	7.4	26.6	136.7	-113.3	180.0	

TABLE 5

dips	metres	horizontal	vertical	distance	height	vert. dist.	height corr.	factor corr.
12	0	0.0	0.0	268.2	285.0	0.0	285.0	-0.69
13	18	17.5	4.0	250.7	281.0	-4.0	282.2	
12	18	17.6	3.7	233.1	277.2	-7.8	279.6	
11	19.8	19.4	3.8	213.6	273.4	-11.6	277.0	
29	19.8	17.3	9.6	196.3	263.8	-21.2	270.3	
25	16.2	14.7	6.8	181.6	257.0	-28.0	265.6	
27	16.2	14.4	7.4	167.2	249.6	-35.4	260.5	
26	18	16.2	7.9	151.0	241.7	-43.3	255.0	
28	18	15.9	8.5	135.1	233.3	-51.7	249.1	
10	18	17.7	3.1	117.4	230.2	-54.8	246.9	
18	18	17.1	5.6	100.3	224.6	-60.4	243.1	
10	18	17.7	3.1	82.5	221.5	-63.5	240.9	
14	18	17.5	4.4	65.1	217.1	-67.9	237.9	
34	19.8	16.4	11.1	48.7	206.0	-79.0	230.2	
26	16.2	14.6	7.1	34.1	198.9	-86.1	225.3	
28	16.2	14.3	7.6	19.8	191.3	-93.7	220.0	

TABLE 6

dips	metres	horizontal	vertical	distance	height	vert. corr.	height corr.	factor corr.

3	0	0	0	180	310	0	310	-0.63
26	18	16.2	7.9	163.8	302.1	-7.9	305.0	
24	18	16.4	7.3	147.4	294.8	-15.2	300.4	
21	18	16.8	6.5	130.6	288.3	-21.7	296.3	
21	18	16.8	6.5	113.8	281.9	-28.1	292.2	
32	19.8	16.8	10.5	97.0	271.4	-38.6	285.5	
32	16.2	13.7	8.6	83.2	262.8	-47.2	280.1	
31	19.8	17.0	10.2	66.3	252.6	-57.4	273.7	
22	16.2	15.0	6.1	51.2	246.5	-63.5	269.8	
28	18	15.9	8.5	35.4	238.1	-71.9	264.5	
23	18	16.6	7.0	18.8	231.1	-78.9	260.0	

TABLE 7

dips	metres	horizontal	vertical	distance	height	vert. dist.	height corr.	factor corr.
10	0	0	O	421.2	315	0	315	-0.63
26	18	16.2	7.9	405.0	307.1	-7.9	310.0	
23	18	16.6	7.0	388.5	300.1	-14.9	305.6	
26	19.8	17.8	8.7	370.7	291.4	-23.6	300.1	
22	16.2	15.0	6.1	355.6	285.3	-29.7	296.2	
16	19.8	19.0	5.5	336.6	279.9	-35.1	292.8	
22	16.2	15.0	6.1	321.6	273.8	-41.2	289.0	
22	19.8	18.4	7.4	303.2	266.4	-48.6	284.3	
15	18	17.4	4.7	285.8	261.7	-53.3	281.3	
27	16.2	14.4	7.4	271.4	254.4	-60.6	276.7	
19	18	17.0	5.9	254.4	248.5	-66.5	273.0	
27	19.8	17.6	9.0	236.7	239.5	-75.5	267.3	
27	16.2	14.4	7.4	222.3	232.2	-82.8	262.6	
26	18	16.2	7.9	206.1	224.3	-90.7	257.6	
23	18	16.6	7.0	189.6	217.2	-97.8	253.2	
21	18	16.8	6.5	172.8	210.8	-104.2	249.1	
23	18	16.6	7.0	156.2	203.8	-111.2	244.7	
20	18	16.9	6.2	139.3	197.6	-117.4	240.8	
23	18	16.6	7.0	122.7	190.6	-124.4	236.3	
22	18	16.7	6.7	106.0	183.8	-131.2	232.1	
23	18	16.6	7.0	89.4	176.8	-138.2	227.6	
24	18	16.4	7.3	73.0	169.5	-145.5	223.0	
28	18	15.9	8.5	57.1	161.0	-154.0	217.7	
32	18	15.3	9.5	41.8	151.5	-163.5	211.6	
21	7.2	6.7	2.6	35.1	148.9	-166.1	210.0	

TABLE 8

dips	metres	horizontal	vertical	distance	height	vert. dist.	height corr.	factor corr.
16	0	O	0	450	320	0	320	-0.67
10	18	17.7	3.1	432.3	316.9	-3.1	317.9	
16	18	17.3	5.0	415.0	311.9	-8.1	314.6	
21	18	16.8	6.5	398.2	305.5	-14.5	310.3	
17	18	17.2	5.3	381.0	300.2	-19.8	306.8	
25	16.2	14.7	6.8	366.3	293.4	-26.6	302.3	
22	19.8	18.4	7.4	347.9	285.9	-34.1	297.3	
20	18	16.9	6.2	331.0	279.8	-40.2	293.2	
19	18	17.0	5.9	314.0	273.9	-46.1	289.3	
23	18	16.6	7.0	297.4	266.9	-53.1	284.7	
24	18	16.4	7.3	281.0	259.6	-60.4	279.8	
22	19.8	18.4	7.4	262.6	252.1	-67.9	274.9	

19	18	17.0	5.9	245.6	246.3	-73.7	271.0	
17	16.2	15.5	4.7	230.1	241.6	-78.4	267.8	
26	18	16.2	7.9	213.9	233.7	-86.3	262.6	
22	18	16.7	6.7	197.2	226.9	-93.1	258.1	
32	18	15.3	9.5	182.0	217.4	-102.6	251.7	
27	18	16.0	8.2	165.9	209.2	-110.8	246.3	
20	18	16.9	6.2	149.0	203.1	-116.9	242.2	
33	18	15.1	9.8	133.9	193.2	-126.8	235.7	
28	18	15.9	8.5	118.0	184.8	-135.2	230.1	
19	18	17.0	5.9	101.0	178.9	-141.1	226.2	
21	18	16.8	6.5	84.2	172.5	-147.5	221.9	
28	18	15.9	8.5	68.3	164.0	-156.0	216.2	
27	18	16.0	8.2	52.3	155.9	-164.1	210.8	
29	18	15.7	8.7	36.5	147.1	-172.9	205.0	

TABLE 9

dips	metres	horizontal	vertical	distance	height	vert. dist.	height corr.	factor corr.
8	0	0	0	342	135	0	135	-0.83
24	18	16.4	7.3	325.6	127.7	-7.3	128.9	
26	18	16.2	7.9	309.4	119.8	-15.2	122.4	
20	18	16.9	6.2	292.5	113.6	-21.4	117.3	
26	18	16.2	7.9	276.3	105.7	-29.3	110.7	
29	18	15.7	8.7	260.5	97.0	-38.0	103.5	
30	18	15.6	9.0	245.0	88.0	-47.0	96.0	
26	19.8	17.8	8.7	227.2	79.3	-55.7	88.8	
18	16.2	15.4	5.0	211.8	74.3	-60.7	84.6	
22	18	16.7	6.7	195.1	67.6	-67.4	79.0	
26	18	16.2	7.9	178.9	59.7	-75.3	72.5	
17	18	17.2	5.3	161.7	54.4	-80.6	68.1	
23	18	16.6	7.0	145.1	47.4	-87.6	62.2	
17	18	17.2	5.3	127.9	42.1	-92.9	57.9	
23	18	16.6	7.0	111.3	35.1	-99.9	52.0	
23	18	16.6	7.0	94.7	28.1	-106.9	46.2	
21	18	16.8	6.5	77.9	21.6	-113.4	40.8	
20	18	16.9	6.2	61.0	15.5	-119.5	35.7	
21	18	16.8	6.5	44.2	9.0	-126.0	30.4	
21	18	16.8	6.5	27.4	2.6	-132.4	25	

TABLE 10

dips	metres	horizontal	vertical	distance	height	vert. dist.	height corr.	factor corr.
17	0	0.0	0.0	249.3	115.0	0	115	-0.48
27	18	16.0	8.2	233.3	106.8	-8.2	111.1	
35	18	14.7	10.3	218.5	96.5	-18.5	106.1	
30	19.8	17.1	9.9	201.4	86.6	-28.4	101.3	
29	18	15.7	8.7	185.6	77.9	-37.1	97.1	
30	18	15.6	9.0	169.9	68.9	-46.1	92.8	
25	16.2	14.7	6.8	155.2	62.0	-53.0	89.5	
31	18	15.4	9.3	139.8	52.8	-62.2	85.0	
30	18	15.6	9.0	124.2	43.8	-71.2	80.7	
29	18	15.7	8.7	108.4	35.0	-80.0	76.5	
32	18	15.3	9.5	93.2	25.5	-89.5	71.9	
29	18	15.7	8.7	77.4	16.8	-98.2	67.7	
35	18	14.7	10.3	62.7	6.4	-108.6	62.7	
30	18	15.6	9.0	47.1	-2.6	-117.6	58.3	

27	15.3	13.6	6.9	33.5	-9.5	-124.5	55.0	

TABLE 11

metres	dip	horizantal	vertical	distance	height	vert. dist.	height corr.	factor corr.
0	7	0	0	478	220	O	220	-0.62
18	4	3.8	1.2	474.2	218.8	-1.2	219.2	
18.9	15	14.2	4.9	460.0	213.9	-6.1	216.2	
16.2	9	8.6	2.5	451.4	211.4	-8.6	214.6	
18	17	16.2	5.3	435.2	206.1	-13.9	211.4	
18	15	14.3	4.6	420.9	201.5	-18.5	208.5	
18	19	18.1	5.9	402.9	195.6	-24.4	204.8	
18	19	18.1	5.9	384.8	189.8	-30.2	201.2	
18	10	9.5	3.1	375.3	186.7	-33.3	199.3	
18	20	19.0	6.2	356.3	180.5	-39.5	195.4	
16.2	22	21.1	6.1	335.1	174.4	-45.6	191.6	
18.9	16	15.1	5.2	320.0	169.2	-50.8	188.4	
16.2	25	24.0	7.0	296.0	162.2	-57.8	184.0	
18	21	20.0	6.5	276.0	155.7	-64.3	180.0	
18	25	23.8	7.7	252.2	148.0	-72.0	175.2	
19.8	20	18.8	6.8	233.4	141.2	-78.8	171.0	
16.2	12	11.5	3.3	221.9	137.9	-82.1	168.9	
19.8	25	23.5	8.5	198.4	129.4	-90.6	163.6	
16.2	20	19.2	5.6	179.2	123.8	-96.2	160.1	
19.8	28	26.3	9.5	152.8	114.3	-105.7	154.2	
16.2	30	28.8	8.4	124.0	106.0	-114.0	149.0	
18	40	38.0	12.4	86.0	93.6	-126.4	141.3	
18	41	39.0	12.7	47.0	80.9	-139.1	133.5	
18	22	20.9	6.8	26.1	74.1	-145.9	129.2	
18	22	20.9	6.8	5.1	67.3	-152.7	125.0	

TABLE 12

dips	metres	horizontal	vertical	distance	height	vert. dist.	height corr.	factor corr.
5	0	0	0	288	290	0	290	-0.62
8	18	17.8	2.5	270.2	287.5	-2.5	288.4	
12	18	17.6	3.7	252.6	283.8	-6.2	286.1	
12	19.8	19.4	4.1	233.2	279.6	-10.4	283.5	
17	16.2	15.5	4.7	259.7	274.9	-15.1	280.6	
15	18	17.4	4.7	242.3	270.2	-19.8	277.7	
22	18	16.7	6.7	225.6	263.5	-26.5	273.4	
15	18	17.4	4.7	208.2	258.8	-31.2	270.5	
16	18	17.3	5.0	190.9	253.9	-36.1	267.4	
14	18	17.5	4.4	173.5	249.5	-40.5	264.7	
17	18	17.2	5.3	156.3	244.3	-45.7	261.4	
17	18	17.2	5.3	139.0	239.0	-51.0	258.1	
13	18	17.5	4.0	121.5	234.9	-55.1	255.6	
18	19.8	18.8	6.1	102.7	228.8	-61.2	251.8	
17	18	17.2	5.3	85.5	223.6	-66.4	248.5	
16	16.2	15.6	4.5	69.9	219.1	-70.9	245.7	
17	19.8	18.9	5.8	51.0	213.3	-76.7	242.1	
12	16.2	15.8	3.4	35.1	209.9	-80.1	240.0	

TABLE 13

dips	metres	horizontal	vertical	distance	height	vert. dist.	height corr.	factor corr.
7	0	0	0	324	295	0	295	-0.23
7	18	17.9	12.2	306.1	282.8	-12.2	292.2	

7	18	17.9	12.2	288.3	270.5	-24.5	289.4	
9	18	17.8	12.2	270.5	258.3	-36.7	286.7	
11	18	17.7	12.2	252.8	246.1	-48.9	283.9	
14	18	17.5	12.2	235.4	233.8	-61.2	281.1	
9	18	17.8	12.2	217.6	221.6	-73.4	278.3	
8	18	17.8	12.2	199.8	209.4	-85.6	275.6	
8	19.8	19.6	13.5	180.1	195.9	-99.1	272.5	
14	16.2	15.7	11.0	164.4	184.9	-110.1	270.0	
10	18	17.7	12.2	146.7	172.7	-122.3	267.2	
20	18	16.9	12.2	129.8	160.5	-134.5	264.4	
11	16.2	15.9	11.0	113.9	149.4	-145.6	261.9	
12	19.8	19.4	13.5	94.5	136.0	-159.0	258.9	
15	18	17.4	12.2	77.1	123.8	-171.2	256.1	
8	18	17.8	12.2	59.3	111.5	-183.5	253.3	
9	18	17.8	12.2	41.5	99.3	-195.7	250.6	
10	18	17.7	12.2	23.8	87.1	-207.9	247.8	
23	18	16.6	12.2	7.2	74.8	-220.2	245.0	

TABLE 14

dips	metres	horizontal	vertical	distance	height	vert. dist.	height corr.	factor corr.
7	0	0	0	788.5	285	0	285	-0.66
11	18	17.7	3.4	770.8	281.6	-3.4	282.7	
5	18	17.9	1.6	752.9	280.0	-5.0	281.7	
9	18	17.8	2.8	735.1	277.2	-7.8	279.9	
17	18	17.2	5.3	717.9	271.9	-13.1	276.4	
25	18	16.3	7.6	701.6	264.3	-20.7	271.4	
28	18	15.9	8.5	685.7	255.9	-29.1	265.8	
33	18	15.1	9.8	670.6	246.1	-38.9	259.4	
12	18	17.6	3.7	653.0	242.3	-42.7	256.9	
25	18	16.3	7.6	636.7	234.7	-50.3	251.9	
21	18	16.8	6.5	619.9	228.3	-56.7	247.7	
6	18	17.9	1.9	602.0	226.4	-58.6	246.4	
24	16.2	14.8	6.6	587.2	219.8	-65.2	242.1	
11	19.8	19.4	3.8	567.7	216.0	-69.0	239.6	
18	18	17.1	5.6	550.6	210.4	-74.6	236.0	
24	18.9	17.3	7.7	533.4	202.8	-82.2	230.9	
24	17.1	15.6	7.0	517.7	195.8	-89.2	226.3	
30	18	15.6	9.0	502.1	186.8	-98.2	220.4	
30	18	15.6	9.0	486.6	177.8	-107.2	214.5	
29	18	15.7	8.7	470.8	169.1	-115.9	208.8	
27	18	16.0	8.2	454.8	160.9	-124.1	203.4	
32	18	15.3	9.5	439.5	151.4	-133.6	197.1	
33	18.9	15.9	10.3	423.7	141.1	-143.9	190.4	
32	17.2	14.6	9.1	409.1	132.0	-153.0	184.4	
12	18	17.6	3.7	391.5	128.2	-156.8	181.9	
20	18	16.9	6.2	374.6	122.1	-162.9	177.9	
29	18	15.7	8.7	358.8	113.3	-171.7	172.1	
29	18	15.7	8.7	343.1	104.6	-180.4	166.4	
34	18	14.9	10.1	328.1	94.5	-190.5	159.8	
26	18	16.2	7.9	312.0	86.7	-198.3	154.6	
27	18	16.0	8.2	295.9	78.5	-206.5	149.2	
22	18	16.7	6.7	279.2	71.7	-213.3	144.8	
34	18	14.9	10.1	264.3	61.7	-223.3	138.1	
20	18	16.9	6.2	247.4	55.5	-229.5	134.1	

23	18	16.6	7.0	230.8	48.5	-236.5	129.5	
23	18	16.6	7.0	214.3	41.4	-243.6	124.8	
28	18	15.9	8.5	198.4	33.0	-252.0	119.3	
31	18	15.4	9.3	182.9	23.7	-261.3	113.2	
32	18	15.3	9.5	167.7	14.2	-270.8	106.9	
25	18	16.3	7.6	151.4	6.6	-278.4	101.9	
30	18	15.6	9.0	135.8	-2.4	-287.4	96.0	
28	18	15.9	8.5	119.9	-10.9	-295.9	90.4	
32	18	15.3	9.5	104.6	-20.4	-305.4	84.2	
24	16.2	14.8	6.6	89.8	-27.0	-312.0	79.8	
27	16.2	14.4	7.4	75.4	-34.4	-319.4	75.0	

TABLE 15

dips	metres	horizontal	vertical	distance	height	vert. dist.	height corr.	factor corr.
7	0	0	0	740	295	0	295	-0.69
6	18	17.9	1.9	722.1	293.1	-1.9	293.7	
8	19.8	19.6	2.8	702.5	290.4	-4.6	291.8	
7	19.8	19.7	2.4	682.8	287.9	-7.1	290.1	
6	16.2	16.1	1.7	666.7	286.3	-8.7	289.0	
6	16.2	16.1	1.7	650.6	284.6	-10.4	287.8	
12	19.8	19.4	4.1	631.2	280.4	-14.6	284.9	
10	18	17.7	3.1	613.5	277.3	-17.7	282.8	
11	16.2	15.9	3.1	597.6	274.2	-20.8	280.6	
11	20	19.6	3.8	578.0	270.4	-24.6	278.0	
13	18	17.5	4.0	560.4	266.4	-28.6	275.2	
11	18	17.7	3.4	542.8	262.9	-32.1	272.8	
10	18	17.7	3.1	525.1	259.8	-35.2	270.7	
14	18	17.5	4.4	507.6	255.4	-39.6	267.7	
13	18	17.5	4.0	490.0	251.4	-43.6	264.9	
11	18	17.7	3.4	472.4	248.0	-47.0	262.5	
12	18	17.6	3.7	454.8	244.2	-50.8	259.9	
11	18	17.7	3.4	437.1	240.8	-54.2	257.5	
10	19.8	19.5	3.4	417.6	237.4	-57.6	255.2	
12	16.2	15.8	3.4	401.8	234.0	-61.0	252.8	
13	18	17.5	4.0	384.2	229.9	-65.1	250.0	
11	16.2	15.9	3.1	368.3	226.8	-68.2	247.9	
12	19.8	19.4	4.1	349.0	222.7	-72.3	245.0	
14	18	17.5	4.4	331.5	218.4	-76.6	242.0	
16	18	17.3	5.0	314.2	213.4	-81.6	238.6	
14	18	17.5	4.4	296.7	209.1	-85.9	235.6	
16	18	17.3	5.0	279.4	204.1	-90.9	232.2	
16	18	17.3	5.0	262.1	199.1	-95.9	228.7	
17	18	17.2	5.3	244.9	193.9	-101.1	225.1	
13	18	17.5	4.0	227.4	189.8	-105.2	222.3	
13	18	17.5	4.0	209.8	185.8	-109.2	219.5	
15	18	17.4	4.7	192.4	181.1	-113.9	216.3	
10	18	17.7	3.1	174.7	178.0	-117.0	214.1	
17	18	17.2	5.3	157.5	172.7	-122.3	210.5	
20	18	16.9	6.2	140.6	166.6	-128.4	206.2	
16	18	17.3	5.0	123.3	161.6	-133.4	202.8	
18	18	17.1	5.6	106.2	156.0	-139.0	199.0	
13	18	17.5	4.0	88.6	152.0	-143.0	196.2	
18	18	17.1	5.6	71.5	146.4	-148.6	192.3	
12	18	17.6	3.7	53.9	142.7	-152.3	189.7	

23	18	16.6	7.0	37.3	135.7	-159.3	184.9	
23	18	16.6	7.0	20.8	128.6	-166.4	180.0	

TABLE 16

dips	metres	horizontal	vertical	distance	height	vert. dist.	height corr.	factor corr.
3	0	0	0	578	405	0	404	-0.86
11	18	17.7	3.4	560.3	401.6	-3.4	402.1	
11	18	17.7	3.4	542.7	398.1	-6.9	399.1	
14	18	17.5	4.4	525.2	393.8	-11.2	395.4	
12	18	17.6	3.7	507.6	390.0	-15.0	392.2	
11	18	17.7	3.4	489.9	386.6	-18.4	389.2	
15	18	17.4	4.7	472.5	381.9	-23.1	385.2	
17	18	17.2	5.3	455.3	376.7	-28.3	380.7	
19	18	17.0	5.9	438.3	370.8	-34.2	375.7	
12	18	17.6	3.7	420.7	367.1	-37.9	372.5	
20	18	16.9	6.2	403.8	360.9	-44.1	367.2	
13	18	17.5	4.0	386.2	356.9	-48.1	363.7	
18	18	17.1	5.6	369.1	351.3	-53.7	358.9	
11	18	17.7	3.4	351.5	347.9	-57.1	356.0	
22	18	16.7	6.7	334.8	341.1	-63.9	350.2	
19	18	17.0	5.9	317.7	335.3	-69.7	345.2	
18	18	17.1	5.6	300.6	329.7	-75.3	340.4	
21	18	16.8	6.5	283.8	323.3	-81.7	334.9	
26	18	16.2	7.9	267.6	315.4	-89.6	328.1	
21	18	16.8	6.5	250.8	308.9	-96.1	322.5	
20	18	16.9	6.2	233.9	302.8	-102.2	317.3	
20	18	16.9	6.2	217.0	296.6	-108.4	312.0	
15	18	17.4	4.7	199.6	291.9	-113.1	308.0	
19	18	17.0	5.9	182.6	286.1	-118.9	303.0	
22	16.2	15.0	6.1	167.6	280.0	-125.0	297.7	
30	19.8	17.1	9.9	150.4	270.1	-134.9	289.3	
32	18	15.3	9.5	135.2	260.6	-144.4	281.1	
26	18.2	16.4	8.0	118.8	252.6	-152.4	274.2	
10	19.8	19.5	3.4	99.3	249.2	-155.8	271.3	
15	18	17.4	4.7	81.9	244.5	-160.5	267.3	
14	18	17.5	4.4	64.5	240.1	-164.9	263.5	
24	18	16.4	7.3	48.0	232.8	-172.2	257.3	
28	18	15.9	8.5	32.1	224.4	-180.6	250.0	

TABLE 17

dips	metres	horizontal	vertical	distance	height	vert. dist.	height corr.	factor corr.
6	0	0	0	234	100	0	100	-0.65
9	18	17.8	2.8	216.2	97.2	-2.8	98.2	
11	18	17.7	3.4	198.6	93.7	-6.3	95.9	
15	18	17.4	4.7	181.2	89.1	-10.9	92.9	
20	18	16.9	6.2	164.3	82.9	-17.1	88.9	
17	18	17.2	5.3	147.0	77.7	-22.3	85.4	
21	18	16.8	6.5	130.2	71.2	-28.8	81.2	
18	18	17.1	5.6	113.1	65.7	-34.3	77.6	
19	18	17.0	5.9	96.1	59.8	-40.2	73.8	
28	18	15.9	8.5	80.2	51.3	-48.7	68.3	
22	18	16.7	6.7	63.5	44.6	-55.4	63.9	
30	18	15.6	9.0	47.9	35.6	-64.4	58.0	
17	18	17.2	5.3	30.7	30.3	-69.7	54.6	

23	18	16.6	7.0	14.1	23.3	-76.7	50.0	

TABLE 18

dips	metres	horizontal	vertical	distance	height	vert. dist.	height corr.	factor corr.
5	0	0	0	216	115	0	115	-0.88
11	18	17.7	3.4	198.3	111.6	-3.4	112.0	
20	18	16.9	6.2	181.4	105.4	-9.6	106.5	
14	18	17.5	4.4	164.0	101.1	-13.9	102.7	
26	18	16.2	7.9	147.8	93.2	-21.8	95.7	
27	18	16.0	8.2	131.7	85.0	-30.0	88.5	
21	18	16.8	6.5	114.9	78.5	-36.5	82.8	
26	18	16.2	7.9	98.8	70.7	-44.3	75.8	
21	18	16.8	6.5	81.9	64.2	-50.8	70.1	
15	18	17.4	4.7	64.6	59.5	-55.5	66.0	
15	18	17.4	4.7	47.2	54.9	-60.1	61.8	
15	18	17.4	4.7	29.8	50.2	-64.8	57.7	
29	18	15.7	8.7	14.0	41.5	-73.5	50.0	

TABLE 19

dips	metres	horizotal	vertical	distance	height	vert. dist.	height corr.	factor corr.
7	0	0	0	432	240	0	240	-0.88
15	18	17.4	4.7	414.6	235.3	-4.7	235.9	
20	18	16.9	6.2	397.7	229.2	-10.8	230.5	
15	18	17.4	4.7	380.3	224.5	-15.5	226.4	
17	18	17.2	5.3	363.1	219.3	-20.7	221.8	
29	18	15.7	8.7	347.4	210.5	-29.5	214.1	
17	18	17.2	5.3	330.1	205.3	-34.7	209.5	
17	18	17.2	5.3	312.9	200.0	-40.0	204.9	
22	18	16.7	6.7	296.2	193.3	-46.7	199.0	
19	18	17.0	5.9	279.2	187.4	-52.6	193.8	
20	18	16.9	6.2	262.3	181.3	-58.7	188.4	
25	18	16.3	7.6	246.0	173.6	-66.4	181.7	
22	18	16.7	6.7	229.3	166.9	-73.1	175.8	
26	18	16.2	7.9	213.1	159.0	-81.0	168.9	
28	18	15.9	8.5	197.2	150.6	-89.4	161.5	
29	18	15.7	8.7	181.5	141.8	-98.2	153.8	
27	18	16.0	8.2	165.5	133.7	-106.3	146.6	
29	18	15.7	8.7	149.7	124.9	-115.1	139.0	
20	18	16.9	6.2	132.8	118.8	-121.2	133.6	
17	18	17.2	5.3	115.6	113.5	-126.5	128.9	
34	18	14.9	10.1	100.7	103.5	-136.5	120.1	
23	18	16.6	7.0	84.1	96.4	-143.6	113.9	
28	18	15.9	8.5	68.2	88.0	-152.0	106.5	
30	18	15.6	9.0	52.6	79.0	-161.0	98.6	
33	18	15.1	9.8	37.5	69.2	-170.8	90.0	

TABLE 20

dips	metres	horizontal	vertical	distance	height	vert. dist.	height corr.	factor corr.
4	0	0	0	504	240	0	240	-0.63
16	18	17.3	5.0	486.7	235.0	-5.0	236.9	
12	18	17.6	3.7	469.1	231.3	-8.7	234.5	
24	18	16.4	7.3	452.6	224.0	-16.0	229.9	
17	18	17.2	5.3	435.4	218.7	-21.3	226.5	
17	18	17.2	5.3	418.2	213.4	-26.6	223.2	
14	18	17.5	4.4	400.8	209.1	-30.9	220.4	

20	18	16.9	6.2	383.8	202.9	-37.1	216.5	
17	18	17.2	5.3	366.6	197.7	-42.3	213.2	
28	18	15.9	8.5	350.7	189.2	-50.8	207.9	
31	18	15.4	9.3	335.3	180.0	-60.0	202.0	
33	18	15.1	9.8	320.2	170.2	-69.8	195.8	
23	18	16.6	7.0	303.6	163.1	-76.9	191.3	
24	18	16.4	7.3	287.2	155.8	-84.2	186.7	
25	18	16.3	7.6	270.9	148.2	-91.8	181.9	
31	18	15.4	9.3	255.5	138.9	-101.1	176.0	
25	18	16.3	7.6	239.1	131.3	-108.7	171.2	
22	18	16.7	6.7	222.5	124.6	-115.4	166.9	
29	18	15.7	8.7	206.7	115.8	-124.2	161.4	
21	18	16.8	6.5	189.9	109.4	-130.6	157.3	
27	18	16.0	8.2	173.9	101.2	-138.8	152.2	
25	19.8	17.9	8.4	155.9	92.9	-147.1	146.9	
26	16.2	14.6	7.1	141.4	85.8	-154.2	142.4	
27	19.8	17.6	9.0	123.7	76.8	-163.2	136.7	
30	16.2	14.0	8.1	109.7	68.7	-171.3	131.6	
28	18	15.9	8.5	93.8	60.2	-179.8	126.2	
32	18	15.3	9.5	78.5	50.7	-189.3	120.2	
27	18	16.0	8.2	62.5	42.5	-197.5	115.0	
26	18	16.2	7.9	32.5	34.6	-205.4	110.0	

Appendix no. 3

Steps in the line-balancing of a cross section

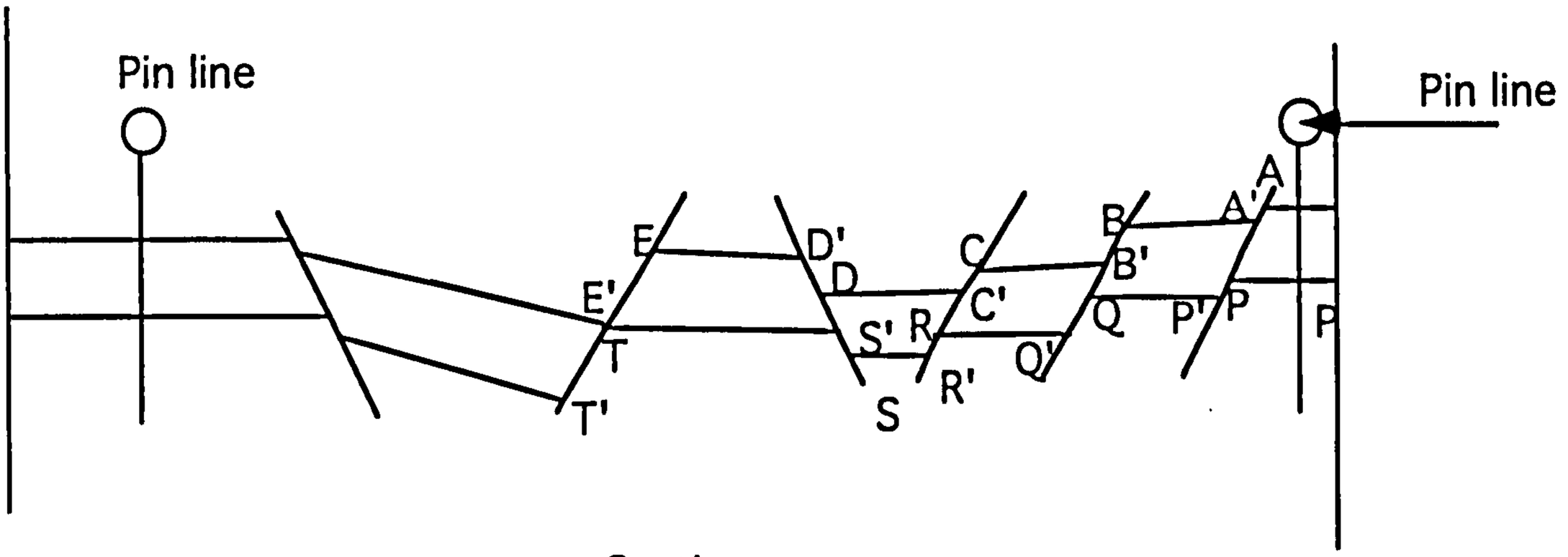

Section

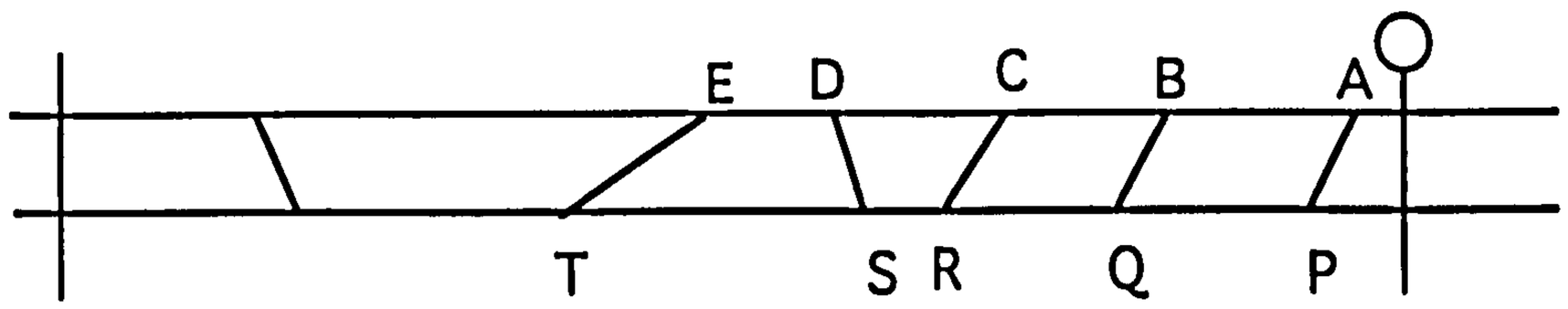

Restored template

Method:
Choose a suitable starting point, for example, where bedding is at the regional dip or in a horst block. Locate the outcrop of faults on the section and draw in the faults using all available data. Proceed from one end of the section to the other. Locate points A and P on the restored section. Knowing point B from the map, draw in AB on the restored template. If the dip of the fault at B is known use its angle with respect to bedding on the restored template, otherwise draw in the interpreted position of the fault on the section i.e. BQ and define points Q and Q'. Take distance PQ from the section and draw it on the restored template. Continue working along the section.
If the dips of faults become shallower than can reasonably be expected, for example, fault ET, then the section should be erased and a new interpretation of the geometry at depth drawn in. The process is repeated until the geological section between the pin lines is restored to a possible pre-faulting geometry.

Appendix no. 4

Measurements of vertical displacement and the length of faults fron maps and field.

Number	Displacement	Length	Number	Displacement	Length
1	3	300	52	20	4500
2	5	780	53	20	4500
3	10	950	54	20	4500
4	10	1000	55	20	4500
5	10	1000	56	20	4550
6	10	1050	57	20	4600
7	10	1150	58	20	4750
8	10	1350	59	20	4850
9	10	1400	60	20	4900
10	10	1650	61	20	4950
11	10	1750	62	20	5000
12	10	1800	63	20	5000
13	10	1900	64	20	5000
14	10	1950	65	20	5000
15	10	2000	66	20	5250
16	10	2150	67	20	5250
17	10	2200	68	20	5250
18	10	2250	69	20	5250
19	10	2400	70	21	5400
20	10	2550	71	30	5450
21	10	2600	72	30	5500
22	10	2600	73	30	5600
23	10	2715	74	30	5650
24	10	2800	75	30	5650
25	10	3000	76	30	5800
26	10	3050	77	30	6000
27	10	3250	78	30	6000
28	10	3250	79	30	6000
29	10	3300	80	30	6150
30	10	3300	81	30	6300
31	10	3350	82	30	6500
32	15	3400	83	31	6500
33	16	3400	84	34	6500
34	16	3500	85	35	6500
35	19	3500	86	37	6550
36	20	3650	87	39	6750
37	20	3650	88	40	6750
38	20	3750	89	40	6750
39	20	3900	90	40	7000
40	20	3950	91	40	7000
41	20	3950	92	40	7200
42	20	4000	93	40	7300
43	20	4000	94	40	7450
44	20	4000	95	40	7500
45	20	4100	96	40	7500
46	20	4150	97	40	7600
47	20	4250	98	40	7650
48	20	4250	99	40	7900
49	20	4250	100	40	8000
50	20	4250	101	40	8000

51	20	4400	102	40	8000
103	40	8050	157	110	14250
104	40	8200	158	110	14350
105	40	8250	159	120	14450
106	40	8250	160	120	14500
107	40	8350	161	120	14500
108	40	8750	162	120	14500
109	41	8750	163	120	15000
110	42	8900	164	127	15500
111	42	9000	165	133	15500
112	47	9000	166	133	16000
113	50	9100	167	140	16000
114	50	9250	168	140	16600
115	50	9250	169	140	16600
116	50	9250	170	148	17000
117	54	9250	171	150	17750
118	60	9300	172	150	17750
119	60	9350	173	150	17750
120	60	9550	174	150	18400
121	60	9650	175	150	18500
122	60	9800	176	160	18600
123	60	9800	177	160	18650
124	60	10000	178	160	19250
125	60	10000	179	160	19550
126	60	10000	180	160	19600
127	60	10000	181	160	19750
128	60	10000	182	160	20000
129	60	10350	183	160	20250
130	60	10350	184	161	20250
131	60	10400	185	168	20800
132	63	10400	186	170	20800
133	66	10500	187	178	21000
134	68	10600	188	180	21000
135	70	10850	189	186	21600
136	80	11000	190	193	22000
137	80	11100	191	196	23500
138	80	11300	192	196	23500
139	80	11300	193	213	24100
140	80	11350	194	213	24300
141	80	11400	195	220	24500
142	80	11400	196	220	24500
143	80	11500	197	220	24500
144	80	11500	198	240	24500
145	85	11700	199	240	25750
146	89	11750	200	240	26000
147	90	11900	201	240	26000
148	100	12000	202	243	27500
149	100	12000	203	261	29200
150	100	12650	204	290	30500
151	100	13100	205	330	31000
152	100	13200	206	371	33000
153	100	13500	207	380	33500
154	100	13500	208	385	36000
155	110	13750	209	391	36200

156	110	14150	210	394	36200
211	460	38300	215	749	59250
212	460	40900	216	1244	59250
213	553	52000	217	1320	6.00E+04
214	690	52000			
Note that the unit is in meter					